uOttawa

L'Université canadienne
Canada's university

FACULTÉ DES ÉTUDES SUPÉRIEURES ET POSTOCTORALES

uOttawa

L'Université canadienne
Canada's university

FACULTY OF GRADUATE AND POSDOCTORAL STUDIES

Audur Atladottir
AUTEUR DE LA THÈSE / AUTHOR OF THESIS

M.A.Sc. (Civil Engineering)
GRADE / DEGREE

Department of Civil Engineering
FACULTÉ, ÉCOLE, DÉPARTEMENT / FACULTY, SCHOOL, DEPARTMENT

Experimental Investigation of Wave-Induced Morphological Changes of Gravel Beaches

TITRE DE LA THÈSE / TITLE OF THESIS

Dr. I. Nistor
DIRECTEUR (DIRECTRICE) DE LA THÈSE / THESIS SUPERVISOR

Dr. Andrew Cornett
CO-DIRECTEUR (CO-DIRECTRICE) DE LA THÈSE / THESIS CO-SUPERVISOR

EXAMINATEURS (EXAMINATRICES) DE LA THÈSE / THESIS EXAMINERS

Dr. Paul Van Geel

Dr. O. Seidou

Dr. C. Rennie

Gary W. Slater
Le Doyen de la Faculté des études supérieures et postdoctorales / Dean of the Faculty of Graduate and Postdoctoral Studies

EXPERIMENTAL INVESTIGATION OF WAVE-INDUCED MORPHOLOGICAL CHANGES OF GRAVEL BEACHES

Audur Atladottir

Submitted under the supervision of
Dr. Ioan Nistor
Dr. Andrew Cornett
Dr. Ronald Townsend

In partial fulfillment of the requirements for the degree of
Master of Applied Science in Civil Engineering

Department of Civil Engineering
University of Ottawa
July, 2008

Ottawa, Canada

Your file Votre référence
ISBN: 978-0-494-48434-0
Our file Notre référence
ISBN: 978-0-494-48434-0

ACKNOWLEDGMENTS

I would first like to thank my parents for their endless encouragement and support.

I sincerely thank my supervisor, Dr. Ioan Nistor, for introducing me to the world of coastal engineering, and for his guidance throughout my studies. I would like to thank my co-supervisor, Dr. Andrew Cornett, for allowing me to conduct my project at the Canadian Hydraulics Centre, the National Research Council (NRC) in Ottawa, and for directing me throughout the thesis project. I would also like to thank my other co-supervisor, Dr. Ronald Townsend, for his valuable comments on the thesis manuscript.

Many thanks to the technical staff at Canadian Hydraulics Centre for making my experimental work possible, especially to Daniel Pelletier and Jean-Pierre Des Becquets.

I would like to thank Nima Aghniaey, Antoine Cousin and Bertrand Oisseuil, undergraduate volunteer students for their help with the physical model construction and various test runs.

Many thanks to Scott Baker, Kirsten Uttley, Vigdís Harðardóttir, Steinunn Björnsdóttir and Elizabeth Jamieson and to all other friends at the University of Ottawa.

The memorial fund of Margrét Björgólfsdóttir and NSERC receive my many thanks for their financial support.

ABSTRACT

Gravel beaches are widespread around the North-Atlantic Ocean shorelines and can also be found along the coastlines of New Zealand, Russia and the Pacific shore of USA. Over the past decades, researchers in coastal morphodynamics have placed their emphasis on studying sand beaches but gravel material is being used more frequently to nourish eroding sand beaches.

The present thesis aims to advance the understanding of the behaviour of gravel beaches under wave attack. A two-dimensional physical model was developed for gravel beach applications. Regular and irregular waves were considered as well as two different initial beach slopes.

An extensive analysis was performed on the time history of the waves, beach morphology, wave reflection and energy dissipation. Additional geotechnical analysis was also performed in order to identify the characteristics of the beach material. Wave height, wave period, wave duration and initial beach slope were all found to influence beach deformation and wave reflection pattern.

TABLE OF CONTENTS

LIST OF TABLES

LIST OF FIGURES

LIST OF SYMBOLS

Symbol	Description
C_{Ew}	Energy damping coefficient [-]
C_r	Average reflection coefficient [-]
C_u	Uniformity coefficient [-]
$C_{u,av}$	Average uniformity coefficient [-]
C_z	Gradation coefficient [-]
$C_{z,av}$	Average gradation coefficient [-]
d	Water depth [m]
d_b	Water depth at wave breaking point [m]
d_t	Water depth at beach toe [m]
D_{10}	Grain size diameter corresponding to 10% finer [mm]
D_{30}	Grain size diameter corresponding to 30% finer [mm]
D_{50}	Median grain size diameter [mm]
D_{60}	Grain size diameter corresponding to 60% finer [mm]
D_{90}	Grain size diameter corresponding to 90% finer [mm]
D_{n50}	Nominal grain size diameter [mm]
e	Void ratio [-]
E_w	Wave energy density [J/m^2]
$E_{w,offshore}$	Average wave energy density at offshore location [J/m^2]
f_p	Peak frequency [Hz]
g	Acceleration due to gravity [m/s^2]
G_s	Specific gravity [-]
$G_{s,av}$	Average specific gravity [-]
h	Height of beach structure [m]
H	Wave height [m]
H_{av}	Average wave height [m]
H_{max}	Maximum wave height [m]
H_{m0}	Significant wave height estimate (4 times the spectrum of the zeroth spectral moment [m]
H_s	Significant wave height [m]
K	K-factor [-]
L	Wave length [m]
M_{50}	Median mass of unit given by 50% on mass distribution curve [kg]
M_s	Mass of soil [kg]

m_0	Initial beach slope [-]
N_w	Number of waves [-]
n	Porosity [-]
P	Rod length [m]
P	Van der Meer's (1988) permeability coefficient [-]
q_x	Sediment transport rate [m^3/s/m]
r	Correlation coefficient [-]
r^2	Coefficient of determination [-]
R	Horizontal position of the axis of rotation of the profiling rod [m]
t	Time [s]
T	Temperature [°C]
T	Wave period [s]
T_{av}	Average wave period [s]
T_p	Peak wave period [s]
V_s	Volume of soil [m^3]
W_1	Mass of flask + water filled to mark [g]
W_2	Mass of flask + soil + water filled to mark [g]
W_s	Mass of dry soil [g]
W_w	Mass of equal volume of water as the soil solids, $W_w = W_1 + W_2 - W_s$ [g]
x	Horizontal cross-shore coordinate [m], x = 0 at north end of flume
y	Horizontal across the flume coordinate [m], y = 0 at east end of flume
z	Vertical coordinate, positive upwards [m], z = 0 at water level (where d = 0.6 m)
z_{wall}	Vertical coordinate, measured manually at the wall of the flume [m]
$\square$	Angle of beach slope [rad]
$\square h$	Change in height of beach structure [m]
$\square h_{max}$	Positive maximum change in height of beach structure (maximum accretion) [m]
$\square h_{min}$	Negative maximum change in height of beach structure (maximum erosion) [m]
$\square q_x$	Change in sediment transport rate [m^3/s/m]
$\square t$	Change in time step [-]
$\square x$	Change in horizontal cross-shore coordinate [m]
$\square_d$	Specific weight of dry soil [N/m^3]
$\square_w$	Specific weight of water [N/m^3]
$\square_c$	Wave crest height [m]
$\square_t$	Wave trough height [m]
$\square(t)$	Sea surface elevation [m]

$\square_i(t)$	Sea surface elevation of incident wave train [m]
$\square_r(t)$	Sea surface elevation of reflected wave train [m]
$\square$	Angle between the profiling beam and the rod [rad]
$\square$	Surf similarity parameter, Iribarren number [-]
$\square_o$	Surf similarity parameter, Iribarren number for regular waves [-]
$\square_p$	Surf similarity parameter, Iribarren number for irregular waves [-]
$\square_{VdM}$	Surf similarity parameter, Iribarren number for equation of Van der Meer (1993) [-]
$\square$	PI constant [3.14159…]
$\square_d$	Density of dry soil [kg/m^3]
$\square_w$	Density of water [kg/m^3]
$\square$	Standard deviation of the zeroth spectral moment [-]
$\square_i$	Standard deviation of the incident wave train [-]
$\square_r$	Standard deviation of the reflected wave train [-]
$\square$	Bed shear stress [N/m^2]
$\square_{cr}$	Critical bed shear stress [N/m^2]

LIST OF ABBREVIATIONS

Abbreviation	Description
AWA	Active Wave Absorption
CHC	Canadian Hydraulics Centre
FFT	Fast Fourier Transform
JONSWAP	JOint North Sea Wave Analysis Project
NRC	National Research Council of Canada
NDAC	(Windows) Nt Data Acquisition and Control
PT	Pressure Transducer
SWL	Still Water Level
WG	Wave Gauge

1 INTRODUCTION

For the most part, researchers in coastal morphodynamics have placed their emphasis on sand beaches (e.g. McKay and Terich, 1992). However, gravel beaches are widespread on the coastlines of the North Atlantic Ocean, especially in the United Kingdom, Ireland, Iceland, Canada, USA, and also on the coastlines of Japan, New Zealand, Russia and Latin America (Buscombe and Masselink, 2006). Studies on gravel beaches are prominent in Great Britain where one third of the coastline consists of gravel material. Many of the field studies mentioned in this thesis have been carried out in the south part of Great Britain.

Similar to sand beaches around the world, gravel beaches also experience erosion. However, gravel beaches are more stable. Coarse material is being used more and more to nourish eroding sand beaches (McFarland *et al.*, 1994; Whitcombe, 1996; Buscombe and Masselink, 2006; Cammelli et al., 2006; Horn and Li, 2006 and Ibrahim *et al.*, 2006). To do so with satisfactory results, it is important to understand the behaviour of gravel beaches under wave attack. Unexpected difficulties have surfaced in gravel material replenishment projects due to lack of understanding of the mechanisms of gravel beach formation, e.g. where finer grains fill up the voids inside gravel replenished beach (Cammelli *et al.*, 2006). Experimental work on gravel beaches is scarce. Due to lack of data, there is a gap in the validation of numerical models describing gravel beach behaviour (San Román-Blanco *et al.*, 2006).

Gravel beaches are one of the most effective types of natural sea defences. The current philosophy is to use soft engineering techniques where appropriate (van Wellen *et al.*, 2000). Replenishment of gravel beaches has less negative environmental impact than some other 'harder' methods such as seawalls, breakwaters or rock, or wooden groynes. Gravel beaches are also capable of dissipating up to 90% of incident wave energy (Powell, 1990, Buscombe and Masselink, 2006).

1.1 Significance and Novelty of the Study

Experimental work on gravel beaches is scarce, so obtaining or generating new data sets is essential for improving our understanding of morphodynamic behaviour of such beaches. A new approach in gravel beach instrumentation was employed in this study where pressure transducers were buried inside the beach and wave gauges were placed at the same locations. New equations were derived in order to describe the relationship between the beach berm development and the wave duration, as well as between the beach trough generation and the wave duration. An extensive analysis of the wave reflection from gravel beaches is performed.

1.2 Objective of the Study

The aim of this study is to generate a large-scale experimental data set in order to improve the understanding of gravel beach behaviour under wave attack. In carefully prepared laboratory experiments it is possible to control better the wave characteristics and the general experimental conditions ensuring better accuracy than experimental data collected in the field. This is particularly advantageous for the development of numerical models. The principal objective of the performed data analysis is to explain the interaction between the wave climate and the behaviour of the gravel beach.

1.3 Scope of the Study

Due to various physical limitations of the available laboratory facilities and other complexities, the physical model used in this project excludes some aspects found in nature. The model is two-dimensional and waves can only be generated perpendicular to the beach face. No currents are involved so that the longshore sediment transport does not occur. The groundwater level is assumed to be the same as the still water level and does not vary. Since the still water level is kept constant throughout the experiment, tidal variations are excluded.

The experiments have been conducted with gravel in a flume where wave heights and wave periods are smaller than ones typically occurring in natural conditions. However, since scale effects are thought to be small, the experimental results are indicative of the behaviour of real gravel beaches in nature.

1.4 Thesis Outline

This thesis is organized into nine main chapters. The organization of the thesis is as follows:

Chapter 1 describes the significance and novelty of the study, explains the object and scope of the research, and describes the general framework of the thesis.

Chapter 2 reviews earlier studies on the subject and presents the state-of-the-art on the studies dealing with the interaction between gravel beach and the wave climate.

Chapter 3 describes the research project in general and the physical model design and construction.

Chapter 4 describes the experimental setup and instrumentation used in these experiments.

Chapter 5 presents the results of the data analysis; the results of the geotechnical analysis, aspects related to the wave climate, beach deformation, the interaction between the beach and the waves, and wave reflection and energy dissipation within the beach inner face.

Chapter 6 includes a discussion of the main findings.

Chapter 7 presents the conclusions of the study.

Chapter 8 gives recommendations for future works on the subject.

Chapter 9 lists the references consulted in the study.

2 LITERATURE REVIEW

2.1 Laboratory Experiments on Gravel Beaches

Sleath (1978) conducted an experiment on sediment transport in an oscillatory tray. Tests with gravel (D_{50} = 4.24 mm), sand (D_{50} = 1.89 mm) and nylon pellets (D_{50} = 3.04 mm) were carried out (D_{50} denotes the median grain size diameter of the particles). The bedload transport rate was measured at each instant of a wave cycle while other researchers had measured the amount of bedload sediment moved after several wave cycles over a flat bed. Sleath concluded that if any transport would occur at all, it would occur over almost the entire half cycle. For sand and gravel, the variation of sediment transport rate with time was quite well represented with regression analysis. For nylon pellets, results scattered with less agreement to the regression line of sand and gravel. The reason could have been the light weight of the pellets, since their specific gravity was 1.138.

Vincent *et al.* (1981) conducted experiments in oscillating trays, where the bed material deposited in the trays was interpreted as a measure of the concentration of material in suspension. After the bed had gained speed and the critical bed shear stress (τ_{cr}) had been exceeded, the number of grains in suspension became a function of the difference between the bed shear stress and the critical bed shear stress; (τ - τ_{cr}). Under critical conditions, the tray would trap any material that had been lifted into suspension. The height of suspension was considered less than 1 cm for bedload transport conditions.

Van Hijum and Pilarczyk (1982) summarized the results of investigations on gravel beaches performed in Delft Hydraulics Laboratory, the Netherlands from 1969 to 1980. It was concluded that sediment transport was a function of the angle between the wave crest and depth contours, grain size diameter, wave height, wave period, beach slope and longshore current. It was stated that the distance over which the grains were carried increased as the diameter of the grains decreased. The authors developed a method describing the optimal initial beach profile. A relationship of the dependant variables was presented. It was stated that an optimal initial beach profile, for beach material with D_{50} = 2 mm, was between 1:5 and 1:20. Van Hijum and Pilarczyk (1982) found no scale effects in a small scale investigation if D_{90}, that is grain size diameter corresponding to 90% finer, was larger than 4 to 6 mm.

Van der Meer (1988) performed laboratory experiments on gravel beaches and rock slopes in a 50 m long wave flume at Delft Hydraulics Laboratory, the Netherlands. Some tests were repeated in a larger flume, (230 m long, 5 m wide and 7 m deep) to evaluate scale effects. Van der Meer also analysed the van Hijum and Pilarczyk (1982) data. Nominal grain size diameter (grain size diameter related to the average mass of the material, $D_{n50} = (M_{50}/\rho_d)^{1/3}$, where M_{50} is the median mass of the unit and ρ_d is the mass density of the rock (Van der Meer, 1993)) varied from 4 to 27.2 mm. Five different spectra for irregular waves were investigated. Several beach slopes were considered; from 1:1.5 to 1:10. Van der Meer (1988) investigated beach profiles of different grain size, grading of the material, wave height, wave period, number of waves, initial slope, shape of the stones, spectral shape, water depth and angle of wave attack. Wave height and wave period were found to have a large influence on profiles. Longer wave periods resulted in longer profiles. Spectral shape had no or only minor influence on the profile (comparison between Pierson Moskowitz spectrum and narrow spectrum). A large part of the profile changes were found to occur within the first few hundreds of waves. Storm duration highly influenced the development of the berm; longer period of wave attack increased the berm height. Comparison studies showed that the shape of the material (rounded, angular, flat/long) had no or only a minor influence on profile changes. A wider grading of the material was found to make a difference below the still water level but had no influence above it. Comparison between initial beach slopes of 1:3 and 1:5 showed that the same profile was reached between the berm and a step below the still water level if boundary conditions were kept the same. Tidal effects were investigated and showed that lowering the water level changed the developed profile significantly and when the water level was raised again, the profile became almost the same again.

Powell (1990) carried out a physical experiment in a wave flume at Hydraulics Research, Wallingford, UK. The flume was 42 m long, 1.5 m wide and 1.4 m deep. Four different gravel material mixes were considered for the experiment, where D_{50} varied from 10 to 30 mm. The overall beach slope was 1:7. The experiments were conducted at a model scale of 1:17. All tests were conducted with irregular waves of JONSWAP spectrum and model water depth was 0.8 m. It was concluded that wave height, wave period, beach material size and angle of wave attack were the principal variables influencing beach profile changes. The beach profiles changed rapidly due to wave attack, 80% of the volumetric change occurred within first the 500 waves. No dependency was found between wave energy dissipation and beach material size. It was stated that gravel beaches are one of the most effective natural sea defences as they are capable of dissipating more than 90% of the wave energy.

Shimizu and Kawata (1997) investigated beach profile changes in a large scale experiment conducted at the Central Research Institute of Electric Power Industry in Japan. The flume was 200 m long, 6 m deep, allowing 4 m of water depth. Cross-shore profile changes due to irregular (JONSWAP) waves were measured. The initial beach slope was 1:30 and the median diameter of the sand particles in the beach was D_{50} = 1 mm. In order to measure wave height, currents, run-up and turbidity, several wave gauges, electromagnetic current meters, a run-up gauge and a sand surface profiler were installed. The beach profile changed and a bar developed as the number of waves increased. It was also noticed that the bar accumulated slightly onshore of the point where significant wave height was observed to reach a maximum value.

Ünal *et al.* (1998) investigated experimentally the effect of coarse sediment and wave characteristics on incipient motion. The beach slope was either 1:6.7 or 1:5. They found that the threshold motion depth of gravel particles (D_{50} = 8.5, 10.5 and 13.5 mm) on a slope under wave attack (plunging waves) increased with increasing wave height, wave period and beach slope and decreased as the particle size increased. They introduced regression equations which can be used to predict the erosion area on a straight gravel slope under wave attack.

San Román-Blanco *et al.* (2006) conducted a large scale experiment on profile changes of gravel beaches. The experiment was conducted in a large wave channel in Hanover, Germany in 2002. The flume was 309 m long, 5 m wide and 7 m deep. The initial slope of the beach was 1:8. The experiments were run at full scale so scaling uncertainties could be avoided. The significant wave height was 0.6 m, peak wave period was 3.22 s, wave steepness 0.05 and the irregular waves where synthesized from a JONSWAP spectrum. The material grain size was distributed between 16 – 32 mm, having a mean diameter of D_{50} = 21 mm. The porosity of the beach was approximately 0.44. Twenty five wave gauges were placed along the flume, 24 pressure transducers were deployed in the beach and 3 Acoustic Doppler Velocimeters (ADVs) and a hydrophone were used. Wave run-up was recorded with a video camera. This experiment was run both for a gravel beach and a mixed sand and gravel beach. The D_{50} of the gravel was 21 mm and the D_{50} of the sand was 0.3 mm. In the case of the mixed beach, the sediment mixture was 30% sand and 70% gravel. San Román-Blanco *et al.* (2006) do not present the results and analysis of their study. Pedrozo-Acuña *et al.* (2006) have used results from this experiment to develop a numerical model to reproduce the morphological changes of the beach under wave attack.

Ibrahim *et al.* (2006) investigated gravel beach morphodynamics with field measurements at Slapton Sands, England and compared the data to the laboratory results gathered in a large wave flume experiment conducted in Hanover during 2002 (San Román-Blanco *et al.*, 2006). In the laboratory model, the beach reached dynamic equilibrium after 2000-3000 wave impacts but in the field at Slapton Sands, the beach never reached a state of equilibrium. During ebb tide, the beach at Slapton Sands exhibited a similar pattern of erosion and accretion to the modelled beach, where accretion generally occurred above the still water level and erosion just seaward of it. All field data represented highly reflective conditions. They stated that the sub-surface hydrodynamics played the key role in the beach morphodynamics over a tidal cycle.

Lee *et al.* (2007) conducted an experiment in a 30 m long wave flume at Nagoya University, Japan. A gravel beach with slope 1:7 and D_{50} = 5 mm was built inside the flume. The flume was capable of changing the groundwater level so it could be different to the water level in front of the beach. It was stated that groundwater does not always follow tidal variations. The difference between the seawater and groundwater levels might cause changes in the volume of infiltration and exfiltration through the beach material. Under average wave conditions, changes in groundwater level did not affect the beach profile changes. However for storm wave conditions, changes in the beach profile were observed. With a decreasing groundwater level, the berm formed at the upper part of the shoreline moved onshore and 'up the beach'. Similarly, for a rising groundwater level, the berm moved seaward. The beach slope below the mean water level was found to be less steep when the ground water level was higher. It was observed that the greatest part of the erosion happened in the vicinity of the wave breaking point.

2.2 Field Experiments on Gravel Beaches

Kirk (1975) carried out a field experiment at a mixed sand and gravel beach in Kaikoura, New Zealand. The aim of the experiment was to investigate the surf and run-up processes at a beach which had a slope of 1:4.8 - 1:11 and grain size varying from 0.25 to 16 mm. Kirk stated that the wave breaking height was the primary control of swash length. Run-up velocities were found to be 20% higher than the backwash velocities. Kirk mentioned that a number of attempts had been made to predict numerically beach processes and responses. However, all such studies were rather weak, both in quality and quantity.

Kirk (1980) gave a general overview of morphology processes and sediments on mixed sand and gravel beaches as they occurred in New Zealand. Beach widths were commonly 100 to 200 m and average elevations above mean sea level were 4 to 6 m. Profiles contained 150 to 250 m^3 of sediment per meter of shoreline. Annual variations were typically of the order of 50 m^3/m. Long-term rates of erosion were found to be 0.5 to 5.5 m per year. Beach cusps were common in mixed sand and gravel beach faces as well as particle segregation, where larger particles were found on the beach berms and smaller particles closer to the sea level.

Caldwell and Williams (1985) conducted field measurements on two beaches at Glamorgan Heritage Coast in Wales in November 1977. Grain size varied from 4 to 256 mm. In total, 180 beach profiles were investigated. The authors' goal was to come up with a classification scheme for gravel beach deformation. They attempted to categorize gravel beaches by the trigonometric shape of their profiles and the location of the berm. They classified beach profiles as concave or linear and further if they presented berms and of what kind: high, low, composite or not present. Concave shape was more commonly observed than the linear shape. They stated that it was difficult to draw any general conclusions on beach morphology from beach profile changes. Beach characteristics could differ significantly within the same coastline.

Sherman (1991) conducted a field experiment at two sites in Malin Head, County Donegal, Ireland, in 1987. At Pebble Strand, (a 100 m long beach), the average beach slope was 1:5.1. Particle sizes ranged from 5 to 200 mm, decreasing downslope. Daily beach profile measurements were collected at 5 m intervals. The other site, Slievebane Beach was 300 m long and with a gentle slope of 1 to 3°. Particle sizes ranged from 4 to 64 mm, also decreasing downslope. A pressure transducer, located 1 km offshore, recorded wave height and wave period. Waves were recorded for 15 minutes every 3 hours. At Pebble Strand, foreshore accretion took place through the time series. At Slievebane Beach, this process did not occur, but a swash bar developed at the foot of the foreshore. It was stated that erosion and accretion of the gravel foreshores were controlled by wave steepness. Sherman (1991) stated that gravel beaches were to be commonly found in latitudes above 40° where shorelines were not ice-bound, but occurred less frequently at lower latitudes.

McKay and Terich (1992) described the morphology and development processes at gravel barriers along the Olympic National Seashore in the state of Washington, USA. Grain size at the site varied from 0.2 to 42 mm. They concluded that the following factors influenced the development of gravel barriers: source and volume of coarse-grained sediment, shoreline configuration and positions of headlands, storm wave conditions and changes in relative sea level. They stated that the barriers along the Olympic Coast displayed many similar characteristics to those found in other parts of the world's coastlines. Nearly all of the surveyed profiles displayed similar profile developments as those found at Malin Head, Ireland (Sherman, 1991).

McFarland *et al.* (1994) presented the results of a gravel beach replenishment project in Whitstable, South-East England. The project, where gravel material was brought from the Thames Estuary to the Whitstable frontage, took place in 1988 – 1989. The grain size diameter of the material was around 9 mm and the material was well sorted. The material used in the nourishment was found to have much greater density than expected and greater than the one found in natural gravel beaches. The formation of a series of 'cliff-like' scarps along the upper part of the beach was also unexpected. This caused the recharged beach to act as a reflective barrier to waves and increased erosion and undercutting along the lower parts of the beach. Further studies would be needed to alleviate these adverse effects, caused by the use of dredged material from offshore, and to better understand the mechanisms governing the development of the formation.

Whitcombe (1996) assessed a beach renourishment project in Hayling Island at the south coast of England. It was stated that little is known on the post-replenishment behaviour of many artificially nourished beaches. The beach at Hayling Island was nourished in 1985, where approximately 530,000 m^3 of shingle material was dredged from offshore and imported to the frontage of around 2 km of the beach. The grain size diameter of the material was around 11 mm and the material was well sorted (McFarland *et al.*, 1994). The berm of the beach was raised by around 5.6 m and the width of the beach was extended by around 30 m. Whitcombe (1996) noticed that an artificial nourished gravel beach might not necessarily exhibit the same characteristics as a natural gravel beach. An artificial beach would be more compact and therefore lack the permeability observed in natural gravel beaches. Some other unknown factors might also be involved. Artificial gravel beaches might also not respond to wave attack in the same way as natural gravel beaches. Observed changes in beach profiles of the nourished beach at Hayling Island suggested that the gravel material was being transported along the shoreline at a relatively constant rate.

Jennings and Shulmeister (2002) suggested a classification scheme for gravel beaches. A field study was undertaken in New Zealand where 42 beaches were investigated. At each site, information on following parameters was collected; beach width, beach slope, storm berm height, number of berms, grain size and local wave climate. They classified gravel beaches into three categories; pure gravel beaches, mixed sand and gravel beaches and composite gravel beaches. The pure gravel beach had linear beach slope, minor berms and strong sediment sorting. Mixed sand and gravel beaches consisted of entirely intermixed sand and gravel particles throughout the beach profiles. In composite gravel beaches, the sand and gravel particles were segregated in the cross-shore direction. Beach face slope was the highest for pure gravel beaches (average value 1:5.6), while the average value for mixed sand and gravel beaches was found to be 1:10 and for composite gravel beaches 1:12.5. The particles in the composite gravel beaches were uniform and with a D_{50} value of around 32 mm. The pure gravel and mixed sand and gravel beaches were non-uniform in sediment sorting, having average grain size of 18.5 mm and 15.2 mm, respectively. The classification scheme took into account beach width, storm berm height, number of berms, active profile slope, average grain size and Iribarren number (Battjes, 1974). It was stated that the model correctly classified 86% of the pure gravel beaches, 92% of the mixed sand and gravel beaches and 91% of the composite gravel beaches.

Conley and Griffin (2004) measured bed stress in the swash zone on Barret Beach, Fire Island, New York, by flush mounted hot film anemometry. They stated that the peak uprush stress was twice the magnitude of the peak backwash stress. The duration of backwash was found to be 35% longer than of the uprush. The friction factor, which is dependent on velocity, was found to be higher for uprush than for backwash.

Austin and Masselink (2006) conducted a field survey at Slapton Sands, on the south coast of England to investigate short-term morphodynamic processes on a gravel beach. The measurements, conducted over 24 tide cycles, were carried out in October 2004. During the tests, the beach profile was surveyed at each low-tide with a total station. Water level changes were measured with pressure transducers and a tide gauge was located approximately 30 km from the coastline. Deep-water wave height and period were measured every hour by an offshore wave station, 40 km away from the coastline. Uprush and backwash sediment transport loads were measured using total load traps. Beach slope was 1:6.7, specified as steep and reflective. Grain size diameter was 6 mm. Beach morphology was found to be directly related to shoreline elevation and characterized by high tide and storm berms. The intertidal beach face was steepened by onshore sediment transport during flood tide and flattened by offshore sediment transport during the ebb. Sediment was also observed being transported by the swash, which is also the case on sand beaches. The author of this thesis has been provided with the whole data set from Slapton Sands from October 16th to October 28th 2004.

Cammelli *et al.* (2006) assessed the performance of gravel material for beach nourishment at Marina di Pisa in Italy. Around 93 m^3 of river-washed material of 40 to 200 mm in diameter was placed per meter of beach on a 330 m long coastline. Material was dumped seaward of an old seawall and groins were built within the study area to avoid losing sediment along the shore. Prior to the construction of the nourished beach, there was a trough in the beach profile just seaward of the seawall. After construction, the trough had been filled and stayed so 15 months after the nourishment. Deepening in the beach profile was observed in some places, but it was uncertain if that happened due to bar migration or wave reflection at the base of the gravel beach. About 40 to 50 m from the shore, changes were found at different times in many of the profiles. These changes might be caused by wave reflection at the base of the foreshore, or possibly due to increment in backwash velocity associated with the reduced permeability observed in the beach caused by sand infiltration into the gravel beach. Sand moved onshore and infiltrated into the gravel beach. The sand filled the voids in the gravel beach so the sand sediment basically got lost inside the beach as the sediment transport did not increase the overall size of the beach. This kind of sand sediment transport could be considered as a temporary loss in the coastal sediment budget. It also changed the permeability of the beach and its responsiveness to waves and swash. The nourishment at Marina di Pisa was successful; the beach became usable for tourist activity and the road close to the seawall did not have to be closed during storms.

2.3 Numerical Studies of Gravel Beaches Morphodynamics under Waves

Lorang (2002) derived two empirical equations to predict the berm height of a gravel beach. The first derivation compared the wave forces acting to move material up the beach face with a weight force acting to hold the material in place. The other derivation compared the potential energy of the beach berm to the total wave energy that transported material above a given water level. Required data for the equations were wave height, wave period, average highest high tide, grain size diameter, beach slope and the average mass per area of the beach berm. The equations were validated with data from a gravel beach located on the Oregon Coast, USA. Both equations were found to predict the berm height with good accuracy for this one data set. Further field testing is however necessary to accept their validity in berm height elevation prediction.

Soulsby and Damgaard (2005) derived formulas for bedload sediment transport in coastal waters. Formulas were classified by the driving forces of the transport; currents, currents with symmetrical waves and currents with asymmetrical waves. The formulas were validated with field and laboratory data with satisfying results. Some data, however, only included sand with grain size diameter of 0.2 – 1 mm. It was stated that for gravel beaches, the grains are too coarse to form ripples. A formula for longshore sediment transport in gravel beaches was also derived and tested with satisfying results against field and laboratory data, primarily from van Hijum and Pilarczyk (1982).

Horn and Li (2006) collected field data at Slapton Sands, UK. The beach slope was 1:5.9 and the beach consisted of relatively uniform material with D_{50} = 9 mm. Swash velocities were measured with three Acoustic Doppler Velocimeters (ADVs), eight pressure transducers measured pressure at the surface of the beach and a total of six pressure transducers were buried inside the beach to measure the subsurface pore water pressures. The field data were analysed by comparison with simulations using the BeachWin model. BeachWin simulated the interacting wave motion, beach groundwater flow and sediment transport in the swash zone and a part of the surf zone. The simulations indicated that swash infiltration is an important factor in gravel beach profile response to waves. The predictions of the model are sensitive to the values of hydraulic conductivity, friction factor and the ratio between uprush and backwash sediment transport rates. It was stated that these parameters are likely to play important roles in profile changes in gravel beaches. Due to lack of data on gravel beach behaviour, the value ranges of these parameters were stated to be unknown.

Hsu *et al.* (2006) developed a model for a new shape function for bar-type beach profiles and compared it to various field data from Da Pong Bay in Taiwan. The new shape function was based on an exponential function and a hyperbolic function to cover both the slope of the beach and the prominent bar-type profile. The bottom material was described as "gravelly sand". Their model was unique for that no separation of the beach profile was required, that is, the model is applicable to the whole profile of berm, trough and nearshore zone. The comparison with field data gave good results. Over one hundred sections were examined and the average best-fit results gave the correlation of 0.99.

Lee *et al.* (2007) investigated the wave field in the swash zone and the surf zone numerically with the numerical model wave tank (NWT). A gravel beach, with slope 1:7 and D_{50} = 5 mm, was built inside a numerical wave flume. Computed results showed exfiltration flowing out of the gravel beach throughout the runup and the rundown processes. The groundwater level was controlled and differed from the relative mean water level. This is contrary to the findings of Masselink and Hughes (1998), who stated that infiltration took place during runup and exfiltration during rundown.

2.4 Discussion

The review of the existing literature indicates that the interest in the behaviour of gravel beaches is increasing. Numerous researchers pointed out that the emphasis has been on sand beaches and coarser sediment beaches received less interest. However, this is changing due to a significant increase in the economic and human development in coastal areas where gravel beaches are present. During the past 10 years, experimental projects have been carried out, both in the field and in laboratories. Large wave flumes such as the ones in Hanover, Germany (San Román-Blanco *et al.*, 2006) and Japan (Shimizu and Kawata, 1997) are essential tools. Field measurements are also giving a new perspective on the behaviour of gravel beaches. Researchers agree on some fundamental topics concerning gravel beaches. Gravel beaches are more stable than sand beaches and offer many advantages for local coastal protection. From an environmental point of view, soft construction of a coarse beach may be preferable to other alternatives such as seawalls, groynes and breakwaters. Replenished gravel beaches were shown to improve recreational opportunities (Cammelli *et al.*, 2006).

The laboratory experiments proved that gravel beach profile changes are found to be dependent on the wave height, wave period, beach material size and angle of wave attack (Van der Meer, 1988 and Powell, 1990). From field investigations, it was shown that currents, tidal variations, storm duration, and groundwater level also make it to the list of important factors (e.g. Lee *et al.*, 2007). A significant gap remains as it would be essential to conduct three-dimensional laboratory experiments on gravel beach and include also currents, longshore sediment transport and tidal effects. Only information on two-dimensional experimental work was found in the literature except for three-dimensional experiments carried out in 1974 and 1980 (van Hijum and Pilarczyk, 1982). However, these references are not available in English. Van Hijum and Pilarczyk (1982) showed that tests of regular and irregular waves under oblique wave attack were run in three dimensional conditions in 1974 and 1980, and the amount of transverse and longshore sediment transport was determined.

Relatively few numerical models have been developed to predict the response of gravel beaches to waves. New laboratory and field data sets, covering a broader range of conditions, are required to help advance our knowledge of the response of gravel beaches to waves.

3 General Project Description

The present experimental program was carried out in a steel and glass flume at the Canadian Hydraulics Centre (CHC) which is part of the National Research Council of Canada (NRC) in Ottawa, Canada. The experimental test series were designed and conducted between July and December 2007. A beach mound was built inside the wave flume and before construction started, significant conceptual design matters had to be carefully considered.

3.1 Geotechnical Characteristics of the Gravel Material

Some of the first parameters of the project to be decided upon were the grain size of the material and the slope of the beach. The literature review offered significant insight on the experimental work of gravel beaches and the properties of the gravel material. This helped determine the sediment grain size and beach slopes found in nature. Sediment particles are often classified according to their diameter. Gravel beaches consist of coarse sediment where the median grain size, D_{50}, is larger than 2 mm. A classification of coarse sediments is provided in Table 3.1.

Table 3.1 – Coarse sediment classification (Kamphuis, 2000)

Unified soils classification	ASTM mesh	Size [mm]	Wentworth classification
Cobble		256.0	Boulder
Coarse gravel		76.0	Cobble
		64.0	
		19.0	Pebble
Fine gravel	4	4.76	
Coarse sand	5	4.0	
	10	2.0	Gravel

Table 3.2 contains a summary of various field experiments performed on the morphodynamics of gravel beaches. The table is adapted from Jennings and Shulmeister (2002), but is edited and enhanced by the author with more recent information.

Table 3.2 – Experimental field measurements performed on gravel beaches

Author	D_{50} [mm]	Beach slope	Location
Buscombe (2007)	0.98 - 6.53	1:5:9 - 1:7.1	Southwest England, UK
Austin and Masselink (2006)	6	1:6.7	Southwest England, UK
Conley and Griffin (2004)	-	Flat	Barret Beach, Fire Island, NY, US
Lorang (2002)	5.93	1:6.7	Oregon, US
Jennings and Shulmeister (2002)	4 - 64	1:4.2 - 1:12.5	New Zealand
McKay and Terich (1992)	0.2 - 42	1:7 - 1:10	Olympic Nat. Park, WA, US
Sherman (1991)	4 - 64	1:8.2 - 1:11	Malin Head, Ireland
Mason and Hansom (1989)	0.26 - 2.6	1:8.2 - 1:14	Holderness coast, UK
Caldwell and Williams (1985)	4 - 256	1:4 - 1:10	South Wales, UK
Kirk (1975, 1980)	0.25 - 16	1:4.8 - 1:11	Kaikoura, New Zealand
Carr (1971)	pebble or larger	1:6.3	Chesil beach, UK

The beach slope in available field data ranged from 1:4 to 1:12.5. The median grain size diameter, D_{50}, ranged from 0.2 mm to 256 mm. Based on this information, it was decided to consider two different beach slopes for the present study: 1:10 and 1:7. Grain size was chosen to be within the range of 2 mm to 20 mm and gravel availability had to be taken into account as well. Gravel material for the experiment came from Greely Sand and Gravel, Greely, Ontario. Playground stone, uniform river-washed material, was chosen and 4.5 m^3 were purchased. The material was trucked to the Canadian Hydraulics Centre in Ottawa.

As general geotechnical information was not available from the supplier, the precise mean diameter or other geotechnical parameters of the gravel were not known. The supplier quoted the diameter as ranging from 5/16" to 3/8" or 7.9 mm to 9.5 mm. Further details of the gravel properties were determined through testing in the Geotechnical Laboratory of the University of Ottawa, (Chapter 5.1).

3.2 Test Program

The response of a gravel beach to both regular waves (monochromatic waves, constant wave height and wave period) and irregular waves (JONSWAP spectrum) was investigated. Table 3.3 shows the characteristics of the 7 tests performed with regular waves while Table 3.4 shows the characteristics of the 12 tests performed with irregular waves.

Tests 1 to 3, 10 to 12 and 19 involved regular waves, where the wave period was kept constant and runs were conducted using three different wave heights and two different beach slopes. Tests 4 to 9 and 13 to 18 involved irregular waves, where three different wave periods, two different wave heights and two different beach slopes were considered. AWA stands for the Active Wave Absorption system which was used in some tests. Details on the AWA system can be found in Chapter 4.2. Test 19 is a repetition of Test 11, and was performed in order to assess the repeatability of the experimental output. Throughout the experiments, the water depth was kept constant at 0.6 m.

Table 3.3 – Experimental program performed with regular waves

Tests	Slope	AWA?	Target wave period, T_{av} [s]	Average wave period, T_{av} [s]	Target wave height, H_{av} [m]	Average wave height, H_{av} [m]
1	1:10	Yes	2.0	2.0	0.15	0.15
2					0.20	0.19
3					0.25	0.25
10	1:7				0.15	0.15
11					0.20	0.21
12					0.25	0.25
19					0.20	0.18

Table 3.4 – Experimental program performed with irregular waves

Tests	Slope	AWA?	Target wave period, T [s]	Peak wave period, T_p [s]	Target wave height, H_{m0} [m]	Significant wave height, H_s [m]
4	1:10	No	1.5	1.5	0.15	0.13
5			2.0	2.0	0.15	0.14
6			2.5	2.5	0.15	0.14
7			1.5	1.5	0.20	0.17
8			2.0	2.4	0.20	0.18
9			2.5	2.9	0.20	0.19
13	1:7	Yes	1.5	1.5	0.15	0.14
14			2.0	2.0	0.15	0.14
15			2.5	2.5	0.15	0.14
16			1.5	1.5	0.20	0.17
17			2.0	2.2	0.20	0.18
18			2.5	2.5	0.20	0.19

In the case of regular waves, the cross-shore profile of the beach face was measured at eight time intervals, as indicated in Table 3.5. At the beginning of the tests, the profile was measured frequently, since the change was quite rapid initially. Eight beach measurements were performed for each test, and even more in a few cases (3000 waves, 3500 waves, 4000 waves, etc.) to ensure that the beach equilibrium profile was reached.

Table 3.5 – Test sequence for regular waves (Tests 1 – 3, 10 – 12 and 19)

Measurement	Cummulative number of waves
1	50
2	100
3	200
4	400
5	800
6	1500
7	2000
8	2500

For irregular waves, measurements of changes in beach profile were made at time intervals indicated in Table 3.6. An exception was Test 4, where only 7 profile measurements were performed.

Table 3.6 – Test sequence for irregular waves (Tests 4 – 9 and 13 – 18)

Measurement	Cummulative number of waves
1	100
2	300
3	750
4	1000
5	2000
6	3000
7	4000
8	5000

3.3 CHC Wave Flume

The steel and glass flume used in the experimental program in this study at CHC is 63 m long, 1.22 m (4 ft) wide and 1.22 m (4 ft) deep. The maximum wave height that can be generated is approximately 0.35 m, depending on the wave period used. The wave generator has active wave absorption capability. The flume has glass windows in the area where the model beach structure was built. Waves can be generated at both ends of the flume, although only one wave generator was used in the present study.

3.4 Physical Model Design and Construction

The gravel beach profile was constructed inside the flume, in front of the glass windows. Two beach profiles were considered. First, a beach with a slope 1:10 was built. It took three people over four days to construct the initial beach in August 2007. Beach mound height was set at 0.8 m, which corresponded to a beach horizontal length of 8.0 m, from the 'top' to the 'toe' sections. The slope at the back of the gravel beach was set at 1:1.8. After water was pumped into the flume, water penetrated the beach structure and in all tests was present behind the beach mound (see Figure 3.1).

The flume itself was clean but the glass windows needed cleaning. Rust on the glass from previous experiments was removed and the windows were thoroughly cleaned. The initial beach face profiles were marked on the glass windows with a marker in order to ensure the accurate construction of the beach and to make re-profiling between tests easier. The gravel material was brought into the flume using a massive concrete bucket, at a rate of about 0.5 m^3 per round. The filled bucket was lifted by means of a crane to a trolley located on top of the flume that delivered the material close to the construction site. The trolley had a hole in the middle so that the material was easily poured directly to the desired location. Figure 3.1 shows the initial beach in the flume (straight slope, 1:10).

Figure 3.1 – Initial beach profile ready for test (beach slope: 1:10)

4 EXPERIMENTAL SETUP

4.1 Wave Generation and Characteristics

Waves were generated using a computer-controlled wave generator located at the North end of the flume. The generator is equipped with an active wave absorption (AWA) system which was deployed during the majority of the tests. The wave generator is a steel piston that moves back and forth. The wave generator is capable of producing regular and irregular waves. Three options are provided for generating regular waves and, for this experiment, a sinusoidal wave train, with a specified wave height and wave period, was chosen. Other options required maximum wave steepness for either specific wave height or wave period. To generate irregular waves, first a target wave spectrum was selected. The widely used JONSWAP spectrum was chosen for all cases (six other possible spectra are available).

The commands were sent to the wave generator using the NDAC software installed on a computer. In the case of irregular waves, the target spectrum (JONSWAP spectrum) had to be defined. Next steps were the synthesis of an irregular target wave train and the calculation of a drive signal for the wave generator. The drive signal was then loaded onto the NDAC software which commands the wave generator, moving its piston back and forth and generating waves according to the prescribed drive signal. For regular waves, the procedure was similar. However, since there is no target spectrum, only the specified wave height and wave period had to be specified instead (Miles and Pelletier, 2001).

4.2 Active Wave Absorption (AWA) System

The active wave absorption (AWA) system is used where structures, such as the model beach considered in this study, can reflect 20% - 80% of the incident wave amplitude back towards the wave generator. This energy may be re-reflected by the wave generator back towards the structure. This can generate significant inaccuracies, as the incident wave field is modified by the re-reflected waves. To account for this reflection, an array of three wave gauges was deployed close to the wave generator in order to perform a real-time wave reflection analysis. Real-time reflection analysis uses the Fast Fourier Transform (FFT) technique to separate the reflected waves from the structure from the wave train generated by the wave generator. The wave generator reacts by damping the reflected waves to correct the situation (Miles, 1999).

4.3 Instrumentation

Information on changes in water surface elevation, water pressure near and inside the beach structure and morphological changes of the beach due to wave attack was collected using wave gauges, pressure transducers, and a beach profiler. Figure 4.1 shows a schematic of the experimental set-up, excluding the profiler and Figure 4.2 and Figure 4.3 show detailed technical drawings of the experimetal set-up. The numbers at the bottom of Figure 4.2 and Figure 4.3 denote the distance from the wave generator in resting position in meters, whereas the wave generator in located at 0.0 m.

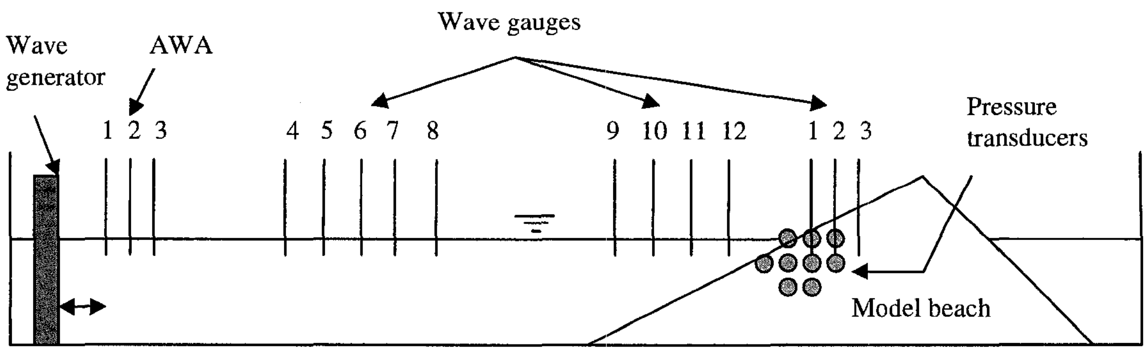

Figure 4.1 – Cross-sectional view of the experimental set-up

In Table 4.1 to Table 4.4, the locations of the wave gauges and pressure transducers are indicated by the coordinate system described in Figure 4.4. The x-coordinate is set as zero at the wave generator (in its resting position) and increases towards the beach structure. The y-coordinate is zero at the East side wall of the flume. The z-coordinate is zero at still water level (which was kept at the same level throughout the experiment) and is positive upwards.

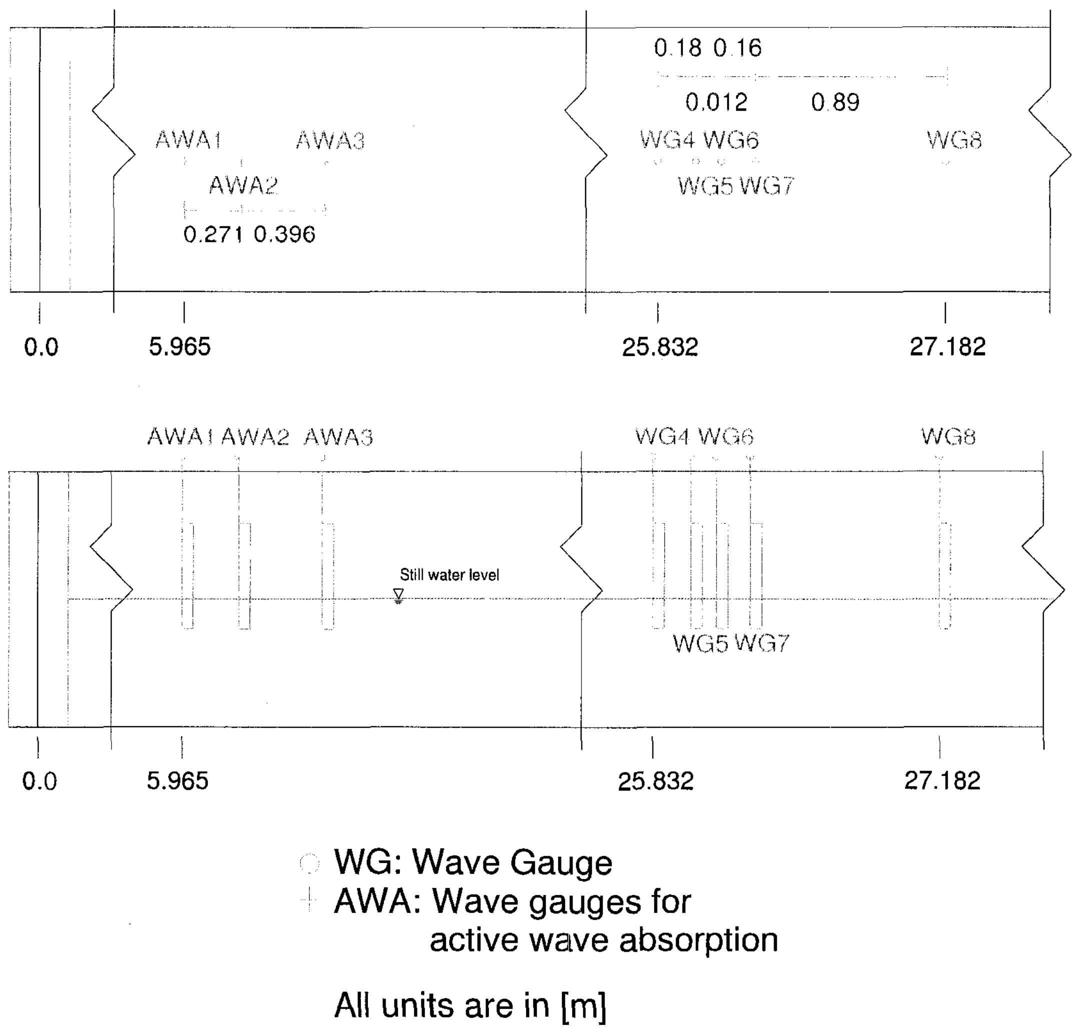

Figure 4.2 – Plan view and cross-sectional view of the flume, near wave generator

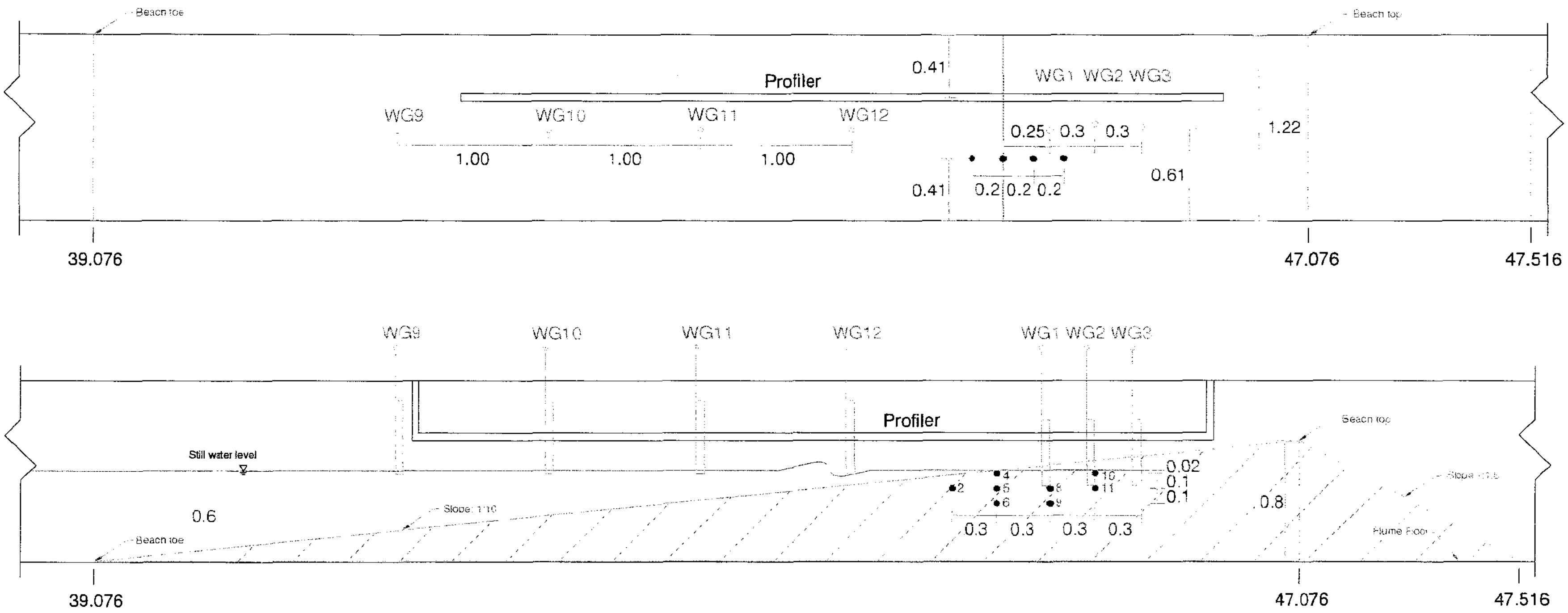

WG: Wave Gauge
● PT: Pressure Transducer

All units are in [m]

Figure 4.3 – Plan view and cross-sectional view of the flume, the beach structure

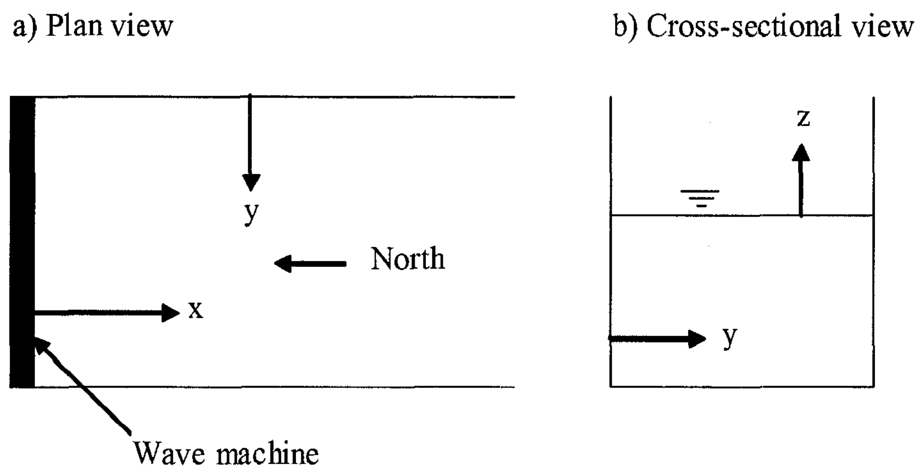

Figure 4.4 – Coordinate system of the flume, a) plan view and b) cross-sectional view

4.3.1 Wave Gauges

The time-history of water elevation was recorded using nine (9) capacitance wave gauges located offshore and in the surf zone. Three additional wave gauges were buried inside the gravel beach in order to measure the fluctuations of the water table inside the beach. Locations of wave gauges, for beach slopes that are 1:10 and 1:7, are listed in Table 4.1 and Table 4.2, respectively. For protection, the buried wave gauges were installed inside perforated Plexiglas tubes, see Figure 4.5. Wave gauges recorded data at the sampling rate of 20 Hz.

Wave gauges AWA1 to AWA3 performed real-time wave reflection analysis and were located close to the wave generator.

Table 4.1 – Location of wave gauges (beach slope 1:10)

Wave gauge	Name	x-location [m]	y-location [m]
1	WG1	45.376	0.61
2	WG2	45.676	0.57
3	WG3	45.976	0.59
4	WG4	25.832	0.61
5	WG5	26.012	0.61
6	WG6	26.132	0.61
7	WG7	26.292	0.61
8	WG8	27.182	0.61
9	WG9	41.076	0.61
10	WG10	42.076	0.59
11	WG11	43.076	0.60
12	WG12	44.076	0.60
27	AWA1	5.965	0.61
28	AWA2	6.236	0.61
29	AWA3	6.632	0.61

After modifying the beach slope from 1:10 to 1:7, WG1 to WG3 and WG9 to WG12 were moved 0.6 m further onshore.

Table 4.2 – Location of wave gauges (beach slope 1:7)

Wave gauge	Name	x-location [m]	y-location [m]
1	WG1	45.976	0.61
2	WG2	46.276	0.57
3	WG3	46.576	0.59
4	WG4	25.832	0.61
5	WG5	26.012	0.61
6	WG6	26.132	0.61
7	WG7	26.292	0.61
8	WG8	27.182	0.61
9	WG9	41.676	0.61
10	WG10	42.676	0.59
11	WG11	43.676	0.60
12	WG12	44.676	0.60
27	AWA1	5.965	0.61
28	AWA2	6.236	0.61
29	AWA3	6.632	0.61

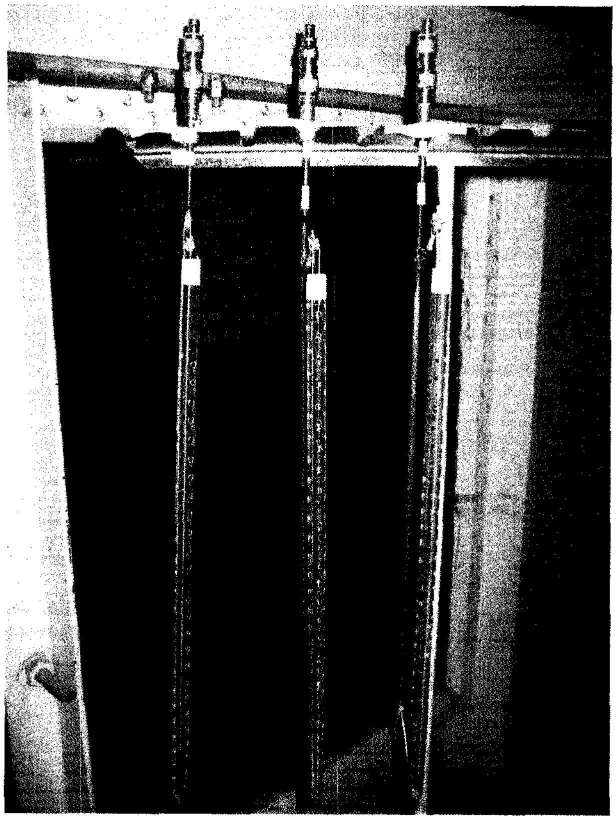

Figure 4.5 – Plexiglas tubes protecting buried wave gauges 1 to 3, prior to installation

Since the spacing between gauges WG1, WG2 and WG3 was of only 30 cm, they could possibly interfere with each other such as WG1 would affect WG2 and WG3, and WG2 would affect WG3. To avoid such situations, WG1 was set as a master wave gauge and WG2 and WG3 were programmed as dependant ("slaves") to WG1. Figure 4.6 shows WG1 to WG3 after installation and after being buried partially into the beach mound.

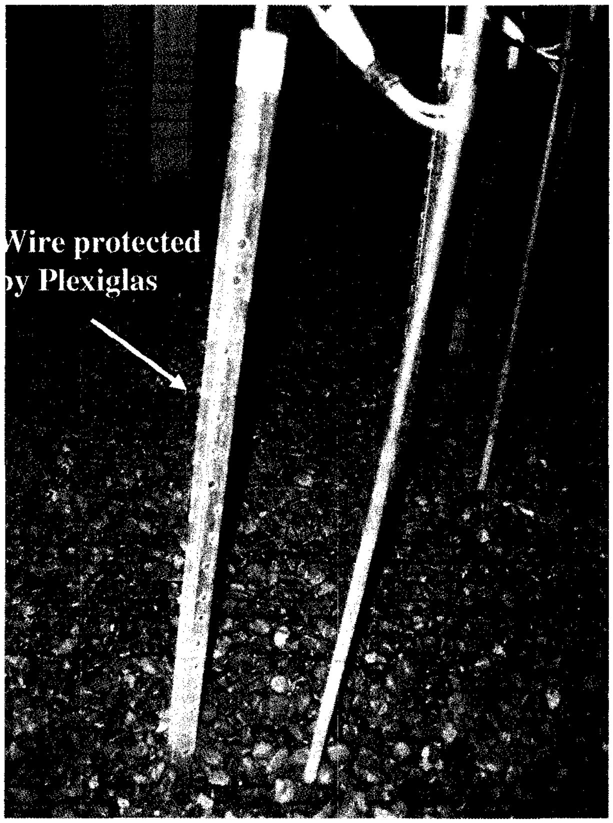

Figure 4.6 – Gauges WG1, WG2 and WG3 after installation (buried)

4.3.2 Pressure Transducers

Nine (9) pressure transducers were buried inside the gravel beach in order to measure water pressure fluctuations inside the porous medium. The transducers were highly sensitive and two of them were damaged during the experimental program. As the damaged ones were not replaced, the last tests had records from only seven pressure transducers. The sampling rate was set at 20 Hz and the signal from the pressure transducers was multiplied 200 times using an amplifier. The pressure transducers were installed on a slender frame constructed using coat hanger wires, duct tape and tie wraps (see Figure 4.7 and Figure 4.8). The space between the pressure transducers in the vertical direction was set to 10 cm (Figure 4.7).

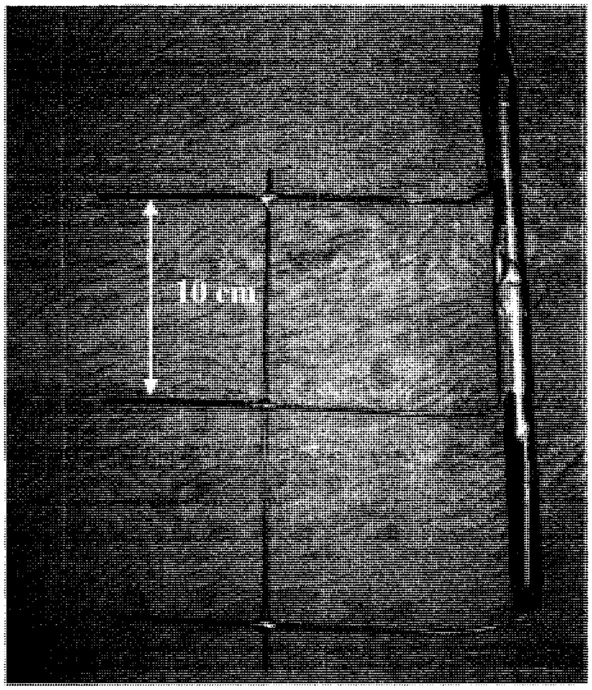

Figure 4.7 – Support frame for the pressure transducers

The four support frames used were capable of holding one, two or three pressure transducers. Figure 4.8 shows how the pressure transducers were mounted on the support frames. The picture was taken before the pressure transducers were buried. The numbers in Figure 4.8 refer to the numbers of the pressure transducers as indicated in Table 4.3 and Table 4.4.

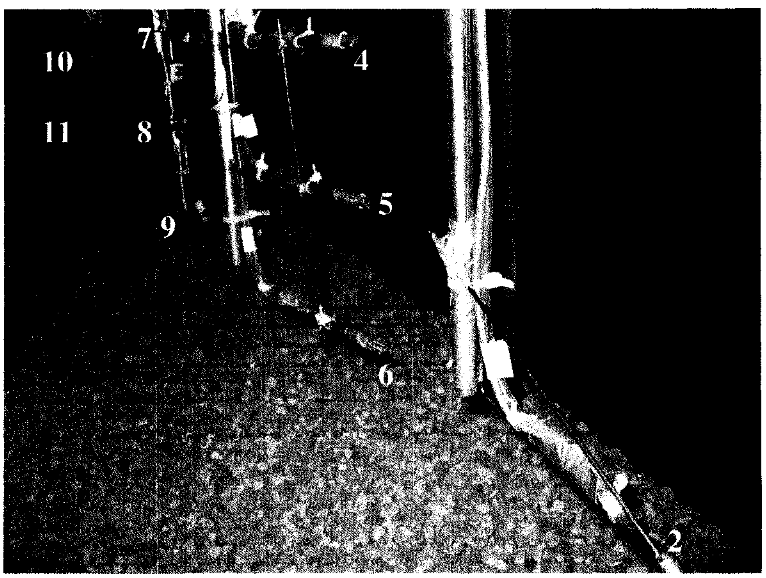

Figure 4.8 – Pressure transducers, before being buried

Table 4.3 and Table 4.4 indicate the locations of the pressure transducers inside the flume for the beach slopes 1:10 and 1:7, respectively.

Table 4.3 – Location of pressure transducers (beach slope1:10)

Pressure Transducer	Name	x location [m]	y location [m]	z location [m]
2	PT2	44.776	0.466	-0,12
4	PT4	45.076	0.452	-0.02
5	PT5	45.076	0.452	-0.12
6	PT6	45.076	0.452	-0.22
7	PT7	45.376	0.463	-0.02
8	PT8	45.376	0.463	-0.12
9	PT9	45.376	0.463	-0.22
10	PT10	45.676	0.478	-0.02
11	PT11	45.676	0.478	-0.12

After modifying the beach slope from 1:10 to 1:7, all pressure transducers were moved 0.60 m further in the onshore direction. This change in configuration was made so that pressure transducers PT4, PT5 and PT6 would be at the location where the water level of 0.6 m touches the beach face. PT7 was damaged during tests and was not replaced so that it only recorded for Tests 1 to 3. PT11 failed following Test 12 and was replaced by PT10, which was removed from its original location. PT11 did not collect data for Tests 13 through 19, (PT10 collected data in its new position for Tests 13 through 19).

Table 4.4 – Location of pressure transducers (beach slope 1:7)

Pressure Transducer	Name	x location [m]	y location [m]	z location [m]
2	PT2	45.376	0.466	-0,12
4	PT4	45.676	0.452	-0.02
5	PT5	45.676	0.452	-0.12
6	PT6	45.676	0.452	-0.22
7	PT7	Damaged		
8	PT8	45.976	0.463	-0.12
9	PT9	45.976	0.463	-0.22
10	PT10	46.276	0.478	-0.02
11	PT11	46.276	0.478	-0.12

4.3.3 Profiler

An electro-mechanical profiler was used to record the morphological response of the beach profile over time under wave forcing. Measurements were collected at a sampling rate of 20 Hz. For a few cases, the changes occurring in the beach profile were out of the profiler's reach, so measurements in these cases were completed manually by measuring through the flume's side window. Figure 4.9 shows a schematic figure of the setup. The profiler recorded the distance travelled in the cross-shore direction, R, and the angle, □ between the profiling beam and the rod with the wheel (which has the length P, measured from the center of the wheel).

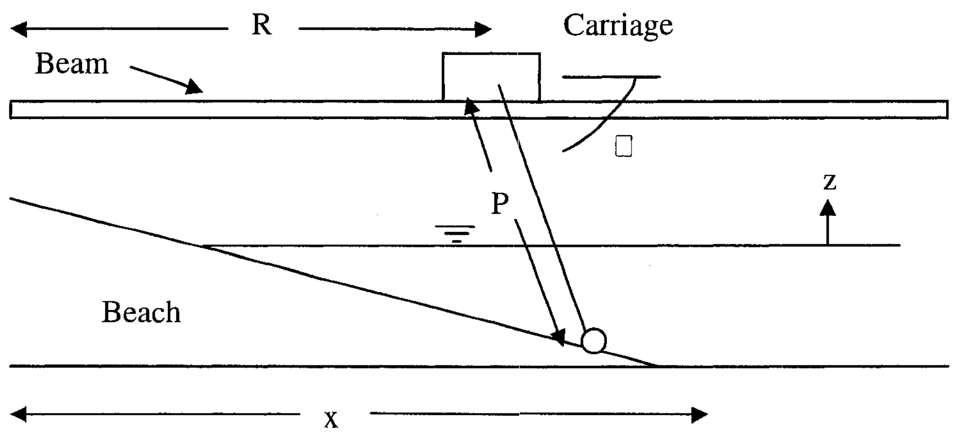

Figure 4.9 – Schema of the beach profiler (adopted from Davies et al., 1995)

The (R,□) array of coordinates needed to be converted to a (x,z) array of coordinates. That was done using a GEDAP program, MERGE_BW, which uses the following equations;

$$x = R + P \cdot \cos(\theta) \tag{4.1}$$

$$z = P \cdot \sin(\theta) - 0.719 \tag{4.2}$$

where 0.719 m is the distance between the profile beam and the still water level (SWL).

Figure 4.10 shows the profiler in its position when it was not in use. The wheel of the profiler was located 46.3 cm away from the West wall of the flume. When measurements were taken, the bar with the wheel at the end moved in the cross-shore direction of the beach. The profiler was always driven from the toe towards the top of the beach in order to minimize the risk of the profiler getting stuck in the beach structure.

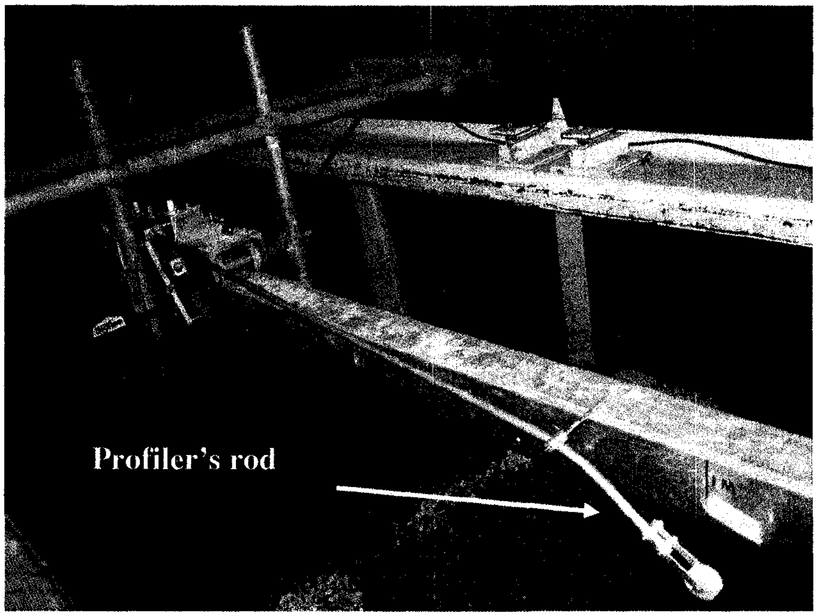

Figure 4.10 – Electro-magnetic beach profiler in resting position

4.3.4 Data Acquisition System

The Canadian Hydraulics Centre (CHC) uses the NDAC data acquisition system which operates in conjunction with the GEDAP analysis software on computers using the Windows NT operating system. NDAC was used for real-time data collection and display during acquisition, sensor calibration and to give commands to the wave generator (Miles, 1997).

4.3.5 Video Analysis and Image Processing

Photographs of instrumentation and profile changes were taken using a Canon Ixus 500 digital camera. Panorama photographs were taken after each test (excluding Tests 3 and 19) and photos were merged using the Canon PhotoStitch software. The Canon Ixus 500 was also used for limited video recordings of wave breaking and sediment transport. More detailed video recordings were performed using a Panasonic digital video camera, with DV mini tape. The camera was used to record more than 40 minutes of wave breaking and sediment transport.

4.4 Instrument Calibration

All recording instruments were calibrated so the difference between the measured and the expected value was within 0.5% admissible range of 100 mm. Wave gauges and pressure transducers were calibrated by keeping the instruments in position and changing the water level in the flume, or by changing the elevation of the instrument while the water level was kept constant. Calibration was performed on wave gauges and pressure transducers in the beginning and repeated when the slope of the beach was modified from 1:10 to 1:7. When the active wave absorption system was in use, these instruments were re-zeroed before every run. The AWA system is sensitive to any changes in water level so water level was set to zero between runs. The wave generator was configured and calibrated before runs started. The profiler was also calibrated, both for movements in the R-direction and θ-direction.

5 DATA ANALYSIS AND RESULTS

5.1 Geotechnical Analysis

Samples of the gravel material used to construct the beach were analysed in the Geotechnical Laboratory of the University of Ottawa. The aim was to determine the following characteristics and parameters of the material:

- Grain size distribution and median diameter (D_{50})
- Uniformity
- Gradation
- Porosity
- Specific gravity

Figure 5.1 shows an example of the gravel material used in the beach construction. The material is river-washed and therefore not very angular. This was fortunate as this is the natural state of gravel found on a beach subjected to the action of waves.

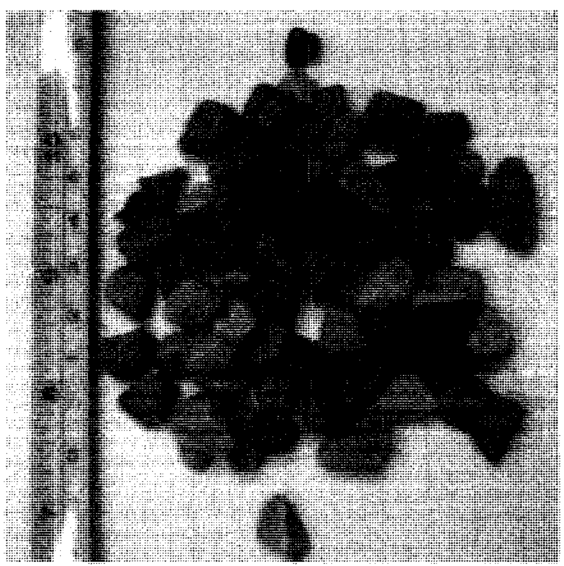

Figure 5.1 – Sample of gravel particles used in the experiment

Three samples were taken from the beach mound after all test runs were performed for the beach slope of 1:10 and before the slope was modified to 1:7. Samples were collected at different surface locations of the beach, as shown in Table 5.1. Each gravel sample weighed around 4 kg.

Table 5.1 – Location of beach sampling

Sample number	Location [m]	Location on the beach
1	40.80	Toe
2	44.00	Center
3	45.50	Top

5.1.1 Grain size distribution

Grain size distribution was determined by dry sieving the material in a series of sieves with different openings. The sieve sequence used is presented in Table 5.2.

Table 5.2 – Sieves used for grain size distribution analysis

Sieve No.	Opening diameter [mm]
3/4"	19.0
1/2"	12.7
3/8"	9.5
No. 4	4.75
No. 8	2.36
No. 10	2.00
No. 20	0.85
Pan	0.0

Two portions (Test A and Test B) of 1600 to 1900 g of each sample were sieved. The median grain size diameter (D_{50}) was determined for each case (Table 5.3).

Table 5.3 – Median grain size diameter at different locations

Location	D_{50} (Test A) [mm]	D_{50} (Test B) [mm]	D_{50} (average) [mm]	D_{50} (average) [mm]
Toe	7.6	7.6	7.6	7.8
Center	7.7	7.6	7.6	
Top	8.3	8.2	8.2	

The average median grain size diameter was determined to be 7.8 mm. Figure 5.2 and Figure 5.3 show grain size distribution charts for Test A and Test B, respectively. Worksheets containing details of the sieve analysis can be found in Table B.1 through Table B.6 in Appendix B.

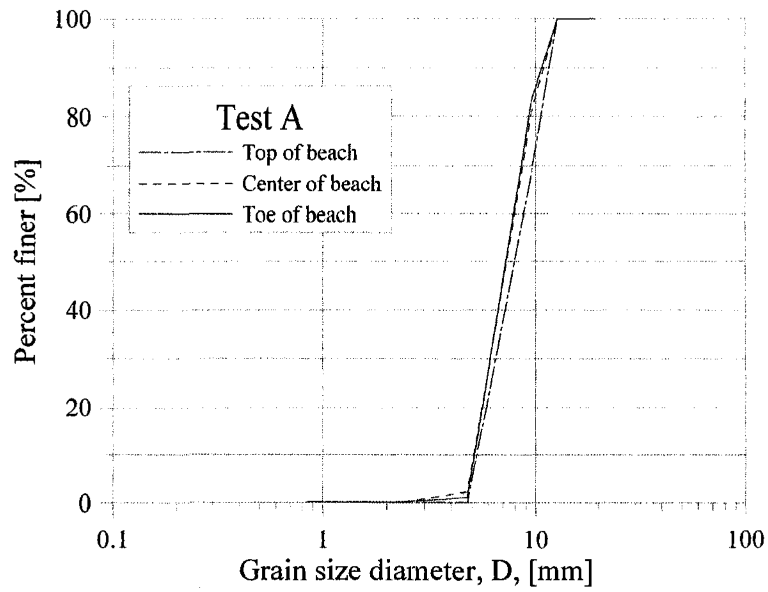

Figure 5.2 – Grain size distribution chart for Test A

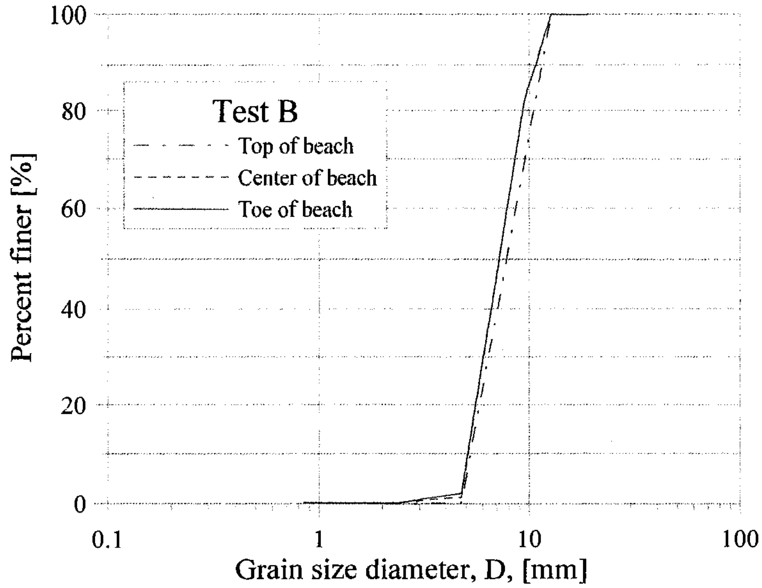

Figure 5.3 – Grain size distribution chart for Test B

5.1.2 Uniformity and Gradation

Figure 5.2 and Figure 5.3 indicate, considering the steep slopes of the grain size distribution represented on the graphs, that the material is very uniform.

The uniformity coefficient, C_u, is defined as:

$$C_u = \frac{D_{60}}{D_{10}} \tag{5.1}$$

where D_{60} is the diameter in the particle size distribution graph corresponding to 60% finer particles. In a similar way, D_{10} is the diameter corresponding to 10% finer grains.

Gradation of the material is described using the coefficient of gradation, C_z. The coefficient is defined as (Das, 2001):

$$C_z = \frac{D^2{}_{30}}{D_{60} \cdot D_{10}} \tag{5.2}$$

The uniformity and grading coefficients for all sieve test performed are shown in Table 5.4. The average value of the uniformity coefficient, $C_{u,av}$, is calculated together with the average value of the grading coefficient, $C_{z,av}$.

Table 5.4 – Uniformity coefficient and grading coefficient

<table>
<tr><th>Test</th><th>Location</th><th>C_u [-]</th><th>C_{u,av} [-]</th><th>C_z [-]</th><th>C_{z,av} [-]</th></tr>
<tr><td rowspan="3">Test A</td><td>Toe</td><td>1.55</td><td rowspan="6">1.59</td><td>0.96</td><td rowspan="6">0.96</td></tr>
<tr><td>Center</td><td>1.57</td><td>0.96</td></tr>
<tr><td>Top</td><td>1.58</td><td>0.96</td></tr>
<tr><td rowspan="3">Test B</td><td>Toe</td><td>1.56</td><td>0.96</td></tr>
<tr><td>Center</td><td>1.64</td><td>0.96</td></tr>
<tr><td>Top</td><td>1.63</td><td>0.96</td></tr>
</table>

A uniformity coefficient close to 1 indicates a 'very uniform' grain size distribution. Graphs in Figure 5.2 and Figure 5.3 also indicate uniformity of the gravel material. The grading coefficient is very low, which indicates very well sorted material.

5.1.3 Porosity

Porosity plays an important part in the following conservation of sediment mass relationship:

$$\frac{\Delta h}{\Delta t} = \frac{1}{(1-n)} \frac{\Delta q_x}{\Delta x} \tag{5.3}$$

where $\Delta h/\Delta t$ is the change in beach profile height over change in time, $\Delta q_x/\Delta x$ is the change of sediment transport rate over distance in cross-shore direction and n is the porosity (Winyu, 1995).

The porosity of a granular material, n, is defined as

$$n = \frac{e}{e+1} \tag{5.4}$$

where, e, the void ratio, is given as

$$e = \frac{G_s \cdot \gamma_w}{\gamma_d} - 1 \tag{5.5}$$

in which G_s is the specific gravity of the material, γ_w is the specific weight of water and γ_d is the specific dry weight of the soil. The specific gravity and the specific dry weight of the gravel were determined in laboratory.

Specific gravity is defined as

$$G_s = \frac{M_s}{V_s \cdot \rho_w} \tag{5.6}$$

where M_s is mass of gravel, V_s is volume of gravel and ρ_w is density of water. In order to determine the specific gravity, a 500 ml volumetric flask was used to measure the volume of sample, by first weighing the flask with 500 ml of distilled water and again with around 100 g of gravel and distilled water added to the 500 ml line. In both cases, air was vacuumed out of the flask. The detailed procedure of the determination of specific gravity is presented in Table B.7 in Appendix B. Table 5.5 presents the specific gravity for gravel samples taken from the toe, center, and top of the beach, as well as their average values.

Table 5.5 – Specific gravity of the gravel

Location	**Specific gravity, G_s**
Toe	2.77
Center	2.79
Top	2.75
Average	**2.77**

The other unknown parameter for the determination of the porosity is the specific weight of the gravel sample. The specific weight is defined as

$$\gamma_d = \rho_d \cdot g \tag{5.7}$$

where ρ_d is the density of the dry gravel and g is the acceleration due to gravity, 9.81 m/s^2.

The density of the gravel was measured by filling a plastic cylinder of known volume and then weighing the gravel, as density is defined as mass over volume. Table 5.6 lists the specific weight of the gravel.

Table 5.6 – Specific weight of the gravel

Location	Mass of soil [kg]	Volume of cylinder [m^3]	Specific weight [N/m^3]
Toe	2.881	0.001647	17160
Center	2.930	0.001647	17452
Top	2.880	0.001647	17154

The specific weight of water is 9810 N/m^3, so it was possible to determine the void ratio using Eq. (5.5) and calculate the porosity using Eq. (5.4). The results are presented in Table 5.7.

Table 5.7 – Porosity of the gravel

Location	Void ratio [-]	Porosity [-]
Toe	0.584	0.369
Center	0.568	0.362
Top	0.573	0.364
Average	**0.575**	**0.365**

The porosity for the gravel was found to be 0.365 and this value was used in Eq. (5.3).

5.2 Wave Analysis

Analysis of wave characteristics was performed using the GEDAP programs developed at the Canadian Hydraulics Centre, NRC. The GEDAP software consists of three main packages:

- NDAC (data acquisition package)
- ANALYSIS (data analysis package)
- GPLOT (interactive graphics package).

Figure 5.4 shows a diagram of the GEDAP system and how component packages are interrelated.

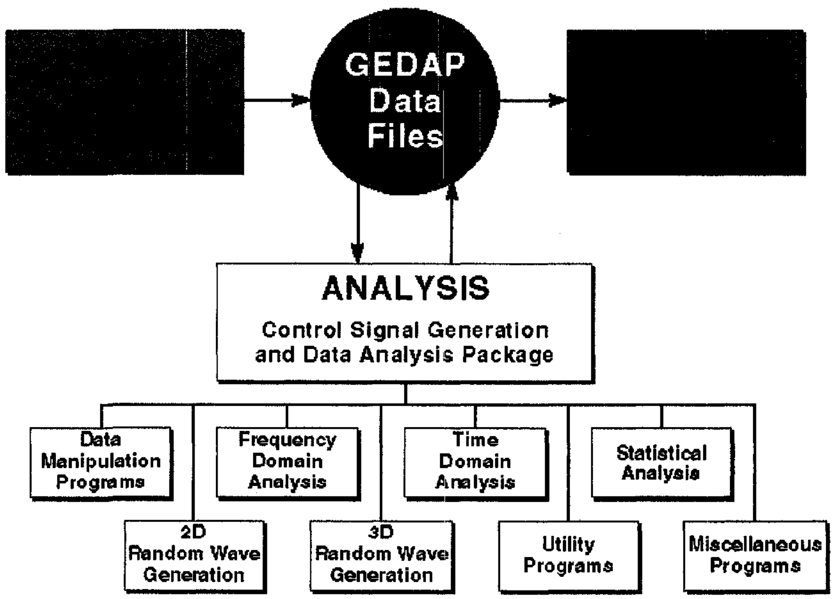

Figure 5.4 – Diagram of the GEDAP system (Miles, 1997)

The ANALYSIS package is the main component of the software. It includes all data analysis functions and subroutines needed for wave data analysis. GPLOT is a two-dimensional graphics package, used to plot data files from GEDAP (Miles, 1997). The GEDAP analysis package is capable of comprehensive wave analysis, both in time and in frequency domain.

The following wave parameters were collected for each test employing regular waves:

- Average wave height, H_{av}

- Maximum wave height, H_{max}
- Average wave period, T_{av}
- Average crest height, $\square_c$
- Average trough height, $\square_t$

These parameters were collected using time domain zero-up crossing analysis of the wave trains. In the zero-up crossing method, a wave is defined when the surface elevation crosses the still water level (z = 0 m) upward and continues until it reaches the next upward crossing point. Zero-down crossing is defined when the surface elevation is chosen when it crosses the still water level downward.

The average wave height, H_{av}, is defined as the average of the average zero-up crossing wave height and the average zero-down crossing wave height. The maximum wave height, H_{max}, is defined as the average of the maximum zero-up crossing wave height and the maximum zero-down crossing wave height. The average wave period, T_{av}, is defined as the average of the average zero-up crossing wave period and the average zero-down crossing wave period (USACE, 2002).

Figure 5.5 shows how the wave height, H and the wave period, T are defined (the still water level is denoted as SWL). The crest of the wave is the uppermost part of the water surface while the trough represents its lowest.

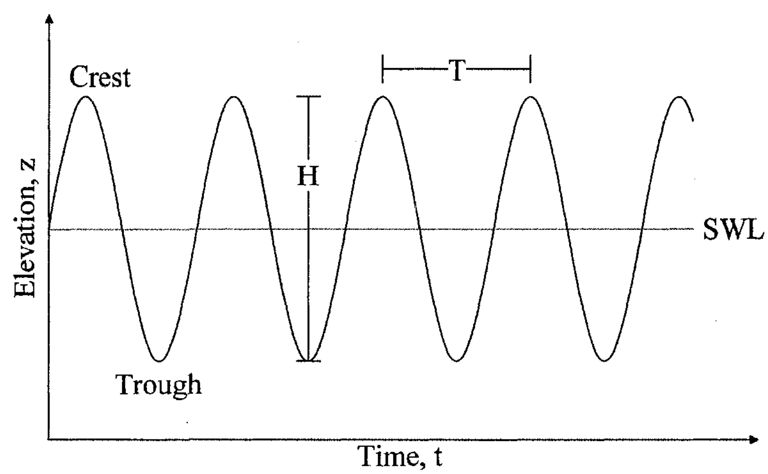

Figure 5.5 – Sinusoidal regular wave characteristics

The following wave parameters were collected during each test employing irregular waves:

- Significant wave height, H_s
- Maximum wave height, H_{max}
- Peak wave period, T_p
- Average wave period, T_{av}
- Average crest height, $\square_c$
- Average trough height, $\square_t$

The significant wave height, H_s, is defined as the average value of the highest one-third of all waves, sometimes denoted as $H_{1/3}$. The significant wave height is evaluated with the zero-down crossing analysis. Wave peak period, T_p, is the period corresponding to the frequency of the spectral peak. Figure 5.6 demonstrates the definition of the significant wave height, H_s and the maximum wave height, H_{max}.

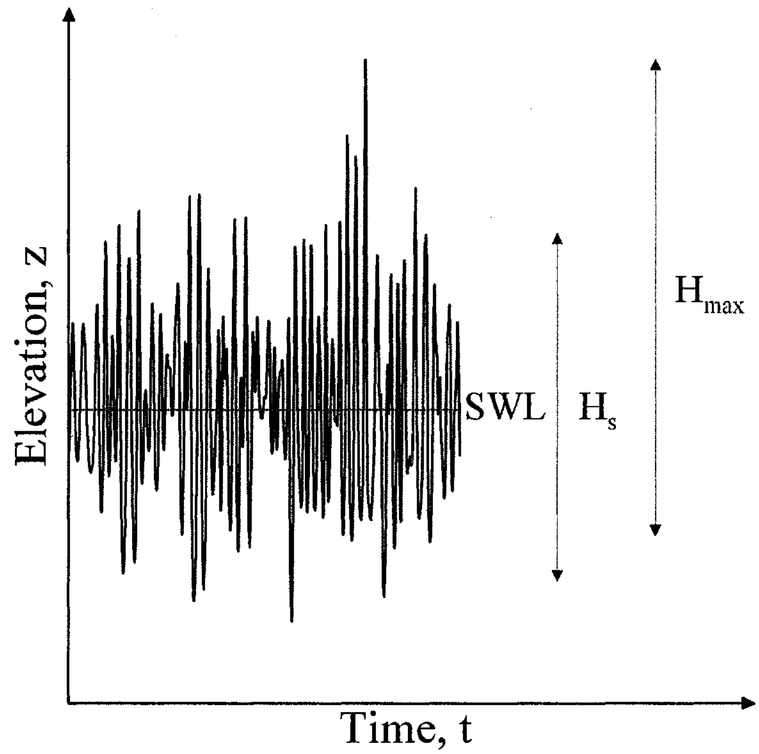

Figure 5.6 – Sequence of irregular waves

The peak wave period is the wave period corresponding to the peak value of the frequency, f_p, as shown in Eq. (5.8);

$$T_p = \frac{1}{f_p} \tag{5.8}$$

Figure 5.7 shows an example of the comparison between the target JONSWAP spectrum and the measured spectrum of the incident waves. The peak frequency of the target spectrum is 0.400 Hz and the frequency of the measured waves was 0.398 Hz. The peak wave period is then determined as indicated by Eq. (5.8).

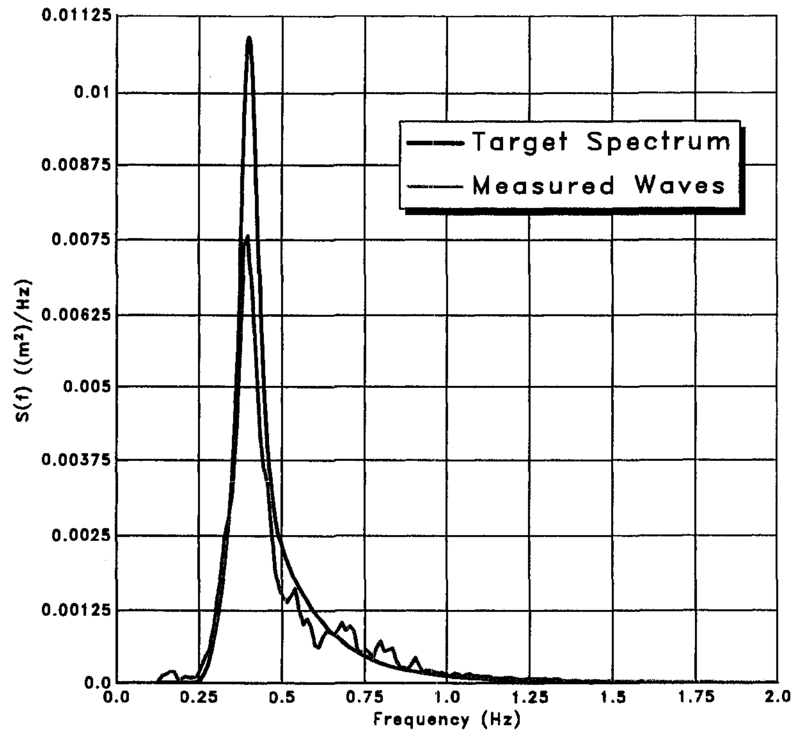

Figure 5.7 –Target spectrum and measured spectrum of incident waves (Test 6)

Tabulations of the average wave height and average wave period for tests with regular waves and of the significant wave height and peak wave period for tests with irregular waves are presented in Appendix E.

5.2.1 Wave Breaking in the Surf Zone

The four wave gauges located in the surf zone (WG9 to WG12) provided information on the changes in wave height in the surf zone. In this section, only results from tests with irregular waves are analyzed. The data needed for this analysis were collected during the first part of each test, during which beach deformation was minimal.

Wave height at wave breaking point, H_b, is a function of the local water depth, d_b, and can be estimated as (Kamphuis 2000):

$$\frac{H_b}{d_b} = 0.78 \tag{5.9}$$

In the following analysis, the wave breaking height for irregular waves was taken as the maximum wave height, H_{max}, so Eq. (5.9) becomes

$$\frac{H_{max}}{d} = 0.78 \tag{5.10}$$

Figure 5.8 shows the maximum wave height across the surf zone for the initial part of Tests 4 through 9. The measurements were taken within the first 100 waves of each test so the change in the beach profile was negligible. According to Figure 5.8, the maximum values of the wave height occurred at 42.08 m or 43.08. The beach profile is assumed to be straight (1:10) profile in the calculations shown in Table 5.8. It should be noted that the distance between wave gauges in the surf zone is 1 m, so that information on the wave height change between the gauges is not available.

Table 5.8 – Measured H_{max}/d values in the surf zone for Tests 4 to 9

Test	H_s [m]	T_p [s]	H_{max}/d @ 42.08 m	H_{max}/d @ 43.08 m
Test 4	0.13	1.5	0.74	1.02
Test 5	0.14	2.0	0.77	1.28
Test 6	0.14	2.5	0.78	1.42
Test 7	0.17	1.5	0.92	1.11
Test 8	0.18	2.4	1.08	1.45
Test 9	0.19	2.9	1.09	1.63

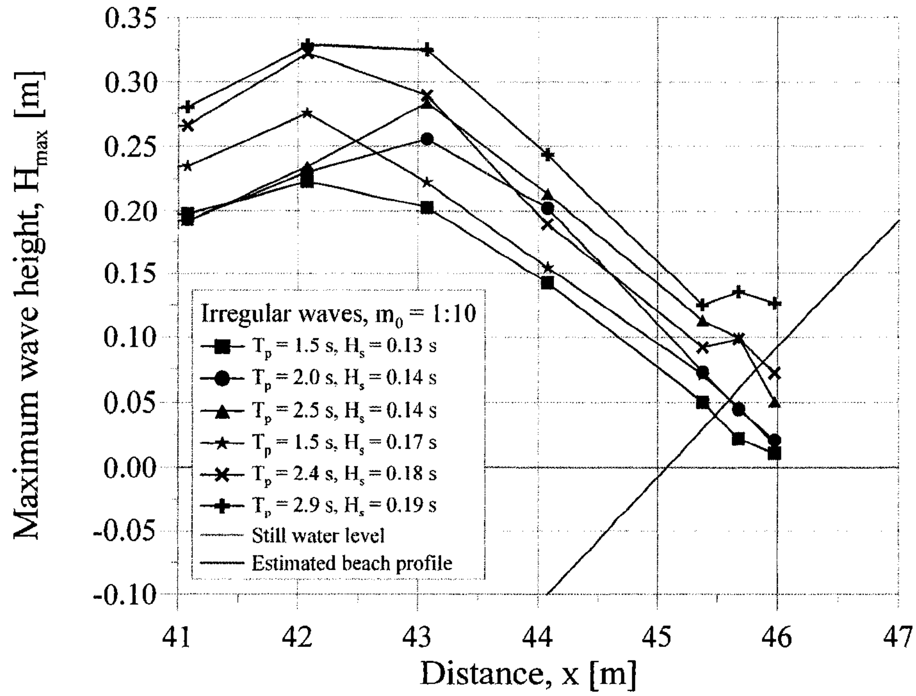

Figure 5.8 – Maximum wave height in the surf zone (Tests 4 to 9, irregular waves, initial beach slope: 1:10)

The maximum values in Table 5.8 are much higher than 0.78. That can partly be explained by the maximum wave height, H_{max}, which consists of both the height of the incident wave and the height of the wave reflected by the beach. The reflected part of the wave increases the value of the maximum wave height, H_{max}, which is not considered in Eq. (5.9). The steepness of the beach slope could also have played a factor.

In Eq. (5.11), the initial beach slope is taken into account. In the Shore Protection Manual (CERC, 1984), it is suggested that the ratio between H_{max} and d can be predicted as,

$$\frac{H_{max}}{d} = \frac{1.56}{1+e^{-19.5 \cdot m_0}} - 43.75\left(1-e^{-19 \cdot m_0}\right) \cdot \frac{H_{max}}{g \cdot T_p^{\,2}} \tag{5.11}$$

where m_0 is the initial beach slope (CERC, 1984).

Table 5.9 presents the H_{max}/d values, when they are evaluated by Eq. (5.11), that is, when the beach slope has been accounted for, as well as the peak wave period.

Table 5.9 – Predicted H_{max}/d values in the surf zone for Tests 4 to 9 (beach slope effect included)

Test	H_s [m]	T_p [s]	H_{max}/d @ 42.08 m	H_{max}/d @ 43.08 m
Test 4	0.13	1.5	**1.00**	0.97
Test 5	0.14	2.0	0.87	**0.89**
Test 6	0.14	2.5	0.82	**0.84**
Test 7	0.17	1.5	**1.09**	0.99
Test 8	0.18	2.4	**0.86**	0.85
Test 9	0.19	2.9	**0.82**	0.82

In Table 5.9, the H_{max}/d values are slightly higher than 0.78 which is expected since both the incident and reflected waves are included in the maximum wave height, H_{max}. The bold values in Table 5.9 indicate the maximum values in the table for each test, and are similar to the estimated wave breaking point in Figure 5.8, that is, the peaks of the plots in Figure 5.8 are at the locations where the H_{max}/d values are highest.

5.3 Beach Morphology Change

The beach morphological change analysis is conducted in the following section. Several elements were analyzed and are discussed: the cross-sectional view of the beach was plotted at different time steps (see Figure 5.9), the sediment transport rate for each test was calculated and plotted, and the beach berm development and beach trough development were also investigated.

5.3.1 Beach Profile Evolution

The beach profile change was recorded at the end of every test with an electro-magnetic profiler. When necessary, profile changes were also measured manually through the glass wall of the flume, especially if profile changes occurred beyond the spatial range of the profiler. This occurred occasionally at the end of some tests, especially when the beach trough became too deep due to erosion and therefore out of the profiler's reach. In addition, manual profile measurements were performed at the end of Tests 1 to 18 to in order to compare the beach profile changes at the wall with the beach profile changes recorded by the profiler.

Tests were run until a state of equilibrium was reached, that is, until no changes occurred in the beach profile between test sequences. When waves were regular, equilibrium was reached much sooner than for the case of irregular waves as such waves generate a wide spectrum of forces to the beach and this can be expected (Van der Meer, 1988). For regular waves, tests were usually stopped after 2500 waves, but for irregular waves, tests usually ran for 5000 wave periods.

Beach profile changes were plotted for each test, at five instants per test. In the case of tests with regular waves, beach profile evolution was plotted after 50, 400, 800 and 2500 waves. In the case of tests with irregular waves, beach profile evolution was plotted after 100, 750, 2000 and 5000 waves. Beach deformation plots for all 19 tests are presented in Appendix C.

Figure 5.9 shows the beach profile evolution at five instants; at the initial state (before wave action, denoted as "0" waves) and at four different time steps throughout Test 14. The number of waves is denoted as N_w. The still water level is at 0.00 m. The initial beach profile (initial slope of 1:7) is plotted as a solid grey line. Profile change is rapid in the beginning. After only 100 waves of wave action, a beach berm of 8.7 cm (at x = 45.94 m) has already formed.

Beach material is eroded and transported onshore and develops a step below the still water level and a berm above it. After 2000 waves, the beach profile is close to equilibrium. After 5000 waves, there is only a slight difference in the profile resulting from the last 3000 waves. This is similar to the findings of Ibrahim *et al.* (2006) from the experiment performed in Hanover in 2002 (San Román-Blanco *et al.*, 2006). Ibrahim *et al.* (2006) stated that the beach in the large wave flume reached equilibrium after 2000 to 3000 waves. The largest profile changes occurred between 500 and 1000 waves in the case of the Hanover experiment and this is similar to the observations made during this study, where the largest beach profile changes generally took place between the first 100 to 750 waves (Figure 5.9).

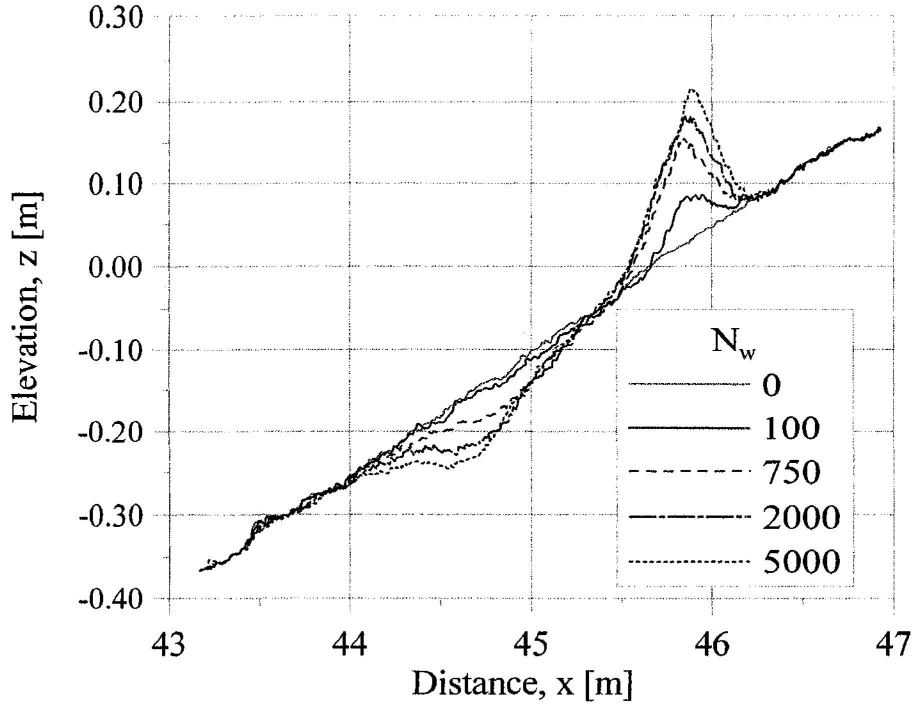

Figure 5.9 – Time evolution of beach deformation, Test 14: Irregular waves, T_p = 2.0 s, H_s = 0.14 m, initial beach slope: 1:7

Ibrahim *et al.* (2006) measured the beach face slope at the state of equilibrium varying between tan(□) = 0.47 and 0.50. The corresponding beach face slope in the present study varied between tan(□) = 0.30 and 0.53 for regular waves and between tan(□) = 0.24 and 0.59 for irregular waves. These are the beach slopes used in the wave reflection analysis in Chapter 5.4 as the beach slopes changed significantly from the initial beach slopes of 1:10 (tan(□) = 0.10) and 1:7 (tan(□) = 0.14). The beach profile evolution shown in Figure 5.9 is equivalent to the beach behaviour also recognized by Pedrozo-Acuña *et al.* (2006) and Van der Meer (1988). Pedrozo-Acuña *et al.* (2006) stated that a plausible reason for the berm to develop so close to the still water level is that the backwash velocity is reduced due to penetration of water into the beach, so the sediment transport in the offshore direction is much less than in the onshore direction.

5.3.1.1 Influence of Wave Height

Figure 5.10 shows the difference in beach profile between Test 15 and Test 18 after 5000 waves, where the significant wave heights are H_s = 0.14 m and H_s = 0.19 m, respectively. Waves are irregular and the peak wave period is constant for the two tests.

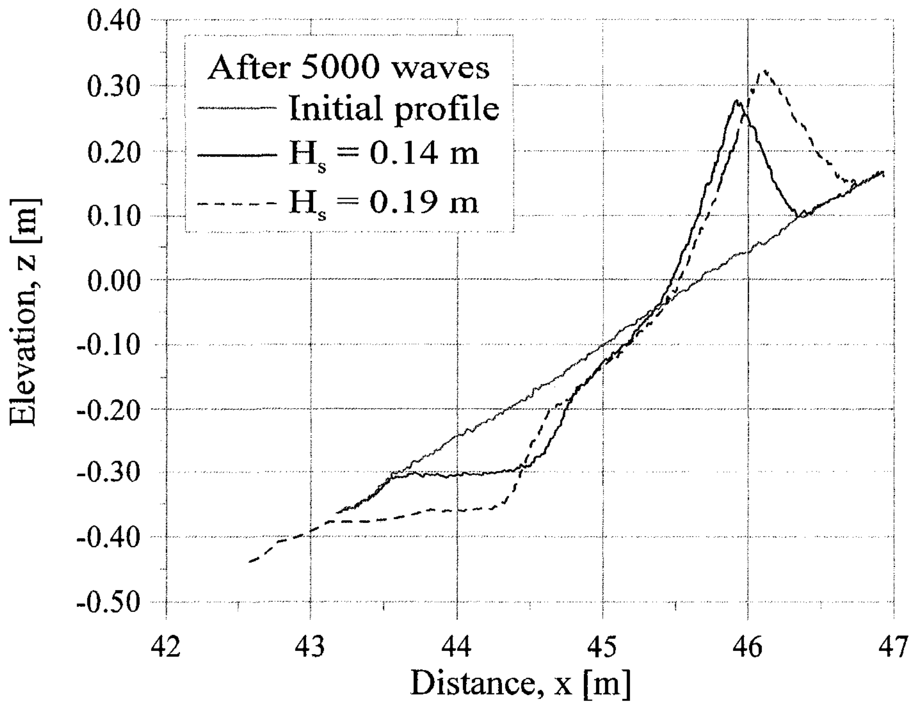

Figure 5.10 – Comparison between Test 15 and 18, after 5000 waves, T_p = 2.5 s, initial slope: 1:7, significant wave height varies

An increase in the wave height leads to an increases in the height of the berm and augments the erosion below the still water level. The trough of the beach below the water level reaches further offshore as the wave height increases. This influence of an increased wave height was also observed in other tests. Higher waves generate higher berms and increase the sediment transport. This is similar to what Ibrahim *et al.* (2006) observed from the laboratory results in the large wave flume in Hanover.

It should be noted however that, in the present study, only two different wave heights were considered for irregular waves. It would be easier to comment on the influence of wave height on beach profiles if additional tests with different wave heights had been performed.

In the case of regular waves, the influence of wave height is less obvious, as seen in Figure 5.11. The beach face maintains similar deformation patterns for H_{av} = 0.15 m, 0.19 m and 0.25 m; however, as the wave height increases, the berms reach a little bit higher. The change is yet rather small. In the cases of H_{av} = 0.19 m and H_{av} = 0.25 m, a second berm is generated below the water level.

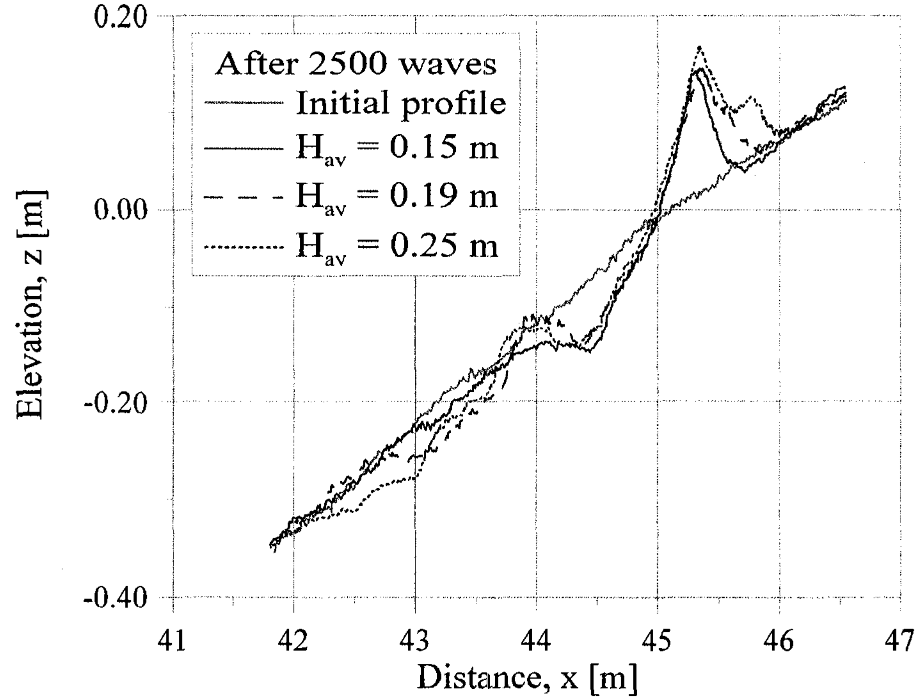

Figure 5.11 – Comparison between Test 1, 2 and 3, after 2500 waves, T_{av} = 2.0 s, slope: 1:10, average wave height varies

Ibrahim *et al.* (2006) stated that the relationship between profile changes and wave height was not linear since, in their study, the largest changes occurred for the intermediate value of the wave height. This observation was confirmed in the present study. For irregular waves, Figure 5.12 shows the maximum accretion (or berm height), □ h_{max}, as a function of significant wave height. Similarly, Figure 5.13 shows the maximum erosion (or maximum trough depth), □ h_{min}, as a function of significant wave height. The observed relation between equilibrium berm or trough amplitude and significant wave height are not linear, as the coefficients of determination, r^2, are only 0.17 or 0.12. However, in this study, the largest values of berm height and trough depth occurred for the largest wave heights.

A careful analysis of Figure 5.12 and Figure 5.13 raises the question on whether the relationship between maximum berm/trough height is polynomial of the second order. At H_s = 0.17 m, the maximum berm height is smaller than for lower and higher significant wave heights.

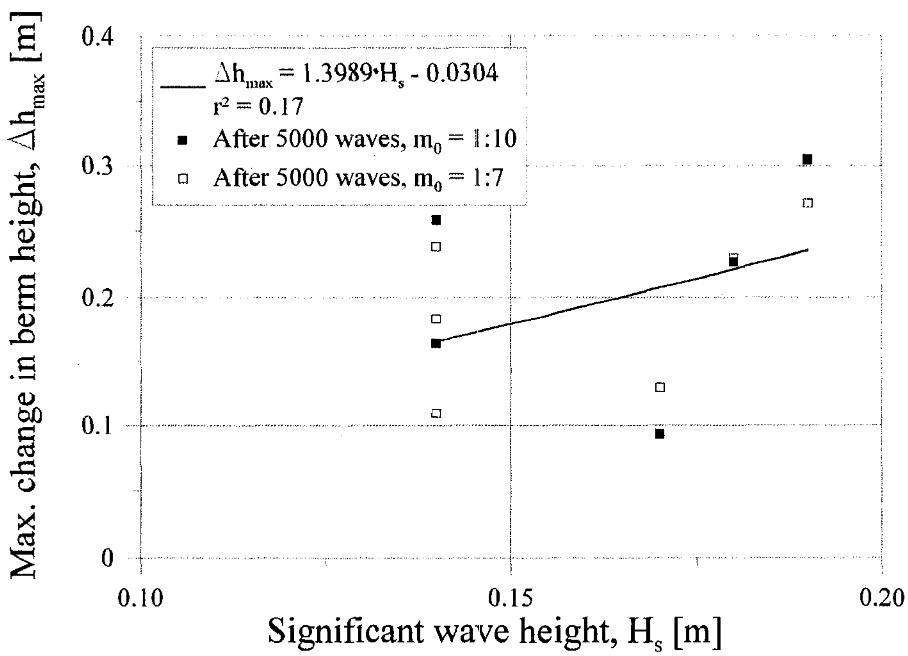

Figure 5.12 – Maximum change in accretion as a function of significant wave height

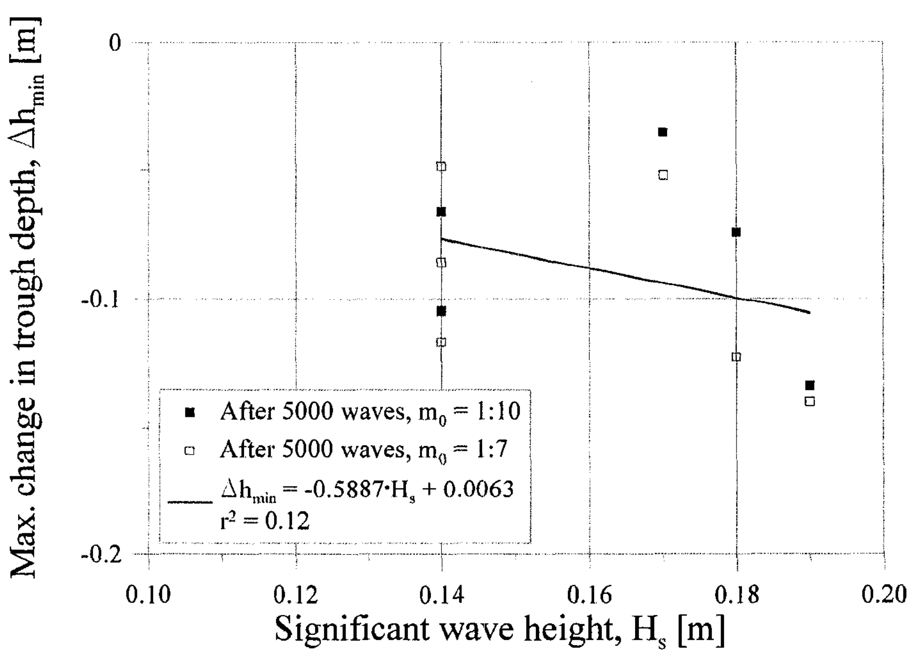

Figure 5.13 – Maximum change in erosion as a function of significant wave height

Results of a similar analysis for tests with regular waves are plotted in Figure 5.14 and Figure 5.15. In Figure 5.14, the linear correlation seems significantly higher than that for irregular waves, especially when separate regression analysis is performed for the two different beach slopes of the tests.

When the initial beach slope is 1:7, the coefficient of determination, r^2, is 0.99, but it is significantly lower for an initial slope of 1:10, $r^2 = 0.63$. In Figure 5.14, only three data points are available for each initial slope. Thus, prudence should be employed when commenting on the relationship between equilibrium berm height and wave height for regular waves.

In Figure 5.15, the relationship between the maximum depth of the beach trough and the average wave height is plotted. The trough develops very differently as the initial beach slope differs. For an initial slope of 1:7, the relationship is not as linear as the one indicated by Figure 5.14. However, it is better for an initial slope of 1:10, even though the regression line is of reverse slope.

The equilibrium trough depth depends weakly on wave height, and also depends on the initial beach slope. The equilibrium berm height shows a weak dependence on wave height for an initial beach slope of 1:10, increases with an increase in wave height for an initial beach slope of 1:7.

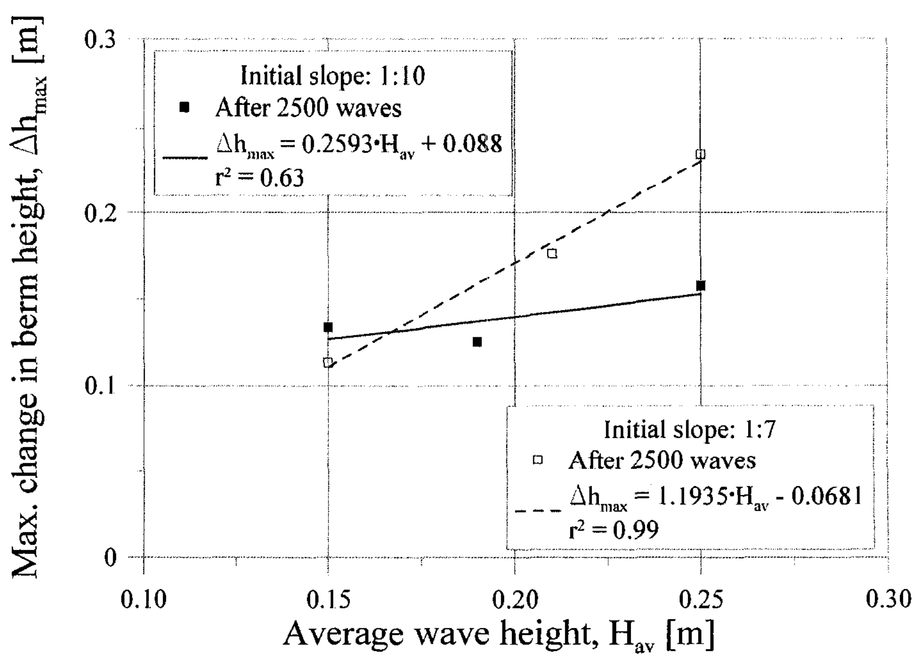

Figure 5.14 – Maximum change in accretion as a function of average wave height

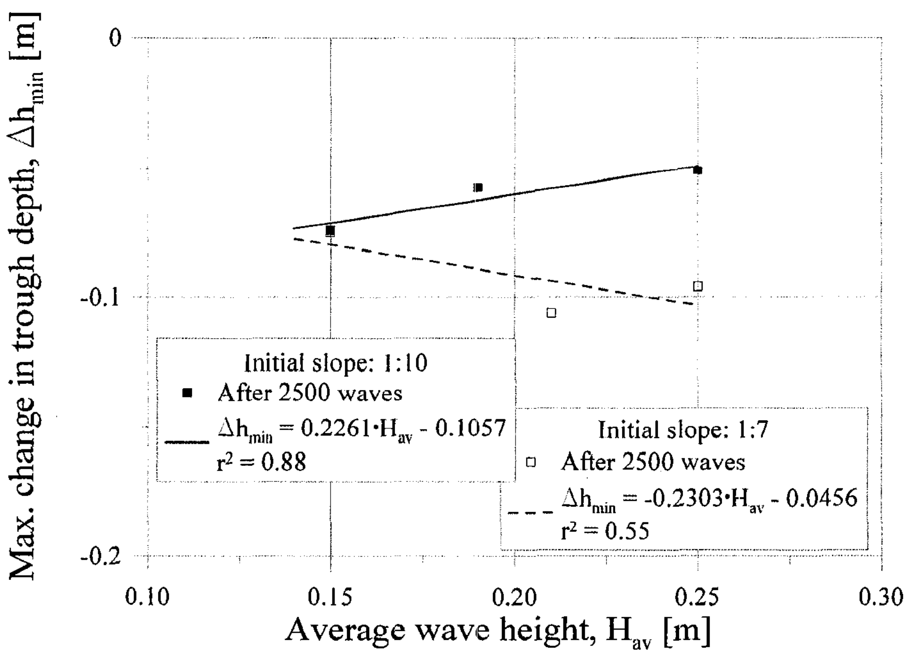

Figure 5.15 – Maximum change in erosion as a function of average wave height

5.3.1.2 Influence of Wave Period

Increasing the wave period increases both the sediment transport and the amplitudes of the berm height and the trough depth, as shown in Figure 5.16.

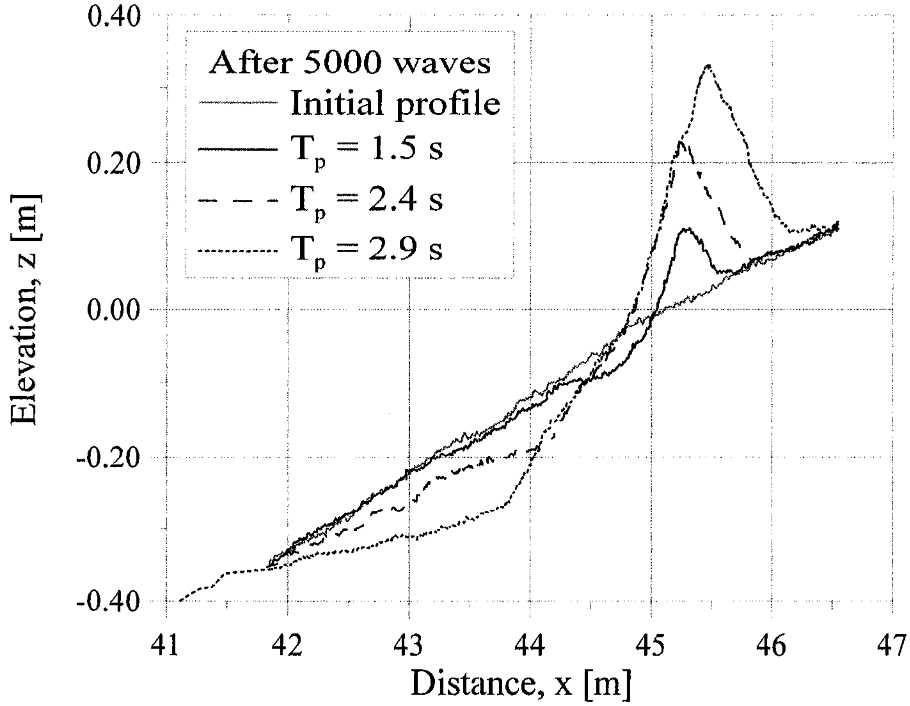

Figure 5.16 – Comparison between Test 7, 8 and 9, after 5000 waves, $H_s = 0.18 \pm 0.01$ m, initial slope: 1:10, peak wave period varies

Results in Figure 5.10 and Figure 5.16 are similar to those of Van der Meer's (1988) and the results in Figure 5.16 are also in agreement with Powell's (1990) findings, which stated that an increasing wave period, for a given wave height, would lead to a higher beach berm. Van der Meer (1988) stated that both the wave height and wave period have a significant influence on the beach profile. He also stated that the wave height and wave period have the same order of influence on the profile.

According to Figure 5.17 and Figure 5.18, the relationship between wave peak period and the maximum berm height or trough depth is linear, especially for the berm height, where the coefficient of determination is $r^2 = 0.96$. For the relationship between wave peak period and the maximum trough depth, the linearity is not determinant as the coefficient of determination ($r^2 = 0.76$) is somewhat lower.

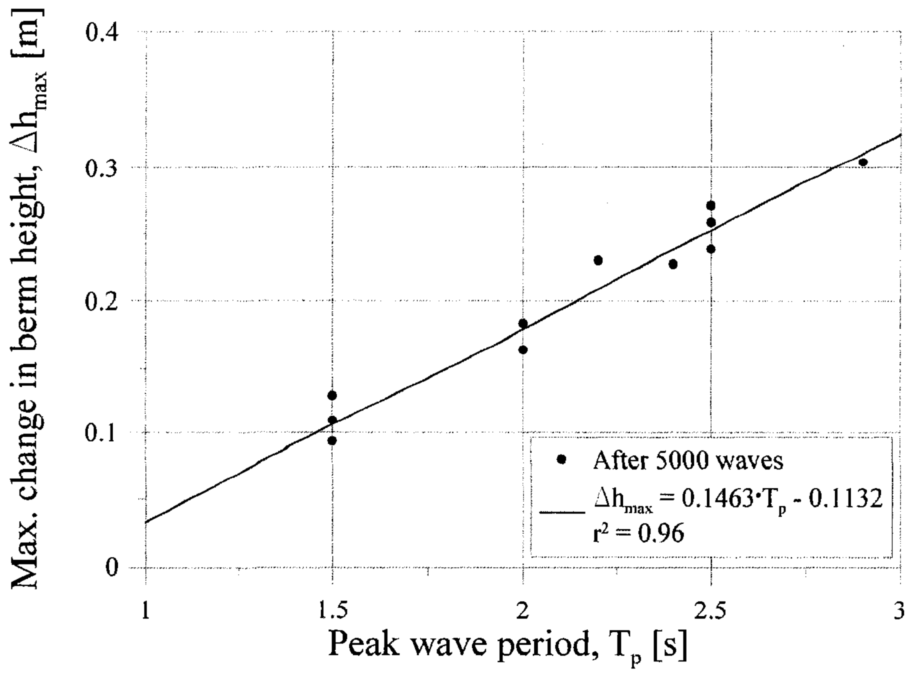

Figure 5.17 – Maximum accretion as a function peak wave period

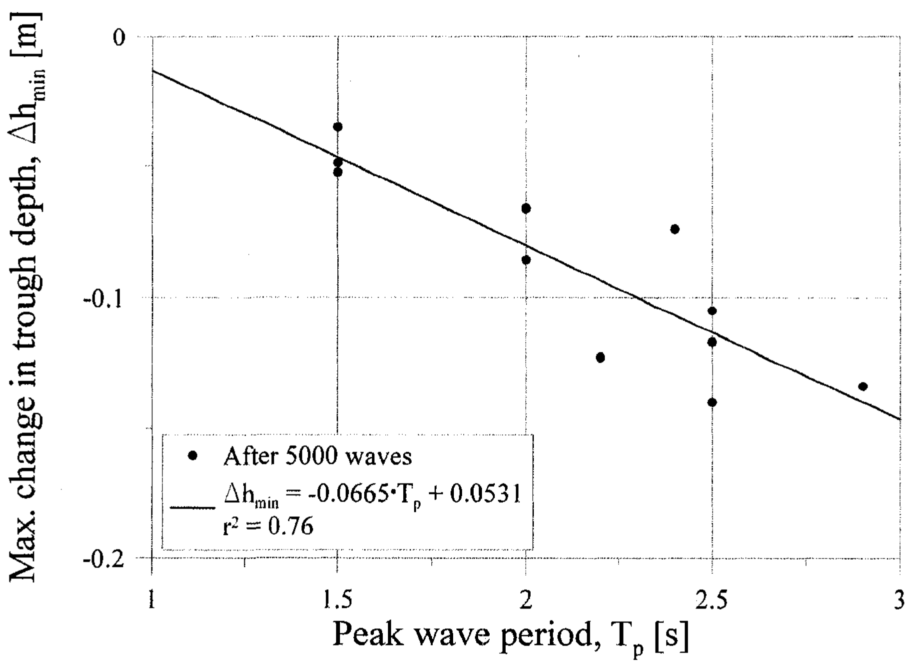

Figure 5.18 – Maximum erosion as a function of peak wave period

The data points in Figure 5.17 and Figure 5.18 come from experiments with irregular waves, with initial beach slopes of 1:7 and 1:10 and various significant wave heights.

Only one average wave period was considered in the tests with regular waves. Similar regression analysis is therefore not possible for regular waves.

5.3.1.3 Influence of Surf Similarity Parameter

The surf similarity parameter, also known as Iribarren number, describes the breaking type of the waves and is defined slightly differently whether waves are regular or irregular.

$$\xi = \begin{cases} \xi_o & \text{for regular waves} \\ \xi_p & \text{for irregular waves} \end{cases} \tag{5.12}$$

The surf similarity parameter for regular waves is defined as (Kamphuis, 2000),

$$\xi_o = \tan(\alpha) \Big/ \sqrt{\frac{2 \cdot \pi \cdot H_{av}}{g \cdot T_{av}^2}} \tag{5.13}$$

In physical terms, ξ_o represents the ratio of beach slope to wave steepness. For irregular waves, H_{av} is replaced by H_s, and T_{av} is replaced by T_p. The equation for the surf similarity for irregular waves becomes therefore,

$$\xi_p = \tan(\alpha) \Big/ \sqrt{\frac{2 \cdot \pi \cdot H_s}{g \cdot T_p^2}} \tag{5.14}$$

The slope of the beach, $\tan(\alpha)$, is defined separately for every test, as the beach face changes with an increase in the wave period.

Table 5.10 shows the wave breaking types according to the surf similarity parameter.

Table 5.10 – Wave breaking types and surf similarity parameter (Kamphuis, 2000)

Breaking type	□
Spilling	< 0.4
Plunging	0.4 – 2.0
Collapsing	> 2.0

Figure 5.19 and Figure 5.20 show the maximum berm height as a function of the surf similarity parameter. When the waves are regular, after 2500 waves and the initial beach slope is 1:10, the breaking waves are of plunging type as they break and the regression coefficient between the change in berm height and the surf similarity parameter is low. For an initial beach slope of 1:7, the waves are of collapsing type as they break and a regression coefficient of $r^2 = 0.89$ is observed between the change in berm height and the surf similarity parameter. However, only three data points are available for each initial slope and additional points would be helpful. Irregular waves mostly collapse as they break. In a few cases the waves plunge due to lower wave height. Measurements are plotted after 5000 wave impacts. For initial beach slope of 1:10, regression is better than for initial beach slope of 1:7.

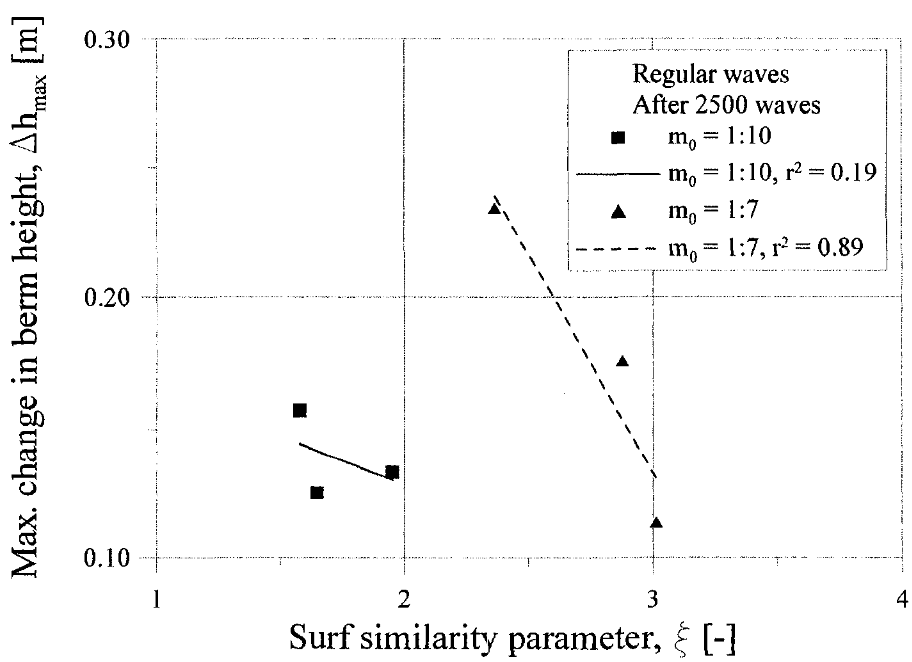

Figure 5.19 – Maximum change in berm height as a function of surf similarity parameter, regular waves

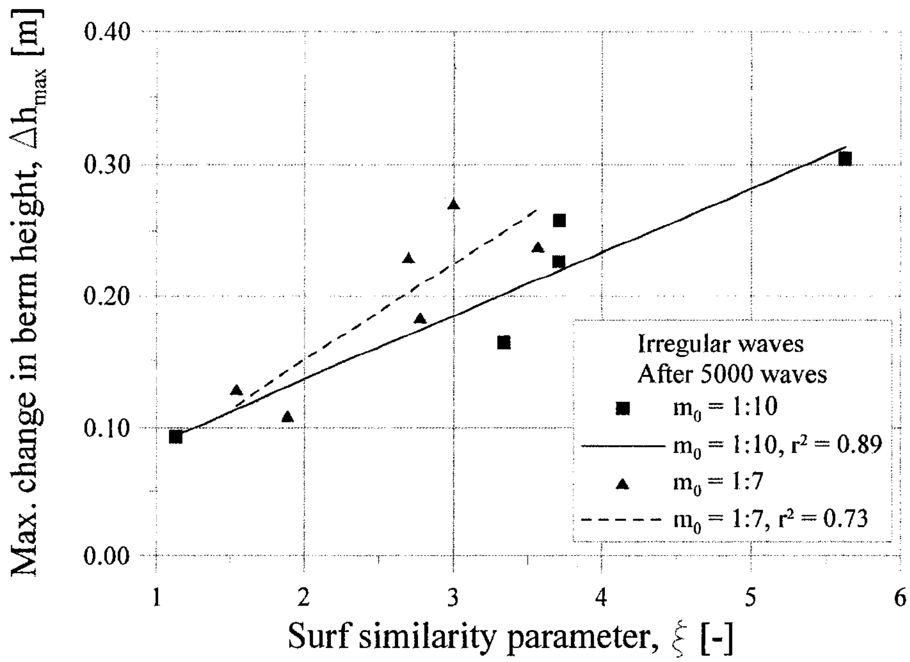

Figure 5.20 – Maximum change in berm height as a function of surf similarity parameter, irregular waves

In Figure 5.21 and Figure 5.22, a normalized berm height is introduced. This transformation is performed as the berm height is divided by the average wave height (in the case of regular waves) and by the significant wave height (in the case of irregular waves). For regular waves and an initial beach slope of 1:10, waves seem to plunge as they break, unlike the collapsing ones which tend to occur for an initial beach slope of 1:7. The regression lines in Figure 5.21 have reverse slopes but both generate good regression coefficients, or $r^2 > 0.93$. Irregular waves mostly collapse as they break. Only in a few cases the waves plunge, as also seen in Figure 5.19. When the initial slope is 1:7, the regression coefficient between the normalized berm height and the surf similarity parameter is high, but when the initial beach slope is 1:10, regression is poor.

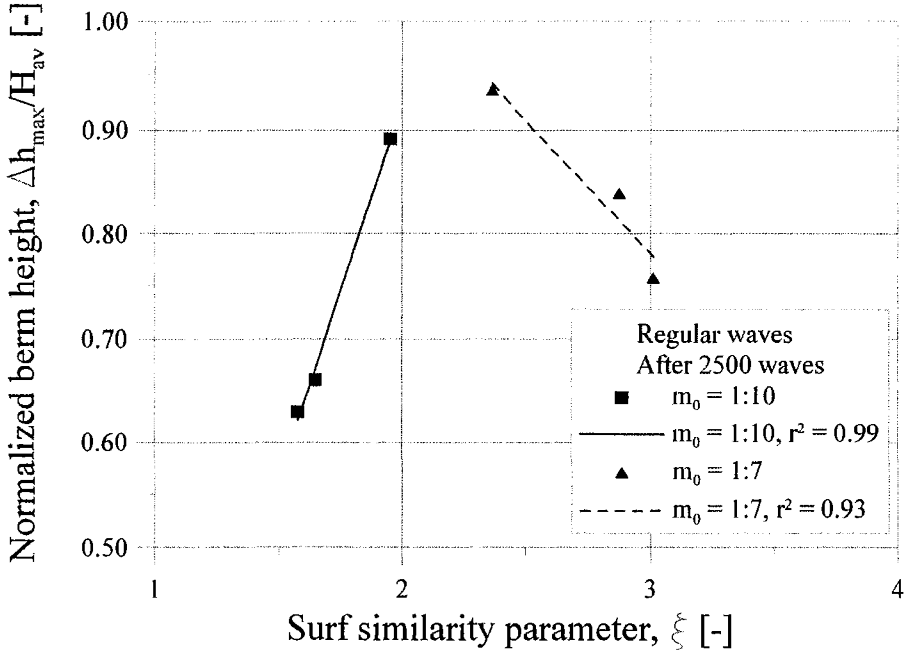

Figure 5.21 – Normalized change in berm height as a function of the surf similarity parameter, regular waves

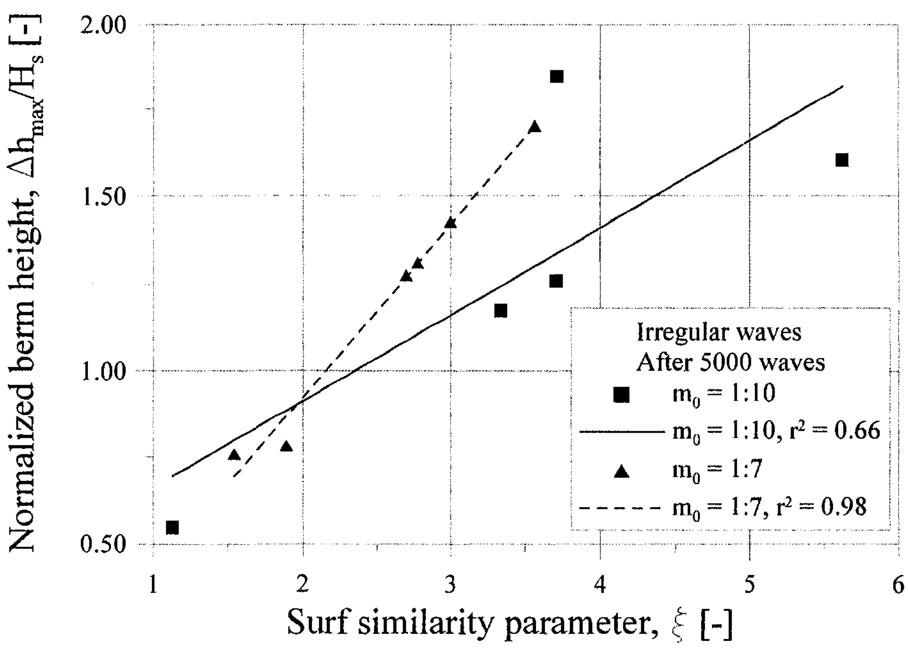

Figure 5.22 – Normalized change in berm height as a function of the surf similarity parameter, irregular waves

5.3.1.4 Influence of Wave Duration

In this section, the influence of wave duration on the beach profile changes is described. An attempt is made to derive a quantifiable relationship between wave duration and the increment in berm height or trough depth until a state of equilibrium beach profile is reached. On the vertical axis, a normalized factor is introduced. □ h is the maximum change at the berm or trough at each time step and □ h_{max} is the maximum berm height reached at the end of each test. Similarly, the maximum trough depth at the end of each test in denoted as □ h_{min}. Thus, the ratio of □ h/□ h_{max} describes the fraction of equilibrium berm development at each time step and □ h/□ h_{min} describes the percentage of trough development at each time step.

In Figure 5.23 and Figure 5.24, the berm development as a function of the wave duration is plotted for irregular waves. In these figures, the initial beach slopes are separated: in Figure 5.23, the initial slope is 1:10, while and the slope is 1:7 in Figure 5.24. By separating the beach slopes, it was possible to derive a power relationship with $r^2 > 0.90$. The figures show that for higher normalized change in berm height, the wave period is lower. Generating a power trendline of combined data values from Figure 5.23 and Figure 5.24 resulted in $r^2 = 0.83$ as seen in Figure 5.25.

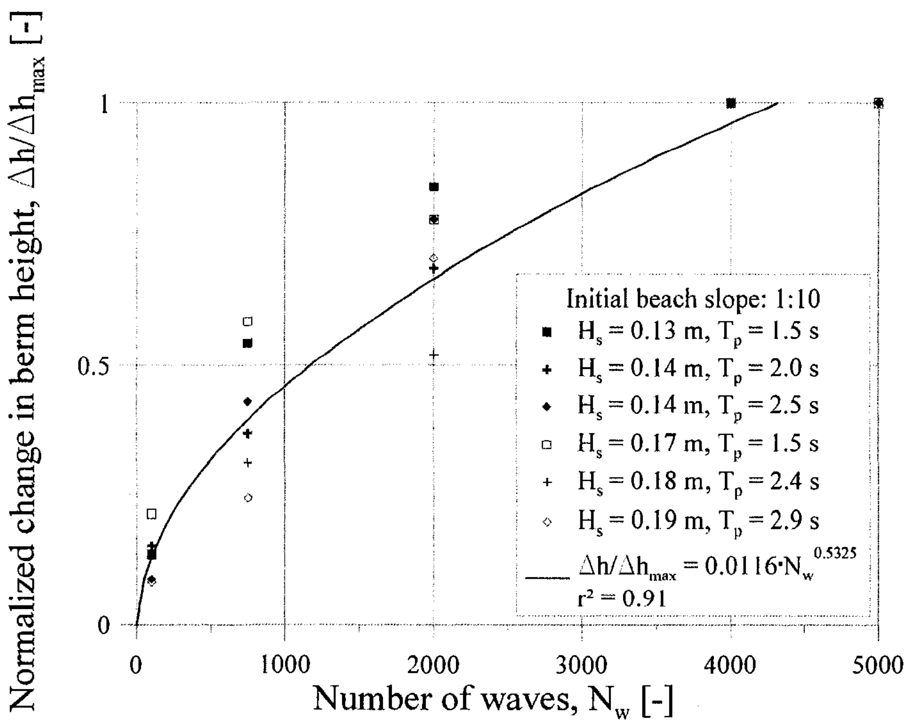

Figure 5.23 – Change in berm height as a function of wave duration, irregular waves, initial beach slope: 1:10

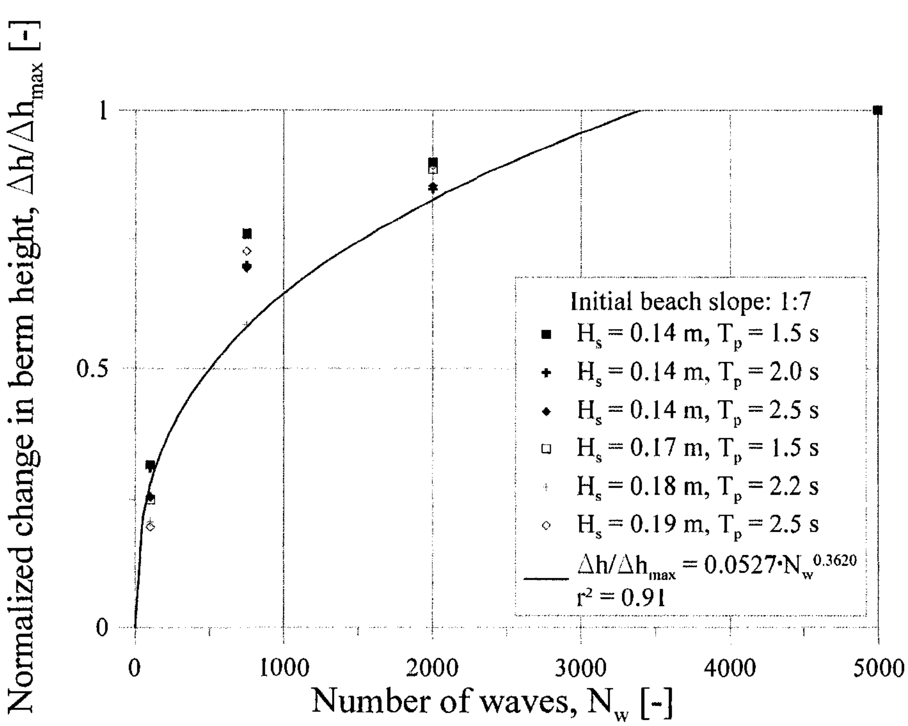

Figure 5.24 – Change in berm height as a function of wave duration, irregular waves, initial beach slope: 1:7

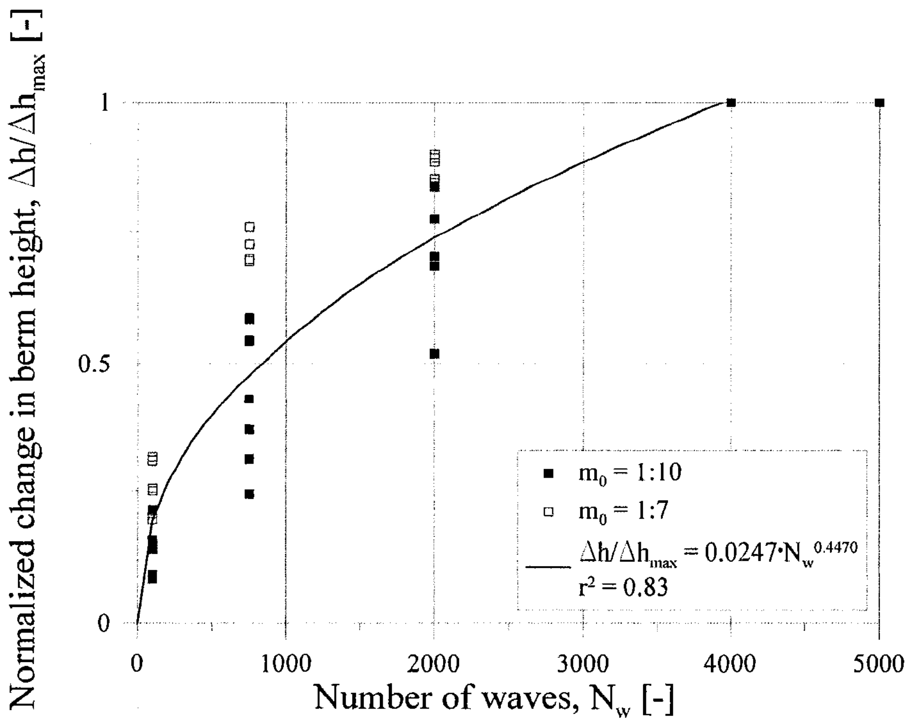

Figure 5.25 – Change in berm height as a function of wave duration, irregular waves

Similarly, the relationship between trough development and wave duration was investigated. Figure 5.26 shows the relationship between the normalized factor $\Delta h/\Delta h_{min}$ and wave duration until the profile equilibrium is reached for an initial beach slope of 1:10. The data points are more scattered for trough generation than in the case of the berm development. The coefficient of determination is $r^2 = 0.72$, compared to $r^2 = 0.91$ for Figure 5.23.

In the case of an initial beach slope of 1:7, the changes are occurring more rapidly at the early stages of the tests, as seen in Figure 5.27. Data points are not as scattered as in the previous figure dealing with an initial beach slope of 1:10.

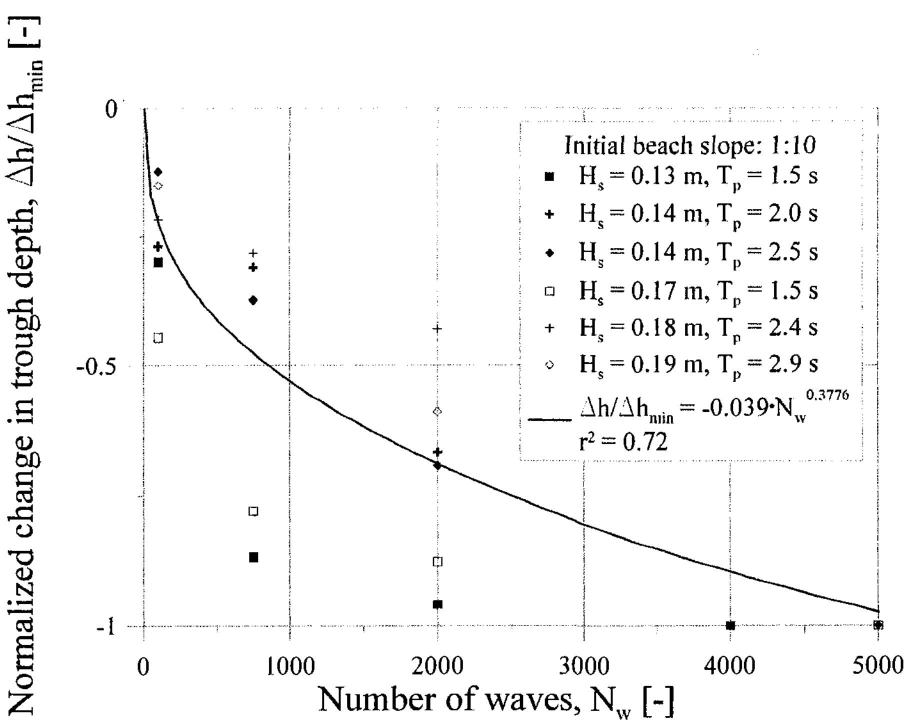

Figure 5.26 – Change in trough depth as a function of wave duration, irregular waves, initial beach slope: 1:10

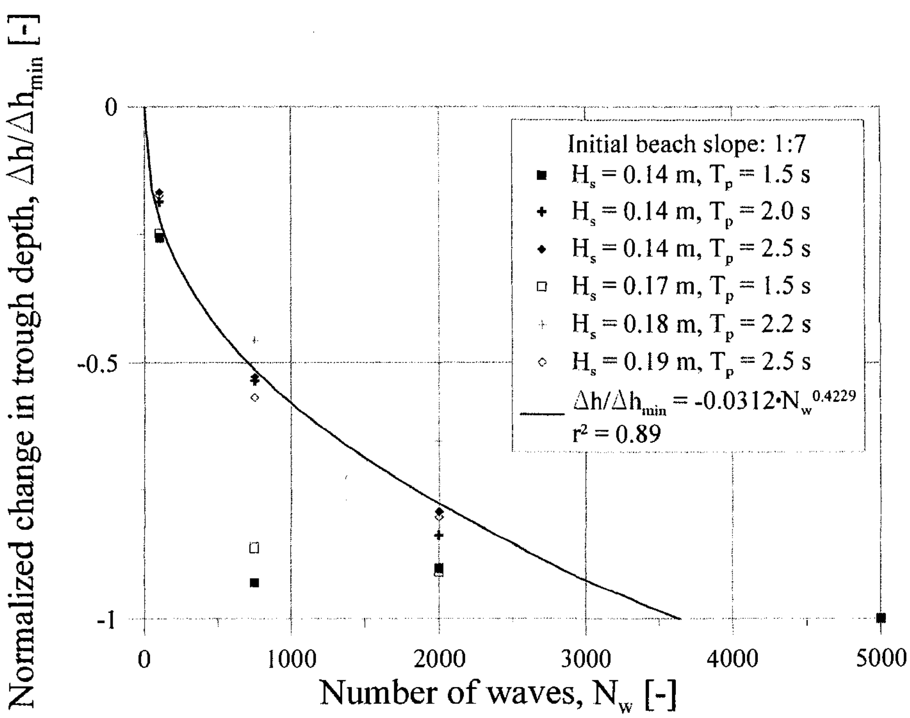

Figure 5.27 – Change in trough depth as a function of wave duration, irregular waves, initial beach slope: 1:7

Combining the results for both initial beach slopes, the power relationship shown in Figure 5.28 was obtained. A power trendline with $r^2 = 0.80$ was derived.

A similar analysis is performed for the case of regular waves. Figure 5.29 shows the beach berm development as a function of wave duration, where a state of equilibrium was reached after 2500 wave periods. The coefficient of determination only reaches 0.39 or 0.58 for the case of regular waves.

Figure 5.30 shows the development of the beach trough as a function of wave duration where the state of equilibrium was reached after 2500 wave periods.

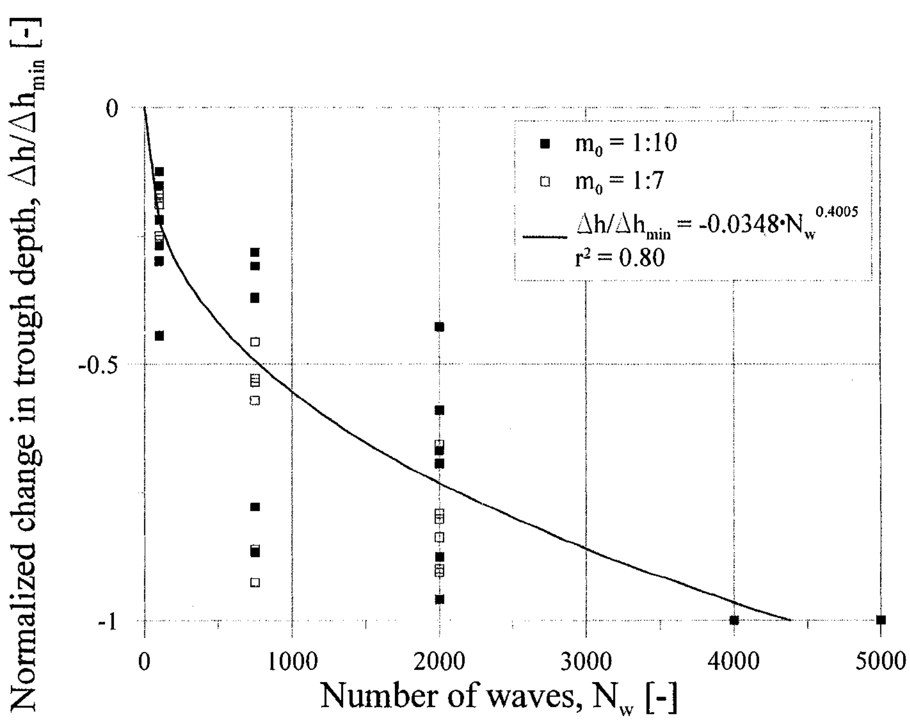

Figure 5.28 – Change in trough depth as a function of wave duration, irregular waves

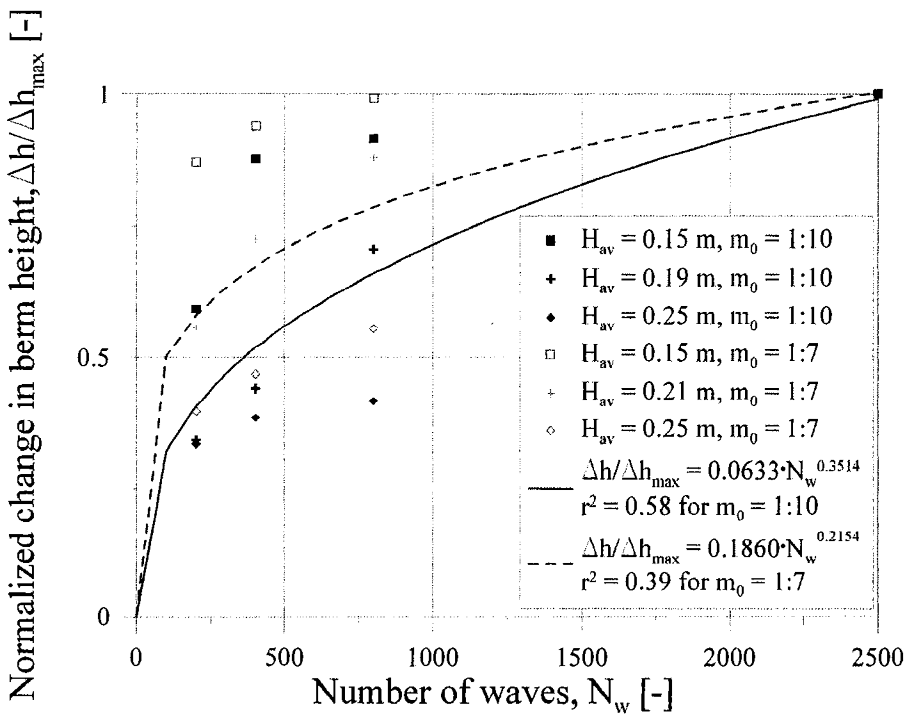

Figure 5.29 – Change in berm height as a function of wave duration, regular waves

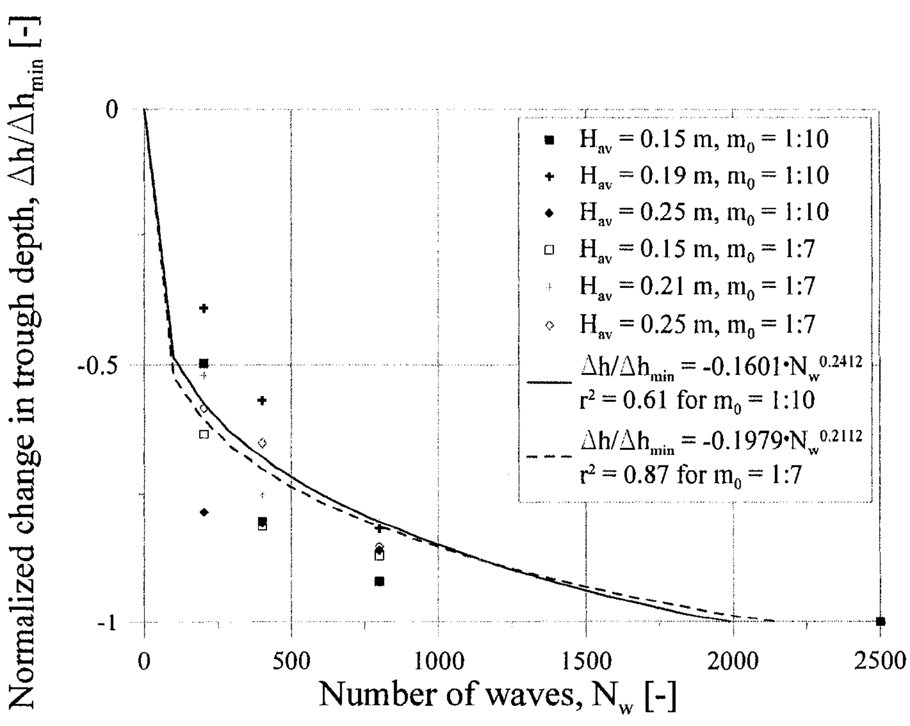

Figure 5.30 – Change in trough depth as a function of wave duration, regular waves

Again, as seen in Figure 5.29, the r^2 values for regular waves are significantly lower than those obtained for the case of irregular waves.

Table 5.11 through Table 5.13 list the relationships developed to describe the relationships between berm and trough development and wave action duration. The coefficient of determination is generally higher for irregular waves than for regular waves.

Table 5.11 – Relationships of berm and trough development and wave duration, initial beach slope: 1:10

Beach slope: 1:10	Berm generation	Trough generation
Irregular waves	$\frac{\Delta h}{\Delta h_{max}} = 0.0116 \cdot N_w^{0.5325}$ $(r^2 = 0.91)$	$\frac{\Delta h}{\Delta h_{min}} = -0.039 \cdot N_w^{0.3776}$ $(r^2 = 0.72)$
Regular waves	$\frac{\Delta h}{\Delta h_{max}} = 0.0633 \cdot N_w^{0.3514}$ $(r^2 = 0.58)$	$\frac{\Delta h}{\Delta h_{min}} = -0.1601 \cdot N_w^{0.2412}$ $(r^2 = 0.61)$

Table 5.12 – Relationships of berm and trough development and wave duration, initial beach slope: 1:7

Beach slope: 1:7	Berm generation	Trough generation
Irregular waves	$\frac{\Delta h}{\Delta h_{max}} = 0.0527 \cdot N_w^{0.3620}$ $(r^2 = 0.91)$	$\frac{\Delta h}{\Delta h_{min}} = -0.0312 \cdot N_w^{0.4229}$ $(r^2 = 0.89)$
Regular waves	$\frac{\Delta h}{\Delta h_{max}} = 0.1860 \cdot N_w^{0.2154}$ $(r^2 = 0.39)$	$\frac{\Delta h}{\Delta h_{min}} = -0.1979 \cdot N_w^{0.2112}$ $(r^2 = 0.87)$

Table 5.13 – Relationships of berm and trough development and wave duration, for both initial slopes

Combined beach slopes	Berm generation	Trough generation
Irregular waves	$\frac{\Delta h}{\Delta h_{max}} = 0.0247 \cdot N_w^{0.4470}$ $(r^2 = 0.83)$	$\frac{\Delta h}{\Delta h_{min}} = -0.0348 \cdot N_w^{0.4005}$ $(r^2 = 0.80)$
Regular waves	$\frac{\Delta h}{\Delta h_{max}} = 0.1085 \cdot N_w^{0.2834}$ $(r^2 = 0.46)$	$\frac{\Delta h}{\Delta h_{min}} = -0.6993 \cdot N_w^{0.2262}$ $(r^2 = 0.70)$

5.3.1.5 Influence of the Initial Beach Slope

Figure 5.31 and Figure 5.32 compare two tests with the same wave characteristics, but different initial beach slopes, 1:7 and 1:10. The profile changes are similar for both cases. Van der Meer (1988) compared gravel beaches with initial slopes of 1:3 and 1:5. In his experiments, the median grain size diameter was 11 mm, while the wave height and wave period were $H_s = 0.24$ m and $T_{av} = 1.8$ s, respectively. It was concluded that, in spite of different initial slopes, similar beach profile was reached between the berm and the step where erosion occurred. The same trend was observed in the case of the present experiment where the final slopes of the equilibrium beach profiles were similar, as seen in Figure 5.31.

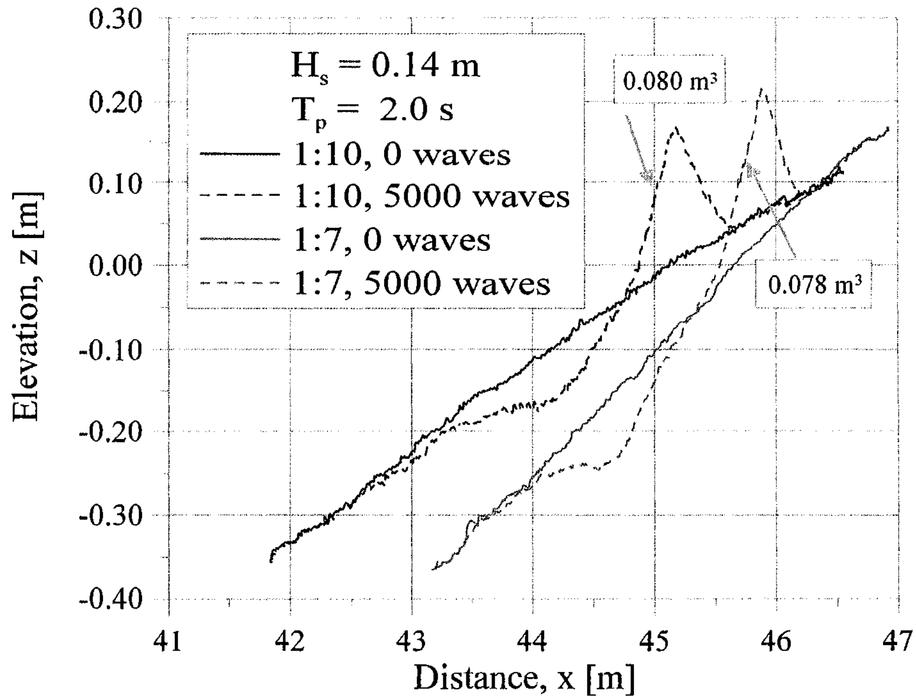

Figure 5.31 – Comparison between Test 5 and 14, after 5000 waves, $H_s = 0.14$ m, $T_p = 2.0$ s, irregular waves, different initial slope

In the case shown in Figure 5.31, the different initial slope did not seem to change the amount of transported sediment. For an initial beach slope of 1:10, 0.080 m^3 of material was transported after 5000 waves compared to 0.078 m^3 when the initial beach slope was 1:7.

A similar behaviour however, is not the case in Figure 5.32. In this case there is a significant difference in the amount of transported sediment; 0.032 m^3 when the initial beach slope is 1:10, but 0.041 m^3 when the initial beach slope is 1:7.

Figure 5.25 shows the berm generation for irregular waves as a function of wave duration. The solid squares are data points for an initial beach slope of 1:10 and the hollow squares are data points for an initial beach slope of 1:7. Clearly, there is a difference between these two data sets. In the case of the 1:7 beach slope, the generation of the berm occurs faster at the early stages of wave action. The higher ratio of □ h/□ h_{max} at 100, 750 and 2000 waves for m_0 = 1:7 indicates that changes in the profile occur more rapidly in the beginning than for m_0 = 1:10. However, the state of equilibrium was reached at the same time, or after 5000 waves. Also recalling Figure 5.28, the change in trough depth as a function of wave duration is obvious, but the trend observed in Figure 5.25 is not noticed; the data points for m_0 = 1:10 and m_0 = 1:7 are not separated.

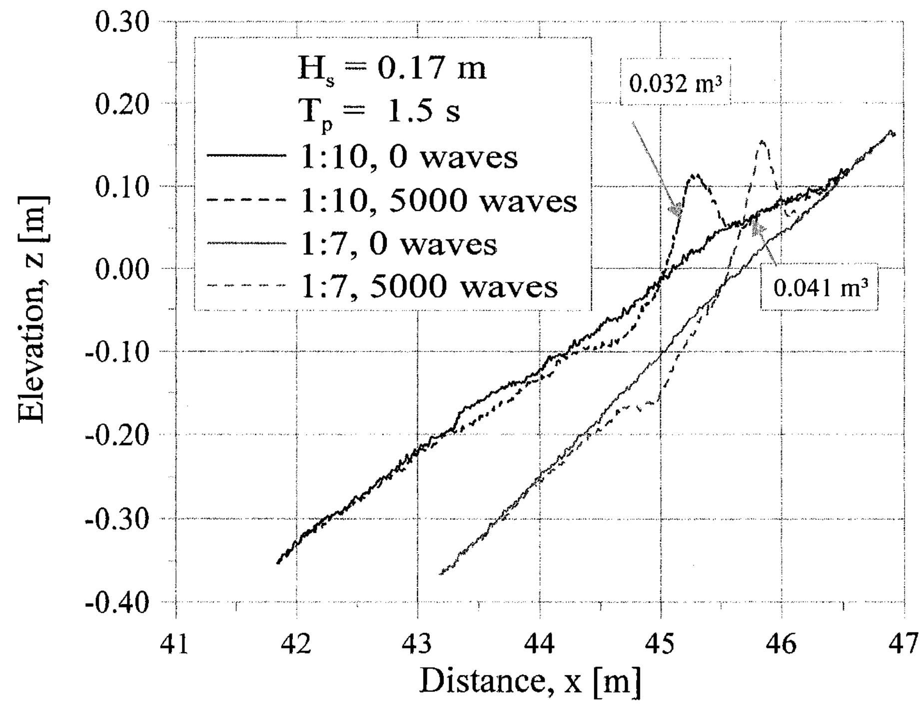

Figure 5.32 – Comparison between Test 7 and 16, after 5000 waves, H_s = 0.17 m, T_p = 1.5 s, irregular waves, different initial slope

5.3.2 Comparison between Tests with Similar Wave Characteristics

As mentioned earlier, Test 11 was repeated using similar wave characteristics in order to check whether the beach response is, as expected, similar in both cases. The repeated test, Test 19, was run at the end of the testing program. In these tests, waves were regular and the average wave period was $T_{av} = 2.0$ s. The target average wave height was $H_{av} = 0.20$ m in both cases. However, the measured values varied slightly. For Test 11, the average wave height was 0.21 m, while for Test 19 it was 0.18 m. Figure 5.33 shows the comparison of the beach profiles change for Tests 11 and 19. The initial beach slope was the same during both tests, 1:7.

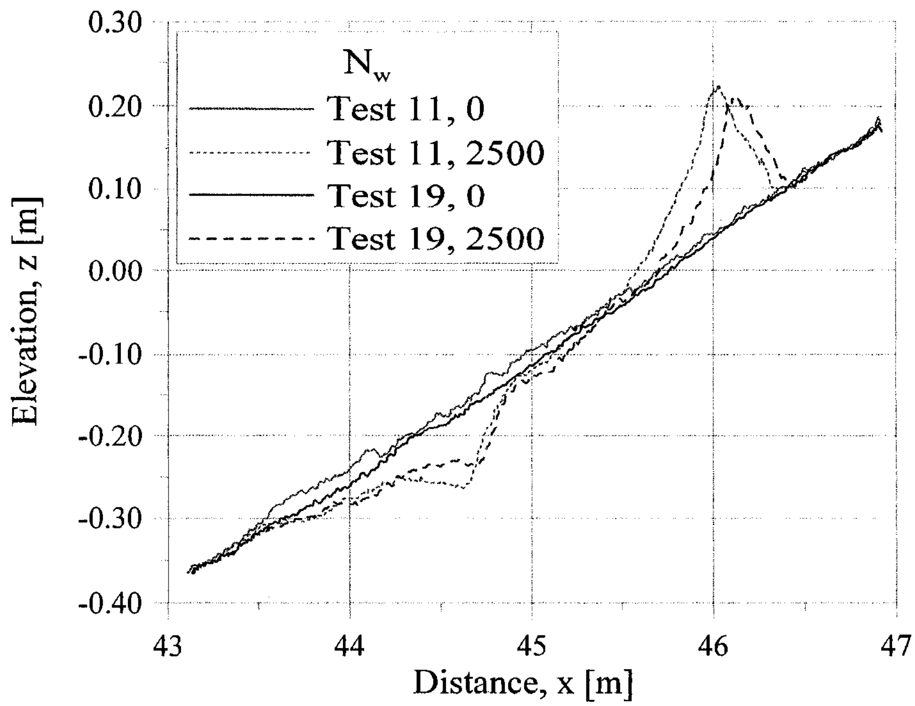

Figure 5.33 – Comparison of beach response in Test 11 and Test 19, similar wave characteristics

In both tests, the beach deformation pattern follows similar trends. However, in Test 19, the berm developed further onshore compared to Test 11 and the trough is not as deep. One explanation could be the initial beach slope. In both cases, the beach slope is 1:7 with 0.5% accuracy; however, the beach slope in Test 11 extends a little more offshore. Another explanation could be the difference in the average wave height. The average wave height turned out to be 0.18 m for Test 19 compared to 0.21 m for Test 11, which could explain the lower berm height and the lower trough depth for Test 19.

5.3.3 Cross-Shore Sediment Transport Rate

The relationship between the cross-shore sediment transport rate, q_x, and beach profile change, Δh, can be written as,

$$\frac{\Delta h}{\Delta t} = \frac{1}{(1-n)} \frac{\Delta q_x}{\Delta x} \tag{5.15}$$

and considering the porosity of the material used in the present experiment, n = 0.365, the equation above can be re-written as,

$$\frac{\Delta h}{\Delta t} = 1.575 \frac{\Delta q_x}{\Delta x} \tag{5.16}$$

By separating variables and integrating this partial differential equation, it is possible to determine the cross-shore sediment transport rate, q_x [$m^3/m/s$], at any given time and at given location in the onshore-offshore direction. A positive sediment transport rate denotes accumulation or accretion while a negative value indicates erosion.

The sediment transport rate was calculated and plotted for all tests. In the case of regular waves, the sediment transport rate was calculated after 50, 400, 800 and 2500 waves, that is, simultaneously with the beach profile measurements. For irregular waves, the sediment transport rate was calculated after 100, 750, 2000 and 5000 waves. Sediment transport rate plots for all 19 tests are presented in Appendix D. The graphs showing the time-evolution of the sediment transport rate are indicative of the development towards the state of equilibrium in the beach profiles. As seen in Figure 5.34, the magnitude of the rate of sediment transport is highest between 50 and 400 waves, with erosion reaching (-0.08) $m^3/m/s$ (cubic meters per second per meter of the flume's width) and accretion as high as 0.12 $m^3/m/s$. As the duration of wave action increases, the sediment transport rate decreases. Between 800 and 2500 waves, the highest value for accretion is 0.01 $m^3/m/s$ and (-0.03) $m^3/m/s$ for erosion, which is significantly lower than the rate calculated for the period between 50 and 400 waves, even though the earlier duration of wave action is significantly shorter.

The trend shown in Figure 5.34 (regular waves) and in Figure 5.35 (irregular waves), where the sediment transport is the highest at the early stages of beach profile development is typical for all tests, as can be seen in the graphs presented in Appendix D. However, there are a few exceptions (as found in Tests 3, 7 and 8), where the highest sediment transport rate is found within the last range of wave duration. In the case of Test 3, the profile was still changing a lot after 2500 wave impacts and measurements were continued throughout 12000 waves.

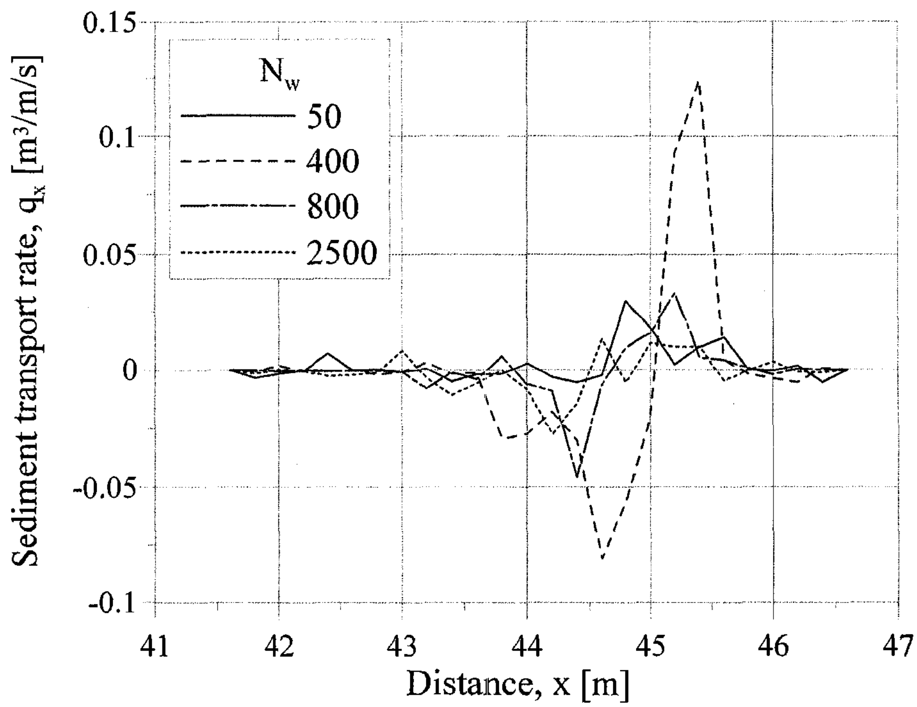

Figure 5.34 – Sediment transport rate, Test 1: Regular waves, T_{av} = 2.0 s, H_{av} = 0.15 m, initial beach slope: 1:10

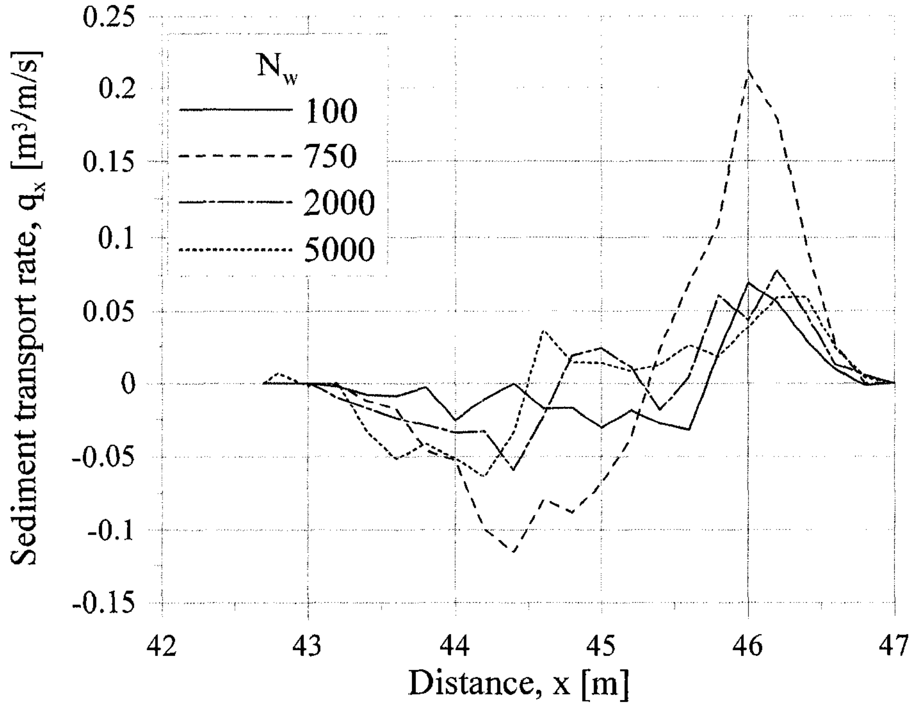

Figure 5.35 – Sediment transport rate, Test 18: Irregular waves, T_p = 2.5 s, H_s = 0.19 m, initial beach slope: 1:7

5.3.4 Interaction between Beach Morphology Evolution and the Wave Climate

Some interesting observations were made on the changes in wave characteristics as the beach profile changed under wave attack over time. As the beach profile changed over time, the decay of wave height across the beach also modified. As the depth of the beach trough increased, wave heights increased while where accumulation took place, wave heights decreased. Information on the average crest height, □c, and average trough excursion, □t, can be determined at each location where wave gauges were positioned.

Figure 5.36 shows the average crest height (positive values) and the average trough depth (negative values) after 100, 750, and 5000 waves. The beach profiles after 100, 750, and 5000 waves are also plotted in Figure 5.36. In this figure, the average crest heights and trough depths are also plotted using data from the three wave gauges located in the surf zone. The still water level is denoted as SWL. Waves were irregular and the beach slope was 1:10.

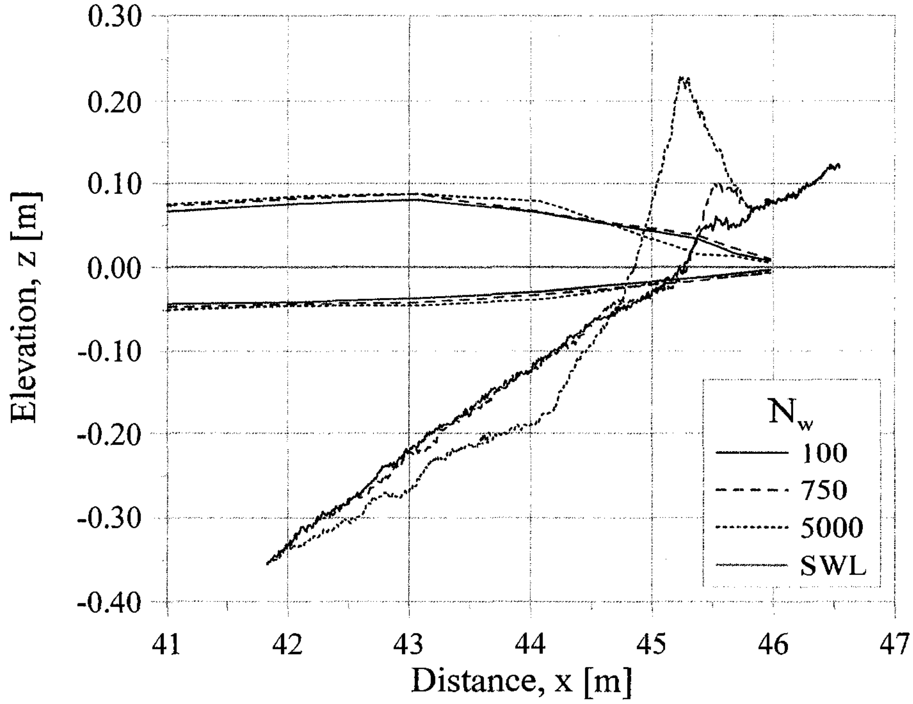

Figure 5.36 – Average crest height and trough depths, Test 8:
T_p = 2.4 s, H_s = 0.18 m, initial beach slope: 1:10

As the number of waves increased, erosion occurred between 42 m and 44.5 m. As the water depth in that particular range increased due to erosion, the wave height slightly increased, resulting in higher wave crest heights and lower wave trough depths. This is expected when looking at the relationship between water depth and wave height in Eq. (5.9).

Figure 5.37 shows the average crest and trough amplitudes for irregular waves and when the beach slope is 1:7.

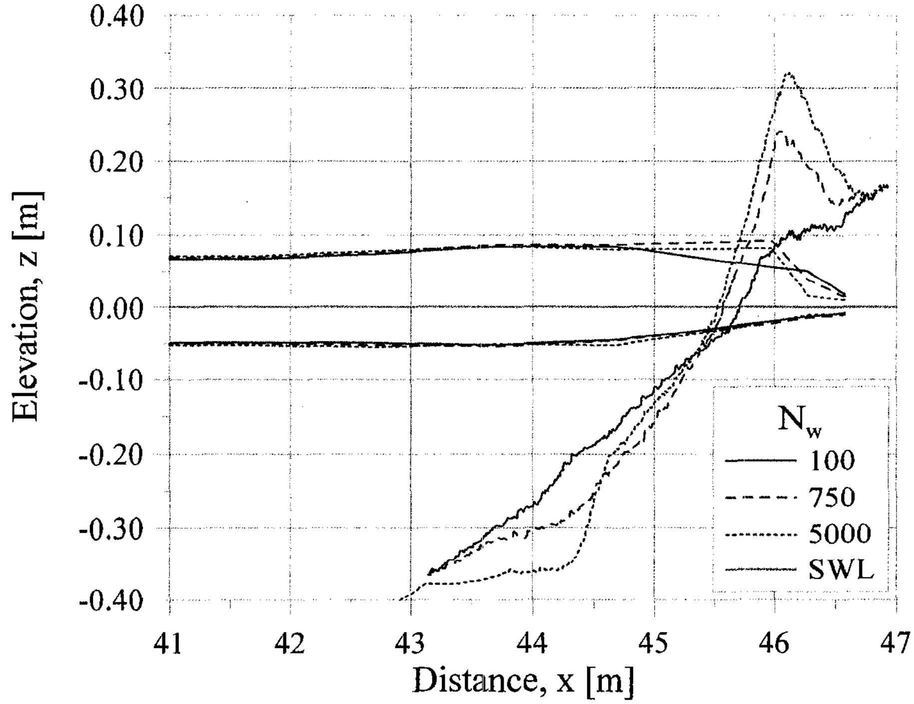

Figure 5.37 – Average crest heights and trough depths, Test 18:
T_p = 2.5 s, H_s = 0.19 m, initial beach slope: 1:7

Changes in the wave amplitudes are not significant but it is interesting to notice that from x = 44.5 to 45.5 m wave amplitudes are higher after 750 waves than after 5000 waves. At that location, the water depth is reduced after 5000 waves due to movement of the sediment.

In the case of regular waves, the first reliable results of the average crest and trough heights are available after 200 waves. The first two wave runs consisted of only 50 waves each, which is not enough to perform the zero-up crossing analysis on the wave data. For regular waves, the average crest and trough height are plotted together with the beach deformation after 200, 400 and 2500 waves.

Figure 5.38 presents the interaction between the beach deformation evolution and wave crest and trough height of the waves for a case with regular waves. The influence of the water depth on the change in wave height is obvious at x = 44.7 m (as indicated by the arrows) where the beach erodes significantly the wave height increases. In this case, fortunately, the wave gauge is perfectly located, i.e. just above the eroded area of interest.

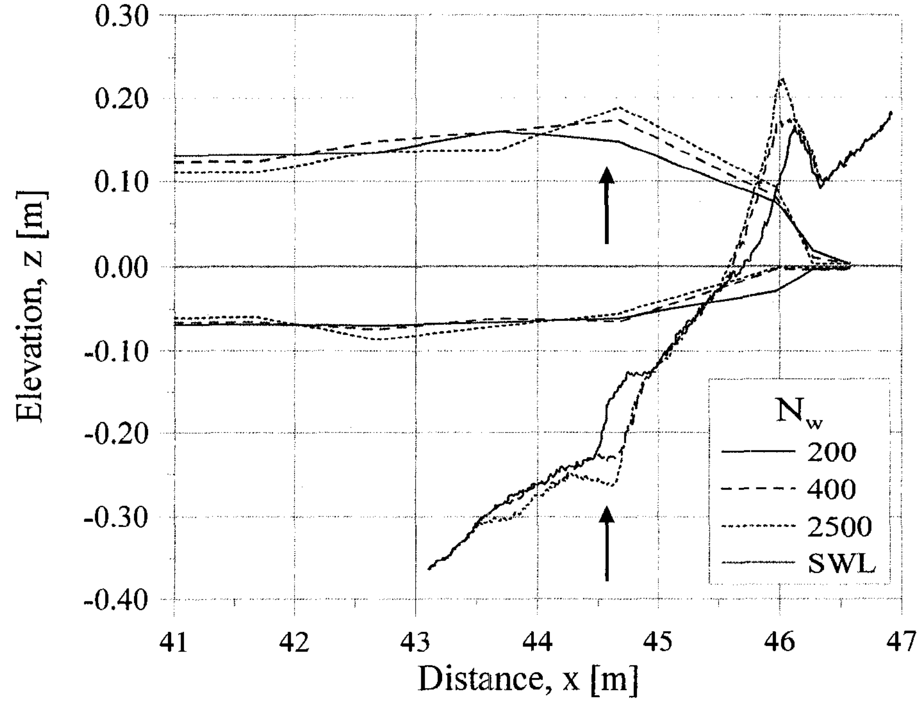

Figure 5.38 – Average crest and trough heights, Test 11:
T_{av} = 2.0 s, H_{av} = 0.21 m, initial beach slope: 1:7

5.4 Wave Reflection Analysis

Waves are reflected by beaches and coastal structures such as breakwaters and seawalls. When hitting a vertical impermeable wall, waves are completely reflected. However, when they impact a beach or a breakwater, a part of their energy is dissipated by the structure and this results in waves being partially reflected (Kamphuis, 2000). In the flume used, waves were reflected by the beach and again re-reflected by the board of the wave generator. To minimize the re-reflection, an active wave absorption system (AWA) was employed by the wave generator in Tests 1 to 3 and 10 to 19. In Tests 4 to 9, reflection was not considered to be significant since the beach slope was gentle and the waves were irregular.

The water surface elevation consists of two parts: the surface elevation of the incident wave train □(t) and the surface elevation of the reflected wave train □(t) (Hughes, 1993).

$$\eta(t) = \eta_i(t) + \eta_r(t) \tag{5.17}$$

A method to separate the incident waves and the reflected waves in the flume has been developed at CHC and this method was used in this study. Figure 5.39 shows a sample of irregular waves separated into incident and reflected waves (Test 5, after 5000 waves).

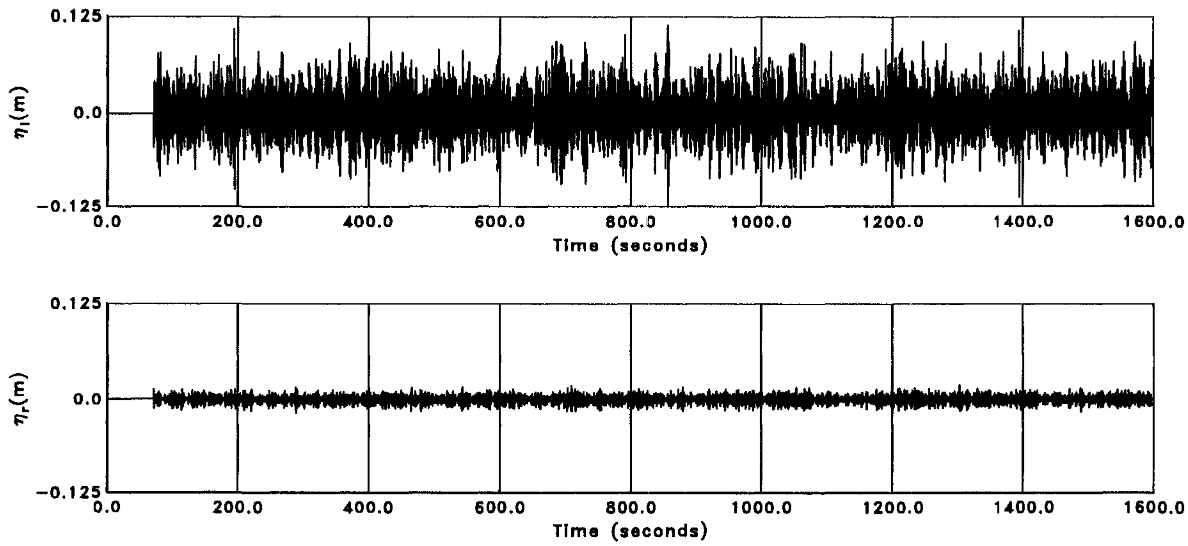

Figure 5.39 – Samples of separated incident wave train (η_i) and reflected wave train (η_r), irregular waves (Test 5)

An array of five wave gauges (WG4 to WG9) was located approximately 26 metres away from the wave generator. These wave gauges were used for the wave reflection analysis. A GEDAP program, PRBSP, chose three optimal wave gauges out of five for further analysis. For each data set, the reflection analysis procedure generates the following information (Mansard and Funke, 1987):

- The wave train for incident waves
- The wave train for reflected waves
- The incident wave spectrum
- The reflected wave spectrum

- The average reflection coefficient
- The reflection coefficient spectrum
- The error as a function of the reflection coefficient spectrum

The GEDAP analysis package includes several programs for determining the wave reflection coefficient:

- REFLA – Separates the incident and the reflected spectra from a measured sea state. The method is based on the least square analysis with data collected from three wave gauges.
- REFLM – Applies only to regular waves. The method is based on the least square analysis of a sinusoidal wave. The method does not account for secondary waves.
- REFLS – The method is based on linear wave theory. The average reflection coefficient (C_r) is quantified as

$$C_r = \frac{\sigma_r}{\sigma_i} \tag{5.18}$$

where σ_r is the standard deviation of the reflected wave train, $\eta_r(t)$ and σ_i is the standard deviation of the incident wave train, $\eta_i(t)$.

For regular waves, the programs REFLM and REFLS should generate similar values for the average reflection coefficient. Also, for irregular waves, REFLA and REFLS should generate similar values for the average reflection coefficient. However, that was not the case in this study, especially for large wave heights. This can be explained by the fact that REFLS is based on the linear wave theory and relies on small wave amplitudes and deep water conditions. Accordingly, incident and reflected waves are not always separated with accuracy. Thus, the average reflection coefficient is not always correctly calculated by REFLS. In this study, the average reflection coefficient was therefore calculated using REFLM for the case of regular waves and with REFLA for the cases involving irregular waves. Tests were run until the state of equilibrium profile was reached, that is until very little or no change occurred with respect to the beach profile under wave action. This state of equilibrium can also be noticed in the following graphs outlining the variation of the reflection coefficient with respect to the test duration. In Figure 5.40, the reflection coefficient, C_r, is plotted against the duration of the wave action. In this case, waves are regular and the wave height and period are constant. The initial beach slopes, m_0, are 1:10 and 1:7.

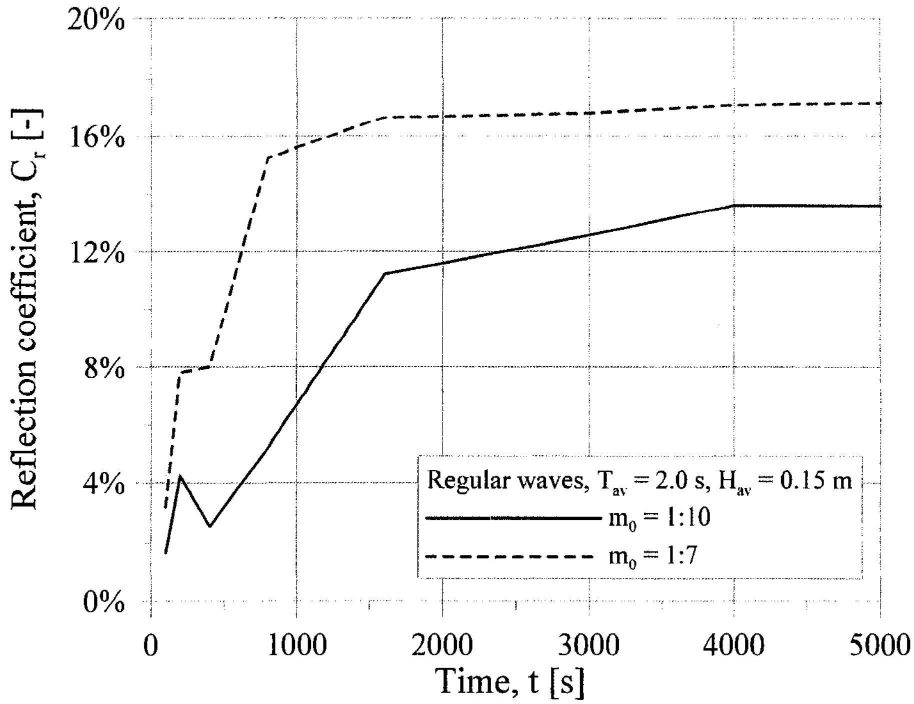

Figure 5.40 – Variation of the reflection coefficient, regular waves, T_{av} = 2.0 s, H_{av} = 0.15 m

Figure 5.40 is indicative of how the state of equilibrium is reached. The reflection coefficient increases rapidly at the beginning of the test during which time the beach profile is also changing rapidly. As expected, the steeper 1:7 beach is also more reflective than the 1:10 beach. This is not surprising, since a steeper beach slope is more reflective. Figure 5.41 prepared for the case of irregular waves shows a similar trend to that shown in Figure 5.40. Wave height and period are both constant. The initial beach slopes, m_0, are 1:10 and 1:7.

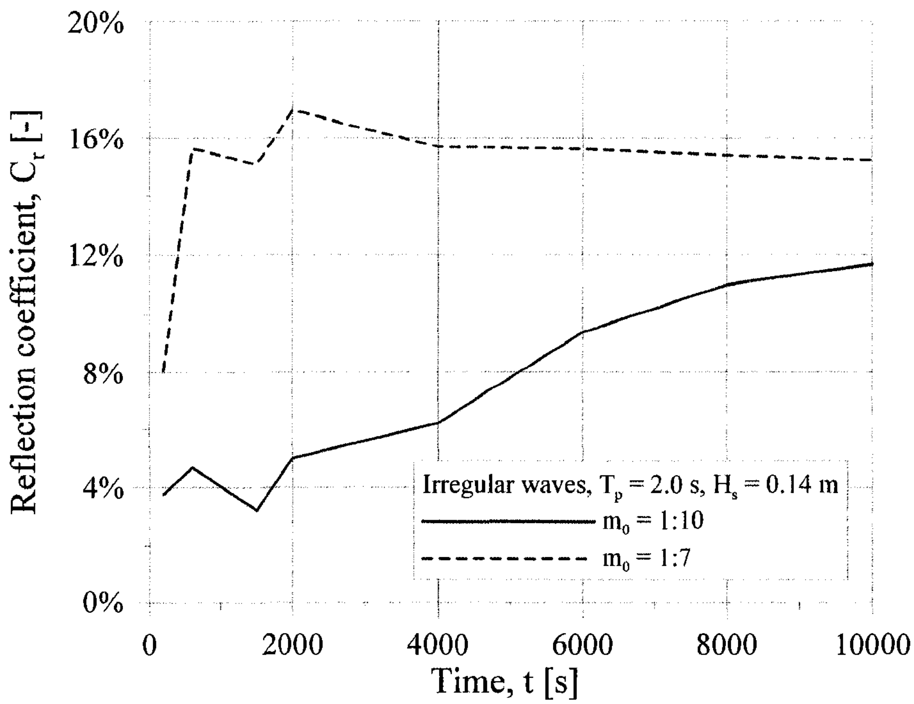

Figure 5.41 – Variation of the reflection coefficient, irregular waves, T_p = 2.0 s, H_s = 0.14 m

As in the case shown in Figure 5.40, the rate of change of the reflection coefficient is significant during the initial wave action period and reduces thereafter. For m_0 = 1:10, the changes are not as rapid as in the case of m_0 = 1:7. The influence of the wave period on the reflection coefficient is illustrated in Figure 5.42. Larger period waves are clearly reflected more than waves with shorter periods.

The influence of the significant wave height on the wave reflection is illustrated in Figure 5.43 and Figure 5.44. Wave reflection decreases with an increase in the significant wave height. This could be due to increased energy dissipation through wave breaking.

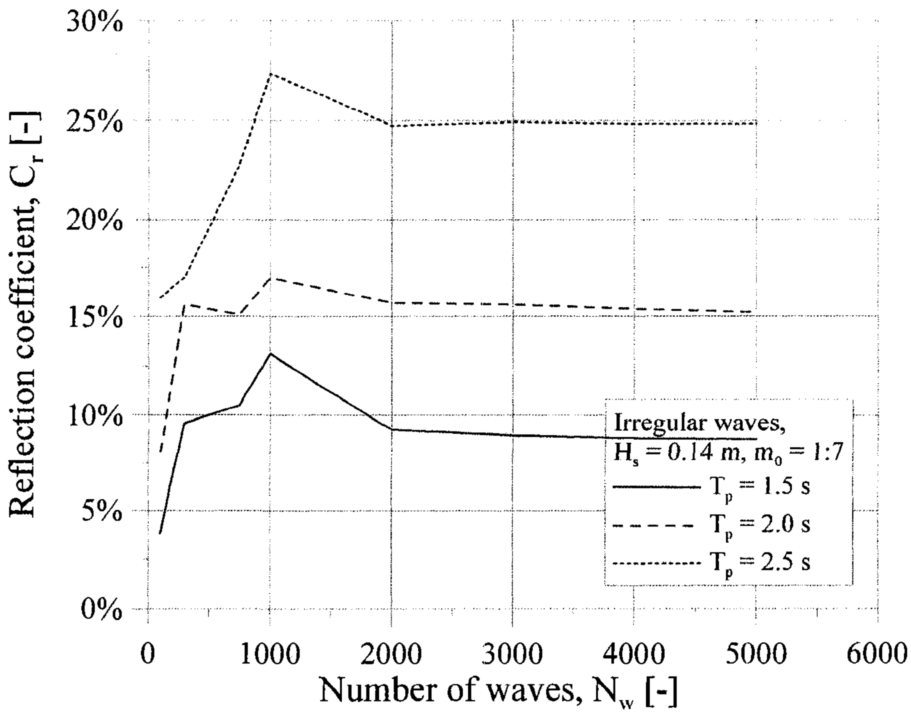

Figure 5.42 – Variation of the reflection coefficient, irregular waves, H_s = 0.14 m, m_0 = 1:7

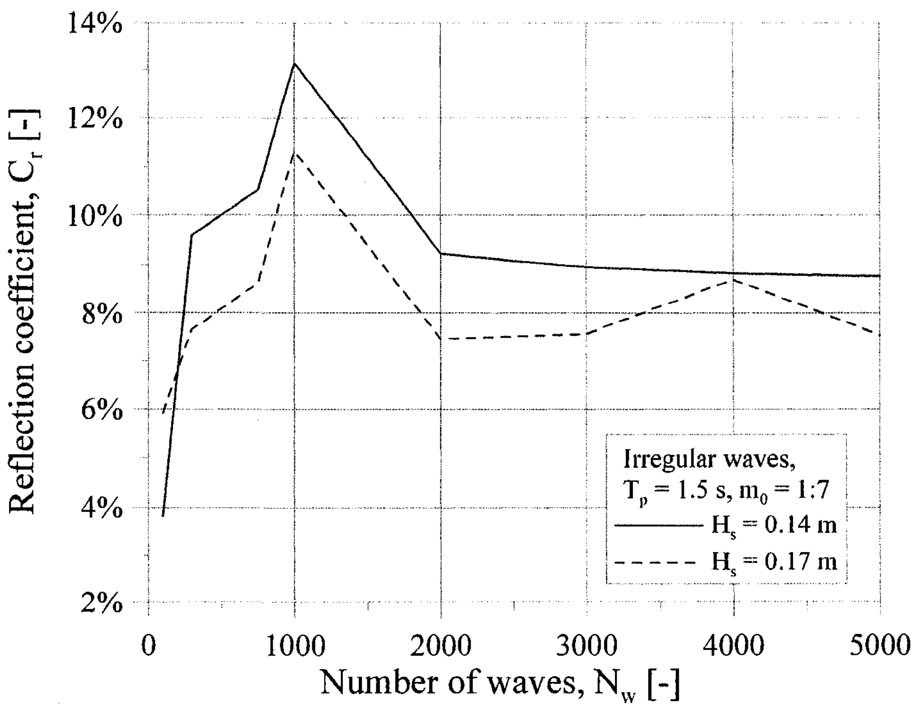

Figure 5.43 – Variation of the reflection coefficient, irregular waves, T_p = 1.5 s, m_0 = 1:7

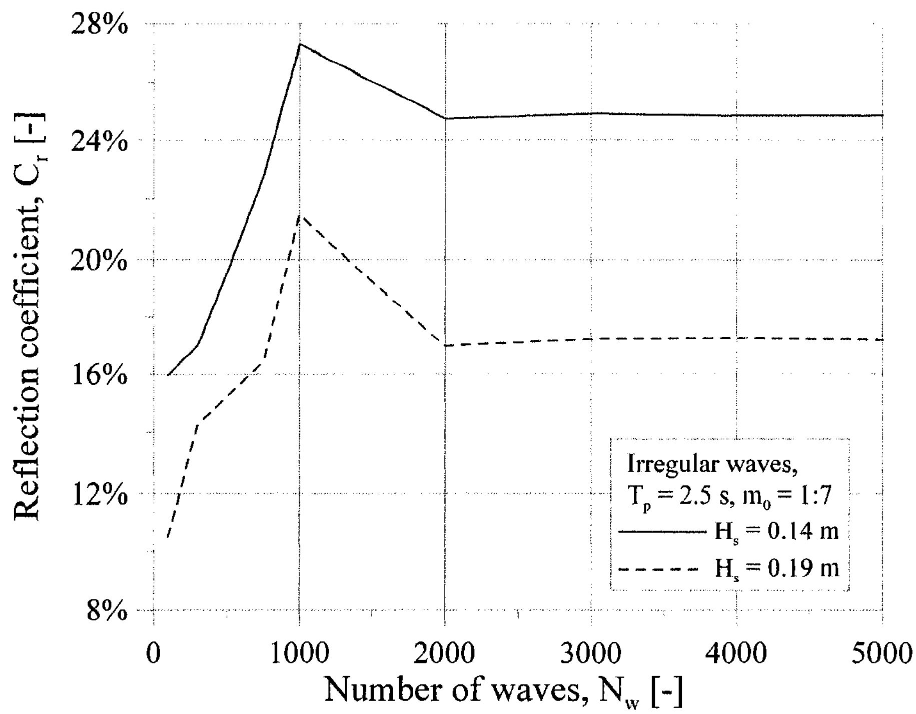

Figure 5.44 – Variation of the reflection coefficient, irregular waves, $T_p = 2.5$ s, $m_0 = 1:7$

The trend observed in Figure 5.43 and Figure 5.44 with respect to the reflection coefficient's maximum value after 1000 waves can be further explained. The wave reflection coefficients seem to reach a peak value and then decrease to a constant value. In both previously mentioned figures, during the first 1000 waves, the beach faces become steeper and the beach berms become higher. Following 1000 waves, the beach berms retain their equilibrium profile.

Several researchers developed equations to predict the variation of the wave reflection coefficient with wave and beach characteristics. The surf similarity parameter is used to account for the wave characteristics (see Table 5.14).

As noted by Postma (1989), one has to compare prudently different wave reflection data sets and formulas. Large differences in wave flume test set-up and used methodology may lead to significant differences in the determination of the wave reflection coefficient.

Table 5.14 – Empirical reflection coefficients by various researchers

Author	Equation	Structure/Limitations
Battjes (1974)	$C_r = 0.1 \cdot \xi^2$ (5.19)	Impermeable slope, beach slope: 1:3.3-1:10, valid for □< 2.5
Seelig and Ahrens (1981)	$C_r = \dfrac{0.6 \cdot \xi^2}{6.6 + \xi^2}$ (5.20)	Rough permeable slope (Benassai, 2006))
Losada and Giménez-Curto (1981)	$C_r = 0.503 \cdot \left(1 - e^{-0.1248 \cdot \xi}\right)$ (5.21)	Rough, rubble permeable slope, beach slope: 1:1.5, Regular waves
Postma (1989)	$C_r = 0.14 \cdot \xi^{0.73}$ (5.22)	Impermeable/permeable slope, straight beach slope: 1:1.5-1:6, D_{50} = 40 mm, valid for □< 8
Zanuttigh and Van der Meer (2007)	$C_r = \tanh\left(0.12 \cdot \xi^{0.87}\right)$ (5.23)	Permeable rock slopes, formula slightly overestimates C_r for □< 4

It should be emphasized that none of the equations in Table 5.14 apply to the conditions used in the present study. Therefore, care should be taken in drawing any clear-cut conclusions from comparing the present experimental data with the above mentioned equations. However, looking at the relationships that have been proposed between reflection coefficients, wave characteristics and rubble-mound slopes is a worthwhile exercise.

Equations shown in Table 5.14 are derived mostly from studies on breakwaters which are steeper and rougher structures than gravel beaches and are expected to dissipate less energy than gravel beaches. To the author's knowledge, no formulas describing wave reflection from gentle gravel beaches exist. Postma (1989) used data collected by Van der Meer (1988) and investigated wave reflection from trapezoidal rubble mound breakwaters, where mean grain size diameter was 40 mm. Postma (1989) stated that the wave period apparently influenced more the reflection behaviour than wave height.

Also, the current literature review outlined the lack of theoretical formulations which would include the porosity in order to describe the relationship between the reflection coefficient and the surf similarity parameter. Only Van der Meer (1993) categorized structures depending on whether they had an impermeable core and different types of armour layers, with or without filters or permeable armour with no core or filter. Van der Meer's (1993) proposed equation is,

$$C_r = 0.071 \cdot P^{-0.082} \cdot \xi_{vdM} \tag{5.24}$$

where the surf similarity, ξ is determined as

$$\xi_{VdM} = \tan^{0.62}(\alpha)\left(\frac{2 \cdot \pi \cdot H}{g \cdot T^2}\right)^{-0.46} \tag{5.25}$$

and is valid for $\xi_{VdM} < 9$. The parameter P is Van der Meer's permeability coefficient which has no physical meaning. For uniformly distributed material (as in this study), with no core or layers, Van der Meer (1988) recommends using P = 0.6.

In Figure 5.45 and Figure 5.46, the reflection coefficient values for tests employing regular and irregular waves are plotted as functions of the surf similarity parameter, respectively. Curves fitted by Eqs. (5.19) – (5.23) in Table 5.14 are plotted alongside for comparison. Eq. (5.24) is also included in the figures where Van der Meer's surf similarity parameter, ξ_{VdM}, is taken as ξ and is plotted as a function of the reflection coefficient.

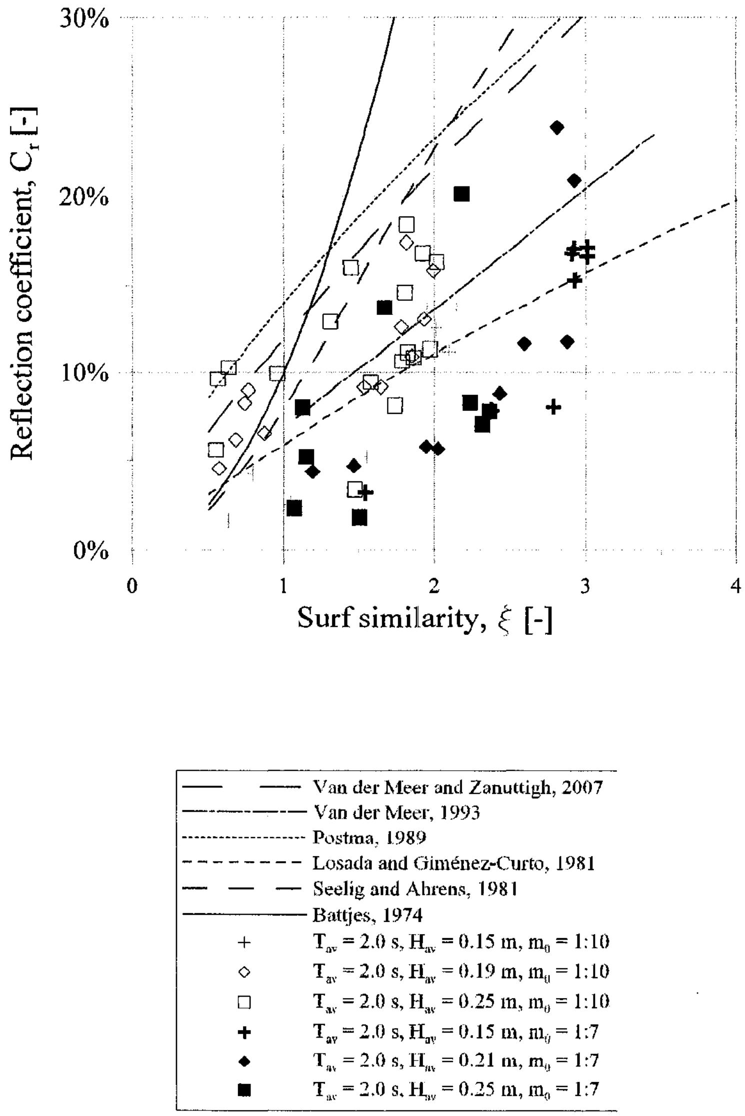

Figure 5.45 – Comparison between reflection coefficients observed in experiment (regular waves) with existing formulas

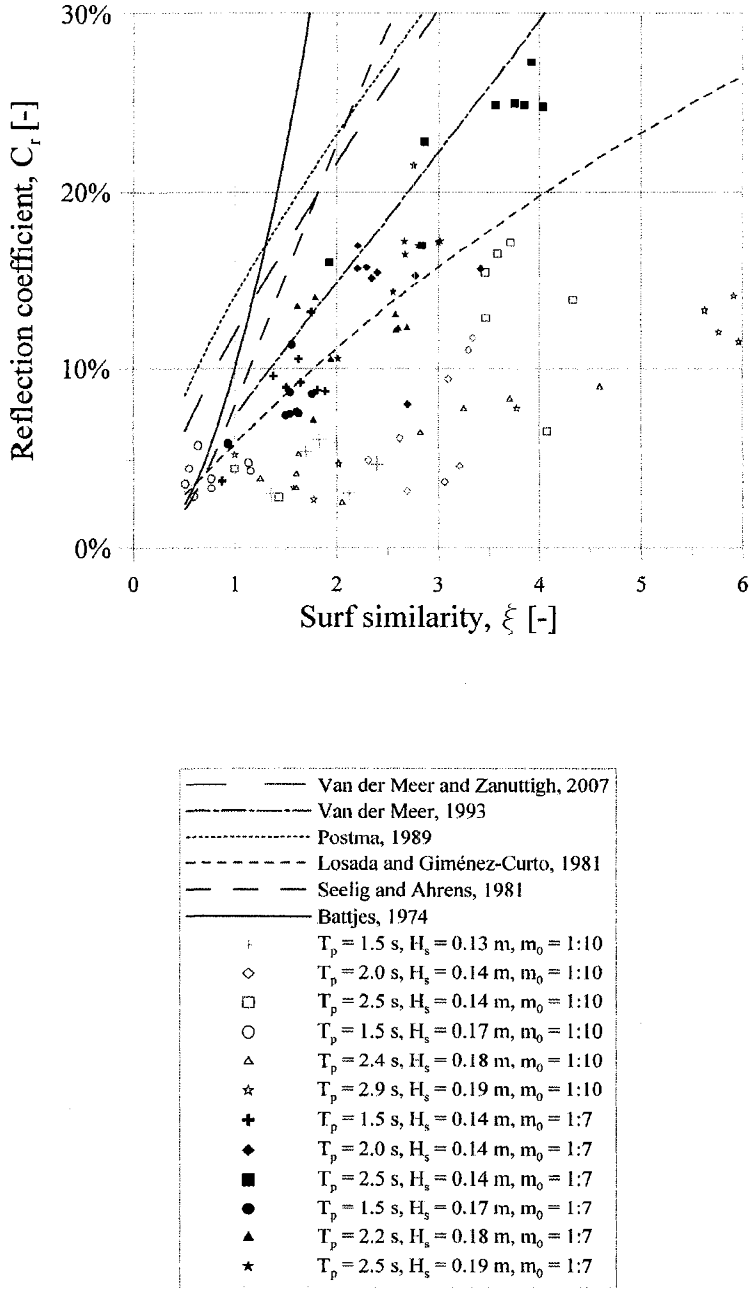

Figure 5.46 – Comparison between reflection coefficients observed in experiment (irregular waves) with existing formulas

As mentioned earlier, the equations plotted along with the experimental data are mainly from breakwater studies were the slope is steeper and the surface significantly rougher. Considering the different characteristics of a gravel beach comparing to the surface roughness of a breakwater, the positions of the reflection coefficients from experimental data below the equation curves in Figure 5.45 and Figure 5.46 make physical sense.

The only two equations closer to the experimental data points in Figure 5.45 and Figure 5.46 are the ones from Eq. (5.21) developed by Losada and Giménez-Curto (1981) and Eq. (5.24) proposed by Van der Meer (1993). Losada and Giménez-Curto (1981) developed a model for regular wave reflection on rough and permeable 1:1.5 slopes. The rubble was quarry stone of unknown diameter. The ratio between depth at the toe of the slope and wave height was d_t/H 3.95. In the present study, this ratio is $d_t/H = 2.40 - 4.00$.

Interesting enough, for regular waves (Figure 5.45), data points for an initial beach slope of 1:7 lie higher than the ones generated for an initial beach slope of 1:10, while for irregular waves (Figure 5.46), the data points for the 1:10 slope beach lie higher. This separation is more obvious in Figure 5.46. It seems like the influence of beach slope in the surf similarity parameter is not enough to offset the variation of the beach slope. This is also indicative of the fact that the same formula may not work for both regular and irregular waves, nor for the two different beach slopes.

It should be noted that after the beach deformation occurred, the beach became a composite beach structure from a slope point of view, whereas available formulas only consider linear, uniform slopes. Therefore, one should investigate the wave reflection before any significant changes occur in the beach face. Figure 5.47 shows the reflection coefficients and the corresponding surf similarity for case of tests with irregular waves. The dots in the graph represent data from the first 100 waves for each of the 12 tests performed with irregular waves. At that particular instant, the beach deformation is negligible and the beach slope is therefore not a composite one. Beach slope is therefore considered to be the initial beach slope.

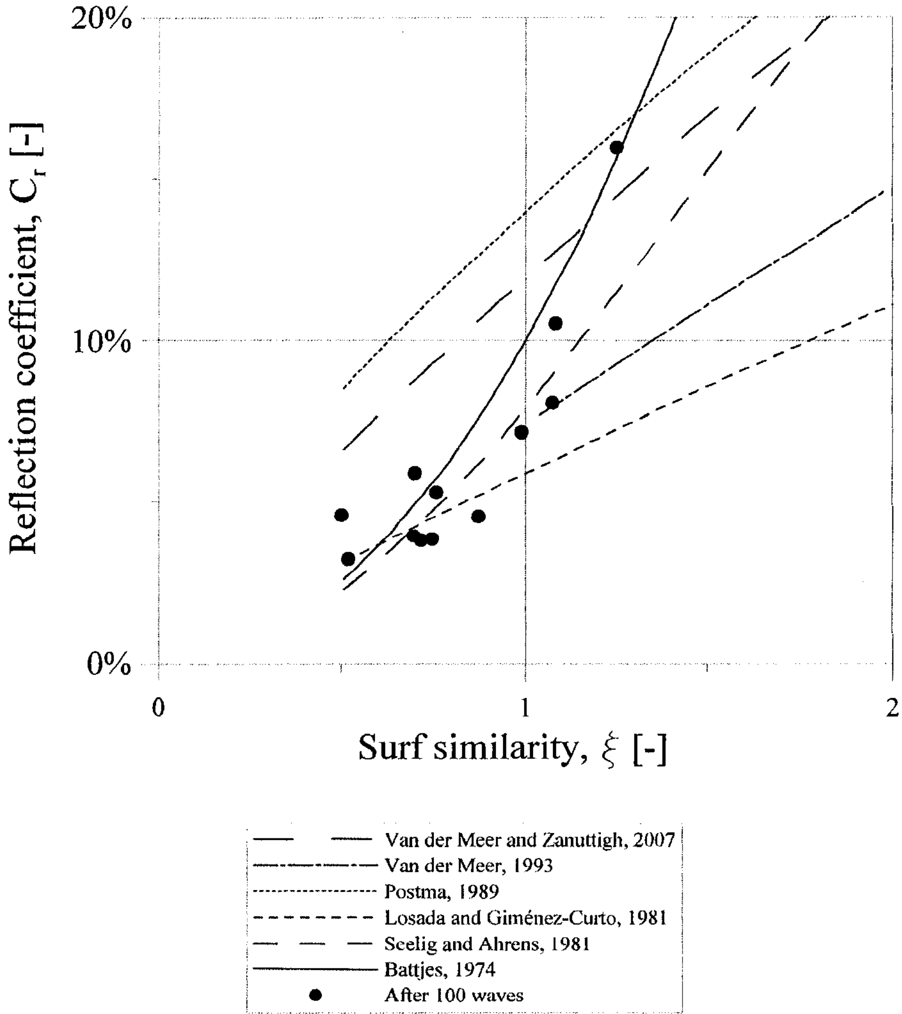

Figure 5.47 – Comparison between reflection coefficients observed in experiment (irregular waves) with existing formulas, after 100 waves

In this case, the experimental data points plotted on Figure 5.47 seem to be much closer to some of the formulas previously mentioned (Eq. (5.19) through (5.25)). The correlation coefficients between the data points and the formulas are as listed in Table 5.15.

Table 5.15 – Correlation between experimental data and proposed formulas for wave reflection (constant initial beach slope)

Author	Correlation coefficient, r	Determination coefficient, r^2
Battjes (1974)	0.96	0.92
Seelig and Ahrens (1981)	0.95	0.90
Losada and Giménez-Curto (1981)	0.91	0.82
Postma (1989)	0.87	0.75
Van der Meer (1993)	0.89	0.79
Zanuttigh and Van der Meer (2007)	0.89	0.79

According to Table 5.15, both the formulas of Battjes (1974) and Seelig and Ahrens (1981) seem to agree with the experimental data points with acceptable accuracy (r^2 is higher than 0.90). It should be emphasized that the data points in Figure 5.47 resulted after the first 100 waves in all 12 tests considered and that any beach deformation is neglected. However, some level of beach deformation was noticed within the first 100 waves for all 12 tests. A small berm started to occur in all cases. This clearly affects the wave reflection coefficient as the beach face becomes steeper (see Appendix C for the beach deformation profiles). Determining the correlation and taking the beach deformation into account generates different results. Instead of considering a constant initial beach profile slope, the slope of the newly generated berm (the new beach face of reflection) is used in the calculations. Table 5.16 lists the values of correlation coefficients and the determination coefficient calculated for this case when the beach slope is no longer constant.

Table 5.16 – Correlation between experimental data proposed formulas for wave reflection (variable beach slope)

Author	Correlation coefficient, r	Determination coefficient, r^2
Battjes (1974)	0.54	0.29
Seelig and Ahrens (1981)	0.69	0.48
Losada and Giménez-Curto (1981)	0.73	0.54
Postma (1989)	0.75	0.57
Van der Meer (1993)	0.71	0.51
Zanuttigh and Van der Meer (2007)	0.86	0.74

According to Table 5.16, as well as to Figure 5.45 and Figure 5.46, it appears that formulas developed to describe wave reflection form breakwaters and revetments should not be used to describe and predict wave reflection from an active and deforming gravel beach. Hence, a thorough investigation of wave reflection on gravel beaches may be one of the necessary, yet least studied aspect in literature.

5.5 Wave Transmission within the Beach Face

Three wave gauges and nine (9) pressure transducers were buried within the beach face, near the waterline, where significant deformation was expected. Using the output of the pressure transducers, it is possible to assess the spatial variation in wave-induced water motion (wave transmission) inside the gravel beach. Figure 5.48 shows the location of the pressure transducers and of the buried wave gauges. Figure 5.49 represents a 'zoom-in' of the pressure transducers, indicating the number of each gage, further referred to in Figure 5.50.

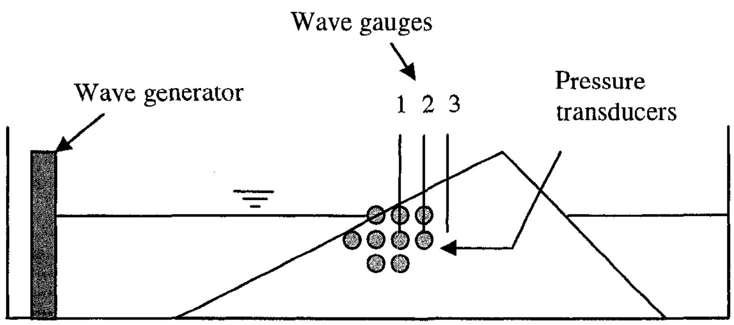

Figure 5.48 – Cross-sectional view of the experimental set-up (not at scale)

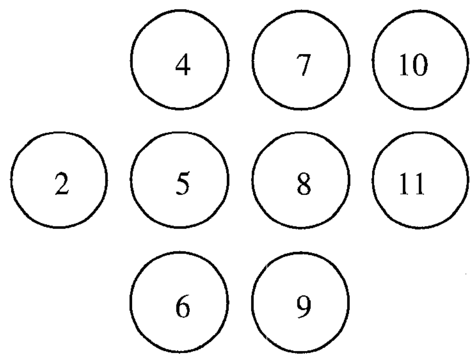

Figure 5.49 – Location of each pressure transducer and their identification numbers

Figure 5.50 shows wave trains recorded by the pressure transducers in the case of irregular waves (Test 6). The pressure on the vertical axis is measured in Pascals (Pa) where 1 m of water indicates 9781 Pa. The vertical axis has the same scale in all cases. At the left of the wave trains, number of the pressure transducer is denoted as PT "number". Recall that PT7 failed early in the experiments and data from it are not available for the case shown in Figure 5.50.

As the waves travel further inside the beach, the wave heights decrease. Table 5.17 lists the mean values and the standard deviations describing the fluctuations in the water level for the case shown in Figure 5.50. Fluctuations are higher at the instruments located closest to the beach face and decrease as the waves travel into the porous beach. The mean values are in all cases higher than zero and decrease away from the beach face. This indicates a water level set-up inside the gravel beach.

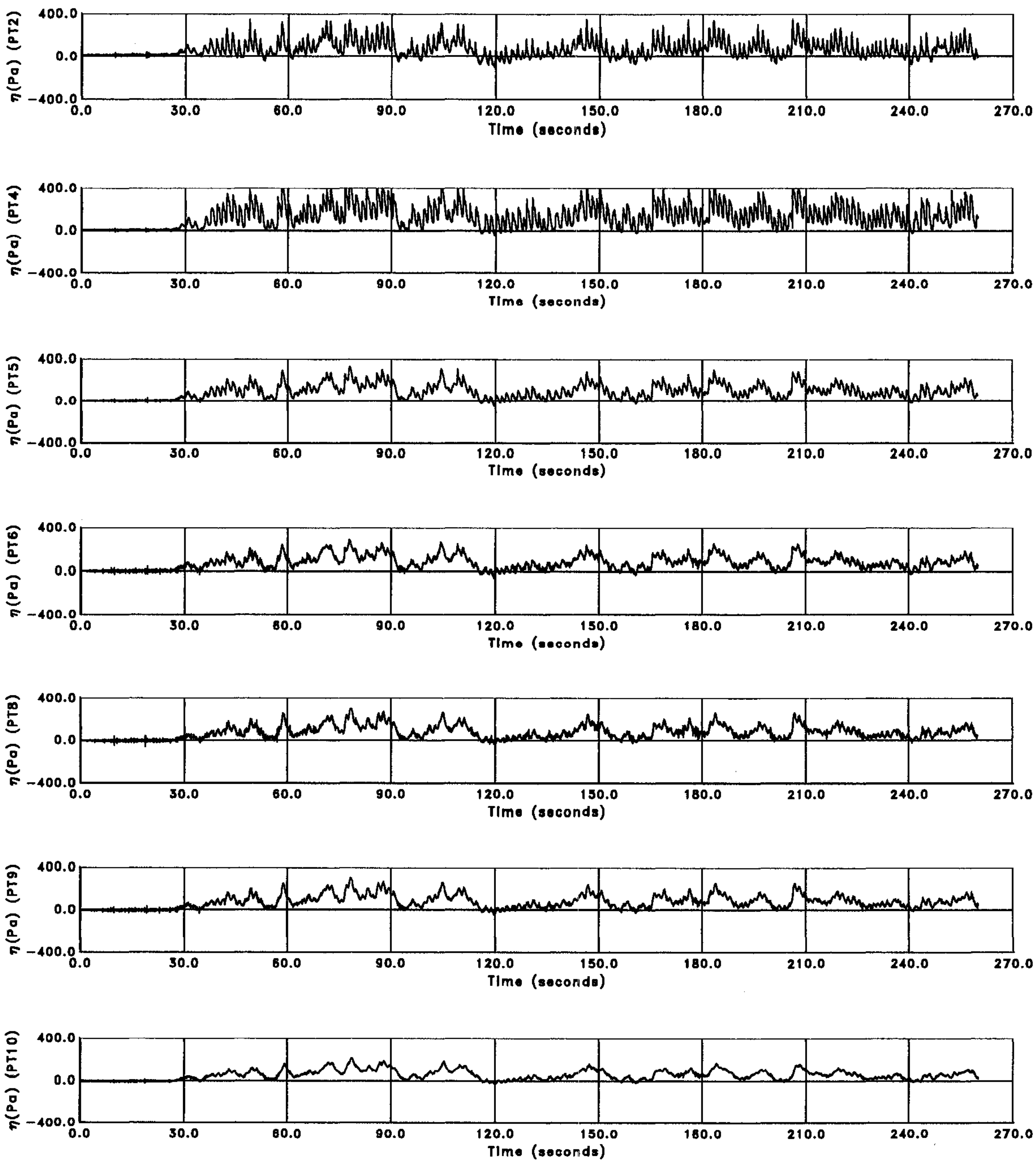

Figure 5.50 – Wave motion recorded by pressure transducers, Test 6, for 100 – 300 waves

Table 5.17 – Mean values recorded by the pressure transducers and standard deviations

Pressure Transducer	Mean value [Pa]	Standard deviation [Pa]
PT2	70.08	74.73
PT4	130.51	103.73
PT5	93.28	70.22
PT6	79.77	62.72
PT8	75.96	62.53
PT9	74.27	62.41
PT10	53.16	46.79
PT11	73.34	45.10

Figure 5.51 shows an example of the wave transmission pattern inside the beach mound. The uppermost wave train is recorded at WG1, the middle one at WG2 while the lowest one is from WG3. The water surface elevation is denoted on the vertical axis and the scale is the same in all cases.

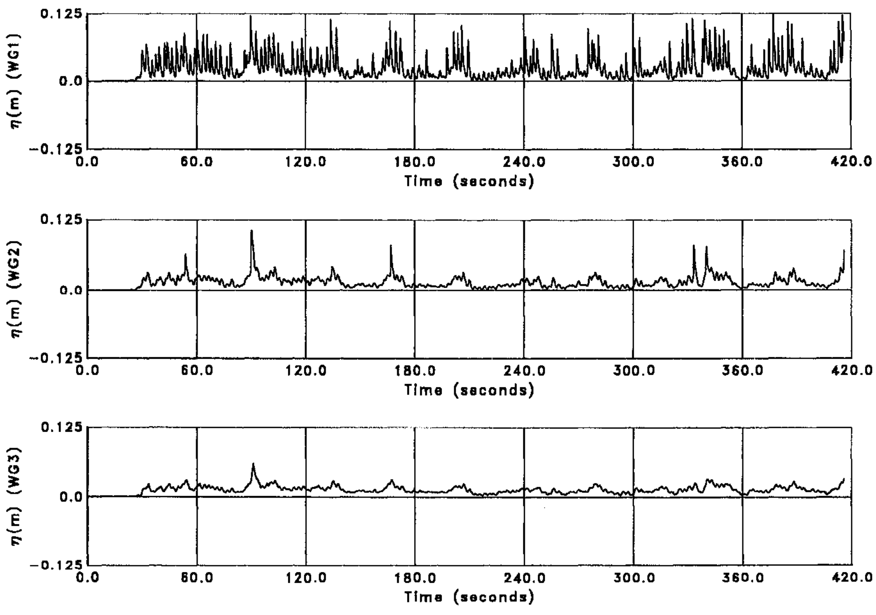

Figure 5.51 – Output from WG1, WG2 and WG3 for irregular waves, Test 6, for 100 – 300 waves

The wave gauges can measure the free water surface within the beach mound. The larger amount of water surface fluctuations recorded by WG1 is recorded backwash seepage flow not recorded at WG2 or WG3. This observation is confirmed by the standard deviation in the pressure fluctuation at PT4 (Table 5.17) which is sensibly higher than those recorded by PT5 and PT6 (further away from the surface of the berm).

5.6 Energy Dissipation within the Beach

Gravel beaches have been found to be effective wave energy dissipators. According to Powell (1990) and Buscombe and Masselink (2006), up to 90% of incident wave energy can be dissipated by gravel beaches.

The wave energy density, E_w, is defined as

$$E_w = \frac{1}{8} \cdot \rho_w \cdot g \cdot H^2 \tag{5.26}$$

The wave height, H, is replaced by H_{av} for regular waves, and by H_s for irregular waves. The unit measure for the wave energy density is J/m^2, or joule per unit surface area of the wave. The wave energy density is proportional to the square of the wave height and, as the density of water and the acceleration due to gravity do not change for a given location, the wave energy density depends solely on the wave height.

In the following figures, the energy density is calculated between the first 100 to 300 waves in the case of irregular waves. In a few cases, no information on H_s was recorded at WG1 to WG3 up to the first 100 waves step because of lack of data points caused by the short time step. For regular waves, the energy density is determined between the first 100 and 200 waves, where the number of data points was enough to calculate required parameters such as the average wave height.

Figure 5.52 and Figure 5.53 show the wave energy density for regular waves and irregular waves, respectively. The right-hand side vertical axis represents the elevation and the estimated beach slope is plotted with a solid grey line. The energy density first increases in the surf zone as a result of an increase in the wave height and further decreases again in the surf zone as waves break. When waves hit the beach, the energy density drops significantly and progressively reduces to zero as recorded by the three wave gauges located inside the beach (between x = 45 – 46 m).

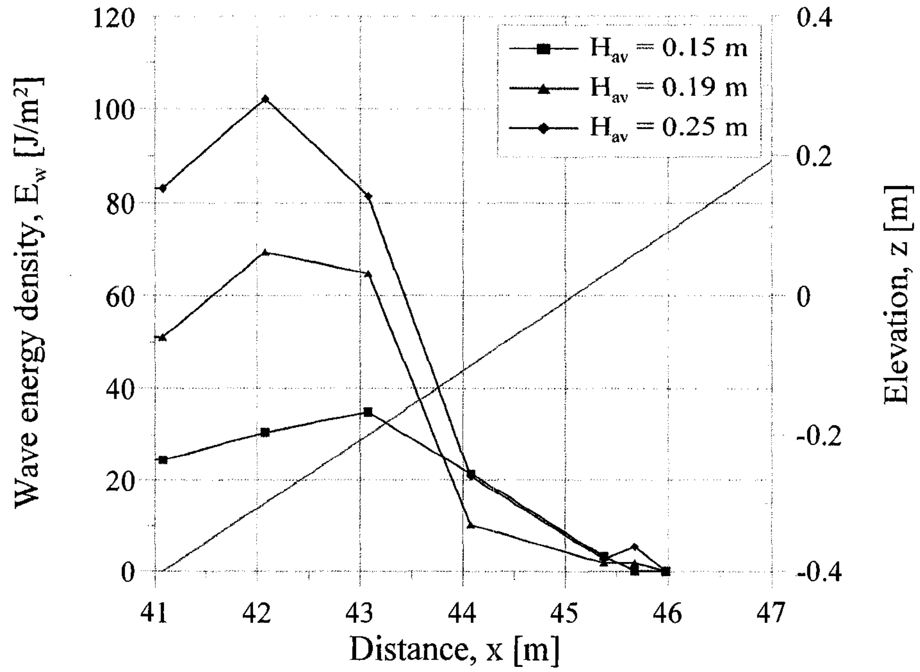

Figure 5.52 – Wave energy density, regular waves, initial beach slope: 1:10

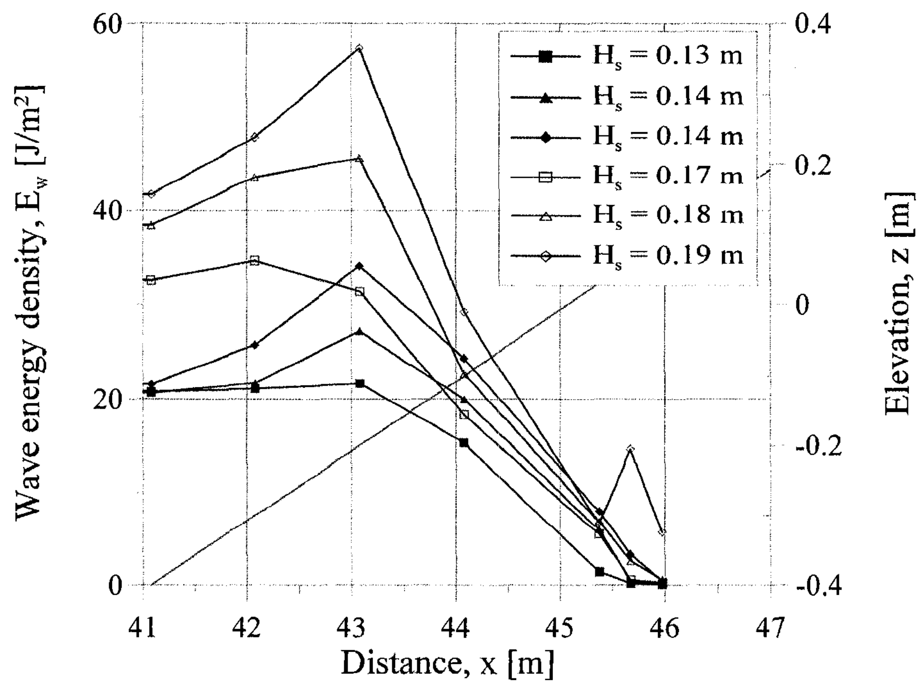

Figure 5.53 – Wave energy density, irregular waves, initial beach slope: 1:10

In order to investigate the dissipation of energy within the gravel medium, a coefficient of energy damping, C_{Ew}, is proposed as,

$$C_{E_w} = \frac{E_w}{E_{w,offshore}} \tag{5.27}$$

where E_w is the energy density at various locations: offshore, within the surf zone and inside the beach mound. $E_{w,offshore}$ is a constant value for each test, defined as the average of the energy density measured at the five wave gauges located offshore (WG4 to WG9).

Figure 5.54 shows the energy damping coefficient for regular waves when the initial beach slope is 1:10. In the surf zone, the energy damping coefficient exceeds 1.00 but as waves approach the beach and inside of the beach mound, the damping coefficient decreases sharply. At the backmost buried wave gauge (WG3), the values of the damping coefficient vary between 0.0007 and 0.0011, which can be regarded as more than 99% energy dissipation (loss). Similarly, Figure 5.55 shows the energy damping coefficient for irregular waves. The energy loss measured at the backmost wave gauge inside the beach (WG3) is equivalent to 85% to 99% (where energy loss can be evaluated as $1\text{-}C_{Ew}$).

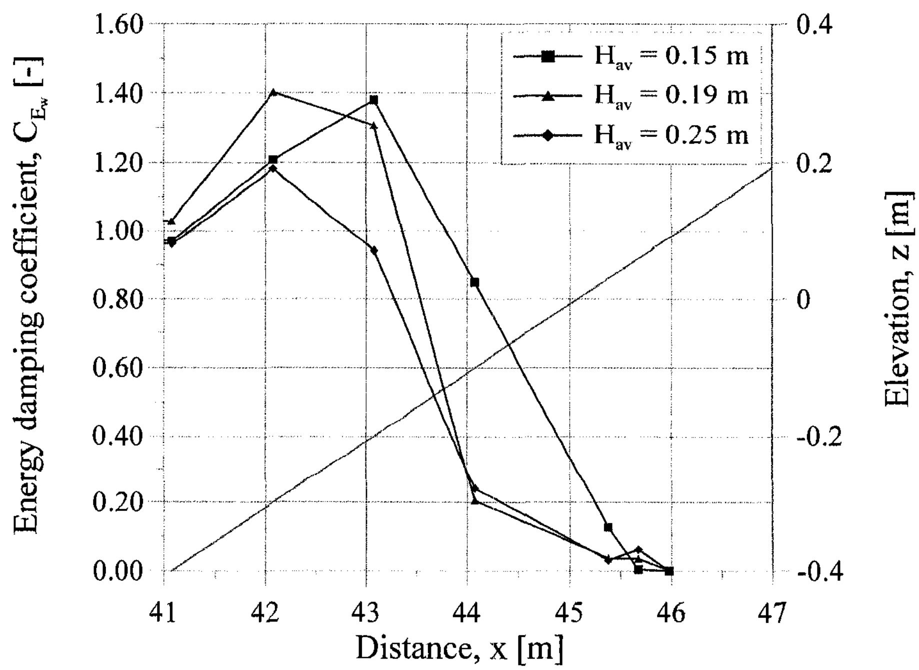

Figure 5.54 – Energy damping coefficient, regular waves, initial beach slope: 1:10

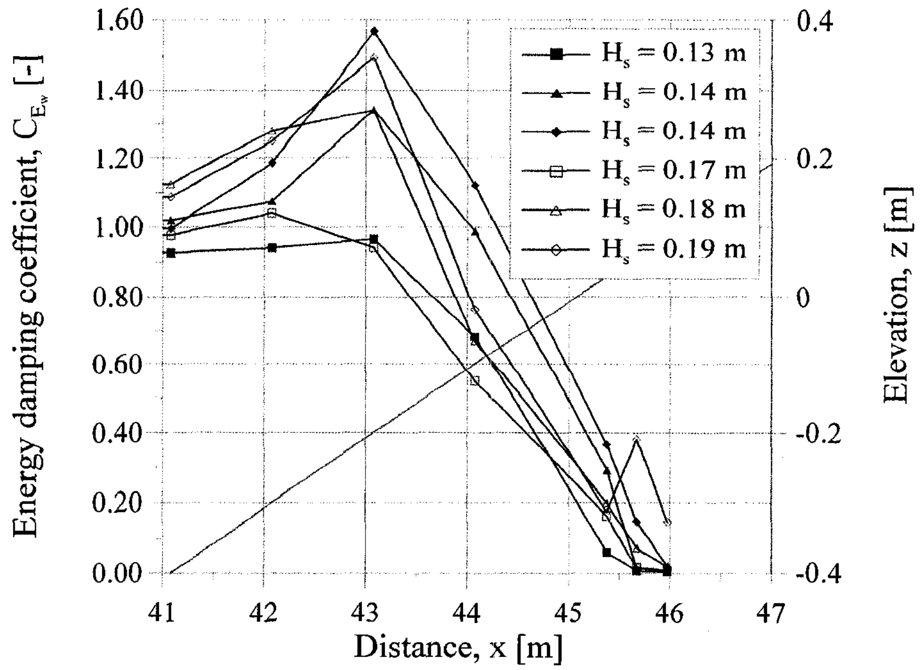

Figure 5.55 – Energy damping coefficient, irregular waves, initial beach slope: 1:10

Similar analysis was carried out for an initial beach slope of 1:7. Figure 5.56 and Figure 5.57 show the energy density variation for regular and irregular waves, respectively.

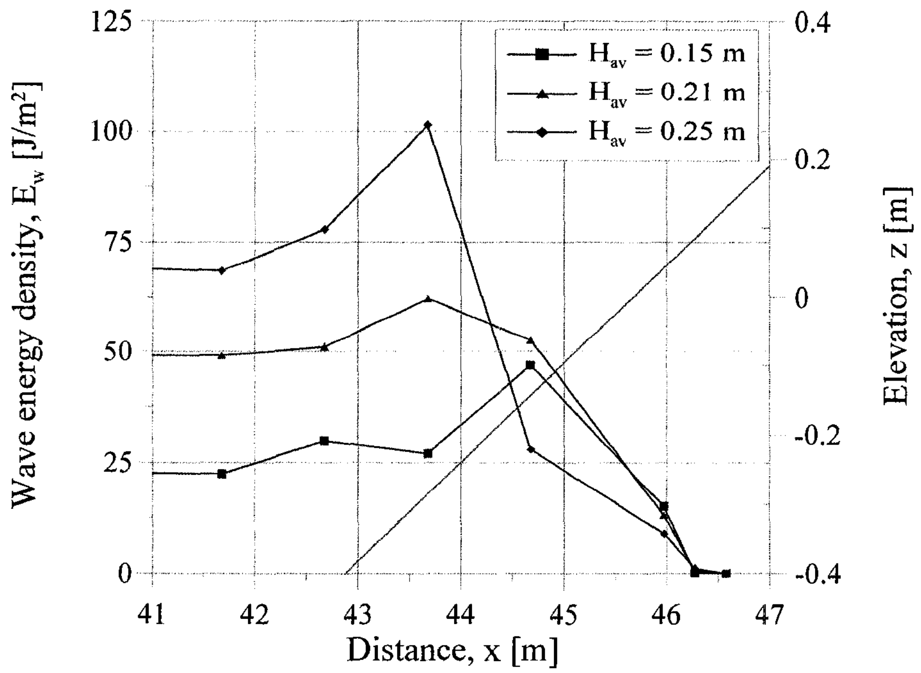

Figure 5.56 – Wave energy density, regular waves, initial beach slope: 1:7

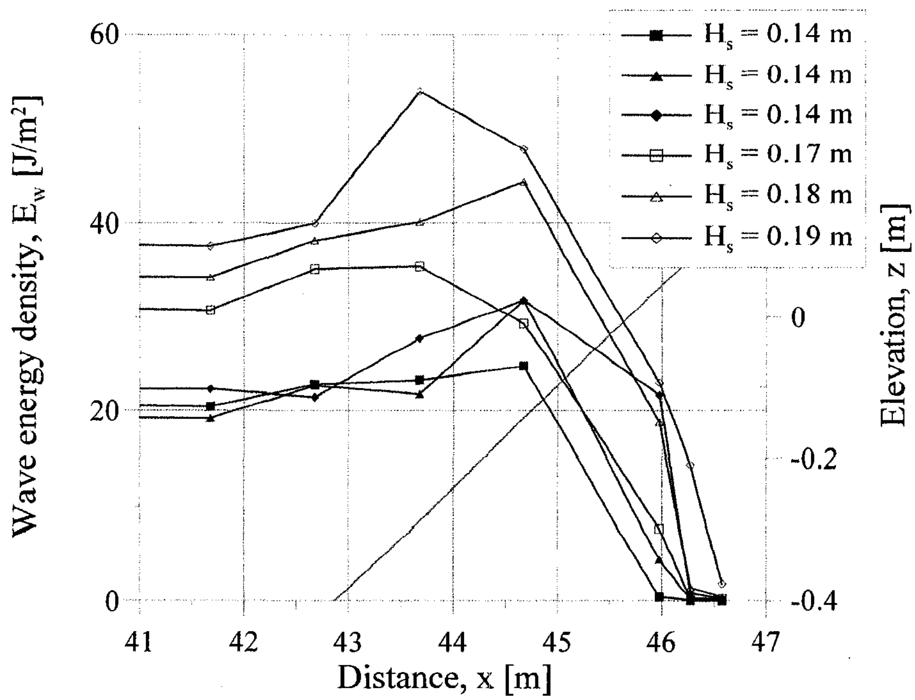

Figure 5.57 – Wave energy density, irregular waves, initial beach slope: 1:7

Figure 5.58 and Figure 5.59 show the energy damping coefficient for regular and irregular waves, respectively. The initial beach slope is 1:7. Again, the wave energy damping coefficient increases in the surf zone as waves break and approach the beach and the gravel beach significantly reduces the amount of energy as the broken waves dissipate through the porous medium created by the presence of the gravel.

The results above show that energy is significantly dissipated as waves penetrate into the gravel beach. The porous gravel beach is therefore very effective in dissipating wave energy. This can be observed in Table 5.18 and Table 5.19 wherein the energy loss at the three buried wave gauges is listed. There is a horizontal distance of 30 cm between WG1 and WG2, as well as between WG2 and WG3.

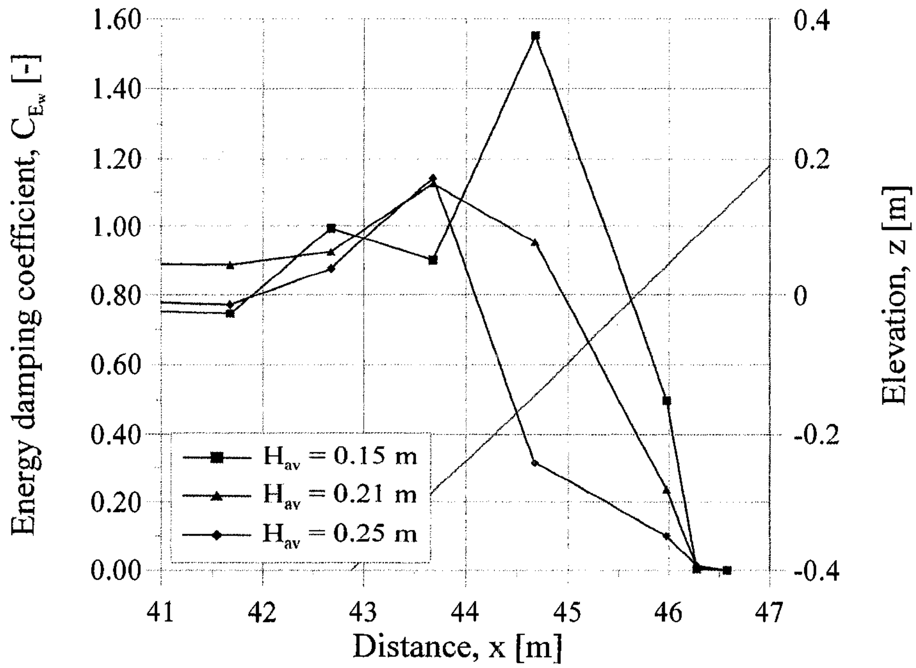

Figure 5.58 – Energy damping coefficient, regular waves, initial beach slope: 1:7

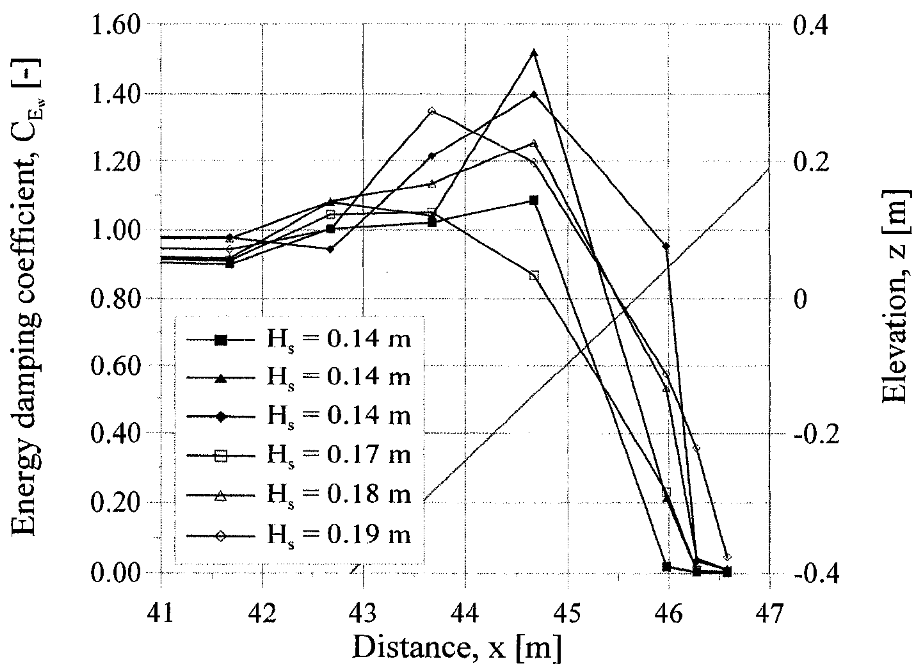

Figure 5.59 – Energy damping coefficient, irregular waves, initial beach slope: 1:7

Table 5.18 – Energy loss inside the beach, regular waves

Test no.	m_0	H_{av} [m]	Energy loss [%]		
			WG1	WG2	WG3
1	1:10	0.15	87	100	100
2		0.19	96	96	100
3		0.25	97	94	100
10	1:7	0.15	50	100	100
11		0.21	76	99	100
12		0.25	90	99	100

In Table 5.18 and Table 5.19, a few numbers may look erroneous, mainly for Tests 9, 10 and 15. However, the main reason for the low energy loss in these cases is due to the high wave heights recorded at the wave gauges for these tests.

Table 5.19 – Energy loss inside the beach, irregular waves

Test no.	m_0	H_s [m]	Energy loss [%]		
			WG 1	WG 2	WG 3
4	1:10	0.13	94	99	100
5		0.14	71	98	99
6		0.14	64	85	98
7		0.17	84	98	99
8		0.18	80	93	98
9		0.19	83	62	85
13	1:7	0.14	98	100	100
14		0.14	79	99	100
15		0.14	5	97	99
16		0.17	77	99	99
17		0.18	47	96	99
18		0.19	43	64	95

Figure 5.60 shows the locations of the three buried wave gauges, WG1, WG2 and WG3. As the beach profiles changed due to wave attack, the amount of gravel on top of these three wave gauges changed as well. The build-up of the gravel berm on top of the wave gauge locations, may affect the recordings of the wave gauges. This was further investigated in Figure 5.61. The

two arrows in Figure 5.60 indicate the increment in the sediment build-up in horizontal and vertical direction, occurring in front of and above the wave gauges. This change in beach profile was found to affect the energy damping coefficient as the wave duration increased, as indicated in Figure 5.61.

At the location of WG1, the energy damping coefficient is higher for N_w = 300 than for N_w = 5000, with one exception (for H_s = 0.19 m). The reason for such a high value for H_s = 0.19 m is the recorded significant wave height at WG1, which was found to be H_s = 0.17 m. As waves penetrate into the gravel berm, the water surface elevation decreases rapidly and reaches zero at the location of WG3. One can estimate that time and spatial evolution of the beach deformation has the potential to significantly affect the damping of wave energy.

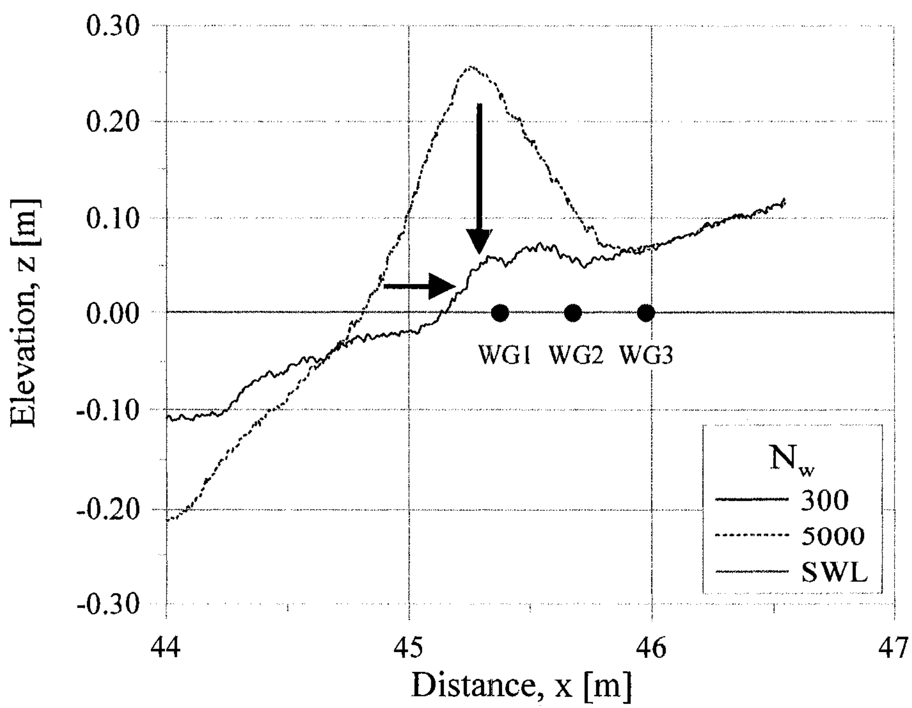

Figure 5.60 – Location of WG 1, WG 2 and WG 3 and the variation in distance to beach face and to the top of the berm

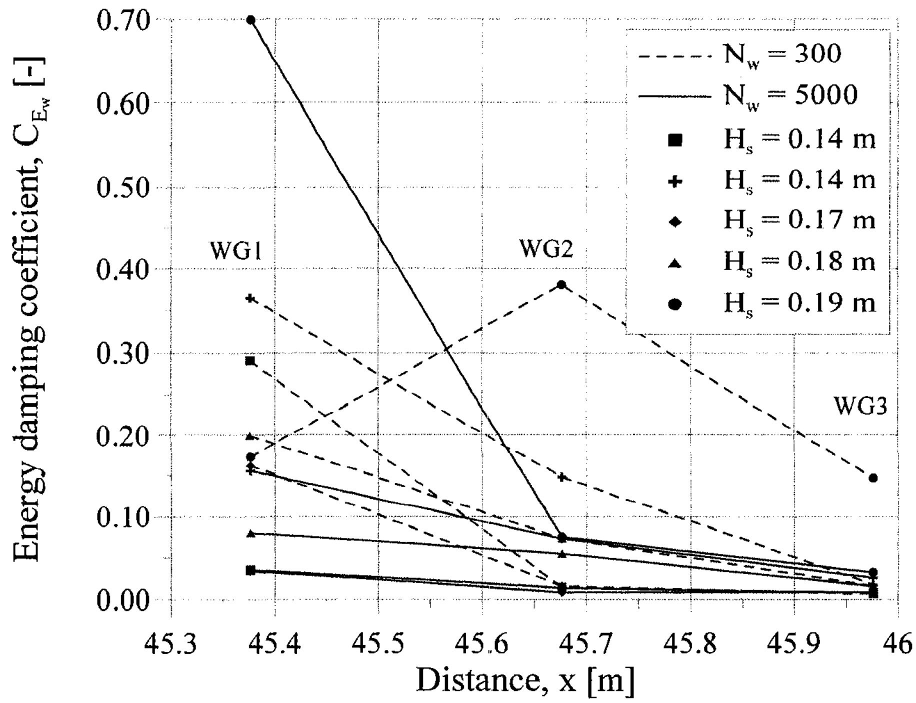

Figure 5.61 – Energy damping coefficient, irregular waves, initial beach slope: 1:10, comparison at $N_w = 300$ waves and $N_w = 5000$ waves

5.7 Model Effects and Distortions

In controlled physical model conditions such as the ones used in this study, it is necessary to account for model effects.

One of the factors affecting such laboratory measurements is the presence of the reflected waves travelling back and forth inside the wave flume. However, in this experiment, the wave reflection from the beach structure in the offshore direction and the wave re-reflection of the waves from the wave generator has been eliminated through the use of a machine-controlled active wave absorption system of the wave generator.

The flume and the beach structure are only 1.22 m (4 ft) wide. The side walls of the flume at the location of the beach are made of glass and represent the side boundaries of the experiment. The influence of the walls on the sediment transport has been previously identified by researchers, mainly due to the characteristics of these side boundaries. However, the influence of the lateral boundaries for the case of experimental work involving gravel sediment has been assumed to be less important that in the case of experiments involving sand.

Measurements of the beach deformations using the electro-magnetic profiler were carried out 46.3 cm from the longitudinal axis (west side)of the flume. Manual measurements of the beach deformation were performed on the lateral (east side) boundary of the flume at the end of each test; that is, usually after 2500 waves for tests involving regular waves and after 5000 in the case of tests involving irregular waves. Figure 5.62 shows the results of the measurements from the two different profile measuring methods plotted together. The solid line represents the measurements performed along the side flume window while the dotted line represents the output generated using the profiler.

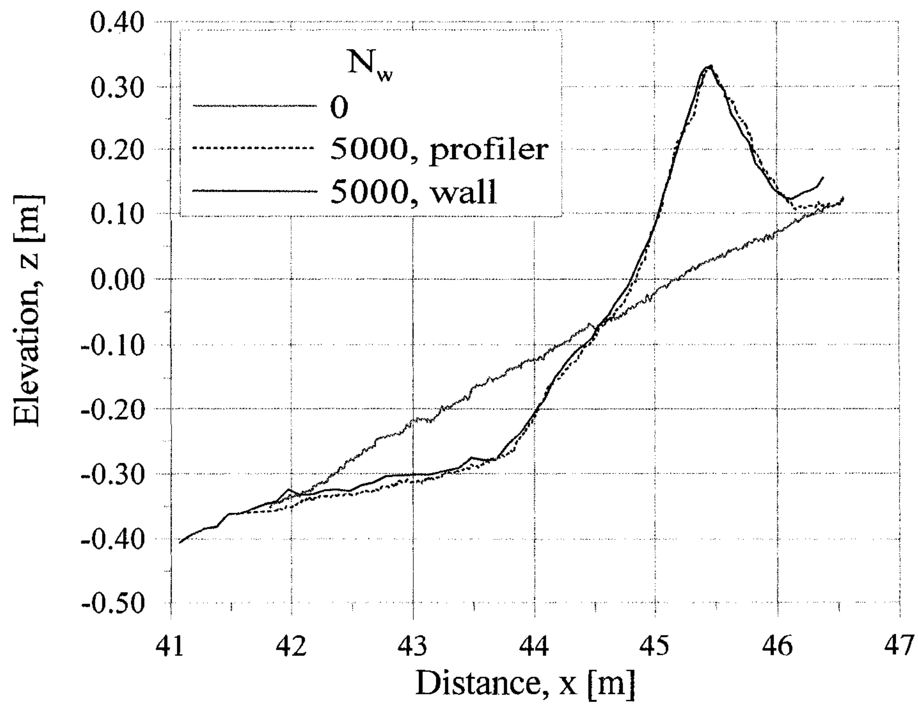

Figure 5.62 – Comparison of the beach profile measured by profiler and the wall, Test 9, irregular waves, after 5000 waves

In Figure 5.63 , the results of the two beach profile methods were plotted for tests involving irregular waves after 5000 waves, for an initial beach slope of 1:10 (Tests 5 – 9). The output from the profiler is on the vertical axis and measurements from the wall on the horizontal axis.

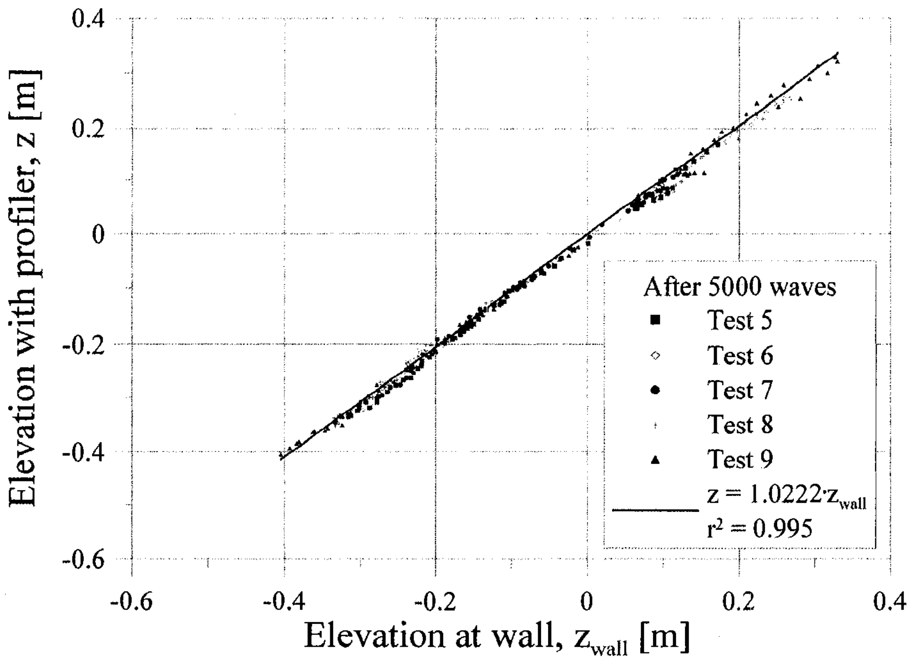

Figure 5.63 – Comparison of elevations measured by profiler and manually at the side flume wall, irregular waves, beach slope: 1:10

Similarly, Figure 5.64 compares the two profiling methods for tests involving regular waves after 2500 waves (Test 10) or 3000 waves (Test 11 and 12) when the initial beach slope was 1:7.

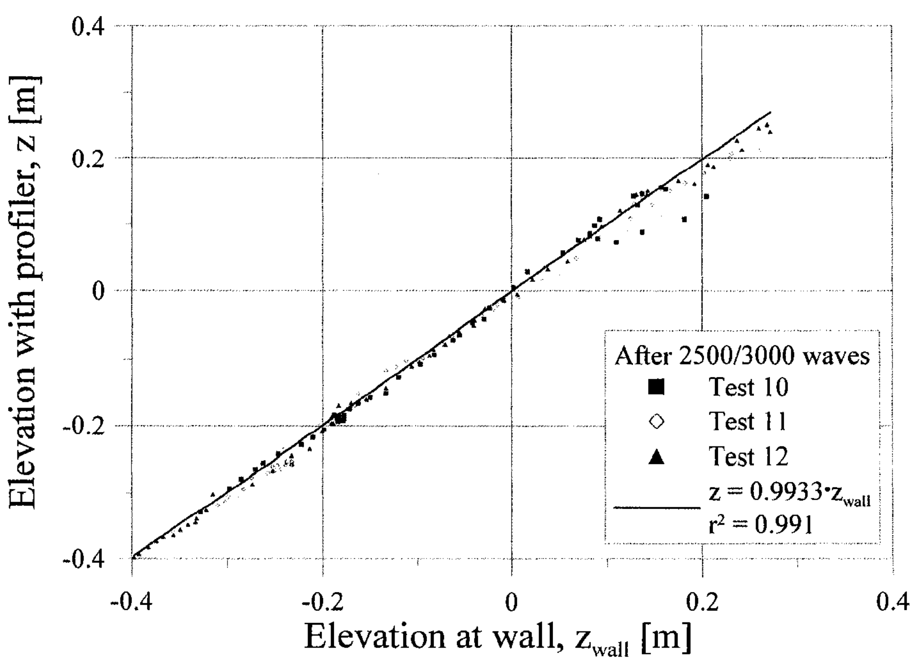

Figure 5.64 – Comparison of elevation measured by profiler and at wall, regular waves, beach slope: 1:7

Analyzing Figure 5.62 through Figure 5.64, one can draw the conclusion that the two profiling methods provide similar results below the still water level (0.0 m). Above the still water level however, where the accretion berm is located, some minor discrepancies are observed. The calculated correlation, for both tests employing regular and irregular waves, is very high ($r^2 > 0.99$). Hence, one can safely assume that model distortions and measurement errors due to irregularities induced by the transversal differences in beach profile are negligible in this particular study.

6 DISCUSSION

6.1 Geotechnical Analysis

In the relatively limited previous studies, information on the geotechnical characteristics of the beach material is either limited or simply absent. In this study, carrying out a geotechnical investigation was considered essential in order to identify the characteristics and composition of the gravel material. Grain size distribution graphs supply useful information on the gravel material and its porosity. The latter is particularly an important factor that was frequently overlooked in previous studies (reference to the porosity was only found in one reference, Pedrozo-Acuña *et al.*, 2006). The voids present in the gravel beach are likely an important factor when determining, for instance, the wave reflection due to a gravel beach. An analysis of the material uniformity is essential as this can provide the information required to distinguish mixed sand and gravel beaches from pure gravel beaches. These two different types of beaches have been found to behave differently and should not be confused.

6.2 Wave Analysis

Near the beginning of every test, it was considered necessary to keep the wave action duration steps short since beach deformation at the early stages is rapid. This also enabled examining in detail the morphological changes occurring on the beach. However, analysing the time history of the waves below a sequence of 50 wave periods was problematic. In order to improve the analysis of waves in the time domain, it would be more practical to choose a minimum time step of 100 waves.

Also, the ratio between maximum wave height and the water depth was measured. Linear wave theory does not properly account for rapid changes in water depth in the direction of wave propagation. The reason for that is likely the additional increment in wave height due to wave reflection from the beach and the steep beach slope. One limitation of the experimental setup was the fact that the water surface measurements are also taken at one meter interval in longitudinal direction. It would have been useful to provide additional wave gauges throughout the surf zone at short distances.

6.3 Beach Morphology

In the analysis of the beach response due to wave attack, the influences of the wave characteristics on the beach morphology were investigated. The wave period was found to be linearly related to the development of beach berm height and trough depth. The wave height was also found to affect the development of the beach berm and trough but no clear quantitative relationship was found between those variables. The relationship between wave characteristics and the wave-induced beach morphology is rather complex. Wave duration has a clear impact on the beach morphology. Quantitative analysis was performed and formulas derived to describe the relationship between the beach berm or trough development and the duration of the wave action. The observed influences of the wave height, wave period and storm duration have been found to be similar to those of Van der Meer (1988).

The influence of the initial slope on the beach morphology was also examined. Since only two different initial beach slopes were considered in the current experiment, it is rather difficult to draw clear-cut conclusions with respect to the relationship between the initial slope and the beach morphodynamic response. In tests involving irregular waves, it was observed that the development of the beach berm occurred faster when the initial beach slope was 1:7. It was however not possible to draw a similar conclusion for the development of the trough.

One of the experimental tests was repeated to investigate whether similar wave characteristics would generate similar results with respect to the deformation pattern and magnitude of the beach changes.

The sediment transport rate was calculated for selected time steps during each test. For the majority of the tests, the maximum sediment transport occurred at the early stages of the wave action and decreased as the state of equilibrium in the beach profile was reached.

The analysis of the wave characteristics, mainly of the wave height, indicated that, as the beach deformed, wave characteristics changed. As a beach trough deepened, the wave height increased at the location of the trough.

6.4 Wave Reflection

Numerous studies of wave reflection on coastal structures such as vertical seawalls and different types of breakwaters have been performed in the past. With increasing interest in applying softer engineering methods in shoreline protection, such as gravel beach nourishment and/or replenishment, it was considered important to investigate the performance of gravel beaches with respect to wave energy dissipation.

The wave energy approaching a gravel beach is either reflected or dissipated through wave breaking, sediment transport, friction or other dissipative mechanism. The small reflection coefficients measured in the study suggest that gravel beaches are effective at dissipating wave energy. It was observed that wave reflection increased as the peak wave period became larger, but that wave reflection decreased as the significant wave height became larger.

The wave reflection coefficients determined in this experimental study were compared to similar data for wave reflection analyses performed on steep rock structures and breakwaters. The gravel beach in the present study was found to dissipate more energy than breakwater-type structures. This is, however, a very general conclusion and further investigations on the wave reflection from gravel beaches is needed. In this sense, it would be worthwhile to analyse wave reflection from gravel beaches with different porosities. To the author's knowledge, no quantitative methods exist currently which would relate porosity in gravel beaches to wave reflection or wave energy dissipation.

In the present wave reflection analysis, inconsistencies were found in the GEDAP software developed at CHC. Modules REFLA and REFLS of GEDAP should have provided results for the wave reflection coefficient in the case of irregular waves, but that was not the case. One of the possible explanations could be the fact that the module REFLS, which is based on the linear wave theory, cannot yield reliable reflection coefficients considering the strong non-linearity of the wave conditions considered in these experiments.

6.5 Wave Motion Transmission within the Beach Mound

As the waves travelled through the porous gravel beach, the water surface elevation decreased rapidly. Both the buried wave gauges and the submerged pressure transducers demonstrated this behaviour inside the beach mound. The fluctuations in the dynamic pressure measured by the pressure transducers decreased as the distance from the beach face increased, both in the horizontal and vertical (downwards) direction. The percolation of the water down-rush was recorded both by a wave gauge (WG1) and one array of the pressure transducers.

6.6 Energy Dissipation within the Beach

The wave energy density and wave energy damping were calculated for the offshore, the surf zone and inside the beach mound. The comparison of the energy density at all wave gauge locations with the energy density calculated using the offshore gauges generated the energy damping coefficient. The latter indicated an increase of energy due to shoaling prior to the wave breaking zone and a significant loss of energy throughout the surf zone and within the beach mound. The porous gravel (n = 0.365) was found to be highly effective in wave energy dissipation. At the backmost buried wave gauge, energy loss was found to exceed 95% in all cases, except for one case where energy loss was 85%. These results are similar to the findings of Powell (1990) and Buscombe and Masselink (2006), who stated that gravel beaches can dissipate up to 90% of the wave energy. In this study, the effects (in 17 out of 18 tests) indicate even larger levels of energy dissipation. As the beach profiles changed, the energy damping coefficient changes were in sync. Generally, sediment is being transported in front of the buried wave gauges so the amount of porous material that the turbulent water bore has to penetrate through to reach the wave gauges, increases. This results in an increase in turbulent energy dissipation. The energy damping coefficient was observed to be smaller after 5000 waves than after 300 waves. This could also be attributed to a steeper beach face that results in more reflection and less energy to be dissipated through the gravel mound.

6.7 Model Effects and Distortions

The wave reflection and the possible re-reflection of the waves by the wave board were effectively suppressed by an active wave absorption system.

Moreover, the flume side boundaries were found not to distort the sediment transport. Comparison between beach profile measurements performed on the side wall of the flume and outputs from the electro-magnetic profiler showed good agreement. The coefficient of determination obtained in this comparison was $r^2 > 0.99$.

7 CONCLUSIONS

As stated by previous researchers and outlined by some of the findings in this work, gravel beaches are an effective type of natural sea defences. Gravel material is increasingly used to nourish eroding sand beaches. However, the understanding of the behaviour of gravel beaches under wave attack is not yet fully understood. The aim of this study was to conduct a large-scale experiment in order to advance our understanding of the behaviour of gravel beach under wave attack.

A geotechnical analysis was also performed and several important geotechnical parameters, such as median grain size diameter, porosity and specific gravity were quantified.

Beach profile changes under regular and irregular waves were analysed. Morphologic changes were found to be rapid at the early stages of each test. The beach profiles reached an equilibrium state after around 2500 waves in the case of regular waves and after around 5000 waves in the case of irregular waves. As the wave period increased, the beach berm height and the beach trough depth increased. Wave height also affected beach morphology, however the correlation is highly non-linear. Wave duration influences the beach profile changes and, in most cases, a state of equilibrium was reached. These observations are similar to those of Van der Meer (1988) and Powell (1990). The initial beach slope was found to influence the development of the beach berm height and beach trough depth in the case of irregular waves, but not so in the case of regular waves. The calculation of the sediment transport rates indicated agreement with the rapid changes at the beach profile at the beginning of the wave action. Later on, the sediment transport rate decreased as the beach profile tended to evolve towards a state of equilibrium.

An analysis of the wave reflection from the gravel beach was performed. The initial beach slope, wave duration and wave period all had a significant impact on the reflection coefficient. Before the gravel beach deforms, reflection data are comparable to the results of the empirical formulas of Battjes (1974) and Seelig and Ahrens (1981). However, empirical formulas developed for breakwaters and revetments are unable to describe the reflective behaviour of gravel beaches with non-linear profiles.

Records from the buried wave gauges and the pressure transducers were analysed. Water fluctuations attenuate as the waves travel further into the beach mound and away from the beach face. The buried wave gauges closest to the beach face recorded the motion of water percolating through the beach berm following wave breaking and swash motion.

Energy dissipation within the beach mound was investigated. At the inner-most wave gauge inside the beach mound, 85-100% of the incident energy was dissipated. Beach deformation also affected the energy dissipation.

Model distortions were not found to play a significant role in the current experiments. The side boundaries of the wave flume were not found to affect the sediment transport close to the walls. Wave re-reflection from wave generator was minimized by including an active wave absorption (AWA) system in the experiment.

8 RECOMMENDATIONS FOR FUTURE WORK

The following future work is suggested:

- Perform three-dimensional laboratory experiments on gravel beaches in order to investigate beach morphology and include the effect of the longshore current and associated sediment transport.
- Perform (long term) laboratory experiments on gravel beach deformation with the inclusion of tidal effects.
- Investigate wave reflection from gravel beaches and measuring wave reflection from gravel beaches with various initial beach slopes, wave heights, wave periods, porosities, gradations and grain sizes. Based on the current experiment, future researchers should be able to develop relationships quantifying the wave reflection from gravel beaches and its influencing factors.
- Study the effects of the gravel beach nourishment of sand beaches in order to determine the impact of the mixed sand and gravel beaches.
- Apply the collected data base from the present experimental study in order to validate a predictive numerical model for gravel beach deformation.

9 REFERENCES

Austin, M.J. and Masselink, G. (2006). Swash-groundwater interaction on a steep gravel beach. *Continental Shelf Research*, 26, 2503-2519.

Battjes, J.A. (1974). Surf similarity. *Proceedings of the 14th Conference on Coastal Engineering*, ASCE, 466-480.

Benassai, G. (2006). *Introduction to coastal dynamics and shoreline protection.* Wit Press, Southampton, 331 pp.

Buscombe, D. (2007). (Personal communication, March 21st, 2007).

Buscombe D. and Masselink G. (2006). *Concepts in gravel beach dynamics.* Earth-Science Reviews, 79, 33-52.

Caldwell, N.E. and Williams, A.T. (1985). The role of beach profile configuration in the discrimination between differing depositional environments affecting coarse clastic beaches. *Journal of Coastal Research*, 1(2), 129-139.

Cammelli, C., Jackson, N.L., Nordstrom, K.F. and Pranzini, E. (2006). Assessment of a gravel nourishment project fronting a seawall at Marina di Pisa, Italy. *Journal of Coastal Research, Special Issue*, 39, 770-775.

Carr, A.P. (1971). Experiments on longshore transport and sorting of pebbles: Chesil beach England. Journal of Sedimentary Petrology, 41 (4), 1084-1104.

Coastal Engineering Research Center, CERC. (1984). *Shore Protection Manual.* Coastal Engineering Research Center, U.S. Army Corps of Engineers, Vicksburg, USA.

Conley, D.C. and Griffin, J.G. (2004). Direct measurements of bed shear stress under swash in the field. *Journal of Geophysical Research*, 109 (C03050), 1-12.

Das, B.M. (2001). *Principles of geotechnical engineering.* 5th edition. Brooks/Cole Thomson Learning, 589 pp.

Davies, M.H., Mansard, E.P.D., & Cornett, A.M. (1995). *Damage Analysis for Rubble-Mound Breakwaters*. National Research Council of Canada, Institute Report IR-1995-09, Ottawa, Canada, 15 pp.

Horn, D. and Li, L. (2006). Measurement and modelling of gravel beach groundwater response to wave run-up: Effects on beach profile changes. *Journal of Coastal Research*, 22(5), 1241-1249.

Hsu, T., Tseng, I. and Lee, C. (2006). A New Shape Function for Bar-Type Beach Profiles.

Journal of Coastal Research, 22(3), 728-736.

Hughes, S.A. (1993). *Physical models and laboratory techniques in coastal engineering*. World Scientific, New Jersey, USA, 568 pp.

Ibrahim, J.C., Holmes, P. and Blanco, B. (2006). Response of a gravel beach to swash zone hydrodynamics. *Journal of Coastal research*, Special Issue, 39, 1685-1690.

Jennings R. and Shulmeister J. (2002). A field based classification scheme for gravel beaches. *Marine Geology*, 186, 211-228.

Kamphuis, J.W. (2000). *Introduction to coastal engineering and management*. World Scientific, New Jersey, USA, 437 pp.

Kirk, R.M. (1975). Aspects of surf runup processes on mixed sand and gravel beaches. *Geografiska Annaler*, 57, A 1/2, 117-133.

Kirk, R. M. (1980). Mixed sand and gravel beaches: Morphology, processes and sediments. *Progress in Physical Geography*, 4, 189-210.

Lee, K., Mizutani, N., Hur, D. and Kamiya, A. (2007). The effect of groundwater on topographic changes in a gravel beach. *Ocean Engineering*, 34, 605-615.

Lorang, M.S. (2002). Predicting the crest height of a gravel beach. *Geomorphology*, 48, 87-101.

Losada, M.A. and Giménez-Curto, L.A. (1981). Flow characteristics on rough permeable slopes under wave action. *Coastal Engineering*, 4, 187-206.

Mansard E.P.D. and Funke E.R. (1987). *On the Reflection Analysis of Irregular Waves.* National Research Council of Canada, Technical Report TR-HY-017, Ottawa, Canada, 46 pp.

Mason, S.J. and Hansom, J.D. (1989). A Markov model for beach changes on the Holderness coast of England. *Earth Surface Processes and Landforms*, 14, 731-743.

Masselink, G. and Hughes, M.G. (1998). Field investigation of sediment transport in the swash zone. *Continental Shelf Research*, 18, 1179-1199.

McFarland, S., Whitcombe, L. and Collins, M. (1994). Recent shingle beach replenishment schemes in the UK: Some Preliminary observations. *Ocean and Coastal Management*, 25, 143-149.

McKay, P.J. and Terich, T.A. (1992). Gravel barrier morphology: Olympic National Park, Washington state, U.S.A. *Journal of Coastal Research*, 8(4), 813-829.

Miles, M.D. (1997). *GEDAP User's Guide for Windows NT.* National Research Council of Canada, Technical Report HYD-TR-021, Ottawa, Canada, 96 pp.

Miles, M.D. (1999). *The GEDAP/NDAC active wave absorption system for wave generators in flumes.* National Research Council of Canada, Technical Report HYD-CTR-059, Ottawa, Canada, 59 pp.

Miles, M.D. and Pelletier, D. (2001). *User guide for GEDAP wave generation software: Update to Windows NT/Windows 2000 version.* National Research Council of Canada, Ottawa, Canada, 24 pp.

Pedrozo-Acuña, A., Simmonds, D.J., Otta, A.K. and Chadwick, A.J. (2006). On the cross-shore profile change of gravel beaches. *Coastal Engineering*, 52, 335-347.

Postma, G.M. (1989). *Wave reflection from rock slopes under random wave attack.* University of Delft, Netherlands, Master's thesis.

Powell, K.A. (1990). *Predicting short term profile response for shingle beaches.* Hydraulics Research, Wallingford, Report. SR219. 118 pp.

San Román-Blanco, B.L., Coates, T.T., Holmes, P., Chadwick, A.J., Bradbury, A., Baldock, T.E., Pedrozo-Acuña, A., Lawrence, J. and Grüne, J. (2006). Large scale experiments on gravel and mixed beaches: experimental procedure, data documentation and initial results. *Coastal Engineering*, 53, 349-362.

Seelig, W.N. and Ahrens, J.P. (1981). *Estimation of wave reflection and energy dissipation coefficients for beaches, revetments and breakwaters.* CERC Technical paper 81-1, USACE, USA, 43 pp.

Sherman, D.J. (1991). Gravel beaches. *National Geographic Research and Exploration*, 7 (4), 442-452.

Shimizu, T. and Kawata Y. (1997). Simultaneous observations on irregular waves, currents, suspended sediment concentration and beach profile changes in large wave flume. *Coastal Dynamics '97*, ASCE, 486-495.

Sleath, J. (1978). Measurements of bed load in oscillatory flow. *Journal of the Waterway Port Coastal and Ocean Division*, 10 (4), 291–307.

Soulsby, R.L. and Damgaard, J.S. (2005). Bedload sediment transport in coastal water. *Coastal Engineering*, 52, 673-689.

U.S. Army Corps of Engineers, USACE. (2002). *Coastal Engineering Manual.* Engineer Manual 1110-2-1100, U.S. Army Corps of Engineers, Washington, USA, (in 6 volumes).

Ünal, N.E. and Bayazit, M. (1998). Incipient motion of coarse particles on a slope by regular or irregular waves. *Journal of the Waterway, Port, Coastal, and Ocean Division*, 124(1), 32-35.

Van der Meer, J.W. (1988). *Rock slopes and gravel beaches under wave attack.* Delft Hydraulics Laboratory. Netherlands, Publication no. 396, 226 pp.

Van der Meer, J.W. (1993). *Conceptual design of rubble mound breakwaters.* Delft Hydraulics Laboratory. Netherlands, Publication no. 483, 71 pp.

Van der Meer, J.W., Briganti, R., Zanuttigh, B., Wang, B. (2005). Wave transmission and reflection at low-crested structures: Design formulae, oblique wave attack and spectral change. *Coastal Engineering*, 52, 915-929.

Van Hijum, E. and Pilarczyk, K.W. (1982). *Gravel beaches. Equilibrium profile and longshore transport of coarse material under regular and irregular wave attack.* Delft Hydraulics Laboratory. Netherlands, Publication no. 274, 118 pp.

Van Wellen, E., Chadwick, A.J. and Mason, T. (2000). A review and assessment of longshore sediment transport equations for coarse-grained beaches. *Coastal Engineering*, 40, 243-275.

Vincent, C.E., Young, R.A. and Swift, D.J.P. (1981). Bed-load transport under waves and currents. *Marine Geology*, 39, 71-80.

Winyu, R. (1995). *Cross-shore sediment transport and beach deformation model.* Ph.D. thesis. Yokohama National University, Department of Civil Engineering, Yokohama, Japan.

Whitcombe, L.J. (1996). Behaviour of an artificially replenished shingle beach at Hayling Island, UK. *Quarterly Journal of Engineering Geology*, 29, 265-271.

Zanuttigh, B. and Van der Meer, J.W. (2007). Wave reflection from composite slopes. *Coastal Structures*, Venice, Italy.

APPENDICES

A Project Experimental Log

Table A.1 – Time line

Day (2007)	Task
July 1st to August 19th	Design of the structure, search for gravel suppliers Literature review on experiments on gravel beach deformation
August 20th	Material ordered and delivered at CHC, 4.5 m^3 Cleaning the windows of the flume
August 21st	Cleaning of the windows finished Outlines of the beach structure drawn on the windows 2.5 m^3 of material put into the flume
August 22nd	2.0 m^3 of material put into the flume Beach profile shaped
August 23rd	Design changed, amount of extra material allows to make structure higher
August 24th	Learning how the 10 cfs pump and wave generator work Water pumped into flume Four wave gauges set up Learning how NDAC generate regular waves Calibrated wave gauges 1-8
August 27th	Calibrated wave gauges 4-5 for own practice First wave generation on my own, regular waves, H = 0.15 m and T = 3 sec
August 28th	Test run with regular waves, H = 0.15 m and T = 5 sec Learning how to generate irregular waves of JONSWAP spectrum Test run with irregular waves, H = 0.15 m and T = 1.5 sec
August 29th	Test run with irregular waves, H = 0.15 m and T = 2.5 sec
August 30th	Test run with irregular waves, H = 0.20 m and T = 2.0 sec Test run with irregular waves, H = 0.10 m and T = 2.0 sec
August 31st	Learning how to analyze the data in GEDAP
September 1st	Data information on the test run set into a matrix
September 3rd	Writing the chapter on experimental setup started
September 4th	Learning how to analyze the data in GEDAP
September 5th	Learning how to analyze the data in GEDAP Wave gauges 9-12 setup and calibrated
September 6th	Learning how to analyze the data in GEDAP
September 7th	Learning how to analyze the data in GEDAP
September 10th	Progress meeting with supervisors Troubleshooting in GEDAP
September 11th	Introduction to pressure transducers Calibration bucket for the pressure transducers in place by the flume Merging the photos of test runs together
September 12th	Locating pressure transducers in the experiment Final design of instrumentation drawn in AutoCAD
September 13th	Profiler calibrated Steel frame built for wave gauges 1, 2 and 3 and the profiler

September 14th	Profiler configurations, test measurements and learning how profiler works with GEDAP
September 17th	Plexiglas tubes prepared, holes drilled in 3 tubes which will be used around the wave gauges' wires at wave gauges 1, 2 and 3 Wave gauge 1 calibrated
September 18th	Wave gauges 2 and 3 calibrated Had a problem calibrating, changed channel card for wave gauge 2
September 19th	Wave gauges 1, 2 and 3 calibrated with the tubes on
September 20th	Reference ruler, black and yellow tape put on the glass walls Steel frame for wave gauges 1-3 and pressure transducers put into flume Calibration of pressure transducers prepared
September 21st	Wave gauges 1 and 2 set up in the flume Flume drained
September 24th	Calibration bar for pressure transducers designed and built Pressure transducers 2, 4 and 5 calibrated
September 25th	Calibrating pressure transducers 1, 3 and 6-11 Pressure transducers 1 and 3 declared broken and will not be used Yellow boxes for wave gauges 1-3 set up on the steel bar in the flume and connected Preparation for installing pressure transducers into flume
September 26th	Pressure transducers set up, holders for them designed and built Grid marked on one glass wall with 5 cm interval
September 27th	Grid marked on the other glass wall with 5 cm interval Wave gauges and pressure transducers set to exact locations in the flume
September 28th	Further work on setting wave gauges and pressure transducers to exact locations in the flume Settled fine sediments in the flume removed by vacuuming the steel flume floor Meeting with supervisor at school
October 1st	Vacuum cleaner taken out Profiler brought into flume and calibrated
October 2nd	Pressure transducers and wave gauges buried and profile reshaped
October 3rd	Wave gauges 4-12 calibrated
October 4th	Preparing Test 1
October 5th	Test 1 started
October 9th	Test 1 finished Test 2 started
October 10th	Test 2 finished Problem on wave gauge 2 and 6 recognized
October 11th	Pressure transducers lowered Wave gauge 2 fixed and recalibrated
October 12th	Working in DAC_VIEW, first analysis of data
October 16th	Wave gauge 6 fixed and recalibrated Pressure transducer 7 is damaged
October 17th	Pressure transducers repositioned
October 22nd	Profile reshaped and prepared for Test 3
October 23rd	Test 4 started and finished Test 5 started
October 24th	Test 5 finished Test 6 started
October 25th	Test 6 finished Test 7 started and finished
October 26th	Test 8 started
October 29th	Test 8 finished Test 9 started

October 30th	Test 9 finished
November 5th	Decided to redo tests 1 and 2 and make an extra test, test 3 Active wave absorber system ready on the wave generator and will be used for the coming tests Test 1 started
November 6th	Test 1 finished Test 2 started
November 7th	Test 2 finished
November 8th	Test 3 started
November 9th	Test 3 finished
November 13th	Three samples taken from the beach for geotechnical analysis Preparation for changing the beach profile from 1:10 to 1:7
November 14th	Gravel shovelled out of the flume
November 15th	Wave gauges 1-12 recalibrated
November 16th	Pressure transducers recalibrated
November 19th	Wave gauges recalibrated Beach slope 1:7 ready
November 20th	Tests 10 and 11 started and finished
November 21st	Test 12 started and finished
November 22nd	Test 13 started and finished
November 23rd	Test 14 started and finished
November 26th	Test 15 started and finished Test 16 started
November 27th	Test 16 finished Test 17 started
November 28th	Test 17 finished Test 18 started and finished
November 29th	Test 19 started and finished
December 4th	Flume cleaned, instruments taken out
December 5th	Flume cleaned, instruments taken out
December 7th	Video recordings converted to digital files
December 11th	Gravel material shovelled out of the flume
December 12th	Gravel material shovelled out of the flume Flume cleaned, all instruments taken out

Table A.2 – Project log of Test 1

Day: 5/11 – 6/11 2007

GENERAL

Regular / Random:	Regular
Wave spectrum:	Regular, AWA
Water level [m]:	0.60
Wave height [m]:	0.15
Wave period [s]:	2.0
Drive Signal:	AWA_R_1_H0P15_T2P0

Initial profile file:	Pro_1_0.DAC
Trendline slope:	0.0998
R^2 of profile:	0.9995
Initial picture:	127-2763 to 67

TEST

Test name:	Test_1_1	Test_1_2	Test_1_3	Test_1_4
Start time:	14:19	14:37	14:53	15:40
Number of waves:	50	50	100	200
Cumulative waves:	50	100	200	400
Duration [s]:	100 (+20)	100 (+20)	200 (+20)	400 (+20)
Wave DAC file:	Test_1_1.DAC	Test_1_2.DAC	Test_1_3.DAC	Test_1_3.DAC
Profiler DAC file:	Pro_1_1.DAC	Pro_1_2.DAC	Pro_1_3.DAC	Pro_1_3.DAC
Profiler XLS file:	Pro_1_1.XLS	Pro_1_2.XLS	Pro_1_3.XLS	Pro_1_3.XLS
Profile – windows:	No	No	No	No
Pictures:	127-2768 to 71	127-2772 to 75	127-2776 to 79	127-2780 to 83
Video:				

Test name:	Test_1_5	Test_1_6	Test_1_7	Test_1_8
Start time:	8:35	9:03	10:00	10:31
Number of waves:	400	700	500	500
Cumulative waves:	800	1500	2000	2500
Duration [s]:	800 (+20)	1400 (+20)	1000 (+20)	1000 (+20)
Wave DAC file:	Test_1_5.DAC	Test_1_6.DAC	Test_1_7.DAC	Test_1_8.DAC
Profiler DAC file:	Pro_1_5.DAC	Pro_1_6.DAC	Pro_1_7.DAC	Pro_1_8.DAC
Profiler XLS file:	Pro_1_5.XLS	Pro_1_6.XLS	Pro_1_7.XLS	Pro_1_8.XLS
Profile – windows:	No	No	No	Yes
Pictures:	127-2784 to 87	127-2788 to 91	127-2792 to 96	127-2797 to 2800
Video:				

REMARKS

14:14: All instruments re-zeroed.
14:39: Six extra seconds in Test_1_2.DAC.

8:29: All instruments re-zeroed.
9:45: Setup of video camera.
10:15: Video record: 0:00:00 – 0:07:18
10:53: The profile is rather non-uniform.
11:15: Test finished.

Table A.3 – Project log of test 2

Day: 6/11 – 7/11 2007

GENERAL

Regular / Random:	Regular
Wave spectrum:	Regular, AWA
Water level [m]:	0.60
Wave height [m]:	0.20
Wave period [s]:	2.0
Drive Signal:	AWA_R_2_H0P20_T2P0

Initial profile file:	Pro_2_0.DAC
Trendline slope:	0.0995
R^2 of profile:	0.9994
Initial picture:	128-2801 to 05

TEST

Test name:	Test_2_1	Test_2_2	Test_2_3	Test_2_4
Start time:	14:15	1432	14:45	15:04
Number of waves:	50	50	100	200
Cumulative waves:	50	100	200	400
Duration [s]:	100 (+20)	100 (+20)	200 (+20)	400 (+20)
Wave DAC file:	Test_2_1.DAC	Test_2_2.DAC	Test_2_3.DAC	Test_2_3.DAC
Profiler DAC file:	Pro_2_1.DAC	Pro_2_2.DAC	Pro_2_3.DAC	Pro_2_3.DAC
Profiler XLS file:	Pro_2_1.XLS	Pro_2_2.XLS	Pro_2_3.XLS	Pro_2_3.XLS
Profile – windows:	No	No	No	No
Pictures:	128-2806 to 09	128-2810 to 13	128-2814 to 17	128-2818 to 21
Video:	07:19 to 07:41 to 08:32		08:33 to 08:59	

Test name:	Test_2_5	Test_2_6	Test_2_7	Test_2_8
Start time:	15:21	15:47	8:29	8:59
Number of waves:	400	700	500	500
Cumulative waves:	800	1500	2000	2500
Duration [s]:	800 (+20)	1400 (+20)	1000 (+20)	1000 (+20)
Wave DAC file:	Test_2_5.DAC	Test_2_6.DAC	Test_2_7.DAC	Test_2_8.DAC
Profiler DAC file:	Pro_2_5.DAC	Pro_2_6.DAC	Pro_2_7.DAC	Pro_2_8.DAC
Profiler XLS file:	Pro_2_5.XLS	Pro_2_6.XLS	Pro_2_7.XLS	Pro_2_8.XLS
Profile – windows:	No	No	No	No
Pictures:	128-2822 to 25	128-2826 to 29	128-2830 to 33	128-2834 to 37
Video:		09:00 to 09:31		

REMARKS

14:13: All instruments re-zeroed.

14:18: Video Test_2_1. Trash on video. Cut at 07:41 on camera.

14:30: Video Test_2_1. Video of roller.

14:46: Side wall effects visible, erosion more by the windows than in the middle of the flume.

14:52: Video Test_2_3. Video of 2 berms and 2 erosion holes.

16:10: Video Test_2_6. Video of wave breaking on an “extra berm”.

8:23: All instruments re-zeroed.

8:37: Still two berms, “the extra berm” getting bigger.

Table A.4 – Project log of Test 2, continued

Day: 7/11 2007

GENERAL

Regular / Random:	Regular
Wave spectrum:	Regular, AWA
Water level [m]:	0.60
Wave height [m]:	0.20
Wave period [s]:	2.0
Drive Signal:	AWA_R_2_H0P20_T2P0

Initial profile file:	Pro_2_0.DAC
Trendline slope:	0.0995
R^2 of profile:	0.9994
Initial picture:	128-2801 to 05

TEST

Test name:	Test_2_9	Test_2_10	Test_2_11	Test_2_12
Start time:	9:37	10:11	10:41	11:31
Number of waves:	500	500	500	1000
Cumulative waves:	3000	3500	4000	5000
Duration [s]:	1000 (+20)	1000 (+20)	1000 (+20)	2000 (+20)
Wave DAC file:	Test_2_9.DAC	Test_2_10.DAC	Test_2_11.DAC	Test_2_12.DAC
Profiler DAC file:	Pro_2_9.DAC	Pro_2_10.DAC	Pro_2_11.DAC	Pro_2_12.DAC
Profiler XLS file:	Pro_2_9.XLS	Pro_2_10.XLS	Pro_2_11.XLS	Pro_2_12.XLS
Profile – windows:	No	No	Yes	No
Pictures:	128-2838 to 41	128-2842 to 45	128-2846 to 49	128-2850 to 53
Video:				

Test name:	Test_2_13			
Start time:				
Number of waves:	1000			
Cumulative waves:	6000			
Duration [s]:	2000 (+20)			
Wave DAC file:	Test_2_13.DAC			
Profiler DAC file:	Pro_2_13.DAC			
Profiler XLS file:	Pro_2_13.XLS			
Profile – windows:	No			
Pictures:				
Video:				

REMARKS

9:36: Decided to continue to see if these two berms were here to stay.
10:09: After Test_2_9: Very little change with the high berm, low berm getting smaller.
10:18: Small berm flattening out.
10:41: Significant change recognized after Test_2_10 where the small berm was.
11:32: Test_2_12.DAC recorded wrong channels, no wave data.
12:14: Test_2_13 is an extra test for fiber optics group.

Table A.5 – Project log of Test 3

Day: 8/11 2007

GENERAL

Regular / Random:	Regular
Wave spectrum:	Regular, AWA
Water level [m]:	0.60
Wave height [m]:	0.25
Wave period [s]:	2.0
Drive Signal:	AWA_R_3_H0P25_T2P0

Initial profile file:	Pro_3_0.DAC
Trendline slope:	0.0993
R^2 of profile:	0.9995
Initial picture:	
Initial video:	09:32 to 10:01

TEST

Test name:	Test_3_1	Test_3_2	Test_3_3	Test_3_4
Start time:	8:39	8:54	9:08	9:23
Number of waves:	50	50	100	200
Cumulative waves:	50	100	200	400
Duration [s]:	100 (+20)	100 (+20)	200 (+20)	400 (+20)
Wave DAC file:	Test_3_1.DAC	Test_3_2.DAC	Test_3_3.DAC	Test_3_3.DAC
Profiler DAC file:	Pro_3_1.DAC	Pro_3_2.DAC	Pro_3_3.DAC	Pro_3_3.DAC
Profiler XLS file:	Pro_3_1.XLS	Pro_3_2.XLS	Pro_3_3.XLS	Pro_3_3.XLS
Profile – windows:	No	No	No	No
Pictures: PANORAMA	11:36 to 12:01	13:01 to 13:25	15:02 to 15:34	17:07 to 17:24 to 17:41
Video:	10:02 to 11:35	12:02 to 13:00	13:26 to 14:15	15:34 to 16:14
Video:			14:16 to 15:01	16:15 to 17:07

Test name:	Test_3_5	Test_3_6	Test_3_7	Test_3_8
Start time:	9:43	10:08	10:47 / 11:27	11:53
Number of waves:	400	700	500	500
Cumulative waves:	800	1500	2000	2500
Duration [s]:	800 (+20)	1400 (+20)	1000 (+20)	1000 (+20)
Wave DAC file:	Test_3_5.DAC	Test_3_6.DAC	Test_3_7.DAC	Test_3_8.DAC
Profiler DAC file:	Pro_3_5.DAC	Pro_3_6.DAC	Pro_3_7.DAC	Pro_3_8.DAC
Profiler XLS file:	Pro_3_5.XLS	Pro_3_6.XLS	Pro_3_7.XLS	Pro_3_8.XLS
Profile – windows:	No	No	No	No
Pictures: PANORAMA	18:52 to 19:09	20:15 to 20:32	22:10 to 22:32	24:03 to 24: 23
Video:	17:51 to 18:51	19:10 to 20:14	20:33 to 21:08	22:33 to 24:02
Video:			21:09 to 22:09	

REMARKS

8:28: All instruments re-zeroed.

8:56: Record 12:02 to 13:00: Two videos of wave breaking and roller.

9:27: Record 15:34 to 16:14: The mullion on the wall in a bad place.

9:45: record 17:42 to 17:50: Still picture of the two berms.

9:55: Started using small camera on berm generation

10:52: **Electricity out!** No data saved for the first 5 minutes of Test_3_7.

11:27: Started Test_3_7 again, subtracted 5 minutes from the test.

11:51: All instruments re-zeroed, forgot to re-zero before restarting Test_3_7.

Table A.6 – Project log of Test 3, continued

Day: 8/11 – 9/11 2007

GENERAL

Regular / Random:	Regular
Wave spectrum:	Regular, AWA
Water level [m]:	0.60
Wave height [m]:	0.25
Wave period [s]:	2.0
Drive Signal:	AWA_R_3_H0P25_T2P0

Initial profile file:	Pro_3_0.DAC
Trendline slope:	0.0993
R^2 of profile:	0.9995
Initial picture:	
Initial video:	09:32 to 10:01

TEST

Test name:	Test_3_9	Test_3_10	Test_3_11	Test_3_12
Start time:	12:22	13:05	13:34	14:06
Number of waves:	500	500	500	500
Cumulative waves:	3000	3500	4000	4500
Duration [s]:	1000 (+20)	1000 (+20)	1000 (+20)	1000 (+20)
Wave DAC file:	Test_3_9.DAC	Test_3_10.DAC	Test_3_11.DAC	Test_3_12.DAC
Profiler DAC file:	Pro_3_9.DAC	Pro_3_10.DAC	Pro_3_11.DAC	Pro_3_12.DAC
Profiler XLS file:	Pro_3_9.XLS	Pro_3_10.XLS	Pro_3_11.XLS	Pro_3_12.XLS
Profile – windows:	No	No	No	No
Pictures: PANORAMA	24:24 to 24:50	25:38 to 25:58	25:59 to 26:19	27:11 to 27: 36
Video:		24:51 to 25:37		26:19 to 27:10

Test name:	Test_3_13	Test_3_14	Test_3_15	Test_3_16
Start time:	14:36	15:06	8:28	9:26
Number of waves:	500	1000	1000	1000
Cumulative waves:	5000	6000	7000	8000
Duration [s]:	1000 (+20)	2000 (+20)	2000 (+20)	2000 (+20)
Wave DAC file:	Test_3_13.DAC	Test_3_14.DAC	Test_3_15.DAC	Test_3_16.DAC
Profiler DAC file:	Pro_3_13.DAC	Pro_3_14.DAC	Pro_3_15.DAC	Pro_3_16.DAC
Profiler XLS file:	Pro_3_13.XLS	Pro_3_14.XLS	Pro_3_15.XLS	Pro_3_16.XLS
Profile – windows:	No	No	Some	Some
Pictures: PANORAMA	27:37 to 28:01	28:39 to 29:01	29:02 to 29:21	31:41 to 32:00
Video:		28:02 to 28:38		29:22 to 30:39
Video:				30:40 to 31:40

REMARKS

14:22: Record 26:19 to 27:10: Little movement in the state of equilibrium.

8:24: All instruments re-zeroed.

9:20: Extra measurement made on the window; Test_3_15: 2.9: 86.8 ; 2.8: 87.0 ; 2.7: 87.4 ; 2.5: 88.1. Test3_16: 3.1: 86.9 ; 3.0: 87.6 ; 2.9: 88.5 ; 2.8: 89.4 ; 2.7: 89.4 ; 2.5: 90.1 ; 2.4: 89.6 ; 2.3: 90.3 ; 2.2: 91.2 ; 2.1: 92.0

Table A.7 – Project log of Test 3, continued

Day: 9/11 2007

GENERAL

Regular / Random:	Regular
Wave spectrum:	Regular, AWA
Water level [m]:	0.60
Wave height [m]:	0.25
Wave period [s]:	2.0
Drive Signal:	AWA_R_3_H0P25_T2P0

Initial profile file:	Pro_3_0.DAC
Trendline slope:	0.0993
R^2 of profile:	0.9995
Initial picture:	
Initial video:	09:32 to 10:01

TEST

Test name:	Test_3_17	Test_3_18		
Start time:	10:19	11:11		
Number of waves:	1000	1000		
Cumulative waves:	9000	10000		
Duration [s]:	2000 (+20)	2000 (+20)		
Wave DAC file:	Test_3_17.DAC	Test_3_18.DAC		
Profiler DAC file:	Pro_3_17.DAC	Pro_3_18.DAC		
Profiler XLS file:	Pro_3_17.XLS	Pro_3_18.XLS		
Profile – windows:	Some	Yes		
Pictures: PANORAMA	32:01 to 32:19	32:20 to 32:35		
Video:				

Test name:				
Start time:				
Number of waves:				
Cumulative waves:				
Duration [s]:				
Wave DAC file:				
Profiler DAC file:				
Profiler XLS file:				
Profile – windows:				
Pictures: PANORAMA				
Video:				

REMARKS

Extra points for Test_3_17: 3.3: 85.6 ; 3.2: 86.5 ; 3.1: 87.0 ; 3.0: 88.8 ; 2.9: 89.0 ; 2.8: 89.5 ;
2.7: 89.5 ; 2.5: 90.2 ; 2.4: 90.5 ; 2.3: 91.2 ; 2.2: 91.3 ; 2.1: 92.2 ; 2.0: 93.0.

12:20: Test_3 finished.

Table A.8 – Project log of Test 4

Day: 23/10 2007

GENERAL

Regular / Random:	Random
Wave spectrum:	JONSWAP
Water level [m]:	0.60
Wave height [m]:	0.15
Wave period [s]:	$T_p = 1.5$, $T_{av} = 1.2$
Drive Signal:	JS_3a_H0P15_T1P5

Initial profile file:	Pro_4_0.DAC
Trendline slope:	0.0993
R^2 of profile:	0.9971
Initial picture:	124-2473 to 77

TEST

Test name:	Test_4_1	Test_4_2	Test_4_3	Test_4_4
Start time:	9:17	9:56	10:27	11:04
Number of waves:	100	200	450	250
Cumulative waves:	100	300	750	1000
Duration [s]:	120 (+20)	240 (+20)	540 (+20)	300 (+20)
Wave DAC file:	Test_4_1.DAC	Test_4_2.DAC	Test_4_3.DAC	Test_4_3.DAC
Profiler DAC file:	Pro_4_1.DAC	Pro_4_2.DAC	Pro_4_3.DAC	Pro_4_3.DAC
Profiler XLS file:	Pro_4_1.XLS	Pro_4_2.XLS	Pro_4_3.XLS	Pro_4_3.XLS
Profile – windows:	No	No	No	No
Pictures:	124-2479 to 81	124-2483 to 86	124-2488 to 91	124-2494 to 97
Video:	124-2478	124-2482	124-2487	124-2492

Test name:	Test_4_5	Test_4_6	Test_4_7	
Start time:	11:47	12:31	13:11	
Number of waves:	1000	1000	1000	
Cumulative waves:	2000	3000	4000	
Duration [s]:	1200 (+20)	1200 (+20)	1200 (+20)	
Wave DAC file:	Test_4_5.DAC	Test_4_6.DAC	Test_4_7.DAC	
Profiler DAC file:	Pro_4_5.DAC	Pro_4_6.DAC	Pro_4_7.DAC	
Profiler XLS file:	Pro_4_5.XLS	Pro_4_6.XLS	Pro_4_7.XLS	
Profile – windows:	No	No	Yes	
Pictures:	124-2500 to 03	125-2505 to 08	125-2510 to 13	
Video:	124-2499	125-2501	125-2509	

REMARKS

11:19: Wave gauge no. 12 stretched and re-zeroed.

13:00: Took a picture of the profile: 125-2504

Table A.9 – Project log of Test 5

Day: 23/10 – 24/10 2007

GENERAL

Regular / Random:	Random
Wave spectrum:	JONSWAP
Water level [m]:	0.60
Wave height [m]:	0.15
Wave period [s]:	$T_p = 2$, $T_{av} = 1.578$
Drive Signal:	JS_3b_ H0P15_T2P0

Initial profile file:	Pro_5_0.DAC
Trendline slope:	0.0995
R^2 of profile:	0.9969
Initial picture:	125-2514 to 18

TEST

Test name:	Test_5_1	Test_5_2	Test_5_3	Test_5_4
Start time:	15:47	16:03	16:24	8:10
Number of waves:	100	200	450	250
Cumulative waves:	100	300	750	1000
Duration [s]:	159 (+20)	318 (+20)	716 (+20)	398 (+20)
Wave DAC file:	Test_5_1.DAC	Test_5_2.DAC	Test_5_3.DAC	Test_5_3.DAC
Profiler DAC file:	Pro_5_1.DAC	Pro_5_2.DAC	Pro_5_3.DAC	Pro_5_3.DAC
Profiler XLS file:	Pro_5_1.XLS	Pro_5_2.XLS	Pro_5_3.XLS	Pro_5_3.XLS
Profile – windows:	No	No	No	No
Pictures:	125-2520 to 23	125-2525 to 28	125-2530 to 33	125-2535 to 38
Video:	125-2519	125-2524	125-2529	125-2534

Test name:	Test_5_5	Test_5_6	Test_5_7	Test_5_8
Start time:	8:32	9:12	9:56	11:00
Number of waves:	1000	1000	1000	1000
Cumulative waves:	2000	3000	4000	5000
Duration [s]:	1587 (+20)	1587 (+20)	1587 (+20)	1587 (+20)
Wave DAC file:	Test_5_5.DAC	Test_5_6.DAC	Test_5_7.DAC	Test_5_8.DAC
Profiler DAC file:	Pro_5_5.DAC	Pro_5_6.DAC	Pro_5_7.DAC	Pro_5_8.DAC
Profiler XLS file:	Pro_5_5.XLS	Pro_5_6.XLS	Pro_5_7.XLS	Pro_5_8.XLS
Profile – windows:	No	No	No	Yes
Pictures:	125-2540 to 43	125-2545 to 48	125-2550 to 57	125-2559 to 62
Video:	125-2539	125-2544	125-2549	125-2558

REMARKS

8:04: All instruments re-zeroed.
8:30: WG12 lowered and re-zeroed.
8:53: Profile is uniform over the width of the flume.
9:10: Significant change after 2000 waves.
9:38: Range of erosion is getting longer.
10:37: Test_5_7: Two sets of panorama pictures.
11:00: Decided to run 5000 waves.

Table A.10 – Project log of Test 6

Day: 24/10 – 25/10 2007

GENERAL

Regular / Random:	Random
Wave spectrum:	JONSWAP
Water level [m]:	0.60
Wave height [m]:	0.15
Wave period [s]:	$T_p = 2.5$, $T_{av} = 1.978$
Drive Signal:	JS_3c_H0P15_T2P5

Initial profile file:	Pro_6_0.DAC
Trendline slope:	0.1008
R^2 of profile:	0.9975
Initial picture:	125-2563 to 67

TEST

Test name:	Test_6_1	Test_6_2	Test_6_3	Test_6_4
Start time:	14:45	15:04	15:22	15:49
Number of waves:	100	200	450	250
Cumulative waves:	100	300	750	1000
Duration [s]:	198 (+20)	396 (+20)	891 (+20)	495 (+20)
Wave DAC file:	Test_6_1.DAC	Test_6_2.DAC	Test_6_3.DAC	Test_6_3.DAC
Profiler DAC file:	Pro_6_1.DAC	Pro_6_2.DAC	Pro_6_3.DAC	Pro_6_3.DAC
Profiler XLS file:	Pro_6_1.XLS	Pro_6_2.XLS	Pro_6_3.XLS	Pro_6_3.XLS
Profile – windows:	No	No	No	No
Pictures:	125-2577 to 79	125-2580 to 83	125-2585 to 88	125-2590 to 92
Video:	125-2568	125-2573	125-2584	125-2589

Test name:	Test_6_5	Test_6_6	Test_6_7	Test_6_8
Start time:	16:07	8:18	9:05	9:50
Number of waves:	1000	1000	1000	1000
Cumulative waves:	2000	3000	4000	5000
Duration [s]:	1978 (+20)	1978 (+20)	1978 (+20)	1978 (+20)
Wave DAC file:	Test_6_5.DAC	Test_6_6.DAC	Test_6_7.DAC	Test_6_8.DAC
Profiler DAC file:	Pro_6_5.DAC	Pro_6_6.DAC	Pro_6_7.DAC	Pro_6_8.DAC
Profiler XLS file:	Pro_6_5.XLS	Pro_6_6.XLS	Pro_6_7.XLS	Pro_6_8.XLS
Profile – windows:	No	No	No	Yes
Pictures:	125-2594 to 97	125-2600 to 03	126-2604 to 07	126-2610 to 13
Video:	125-2593	125-2598 to 99	126-2601 to 03	126-2608 to 09

REMARKS

14:44: All instruments re-zeroed.
16:29: WG12 not low enough.
16:53: WG12 lowered.
8:10: Water level set and all instruments re-zeroed.
8:47: Berm is steep and is reflecting waves.
11:00: Test finished.

Table A.11 – Project log of Test 7

Day: 25/10 2007

GENERAL

Regular / Random:	Random
Wave spectrum:	JONSWAP
Water level [m]:	0.60
Wave height [m]:	0.20
Wave period [s]:	$T_p = 1.5$, $T_{av} = 1.2$
Drive Signal:	JS_4a_H0P20_T1P5

Initial profile file:	Pro_7_0.DAC
Trendline slope:	0.1007
R^2 of profile:	0.9975
Initial picture:	126-2614 to 18

TEST

Test name:	Test_7_1	Test_7_2	Test_7_3	Test_7_4
Start time:	13:16	13:31	13:50	14:11
Number of waves:	100	200	450	250
Cumulative waves:	100	300	750	1000
Duration [s]:	120 (+20)	240 (+20)	540 (+20)	300 (+20)
Wave DAC file:	Test_7_1.DAC	Test_7_2.DAC	Test_7_3.DAC	Test_7_3.DAC
Profiler DAC file:	Pro_7_1.DAC	Pro_7_2.DAC	Pro_7_3.DAC	Pro_7_3.DAC
Profiler XLS file:	Pro_7_1.XLS	Pro_7_2.XLS	Pro_7_3.XLS	Pro_7_3.XLS
Profile – windows:	No	No	No	No
Pictures:	126-2620 to 23	126-2626 to 29	126-2632 to 35	126-2638 to 40
Video:	126-2619	126-2624 to 25	126-2630 to 31	126-2636 to 37

Test name:	Test_7_5	Test_7_6	Test_7_7	Test_7_8
Start time:	14:27	14:58	15:31	16:05
Number of waves:	1000	1000	1000	1000
Cumulative waves:	2000	3000	4000	5000
Duration [s]:	1200 (+20)	1200 (+20)	1200 (+20)	1200 (+20)
Wave DAC file:	Test_7_5.DAC	Test_7_6.DAC	Test_7_7.DAC	Test_7_8.DAC
Profiler DAC file:	Pro_7_5.DAC	Pro_7_6.DAC	Pro_7_7.DAC	Pro_7_8.DAC
Profiler XLS file:	Pro_7_5.XLS	Pro_7_6.XLS	Pro_7_7.XLS	Pro_7_8.XLS
Profile – windows:	No	No	No	Yes
Pictures:	126-2643 to 45	126-2648 to 50	126-2656 to 58	126-2661 to 63
Video:	126-2641	126-2646	126-2651 to 52	126-2659 to 60

REMARKS

13:15: Water level set to 0.6 m and instruments re-zeroed.

14:35: Pressure transducer no. 4 (PT4) is sometimes above water.

14:43: Video of PT4: 126-2642.

15:14 Video of wave generator in action: 126-2647.

16:03: Pictures 126-2653 to 55 are trash.

8:43 (Oct. 26th): Profiling windows finished, Test 7 finished.

Table A.12 – Project log of Test 8

Day: 26/10 2007

GENERAL

Regular / Random:	Random
Wave spectrum:	JONSWAP
Water level [m]:	0.60
Wave height [m]:	0.20
Wave period [s]:	$T_p = 2$, $T_{av} = 1.578$
Drive Signal:	JS_4b_H0P20_T2P0

Initial profile file:	Pro_8_0.DAC
Trendline slope:	0.1007
R^2 of profile:	0.9984
Initial picture:	126-2664 to 67

TEST

Test name:	Test_8_1	Test_8_2	Test_8_3	Test_8_4
Start time:	10:50	11:10	11:29	11:53
Number of waves:	100	200	450	250
Cumulative waves:	100	300	750	1000
Duration [s]:	159 (+20)	318 (+20)	716 (+20)	398 (+20)
Wave DAC file:	Test_8_1.DAC	Test_8_2.DAC	Test_8_3.DAC	Test_8_3.DAC
Profiler DAC file:	Pro_8_1.DAC	Pro_8_2.DAC	Pro_8_3.DAC	Pro_8_3.DAC
Profiler XLS file:	Pro_8_1.XLS	Pro_8_2.XLS	Pro_8_3.XLS	Pro_8_3.XLS
Profile – windows:	No	No	No	No
Pictures:	126-2670 to 73	126-2676 to 79	126-2682 to 85	126-2688 to 91
Video:				

Test name:	Test_8_5	Test_8_6	Test_8_7	Test_8_8
Start time:	12:13	13:10	13:57	14:35
Number of waves:	1000	1000	1000	1000
Cumulative waves:	2000	3000	4000	5000
Duration [s]:	1587 (+20)	1587 (+20)	1587 (+20)	1587 (+20)
Wave DAC file:	Test_8_5.DAC	Test_8_6.DAC	Test_8_7.DAC	Test_8_8.DAC
Profiler DAC file:	Pro_8_5.DAC	Pro_8_6.DAC	Pro_8_7.DAC	Pro_8_8.DAC
Profiler XLS file:	Pro_8_5.XLS	Pro_8_6.XLS	Pro_8_7.XLS	Pro_8_8.XLS
Profile – windows:	No	No	No	Yes
Pictures:	126-2694 to 97	126-2699 to 2702	127-2703 to 06	No
Video:	126-2692 to 93	126-2698	127-2701 to 02	127-2707 to 11

REMARKS

12:00: WG1 data are different from WG2 and WG3 data. The reason might be that WG1 records reflection waves.
12:31: WG12 needs to be lowered.
12:47: WG12 lowered.
13:02: Forgot to re-zero WG12. Test_8_6 stopped after 100 seconds. Test_8_6a.DAC keeps data of these 100 seconds.
13:10: Test_8_6 is split into 6a and 6b, use 6b for data analysis.
14:33: WG11 and WG12 lowered and re-zeroed.

Table A.13 – Project log of Test 8, continued

Day: 29/10 2007

GENERAL

Regular / Random:	Random
Wave spectrum:	JONSWAP
Water level [m]:	0.60
Wave height [m]:	0.20
Wave period [s]:	$T_p = 2$, $T_{av} = 1.578$
Drive Signal:	JS_4b_H0P20_T2P0

Initial profile file:	Pro_8_0.DAC
Trendline slope:	0.1007
R^2 of profile:	0.9984
Initial picture:	126-2664 to 67

TEST

Test name:	Test_8_9			
Start time:	8:50			
Number of waves:	5000			
Cumulative waves:	10000			
Duration [s]:	7935 (+20)			
Wave DAC file:	Test_8_9.DAC			
Profiler DAC file:	Pro_8_9.DAC			
Profiler XLS file:	Pro_8_9.XLS			
Profile – windows:	No			
Pictures:	126-2716 to 19			
Video:	127-2713 to 15			

Test name:				
Start time:				
Number of waves:				
Cumulative waves:				
Duration [s]:				
Wave DAC file:				
Profiler DAC file:				
Profiler XLS file:				
Profile – windows:				
Pictures:				
Video:				

REMARKS

Extra 5000 waves to see profile changes from 5000 to 10000 waves.

Table A.14 – Project log of Test 9

Day: 29/10 – 30/10 2007

GENERAL

Regular / Random:	Random
Wave spectrum:	JONSWAP
Water level [m]:	0.60
Wave height [m]:	0.20
Wave period [s]:	$T_p = 2.5$, $T_{av} = 1.978$
Drive Signal:	JS_4c_H0P20_T2P5

Initial profile file:	Pro_9_0.DAC
Trendline slope:	0.1007
R^2 of profile:	0.9991
Initial picture:	127-2720 to 24

TEST

Test name:	Test_9_1	Test_9_2	Test_9_3	Test_9_4
Start time:	14:22	14:41	15:00	15:26
Number of waves:	100	200	450	250
Cumulative waves:	100	300	750	1000
Duration [s]:	198 (+20)	396 (+20)	891 (+20)	495 (+20)
Wave DAC file:	Test_9_1.DAC	Test_9_2.DAC	Test_9_3.DAC	Test_9_3.DAC
Profiler DAC file:	Pro_9_1.DAC	Pro_9_2.DAC	Pro_9_3.DAC	Pro_9_3.DAC
Profiler XLS file:	Pro_9_1.XLS	Pro_9_2.XLS	Pro_9_3.XLS	Pro_9_3.XLS
Profile – windows:	No	No	No	No
Pictures:	127-2725 to 28	127-2729 to 32	127-2733 to 36	127-2737 to 40
Video:				

Test name:	Test_9_5	Test_9_6	Test_9_7	Test_9_8
Start time:	15:46	8:25	9:09	9:57
Number of waves:	1000	1000	1000	1000
Cumulative waves:	2000	3000	4000	5000
Duration [s]:	1978 (+20)	1978 (+20)	1978 (+20)	1978 (+20)
Wave DAC file:	Test_9_5.DAC	Test_9_6.DAC	Test_9_7.DAC	Test_9_8.DAC
Profiler DAC file:	Pro_9_5.DAC	Pro_9_6.DAC	Pro_9_7.DAC	Pro_9_8.DAC
Profiler XLS file:	Pro_9_5.XLS	Pro_9_6.XLS	Pro_9_7.XLS	Pro_9_8.XLS
Profile – windows:	No	No	Some	Yes
Pictures:	127-2741 to 44	127-2745 to 48	127-2749 to 52	127-2753 to 57
Video:				

REMARKS

14:17: Water level set to 0.60 m and instruments re-zeroed.

8:21: Water level set to 0.60 m and instruments re-zeroed.
9:55: Extra points for Pro_9_7:
2.4: 89.0 ; 2.5: 88.5 ; 2.7: 87.0 ; 2.8: 86.6 ; 2.9: 85.6 ; 3.0: 85.4

Table A.15 – Project log of Test 9, continued

Day: 29/10 – 30/10 2007

GENERAL

Regular / Random:	Random
Wave spectrum:	JONSWAP
Water level [m]:	0.60
Wave height [m]:	0.20
Wave period [s]:	$T_p = 2.5$, $T_{av} = 1.978$
Drive Signal:	JS_4c_H0P20_T2P5

Initial profile file:	Pro_9_0.DAC
Trendline slope:	0.1007
R^2 of profile:	0.9991
Initial picture:	127-2720 to 24

TEST

Test name:	Test_9_9			
Start time:	11:03			
Number of waves:	5000			
Cumulative waves:	10000			
Duration [s]:	9890 (+20)			
Wave DAC file:	Test_9_9.DAC			
Profiler DAC file:	Pro_9_9.DAC			
Profiler XLS file:	Pro_9_9.XLS			
Profile – windows:	No			
Pictures:	127-2758 to 62			
Video:				

Test name:				
Start time:				
Number of waves:				
Cumulative waves:				
Duration [s]:				
Wave DAC file:				
Profiler DAC file:				
Profiler XLS file:				
Profile – windows:				
Pictures:				
Video:				

REMARKS

Extra points for Pro_9_9:

2.0: 93.0 ; 2.1: 92.2 ; 2.2: 91.6 ; 2.3: 90.8 ; 2.4: 89.7 ; 2.5: 89.7 ; 2.7: 88.0 ; 2.8: 87.1 ;

2.9: 87.0 ; 3.0: 87.0

13:50: Test finished.

Table A.16 – Project log of Test 10

Day: 20/11 2007

GENERAL

Regular / Random:	Regular
Wave spectrum:	Regular, AWA
Water level [m]:	0.60
Wave height [m]:	0.15
Wave period [s]:	2.0
Drive Signal:	AWA_R_1_H0P15_T2P0

Initial profile file:	Pro_10_0.DAC
Trendline slope:	0.1415
R^2 of profile:	0.9997
Initial picture:	128-2881 to 85

TEST

Test name:	Test_10_1	Test_10_2	Test_10_3	Test_10_4
Start time:	8:16	8:32	8:48	9:09
Number of waves:	50	50	100	200
Cumulative waves:	50	100	200	400
Duration [s]:	100 (+20)	100 (+20)	200 (+20)	400 (+20)
Wave DAC file:	Test_10_1.DAC	Test_10_2.DAC	Test_10_3.DAC	Test_10_3.DAC
Profiler DAC file:	Pro_10_1.DAC	Pro_10_2.DAC	Pro_10_3.DAC	Pro_10_3.DAC
Profiler XLS file:	Pro_10_1.XLS	Pro_10_2.XLS	Pro_10_3.XLS	Pro_10_3.XLS
Profile – windows:	No	No	No	No
Pictures:	128-2886 to 90	128-2891 to 95	128-2896 to 2900	129-2901 to 05
Video:				

Test name:	Test_10_5	Test_10_6	Test_10_7	Test_10_8
Start time:	9:24	9:48	10:21	10:49
Number of waves:	400	700	500	500
Cumulative waves:	800	1500	2000	2500
Duration [s]:	800 (+20)	1400 (+20)	1000 (+20)	1000 (+20)
Wave DAC file:	Test_10_5.DAC	Test_10_6.DAC	Test_10_7.DAC	Test_10_8.DAC
Profiler DAC file:	Pro_10_5.DAC	Pro_10_6.DAC	Pro_10_7.DAC	Pro_10_8.DAC
Profiler XLS file:	Pro_10_5.XLS	Pro_10_6.XLS	Pro_10_7.XLS	Pro_10_8.XLS
Profile – windows:	No	No	No	Yes
Pictures:	129-2906 to 10	129-2911 to 15	129-2916 to 20	129-2921 to 25
Video:				

REMARKS

8:48: Water dirty, decided to wait with video recordings.

10:31: Equilibrium reached earlier than for 1:10 slope.

Table A.17 – Project log of Test 11

Day: 20/11 2007

GENERAL

Regular / Random:	Regular
Wave spectrum:	Regular, AWA
Water level [m]:	0.60
Wave height [m]:	0.20
Wave period [s]:	2.0
Drive Signal:	AWA_R_2_H0P20_T2P0

Initial profile file:	Pro_11_0.DAC
Trendline slope:	0.1434
R^2 of profile:	0.9997
Initial picture:	129-2926 to 30

TEST

Test name:	Test_11_1	Test_11_2	Test_11_3	Test_11_4
Start time:	13:02	13:14	13:25	13:44
Number of waves:	50	50	100	200
Cumulative waves:	50	100	200	400
Duration [s]:	100 (+20)	100 (+20)	200 (+20)	400 (+20)
Wave DAC file:	Test_11_1.DAC	Test_11_2.DAC	Test_11_3.DAC	Test_11_3.DAC
Profiler DAC file:	Pro_11_1.DAC	Pro_11_2.DAC	Pro_11_3.DAC	Pro_11_3.DAC
Profiler XLS file:	Pro_11_1.XLS	Pro_11_2.XLS	Pro_11_3.XLS	Pro_11_3.XLS
Profile – windows:	No	No	No	No
Pictures:	129-2931 to 35	129-2936 to 40	129-2941 to 45	129-2946 to 50
Video:				

Test name:	Test_11_5	Test_11_6	Test_11_7	Test_11_8
Start time:	14:02	14:24	15:02	15:29
Number of waves:	400	700	500	500
Cumulative waves:	800	1500	2000	2500
Duration [s]:	800 (+20)	1400 (+20)	1000 (+20)	1000 (+20)
Wave DAC file:	Test_11_5.DAC	Test_11_6.DAC	Test_11_7.DAC	Test_11_8.DAC
Profiler DAC file:	Pro_11_5.DAC	Pro_11_6.DAC	Pro_11_7.DAC	Pro_11_8.DAC
Profiler XLS file:	Pro_11_5.XLS	Pro_11_6.XLS	Pro_11_7.XLS	Pro_11_8.XLS
Profile – windows:	No	No	No	Yes
Pictures:	129-2951 to 55	129-2956 to 60	129-2961 to 65	129-2966 to 70
Video:				

REMARKS

13:00: All instruments re-zeroed.

Table A.18 – Project log of Test 11, continued

Day: 20/11 2007

GENERAL

Regular / Random:	Regular
Wave spectrum:	Regular, AWA
Water level [m]:	0.60
Wave height [m]:	0.20
Wave period [s]:	2.0
Drive Signal:	AWA_R_2_H0P20_T2P0

Initial profile file:	Pro_11_0.DAC
Trendline slope:	0.1434
R^2 of profile:	0.9997
Initial picture:	129-2926 to 30

TEST

Test name:	Test_11_9			
Start time:	15:54			
Number of waves:	500			
Cumulative waves:	3000			
Duration [s]:	1000 (+20)			
Wave DAC file:	Test_11_9.DAC			
Profiler DAC file:	Pro_11_9.DAC			
Profiler XLS file:	Pro_11_9.XLS			
Profile – windows:	Yes			
Pictures:	129-2971 to 75			
Video:				

Test name:				
Start time:				
Number of waves:				
Cumulative waves:				
Duration [s]:				
Wave DAC file:				
Profiler DAC file:				
Profiler XLS file:				
Profile – windows:				
Pictures:				
Video:				

REMARKS

Table A.19 – Project log of Test 12

Day: 21/11 2007

GENERAL

Regular / Random:	Regular
Wave spectrum:	Regular, AWA
Water level [m]:	0.60
Wave height [m]:	0.25
Wave period [s]:	2.0
Drive Signal:	AWA_R_3_H0P25_T2P0

Initial profile file:	Pro_12_0.DAC
Trendline slope:	0.1431
R^2 of profile:	0.9991
Initial picture:	129-2976 to 80

TEST

Test name:	Test_12_1	Test_12_2	Test_12_3	Test_12_4
Start time:	10:45	10:57	11:12	11:30
Number of waves:	50	50	100	200
Cumulative waves:	50	100	200	400
Duration [s]:	100 (+20)	100 (+20)	200 (+20)	400 (+20)
Wave DAC file:	Test_12_1.DAC	Test_12_2.DAC	Test_12_3.DAC	Test_12_3.DAC
Profiler DAC file:	Pro_12_1.DAC	Pro_12_2.DAC	Pro_12_3.DAC	Pro_12_3.DAC
Profiler XLS file:	Pro_12_1.XLS	Pro_12_2.XLS	Pro_12_3.XLS	Pro_12_3.XLS
Profile – windows:	No	No	No	No
Pictures:	129-2981 to 85	129-2986 to 90	129-2992 to 96	129-2997 to 3001
Video:	32:35 to 33:34		33:35 to 34:22	

Test name:	Test_12_5	Test_12_6	Test_12_7	Test_12_8
Start time:	11:48	12:17	12:55	13:22
Number of waves:	400	700	500	500
Cumulative waves:	800	1500	2000	2500
Duration [s]:	800 (+20)	1400 (+20)	1000 (+20)	1000 (+20)
Wave DAC file:	Test_12_5.DAC	Test_12_6.DAC	Test_12_7.DAC	Test_12_8.DAC
Profiler DAC file:	Pro_12_5.DAC	Pro_12_6.DAC	Pro_12_7.DAC	Pro_12_8.DAC
Profiler XLS file:	Pro_12_5.XLS	Pro_12_6.XLS	Pro_12_7.XLS	Pro_12_8.XLS
Profile – windows:	No	Some	Some	Some
Pictures:	130-3001 to 05	130-3006 to 10	130-3011 to 15	130-3016 to 20
Video:				34:23 to 35:00

REMARKS

10:37: All instruments re-zeroed.

Video record 32:35 to 33:34: Run-up.

Video record 33:35 to 34:22: Roller and sediment transport.

Video record 34:23 to 35:00: Run-up on the berm.

Test_12_6 and Test_12_7 extra points: 3.9: 91.2 ; 4.05: 89.9 ; 4.3: 88.5 ; 4.4: 87.6 ; 4.5: 86.9.

Test_12_8 extra points: 3.8: 93.0 ; 3.9: 91.9 ; 4.05: 89.9 ; 4.3: 88.7 ; 4.4: 87.9 ; 4.5: 87.5.

Table A.20 – Project log of Test 12, continued

Day: 21/11 2007

GENERAL

Regular / Random:	Regular
Wave spectrum:	Regular, AWA
Water level [m]:	0.60
Wave height [m]:	0.25
Wave period [s]:	2.0
Drive Signal:	AWA_R_3_H0P25_T2P0

Initial profile file:	Pro_12_0.DAC
Trendline slope:	0.1431
R^2 of profile:	0.9991
Initial picture:	129-2976 to 80

TEST

Test name:	Test_12_9			
Start time:	13:56			
Number of waves:	500			
Cumulative waves:	3000			
Duration [s]:	1000 (+20)			
Wave DAC file:	Test_12_9.DAC			
Profiler DAC file:	Pro_12_9.DAC			
Profiler XLS file:	Pro_12_9.XLS			
Profile – windows:	Yes			
Pictures:	130-3021 to 25			
Video:				

Test name:				
Start time:				
Number of waves:				
Cumulative waves:				
Duration [s]:				
Wave DAC file:				
Profiler DAC file:				
Profiler XLS file:				
Profile – windows:				
Pictures:				
Video:				

REMARKS

14:15: Pressure gauge no. 11 has been acting weird in Test_12_8 and Test_12_8.

14:40: Test finished.

Table A.21 – Project log of Test 13

Day: 22/11 2007

GENERAL

Regular / Random:	Random
Wave spectrum:	JONSWAP
Water level [m]:	0.60
Wave height [m]:	0.15
Wave period [s]:	$T_p = 1.5, T_{av} = 1.2$
Drive Signal:	AWA_JS_T1P5_H0P15

Initial profile file:	Pro_13_0.DAC
Trendline slope:	0.1433
R^2 of profile:	0.9990
Initial picture:	130-3025 to 30

TEST

Test name:	Test_13_1	Test_13_2	Test_13_3	Test_13_4
Start time:	13:27	13:40	13:55	14:14
Number of waves:	100	200	450	250
Cumulative waves:	100	300	750	1000
Duration [s]:	120 (+20)	240 (+20)	540 (+20)	300 (+20)
Wave DAC file:	Test_13_1.DAC	Test_13_2.DAC	Test_13_3.DAC	Test_13_3.DAC
Profiler DAC file:	Pro_13_1.DAC	Pro_13_2.DAC	Pro_13_3.DAC	Pro_13_3.DAC
Profiler XLS file:	Pro_13_1.XLS	Pro_13_2.XLS	Pro_13_3.XLS	Pro_13_3.XLS
Profile – windows:	No	No	No	No
Pictures:	130-3031 to 35	130-3036 to 40	130-3041 to 45	130-3046 to 50
Video:		35:01 to 36:00		

Test name:	Test_13_5	Test_13_6	Test_13_7	Test_13_8
Start time:	14:28	14:57	15:26	15:54
Number of waves:	1000	1000	1000	1000
Cumulative waves:	2000	3000	4000	5000
Duration [s]:	1200 (+20)	1200 (+20)	1200 (+20)	1200 (+20)
Wave DAC file:	Test_13_5.DAC	Test_13_6.DAC	Test_13_7.DAC	Test_13_8.DAC
Profiler DAC file:	Pro_13_5.DAC	Pro_13_6.DAC	Pro_13_7.DAC	Pro_13_8.DAC
Profiler XLS file:	Pro_13_5.XLS	Pro_13_6.XLS	Pro_13_7.XLS	Pro_13_8.XLS
Profile – windows:	No	No	No	Yes
Pictures:	130-3051 to 55	130-3056 to 60	130-3061 to 65	130-3066 to 70
Video:	36:01 to 36:40			36:41 to 37:20

REMARKS

9:33: All instruments re-zeroed. Pressure transducer no. 11 is dead. **PT11 is replaced by PT10.**

13:18: All instruments re-zeroed and test starts.

Table A.22 – Project log of Test 14

Day: 23/11 2007

GENERAL

Regular / Random:	Random
Wave spectrum:	JONSWAP
Water level [m]:	0.60
Wave height [m]:	0.15
Wave period [s]:	$T_p = 2$, $T_{av} = 1.578$
Drive Signal:	AWA_JS_T2P0_H0P15

Initial profile file:	Pro_14_0.DAC
Trendline slope:	0.1426
R^2 of profile:	0.9997
Initial picture:	1303071 to 75

TEST

Test name:	Test_14_1	Test_14_2	Test_14_3	Test_14_4
Start time:	10:51	11:06	11:24	11:46
Number of waves:	100	200	450	250
Cumulative waves:	100	300	750	1000
Duration [s]:	159 (+20)	318 (+20)	716 (+20)	398 (+20)
Wave DAC file:	Test_14_1.DAC	Test_14_2.DAC	Test_14_3.DAC	Test_14_3.DAC
Profiler DAC file:	Pro_14_1.DAC	Pro_14_2.DAC	Pro_14_3.DAC	Pro_14_3.DAC
Profiler XLS file:	Pro_14_1.XLS	Pro_14_2.XLS	Pro_14_3.XLS	Pro_14_3.XLS
Profile – windows:	No	No	No	No
Pictures:	130-3076 to 80	130-3081 to 85	130-3086 to 90	130-3091 to 95
Video:				

Test name:	Test_14_5	Test_14_6	Test_14_7	Test_14_8
Start time:	12:03	12:53	13:30	14:06
Number of waves:	1000	1000	1000	1000
Cumulative waves:	2000	3000	4000	5000
Duration [s]:	1587 (+20)	1587 (+20)	1587 (+20)	1587 (+20)
Wave DAC file:	Test_14_5.DAC	Test_14_6.DAC	Test_14_7.DAC	Test_14_8.DAC
Profiler DAC file:	Pro_14_5.DAC	Pro_14_6.DAC	Pro_14_7.DAC	Pro_14_8.DAC
Profiler XLS file:	Pro_14_5.XLS	Pro_14_6.XLS	Pro_14_7.XLS	Pro_14_8.XLS
Profile – windows:	No	No	No	Yes
Pictures:	130-3096 to 3100	131-3101 to 05	131-3106 to 10	131-3111 to 15
Video:				

REMARKS

10:05: All instruments re-zeroed.

11:22: Pro_14_2.DAC stores data while the car was driving up on the profiler's bar.

15:00: Test finished.

Table A.23 – Project log of Test 15

Day: 26/11 2007

GENERAL

Regular / Random:	Random
Wave spectrum:	JONSWAP
Water level [m]:	0.60
Wave height [m]:	0.15
Wave period [s]:	$T_p = 2.5$, $T_{av} = 1.978$
Drive Signal:	AWA_JS_T2P5_H0P15

Initial profile file:	Pro_15_0.DAC
Trendline slope:	0.1431
R^2 of profile:	0.9998
Initial picture:	131-3117 to 21

TEST

Test name:	Test_15_1	Test_15_2	Test_15_3	Test_15_4
Start time:	9:16	9:30	9:47	10:12
Number of waves:	100	200	450	250
Cumulative waves:	100	300	750	1000
Duration [s]:	198 (+20)	396 (+20)	891 (+20)	495 (+20)
Wave DAC file:	Test_15_1.DAC	Test_15_2.DAC	Test_15_3.DAC	Test_15_3.DAC
Profiler DAC file:	Pro_15_1.DAC	Pro_15_2.DAC	Pro_15_3.DAC	Pro_15_3.DAC
Profiler XLS file:	Pro_15_1.XLS	Pro_15_2.XLS	Pro_15_3.XLS	Pro_15_3.XLS
Profile – windows:	No	No	No	No
Pictures:	131-3122 to 26	131-3127 to 31	131-3132 to 36	131-3137 to 41
Video:				

Test name:	Test_15_5	Test_15_6	Test_15_7	Test_15_8
Start time:	10:30	11:13	11:58	12:40
Number of waves:	1000	1000	1000	1000
Cumulative waves:	2000	3000	4000	5000
Duration [s]:	1978 (+20)	1978 (+20)	1978 (+20)	1978 (+20)
Wave DAC file:	Test_15_5.DAC	Test_15_6.DAC	Test_15_7.DAC	Test_15_8.DAC
Profiler DAC file:	Pro_15_5.DAC	Pro_15_6.DAC	Pro_15_7.DAC	Pro_15_8.DAC
Profiler XLS file:	Pro_15_5.XLS	Pro_15_6.XLS	Pro_15_7.XLS	Pro_15_8.XLS
Profile – windows:	No	No	No	Yes
Pictures:	131-3142 to 46	131-3147 to 51	131-3152 to 56	131-3157 to 61
Video:				

REMARKS

9:12: Profile ready and instruments have been re-zeroed.

11:56: WG12 lowered.

13:50: Test finished.

Table A.24 – Project log of Test 16

Day: 26/11 – 27/11 2007

GENERAL

Regular / Random:	Random
Wave spectrum:	JONSWAP
Water level [m]:	0.60
Wave height [m]:	0.20
Wave period [s]:	$T_p = 1.5$, $T_{av} = 1.2$
Drive Signal:	AWA_JS_T1P5_H0P20

Initial profile file:	Pro_16_0.DAC
Trendline slope:	0.1418
R^2 of profile:	0.9996
Initial picture:	131-3162 to 66

TEST

Test name:	Test_16_1	Test_16_2	Test_16_3	Test_16_4
Start time:	15:23	15:38	15:51	8:31
Number of waves:	100	200	450	250
Cumulative waves:	100	300	750	1000
Duration [s]:	120 (+20)	240 (+20)	540 (+20)	300 (+20)
Wave DAC file:	Test_16_1.DAC	Test_16_2.DAC	Test_16_3.DAC	Test_16_3.DAC
Profiler DAC file:	Pro_16_1.DAC	Pro_16_2.DAC	Pro_16_3.DAC	Pro_16_3.DAC
Profiler XLS file:	Pro_16_1.XLS	Pro_16_2.XLS	Pro_16_3.XLS	Pro_16_3.XLS
Profile – windows:	No	No	No	No
Pictures:	131-3167 to 71	131-3172 to 76	131-3177 to 81	131-3182 to 86
Video:				

Test name:	Test_16_5	Test_16_6	Test_16_7	Test_16_8
Start time:	8:46	9:18	9:48	10:21
Number of waves:	1000	1000	1000	1000
Cumulative waves:	2000	3000	4000	5000
Duration [s]:	1200 (+20)	1200 (+20)	1200 (+20)	1200 (+20)
Wave DAC file:	Test_16_5.DAC	Test_16_6.DAC	Test_16_7.DAC	Test_16_8.DAC
Profiler DAC file:	Pro_16_5.DAC	Pro_16_6.DAC	Pro_16_7.DAC	Pro_16_8.DAC
Profiler XLS file:	Pro_16_5.XLS	Pro_16_6.XLS	Pro_16_7.XLS	Pro_16_8.XLS
Profile – windows:	No	No	No	Yes
Pictures:	131-3187 to 91	131-3192 to 96	131-3197 to 3201	132-3201 to 05
Video:	37:20 to 38:20			
Video:	38:21 to 39:40			

REMARKS

15:21: All instruments re-zeroed.

8:25: All instruments re-zeroed.

9:01: Videos of Test_16_5: Sediment transport in wave breaking zone, the later one zooms in.

10:01: Test_16_7: Forgot to set the time, so the test ran first for default 600 seconds. Test_16_7a stores the rest, 620 seconds.

11:03: Test finished.

Table A.25 – Project log of Test 17

Day: 27/11 – 28/11 2007

GENERAL

Regular / Random:	Random
Wave spectrum:	JONSWAP
Water level [m]:	0.60
Wave height [m]:	0.20
Wave period [s]:	$T_p = 2$, $T_{av} = 1.578$
Drive Signal:	AWA_JS_T2P0_H0P20

Initial profile file:	Pro_17_0.DAC
Trendline slope:	0.1428
R^2 of profile:	0.9998
Initial picture:	132-3206 to 10

TEST

Test name:	Test_17_1	Test_17_2	Test_17_3	Test_17_4
Start time:	12:47	13:01	13:16	13:38
Number of waves:	100	200	450	250
Cumulative waves:	100	300	750	1000
Duration [s]:	159 (+20)	318 (+20)	716 (+20)	398 (+20)
Wave DAC file:	Test_17_1.DAC	Test_17_2.DAC	Test_17_3.DAC	Test_17_3.DAC
Profiler DAC file:	Pro_17_1.DAC	Pro_17_2.DAC	Pro_17_3.DAC	Pro_17_3.DAC
Profiler XLS file:	Pro_17_1.XLS	Pro_17_2.XLS	Pro_17_3.XLS	Pro_17_3.XLS
Profile – windows:	No	No	No	No
Pictures:	132-3211 to 15	132-3216 to 20	132-3221 to 25	132-3226 to 30
Video:	39:41 to 42:00			

Test name:	Test_17_5	Test_17_6	Test_17_7	Test_17_8
Start time:	13:55	14:32	15:22	8:15
Number of waves:	1000	1000	1000	1000
Cumulative waves:	2000	3000	4000	5000
Duration [s]:	1587 (+20)	1587 (+20)	1587 (+20)	1587 (+20)
Wave DAC file:	Test_17_5.DAC	Test_17_6.DAC	Test_17_7.DAC	Test_17_8.DAC
Profiler DAC file:	Pro_17_5.DAC	Pro_17_6.DAC	Pro_17_7.DAC	Pro_17_8.DAC
Profiler XLS file:	Pro_17_5.XLS	Pro_17_6.XLS	Pro_17_7.XLS	Pro_17_8.XLS
Profile – windows:	No	No	No	Yes
Pictures:	132-3231 to 35	132-3236 to 40	132-3241 to 45	132-3246 to 50
Video:				

REMARKS

12:43: All instruments re-zeroed.

12:50: Record 39:41 to 42:00: Sediment transport.

15:00: WG12 is in air. Test_17_6.DAC contains errors on channel 12.

15:15: WG12 lowered.

8:11: All instruments re-zeroed.

9:11: Test finished.

Table A.26 – Project log of Test 18

Day: 28/11 2007

GENERAL

Regular / Random:	Random
Wave spectrum:	JONSWAP
Water level [m]:	0.60
Wave height [m]:	0.20
Wave period [s]:	$T_p = 2.5$, $T_{av} = 1.978$
Drive Signal:	AWA_JS_T2P5_H0P20

Initial profile file:	Pro_18_0.DAC
Trendline slope:	0.1417
R^2 of profile:	0.9997
Initial picture:	132-3252 to 56

TEST

Test name:	Test_18_1	Test_18_2	Test_18_3	Test_18_4
Start time:	11:37	11:52	12:11	12:38
Number of waves:	100	200	450	250
Cumulative waves:	100	300	750	1000
Duration [s]:	198 (+20)	396 (+20)	891 (+20)	495 (+20)
Wave DAC file:	Test_18_1.DAC	Test_18_2.DAC	Test_18_3.DAC	Test_18_3.DAC
Profiler DAC file:	Pro_18_1.DAC	Pro_18_2.DAC	Pro_18_3.DAC	Pro_18_3.DAC
Profiler XLS file:	Pro_18_1.XLS	Pro_18_2.XLS	Pro_18_3.XLS	Pro_18_3.XLS
Profile – windows:	No	No	No	No
Pictures:	132-3257 to 61	132-3262 to 66	132-3267 to 71	132-3272 to 76
Video:	42:01 to 43:04	44:12 to 45:55		
Video:	43:05 to 44:11	45:56 to 47:20		

Test name:	Test_18_5	Test_18_6	Test_18_7	Test_18_8
Start time:	12:58	13:42	14:31	15:17
Number of waves:	1000	1000	1000	1000
Cumulative waves:	2000	3000	4000	5000
Duration [s]:	1978 (+20)	1978 (+20)	1978 (+20)	1978 (+20)
Wave DAC file:	Test_18_5.DAC	Test_18_6.DAC	Test_18_7.DAC	Test_18_8.DAC
Profiler DAC file:	Pro_18_5.DAC	Pro_18_6.DAC	Pro_18_7.DAC	Pro_18_8.DAC
Profiler XLS file:	Pro_18_5.XLS	Pro_18_6.XLS	Pro_18_7.XLS	Pro_18_8.XLS
Profile – windows:	No	No	Some	Yes
Pictures:	132-3277 to 81	132-3282 to 86	132-3287 to 91	132-3292 to 96
Video:				

REMARKS

11:33: All instruments re-zeroed.
11:40: Two videos – A lot of sediment transport in the beginning.
11:53: Record 44:12 to 45:55: Zoom of sediment transport.
11:56: Record 45:56 to 47:20: From long distance.
12:05: Record 47:21 to 49:57: Profiler in action.
12:18: WG12 is in air! WG12 lowered. Test_18_3.DAC contains errors on channel 12.
15:10: Extra points for Pro_18_7: 3.7: 93.9 ; 3.8: 92.7 ; 3.9: 92.0 ; 4.05: 90.5 ; 4.3: 90.0 ;
4.4: 89.5 ; 4.5: 89.0.

Table A.27 – Project log of Test 19

Day: 29/11 2007

GENERAL

Regular / Random:	Regular
Wave spectrum:	Regular, AWA
Water level [m]:	0.60
Wave height [m]:	0.20
Wave period [s]:	2.0
Drive Signal:	AWA_R_2_ H0P20_T2P0

Initial profile file:	Pro_19_0.DAC
Trendline slope:	0.1423
R^2 of profile:	0.9994
Initial picture:	

TEST

Test name:	Test_19_1	Test_19_2	Test_19_3	Test_19_4
Start time:	11:52	12:02	12:12	12:24
Number of waves:	50	50	100	200
Cumulative waves:	50	100	200	400
Duration [s]:	100 (+20)	100 (+20)	200 (+20)	400 (+20)
Wave DAC file:	Test_19_1.DAC	Test_19_2.DAC	Test_19_3.DAC	Test_19_3.DAC
Profiler DAC file:	Pro_19_1.DAC	Pro_19_2.DAC	Pro_19_3.DAC	Pro_19_3.DAC
Profiler XLS file:	Pro_19_1.XLS	Pro_19_2.XLS	Pro_19_3.XLS	Pro_19_3.XLS
Profile – windows:	No	No	No	No
Pictures:				
Video:				

Test name:	Test_19_5	Test_19_6	Test_19_7	Test_19_8
Start time:	12:41	13:03	13:40	14:10
Number of waves:	400	700	500	500
Cumulative waves:	800	1500	2000	2500
Duration [s]:	800 (+20)	1400 (+20)	1000 (+20)	1000 (+20)
Wave DAC file:	Test_19_5.DAC	Test_19_6.DAC	Test_19_7.DAC	Test_19_8.DAC
Profiler DAC file:	Pro_19_5.DAC	Pro_19_6.DAC	Pro_19_7.DAC	Pro_19_8.DAC
Profiler XLS file:	Pro_19_5.XLS	Pro_19_6.XLS	Pro_19_7.XLS	Pro_19_8.XLS
Profile – windows:	No	No	No	No
Pictures:				
Video:				

REMARKS

This test is Test_11 repeated.

Table A.28 – Project log of Test 19, continued

Day: 29/11 2007

GENERAL

Regular / Random:	Regular
Wave spectrum:	Regular, AWA
Water level [m]:	0.60
Wave height [m]:	0.20
Wave period [s]:	2.0
Drive Signal:	AWA_R_2_ H0P20_T2P0

Initial profile file:	Pro_19_0.DAC
Trendline slope:	0.1423
R^2 of profile:	0.9994
Initial picture:	

TEST

Test name:	Test_19_9			
Start time:	14:40			
Number of waves:	500			
Cumulative waves:	3000			
Duration [s]:	1000 (+20)			
Wave DAC file:	Test_19_1.DAC			
Profiler DAC file:	Pro_19_1.DAC			
Profiler XLS file:	Pro_19_1.XLS			
Profile – windows:	No			
Pictures:				
Video:				

Test name:				
Start time:				
Number of waves:				
Cumulative waves:				
Duration [s]:				
Wave DAC file:				
Profiler DAC file:				
Profiler XLS file:				
Profile – windows:				
Pictures:				
Video:				

REMARKS

This test is Test_11 repeated.

B Geotechnical Analysis

Table B.1 – Sieve analysis for toe of beach, sample 1

Opening diameter of sieve [mm]	Accumulated material [g]	Material retained on sieve%
12.70	0.00	100.00
9.51	317.35	83.04
4.75	1849.85	1.16
2.38	1867.98	0.19
2.00	1868.96	0.14
0.85	1869.98	0.09
Pan	1871.59	0.00

Table B.2 – Sieve analysis for toe of beach, sample 2

Opening diameter of sieve [mm]	Accumulated material [g]	Material retained on sieve%
12.70	0.00	100.00
9.51	296.55	82.49
4.75	1655.60	2.25
2.38	1690.10	0.21
2.00	1691.10	0.15
0.85	1692.20	0.09
Pan	1693.70	0.00

Table B.3 – Sieve analysis for center of beach, sample 1

Opening diameter of sieve [mm]	Accumulated material [g]	Material retained on sieve%
12.70	0.00	100.00
9.51	335.35	80.74
4.75	1701.15	2.28
2.38	1737.81	0.17
2.00	1738.63	0.13
0.85	1739.37	0.08
Pan	1740.81	0.00

Table B.4 – Sieve analysis for center of beach, sample 2

Opening diameter of sieve [mm]	Accumulated material [g]	Material retained on sieve%
12.70	0.00	100.00
9.51	324.51	82.66
4.75	1845.92	1.39
2.38	1867.35	0.24
2.00	1868.11	0.20
0.85	1869.32	0.14
Pan	1871.91	0.00

Table B.5 – Sieve analysis for top of beach, sample 1

Opening diameter of sieve [mm]	Accumulated material [g]	Material retained on sieve%
12.70	0.00	100.00
9.51	751.80	68.06
4.75	2352.00	0.07
2.38	2352.27	0.06
2.00	2352.27	0.06
0.85	2352.27	0.06
Pan	2353.59	0.00

Table B.6 – Sieve analysis for top of beach, sample 2

Opening diameter of sieve [mm]	Accumulated material [g]	Material retained on sieve%
12.70	0.00	100.00
9.51	479.36	69.76
4.75	1583.98	0.09
2.38	1584.00	0.09
2.00	1584.12	0.08
0.85	1584.14	0.08
Pan	1585.43	0.00

Table B.7 – Determination of specific gravity of the beach material

Item		Bottom	Center	Top
Mass of flask + water filled to mark	W_1(g)	683.18	683.11	6.83.05
Mass of flask + gravel + water filled to mark	W_2(g)	746.61	749.02	737.49
Mass of dry gravel	W_s(g)	99.21	102.64	85.57
Mass of equal volume of water as the soil solids, $W_w = W_1 + W_2 - W_s$	W_w(g)	35.78	36.73	31.13
Specific gravity, $G_{s(@T,\ °C)}$	W_s/W_w	2.77	2.79	2.75
Temperature of test	T(°C)	23.5	23	23
K-factor	K	0.99921	0.99933	0.99933
Specific gravity, $G_{s(@20°C)} = G_{s(@T,\ °C)} * K$	G_s	2.77	2.79	2.75
Average specific gravity, $G_{s,av}$	$G_{s,av}$	**2.77**		

C Beach Profiles

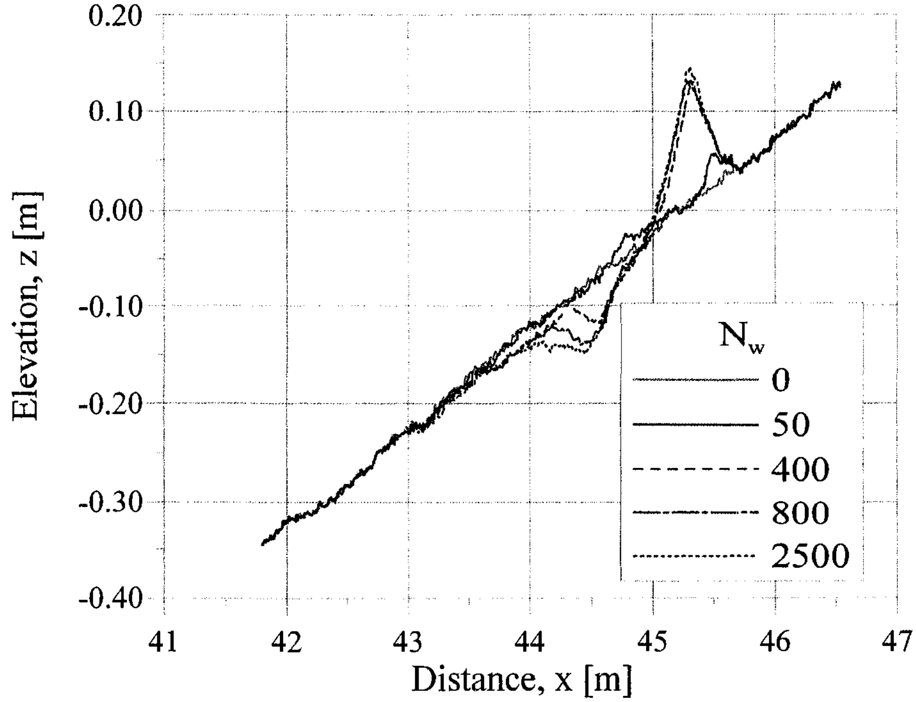

Figure C.1 – Time evolution of beach deformation, Test 1: Regular waves, T_{av} = 2.0 s, H_{av} = 0.15 m, slope: 1:10

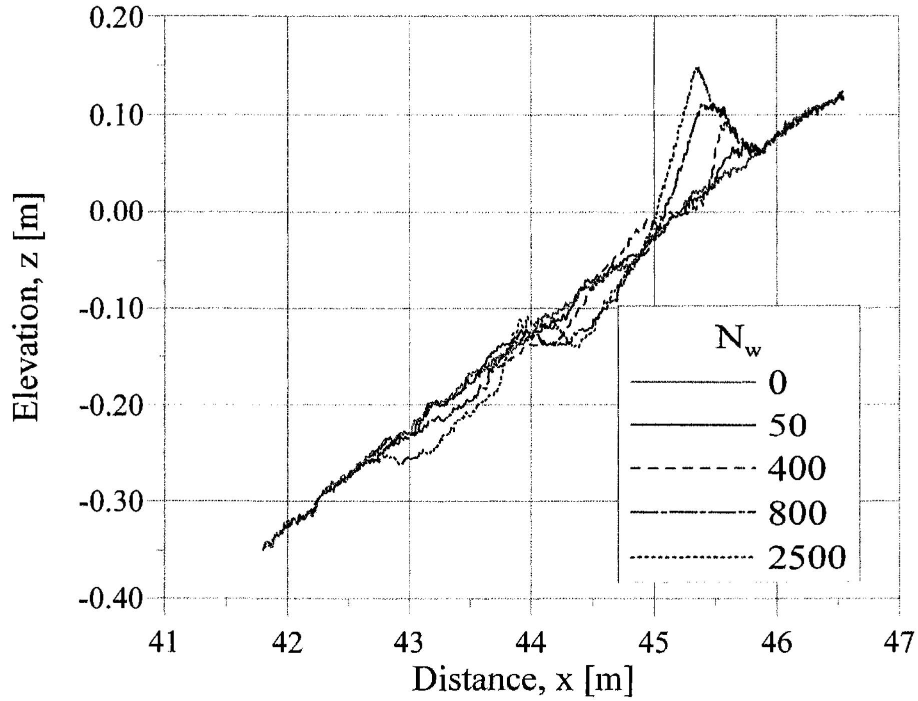

Figure C.2 – Time evolution of beach deformation, Test 2: Regular waves, T_{av} = 2.0 s, H_{av} = 0.19 m, slope: 1:10

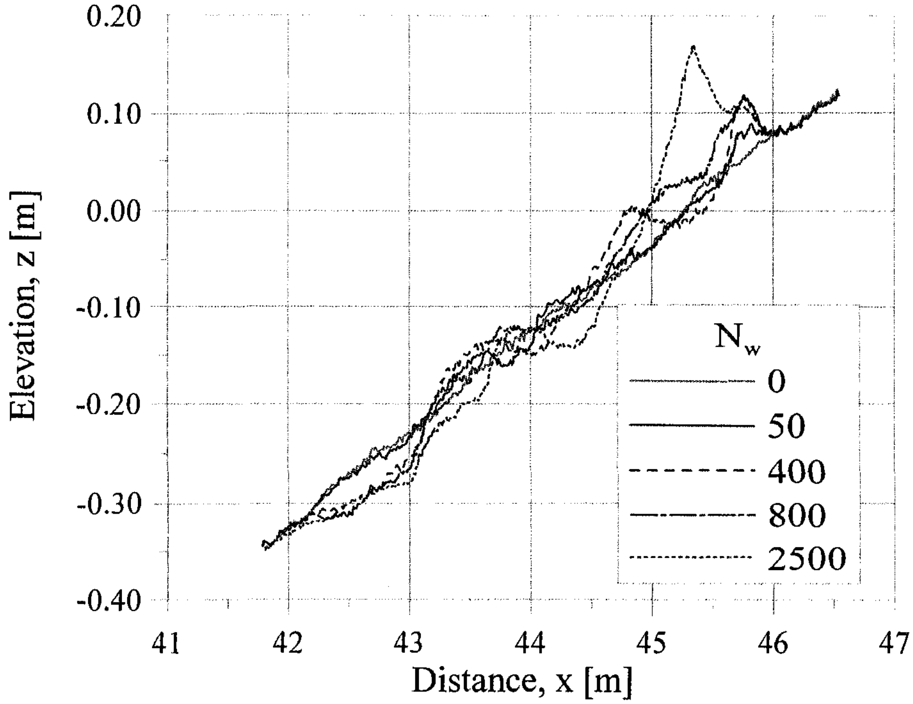

Figure C.3 – Time evolution of beach deformation, Test 3: Regular waves, T_{av} = 2.0 s, H_{av} = 0.25 m, slope: 1:10

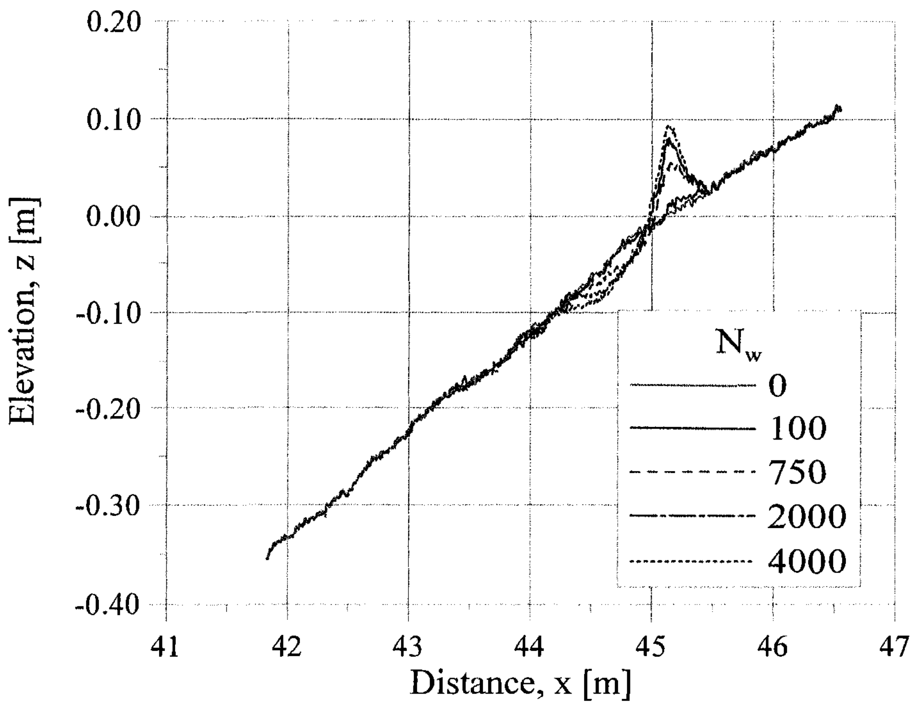

Figure C.4 – Time evolution of beach deformation, Test 4: Irregular waves, T_p = 1.5 s, H_s = 0.13 m, slope: 1:10

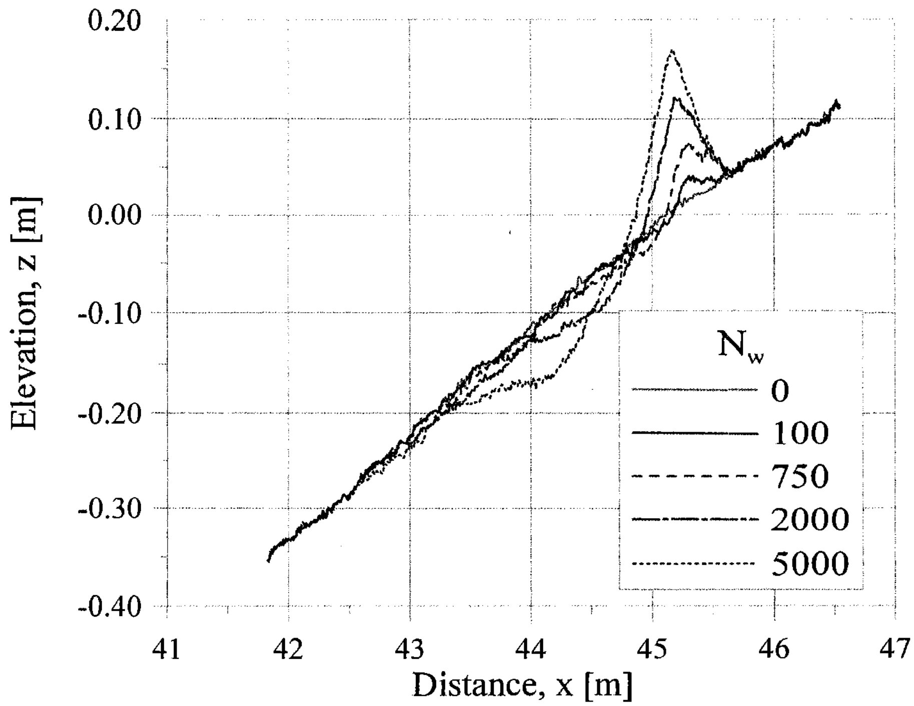

Figure C.5 – Time evolution of beach deformation, Test 5: Irregular waves, $T_p = 2.0$ s, $H_s = 0.14$ m, slope: 1:10

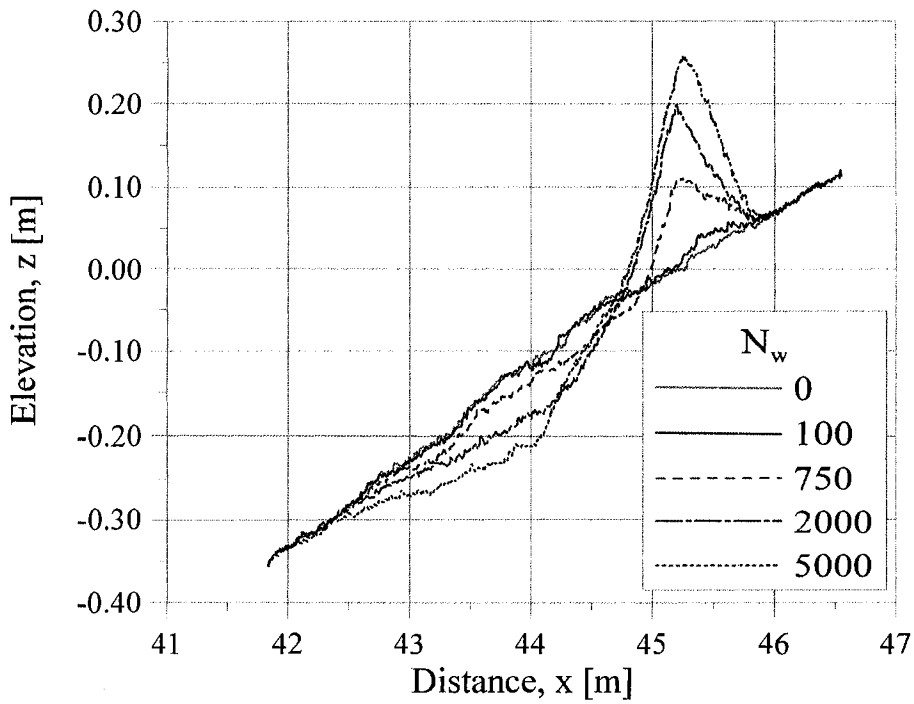

Figure C.6 – Time evolution of beach deformation, Test 6: Irregular waves, $T_p = 2.5$ s, $H_s = 0.14$ m, slope: 1:10

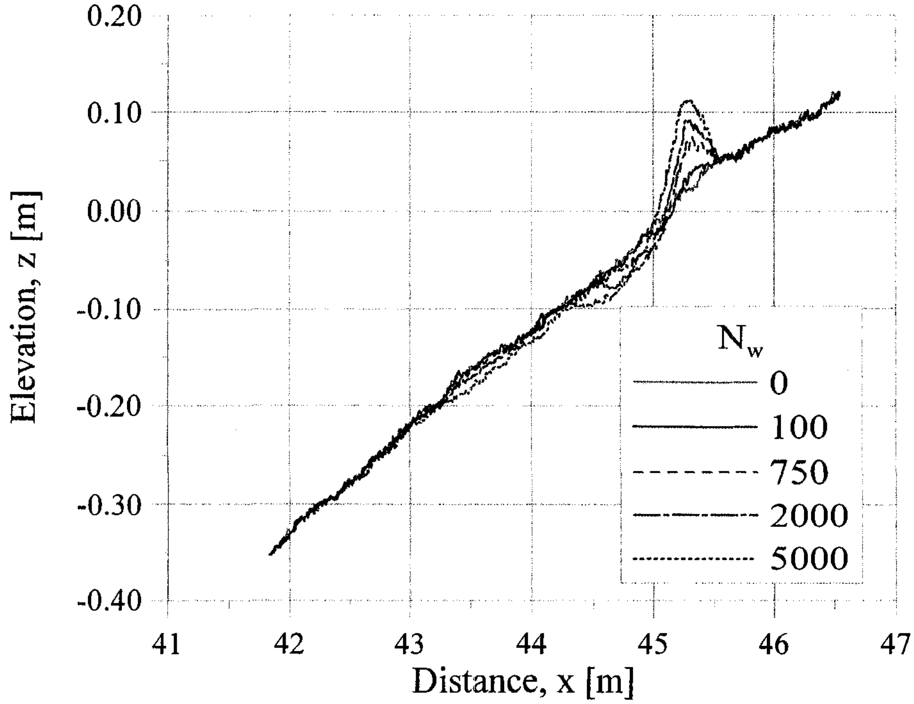

Figure C.7 – Time evolution of beach deformation, Test 7: Irregular waves, T_p = 1.5 s, H_s = 0.17 m, slope: 1:10

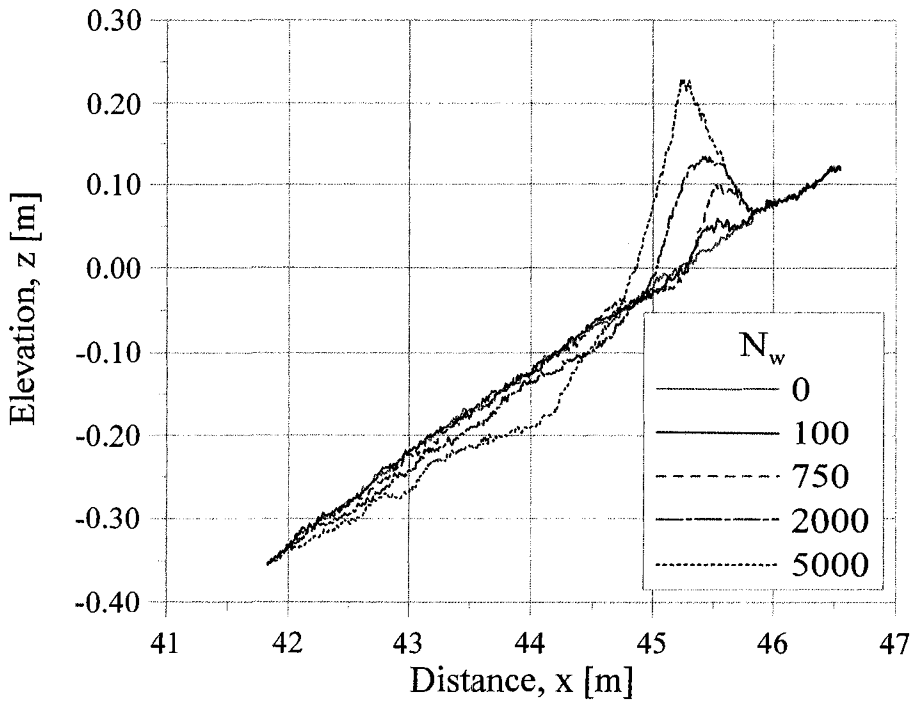

Figure C.8 – Time evolution of beach deformation, Test 8: Irregular waves, T_p = 2.4 s, H_s = 0.18 m, slope: 1:10

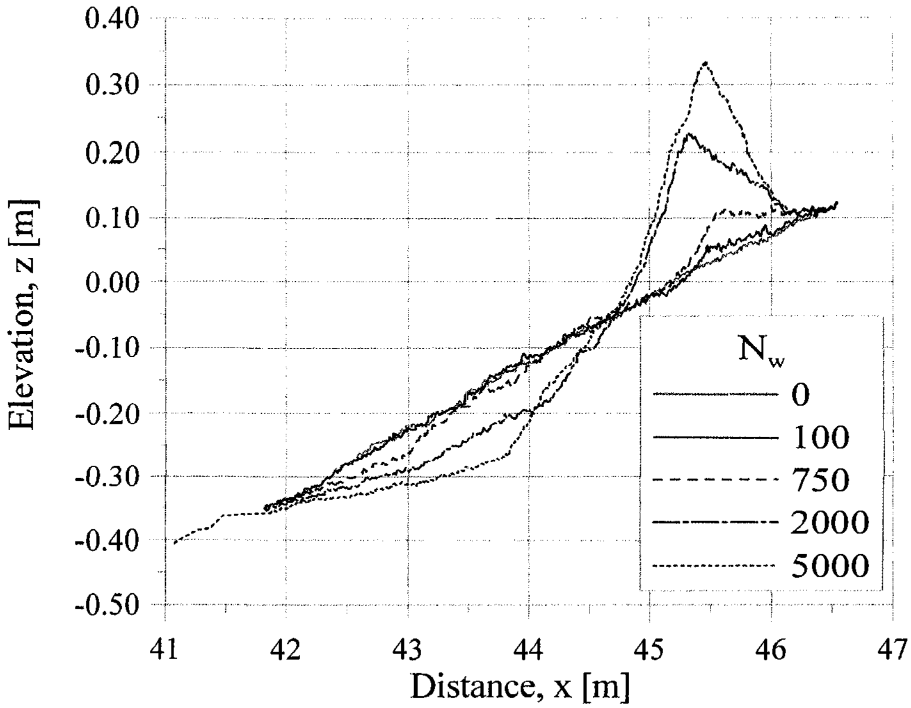

Figure C.9 – Time evolution of beach deformation, Test 9: Irregular waves, T_p = 2.9 s, H_s = 0.19 m, slope: 1:10

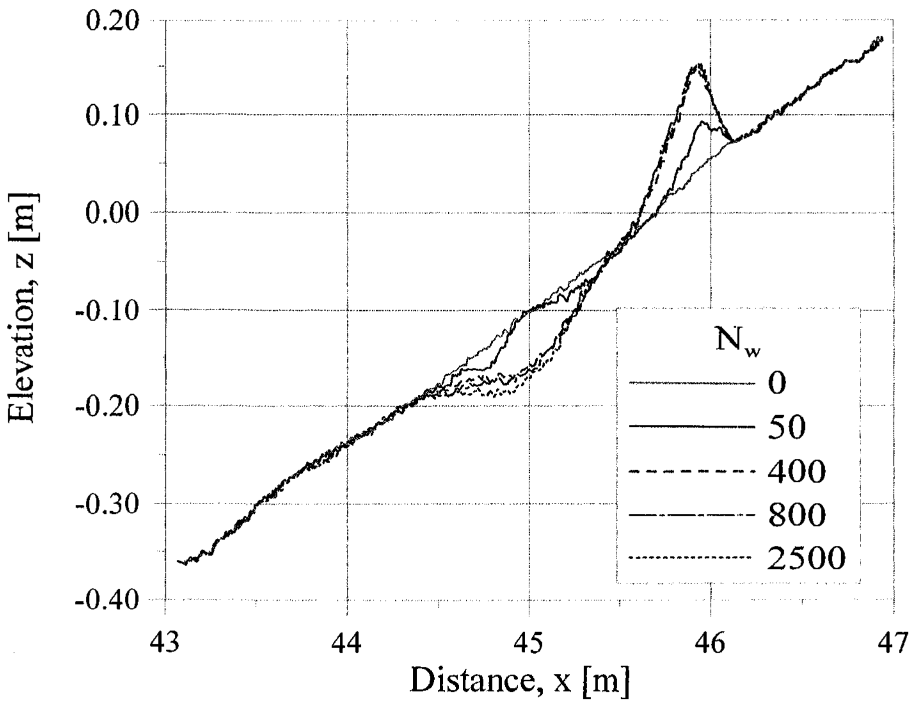

Figure C.10 – Time evolution of beach deformation, Test 10: Regular waves, T_{av} = 2.0 s, H_{av} = 0.15 m, slope: 1:7

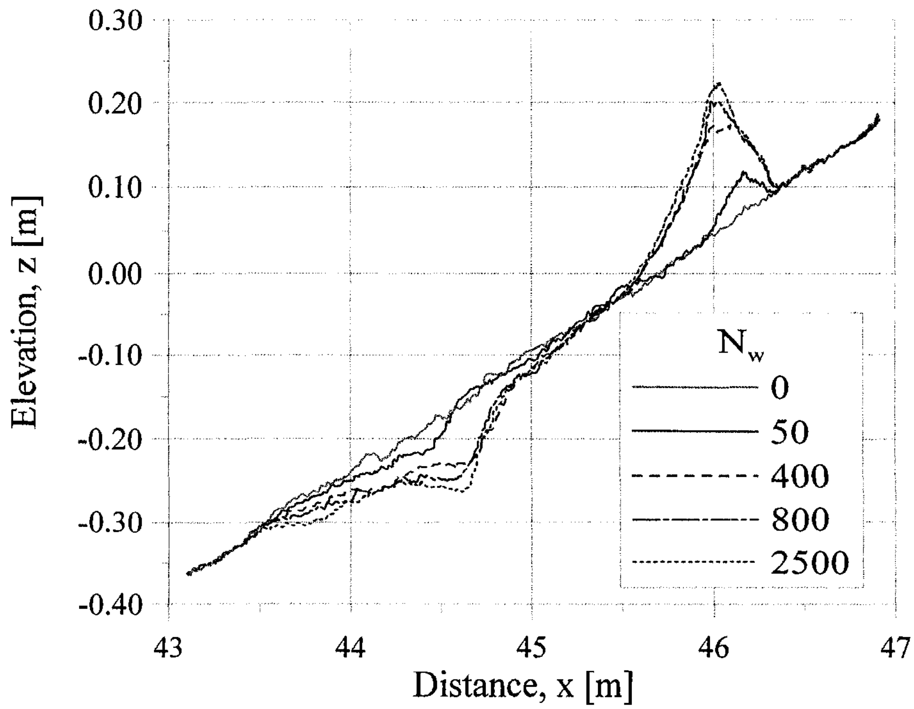

Figure C.11 – Time evolution of beach deformation, Test 11: Regular waves, T_{av} = 2.0 s, H_{av} = 0.21 m, slope: 1:7

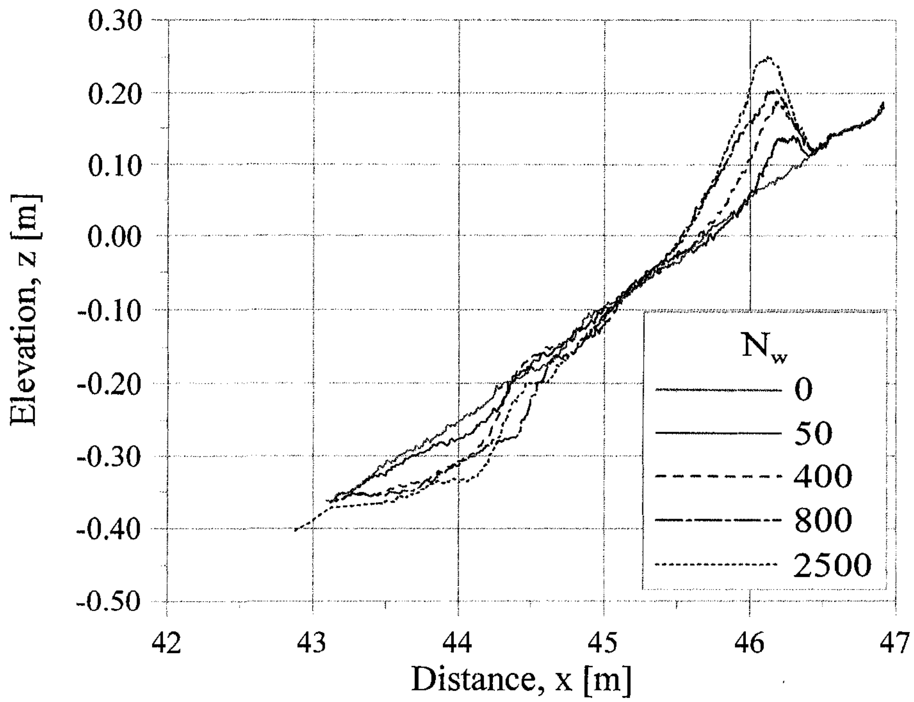

Figure C.12 – Time evolution of beach deformation, Test 12: Regular waves, T_{av} = 2.0 s, H_{av}= 0.25 m, slope: 1:7

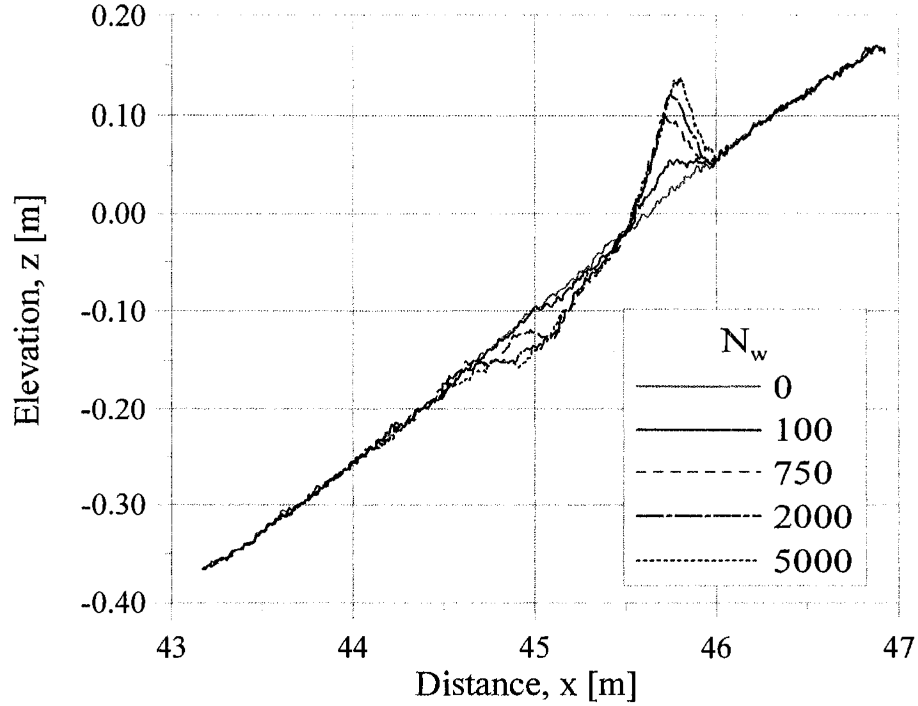

Figure C.13 – Time evolution of beach deformation, Test 13: Irregular waves, T_p = 1.5 s, H_s = 0.14 m, slope: 1:7

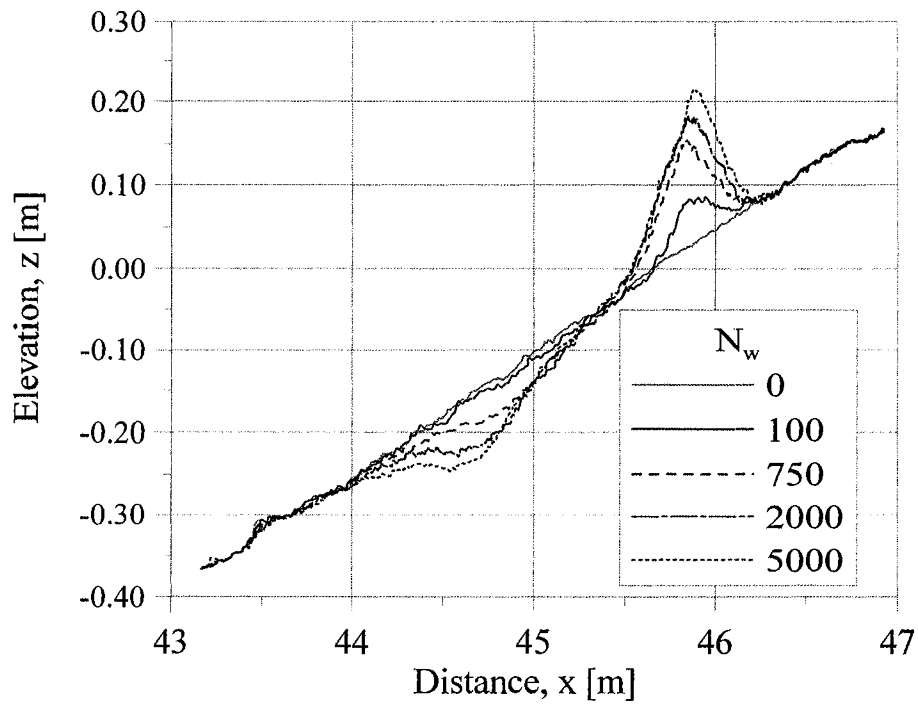

Figure C.14 – Time evolution of beach deformation, Test 14: Irregular waves, T_p = 2.0 s, H_s = 0.14 m, slope: 1:7

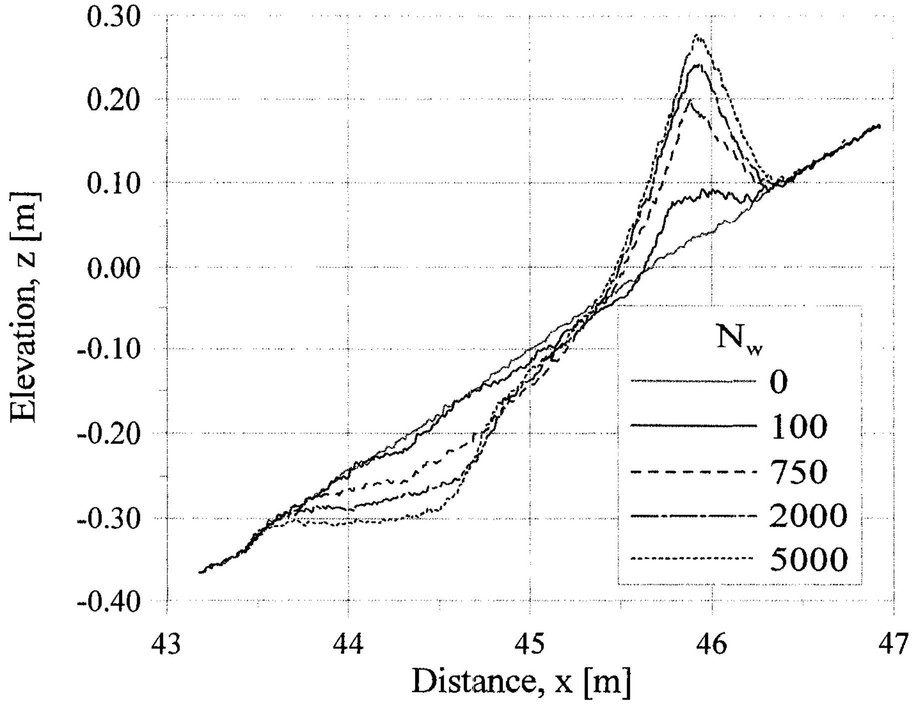

Figure C.15 – Time evolution of beach deformation, Test 15: Irregular waves, T_p = 2.5 s, H_s = 0.14 m, slope: 1:7

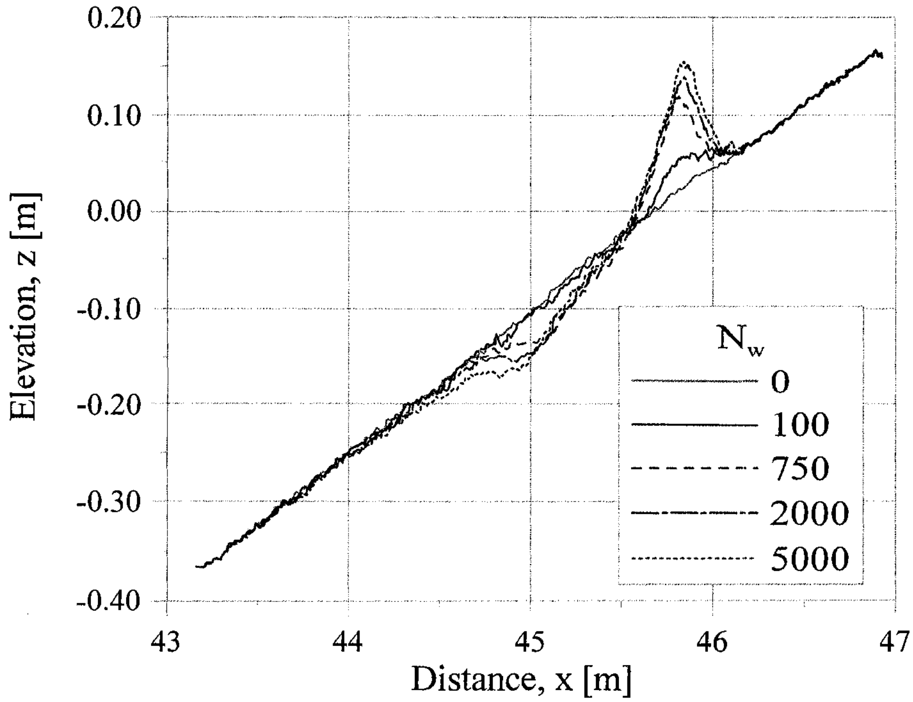

Figure C.16 – Time evolution of beach deformation, Test 16: Irregular waves, T_p = 1.5 s, H_s = 0.17 m, slope: 1:7

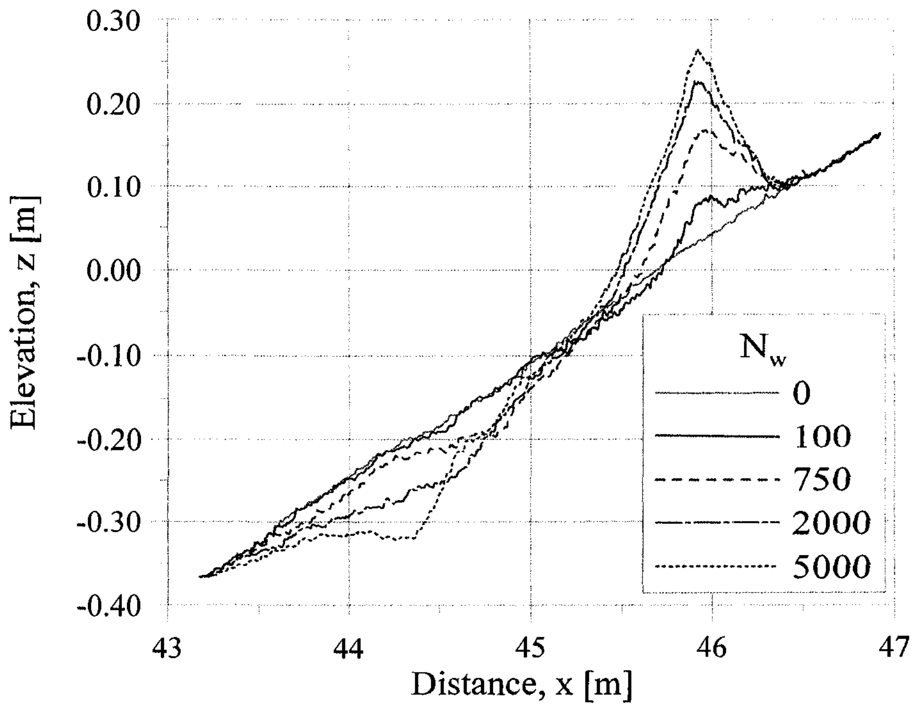

Figure C.17 – Time evolution of beach deformation, Test 17: Irregular waves, T_p = 2.2 s, H_s = 0.18 m, slope: 1:7

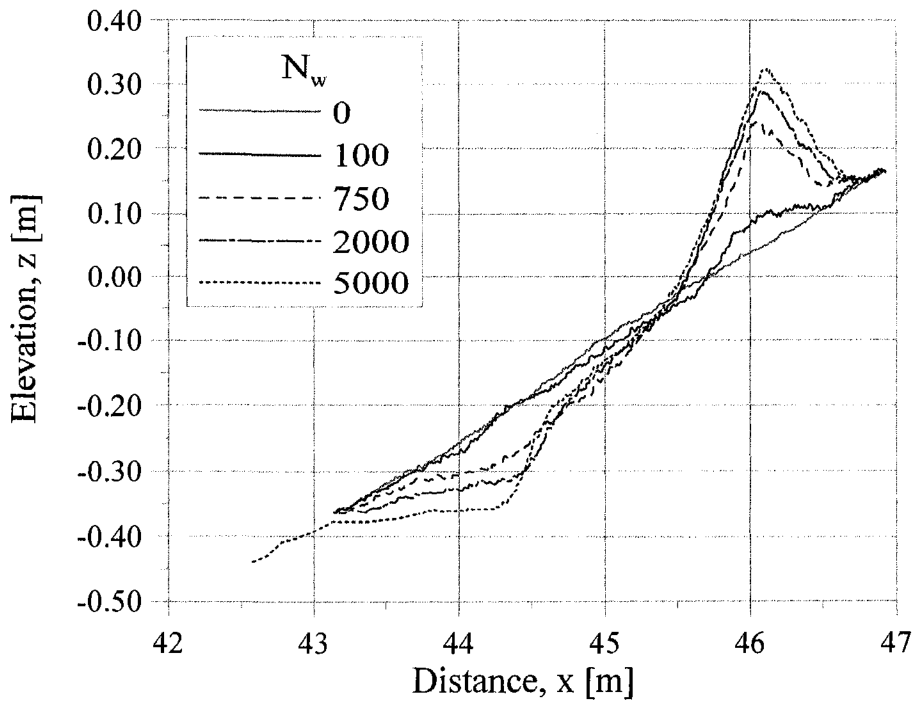

Figure C.18 – Time evolution of beach deformation, Test 18: Irregular waves, T_p = 2.5 s, H_s = 0.19 m, slope: 1:7

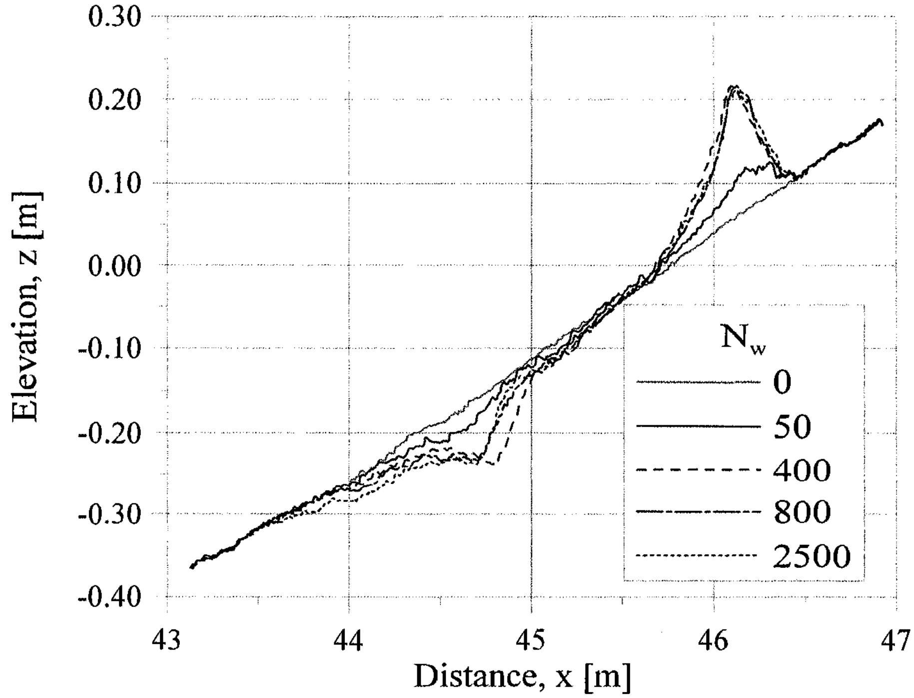

Figure C.19 – Time evolution of beach deformation, Test 19: Regular waves, T_{av} = 2.0 s, H_{av} = 0.18 m, slope: 1:7

D Sediment Transport Rates

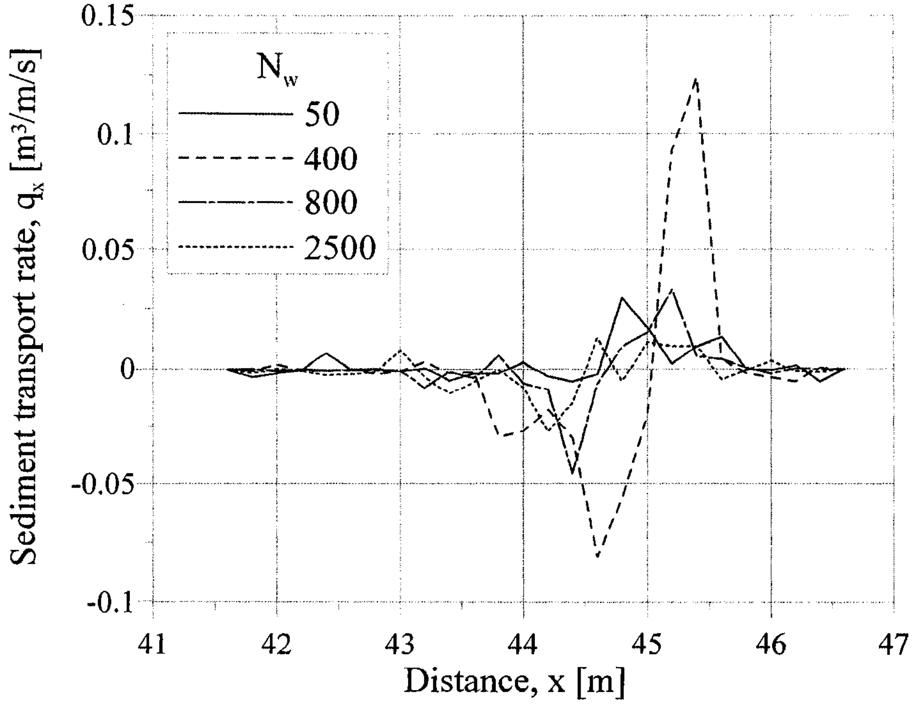

Figure D.1 – Time and space variation of the sediment transport rate, Test 1: Regular waves, T_{av} = 2.0 s, H_{av} = 0.15 m, slope: 1:10

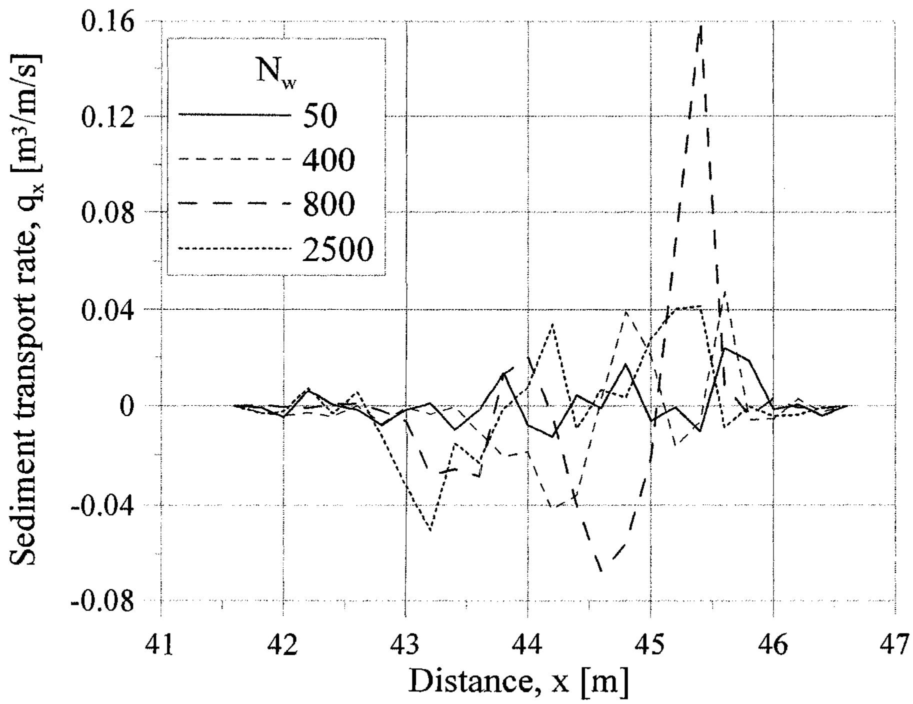

Figure D.2 – Time and space variation of the sediment transport rate, Test 2: Regular waves, T_{av} = 2.0 s, H_{av} = 0.19 m, slope: 1:10

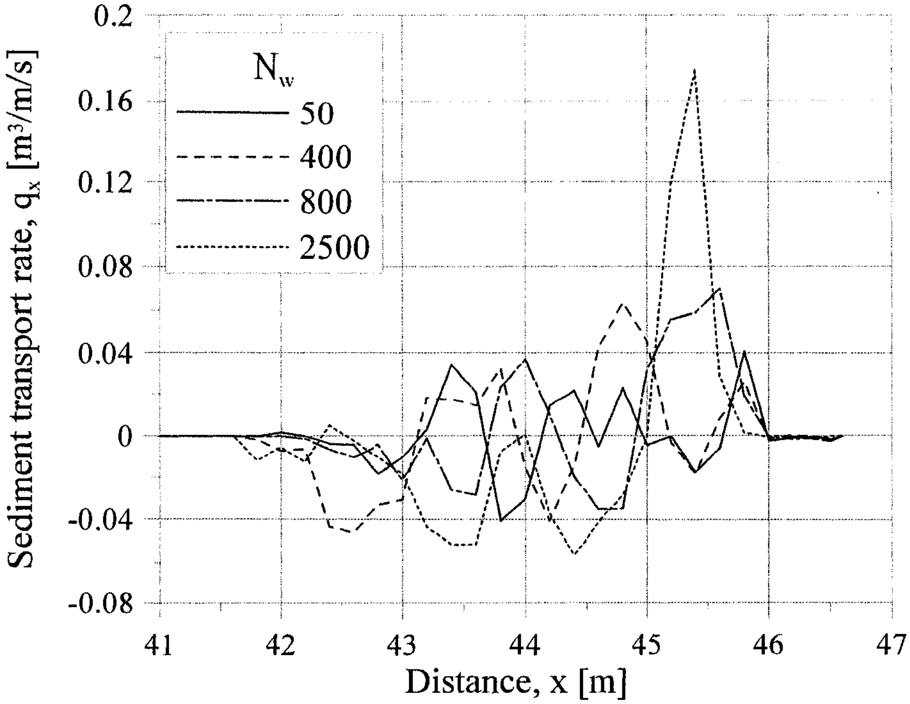

Figure D.3 – Time and space variation of the sediment transport rate, Test 3: Regular waves, T_{av} = 2.0 s, H_{av} = 0.25 m, slope: 1:10

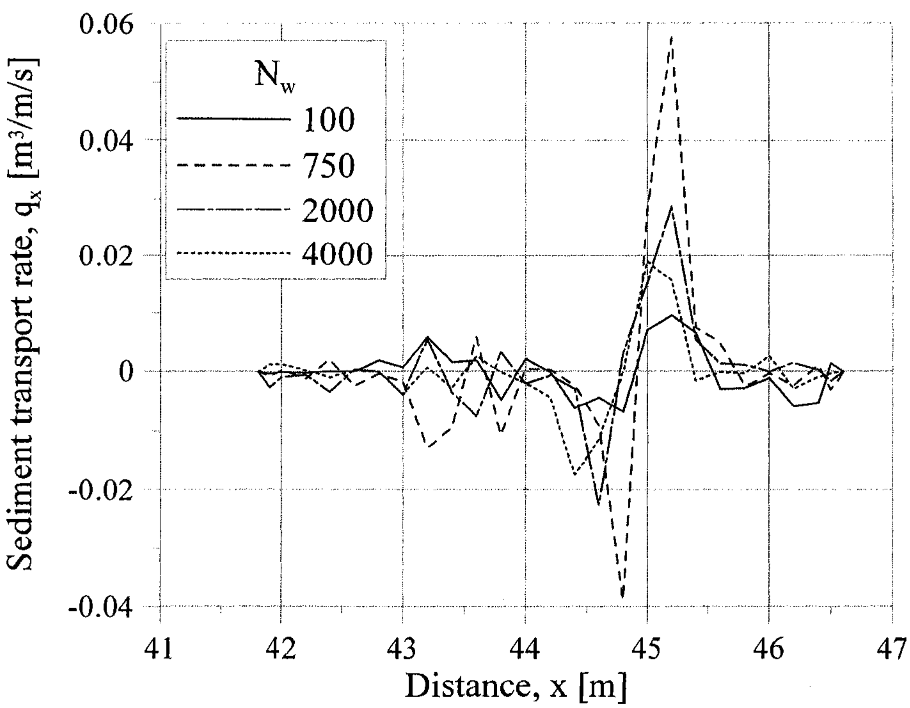

Figure D.4 – Time and space variation of the sediment transport rate, Test 4: Irregular waves, T_p = 1.5 s, H_s = 0.13 m, slope: 1:10

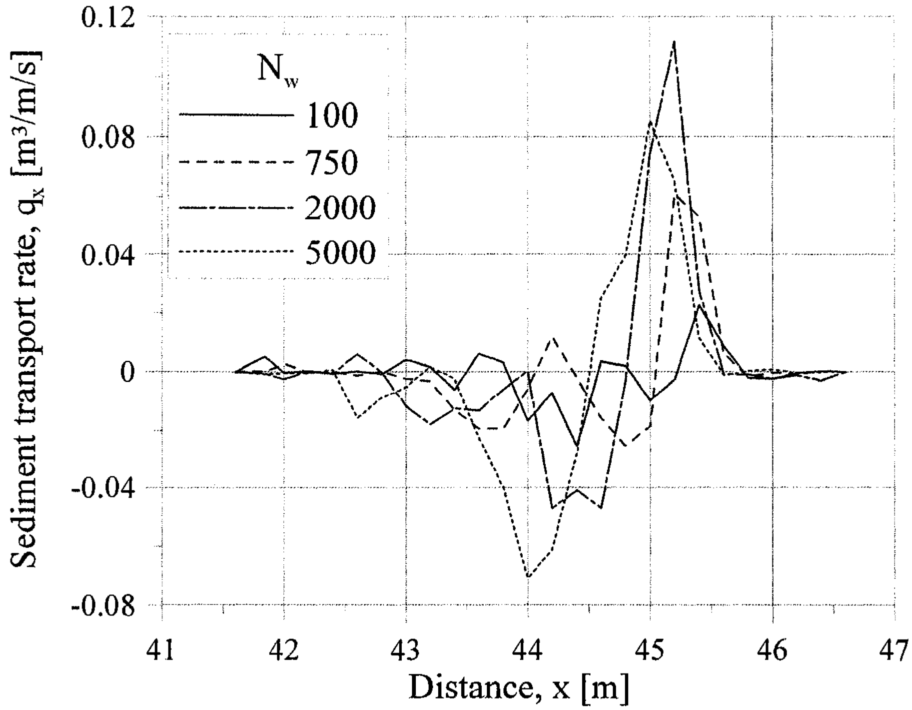

Figure D.5 – Time and space variation of the sediment transport rate, Test 5: Irregular waves, T_p = 2.0 s, H_s = 0.14 m, slope: 1:10

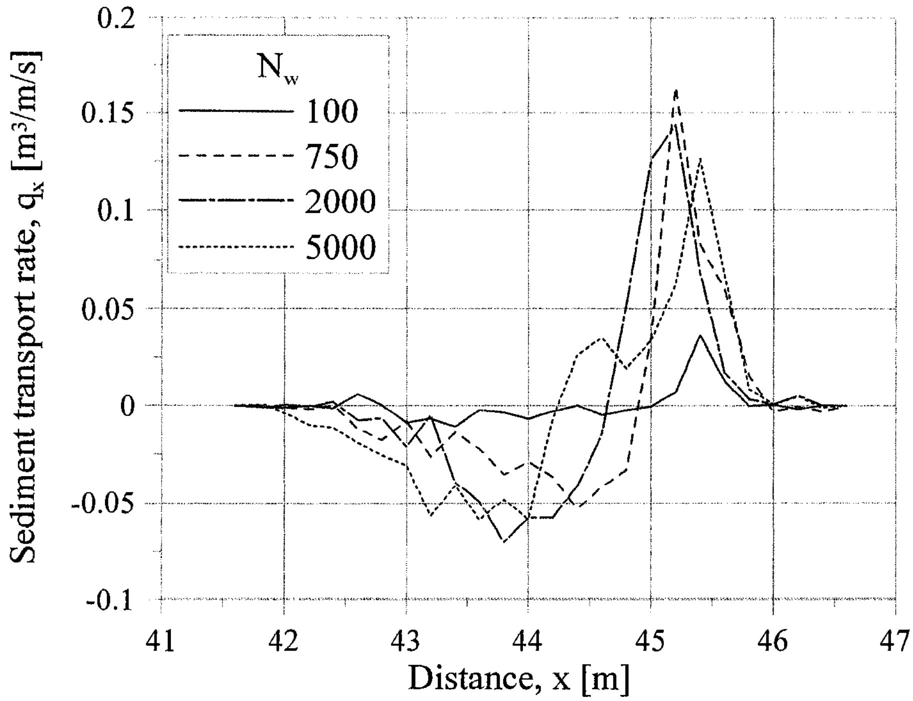

Figure D.6 – Time and space variation of the sediment transport rate, Test 6: Irregular waves, T_p = 2.5 s, H_s = 0.14 m, slope: 1:10

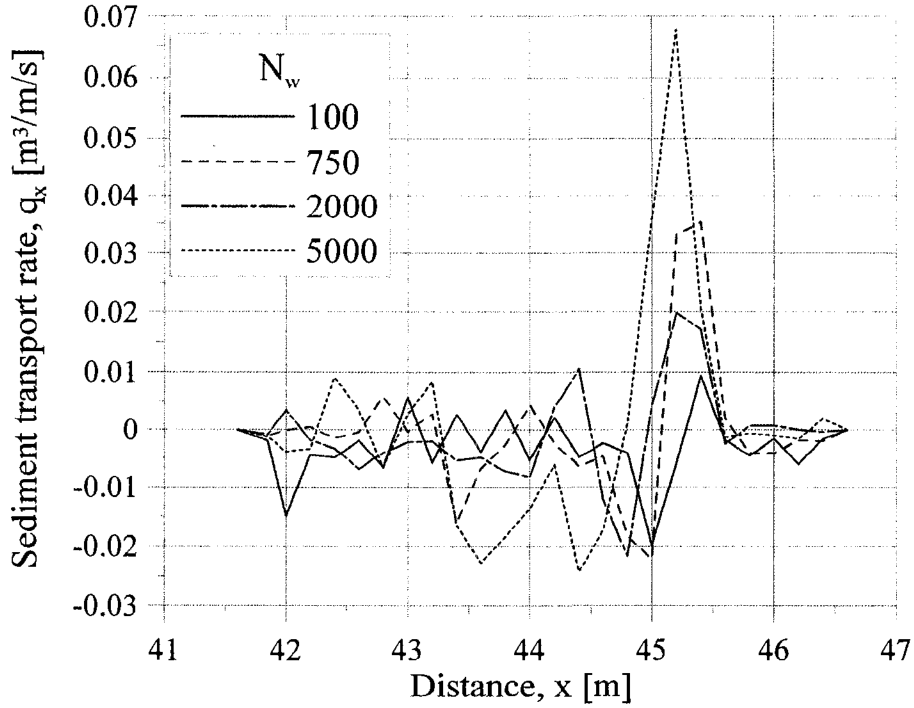

Figure D.7 – Time and space variation of the sediment transport rate, Test 7: Irregular waves, T_p = 1.5 s, H_s = 0.17 m, slope: 1:10

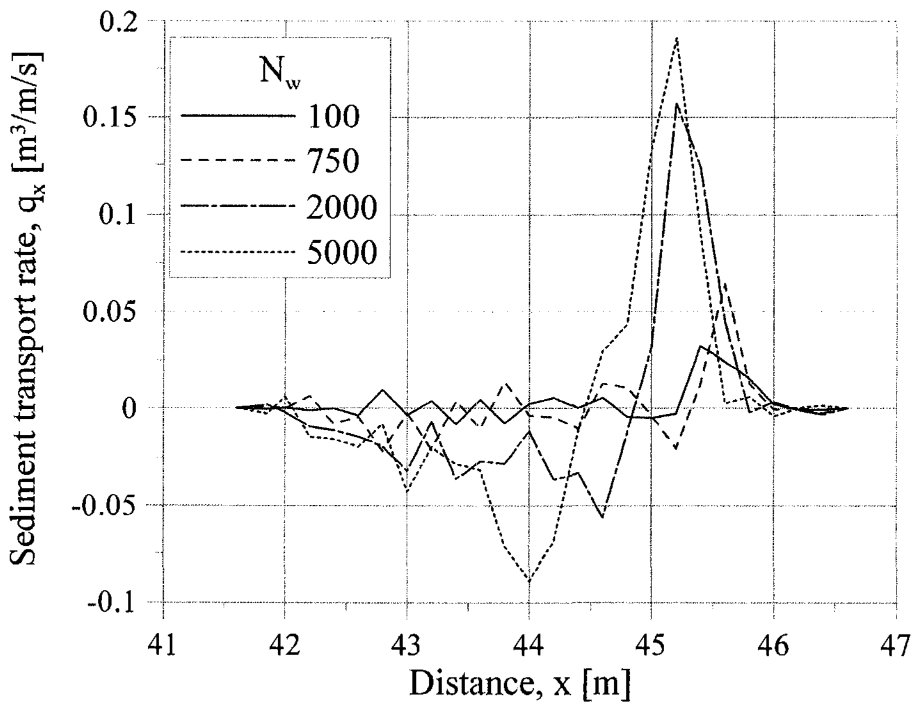

Figure D.8 – Time and space variation of the sediment transport rate, Test 8: Irregular waves, T_p = 2.4 s, H_s = 0.18 m, slope: 1:10

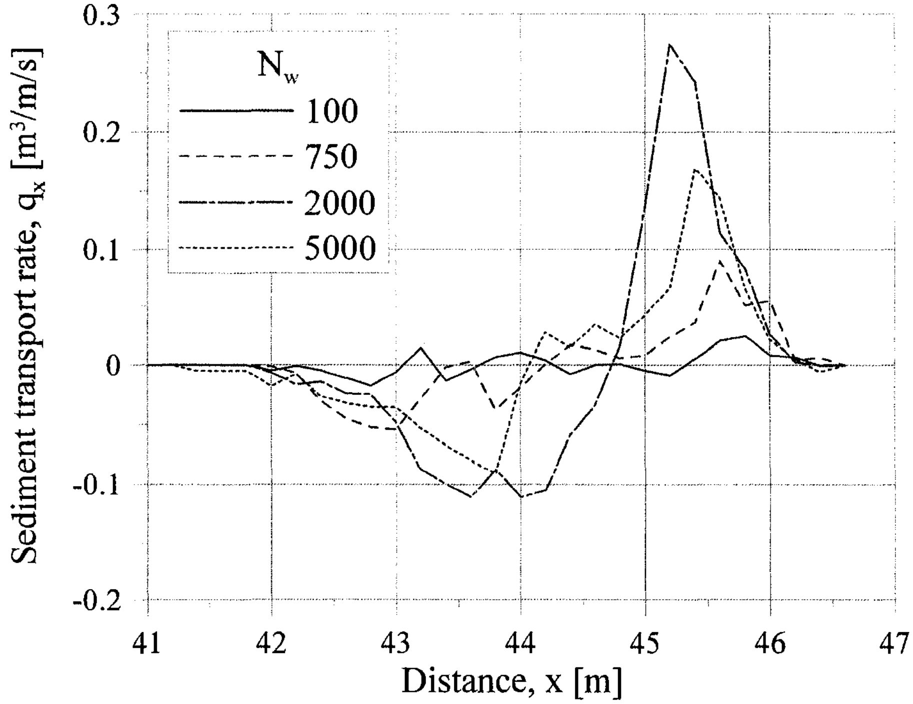

Figure D.9 – Time and space variation of the sediment transport rate, Test 9: Irregular waves, T_p = 2.9 s, H_s = 0.19 m, slope: 1:10

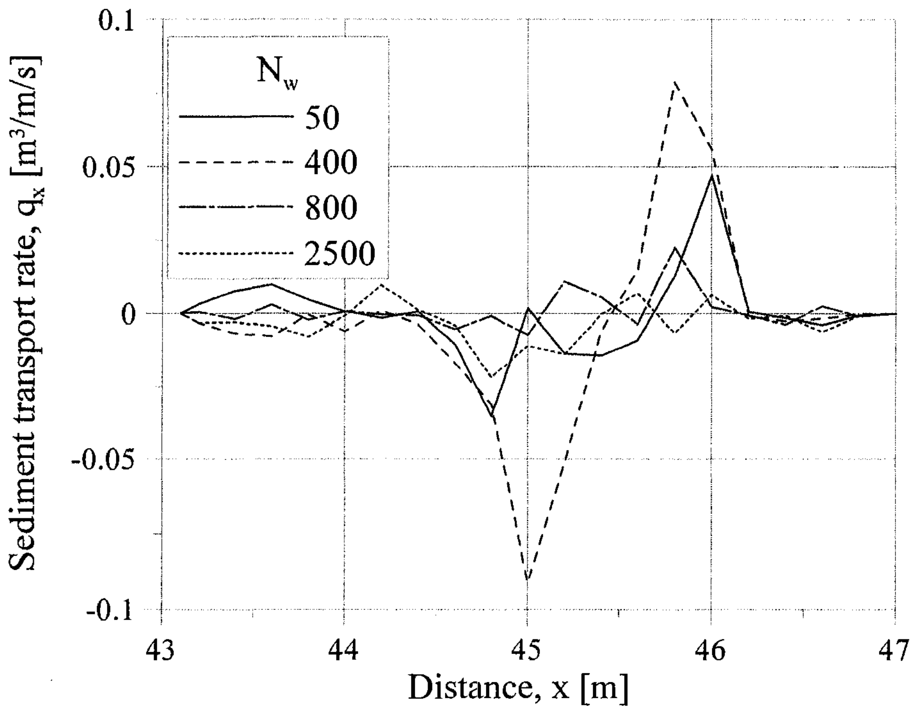

Figure D.10 – Time and space variation of the sediment transport rate, Test 10: Regular waves, T_{av} = 2.0 s, H_{av} = 0.15 m, slope: 1:7

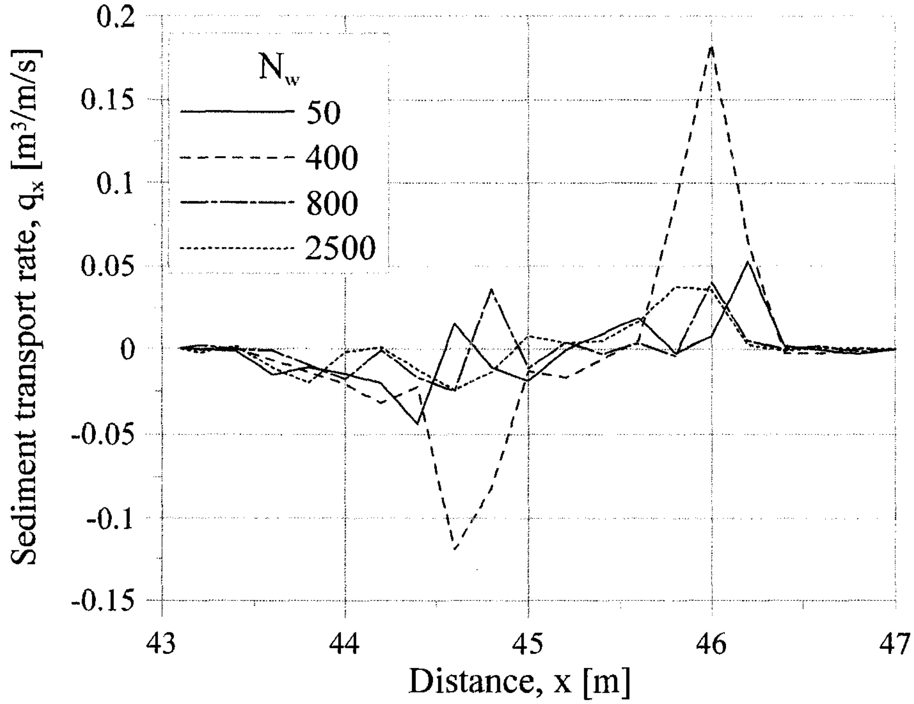

Figure D.11 – Time and space variation of the sediment transport rate, Test 11: Regular waves, T_{av} = 2.0 s, H_{av} = 0.21 m, slope: 1:7

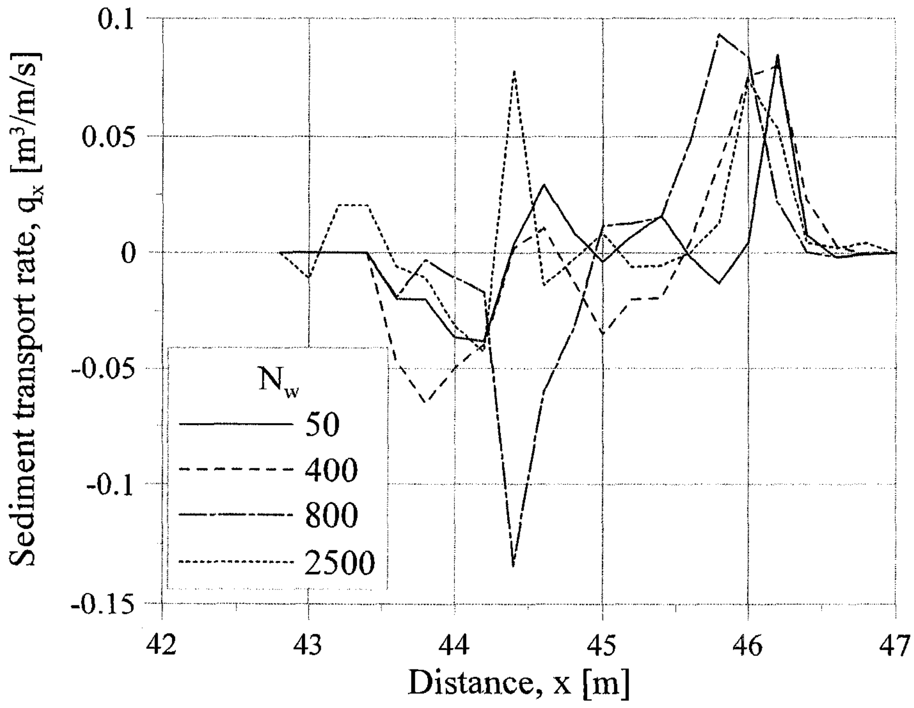

Figure D.12 – Time and space variation of the sediment transport rate, Test 12: Regular waves, T_{av} = 2.0 s, H_{av} = 0.25 m, slope: 1:7

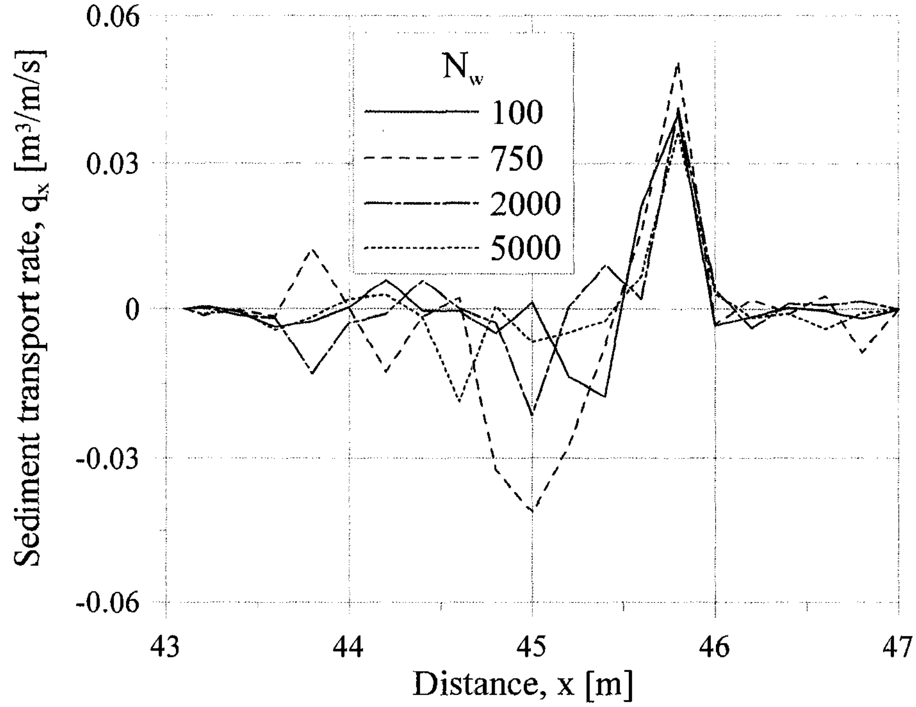

Figure D.13 – Time and space variation of the sediment transport rate, Test 13: Irregular waves, T_p = 1.5 s, H_s = 0.14 m, slope: 1:7

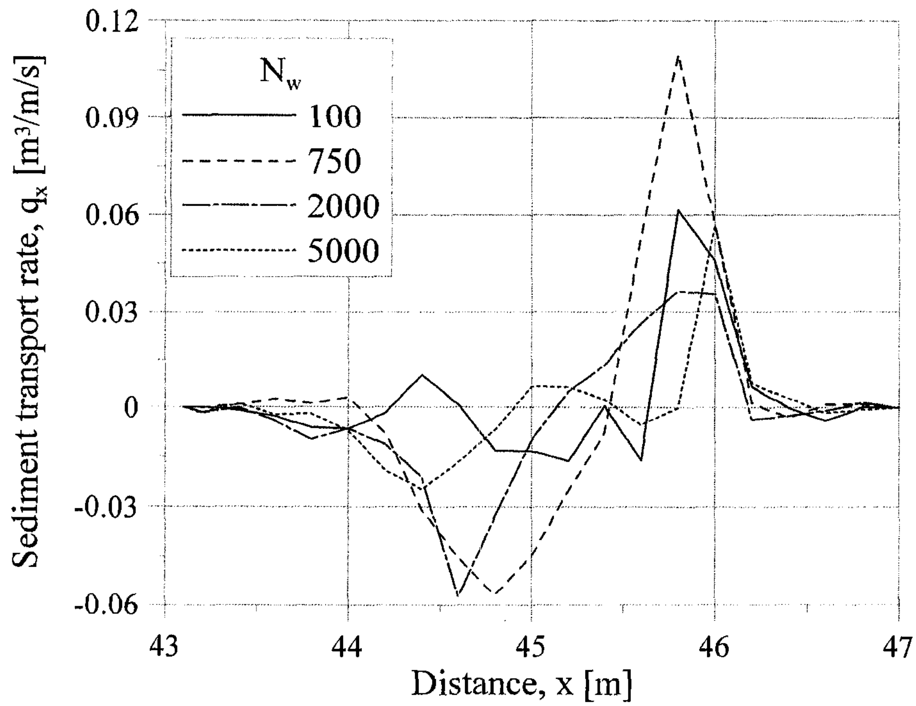

Figure D.14 – Time and space variation of the sediment transport rate, Test 14: Irregular waves, T_p = 2.0 s, H_s = 0.14 m, slope: 1:7

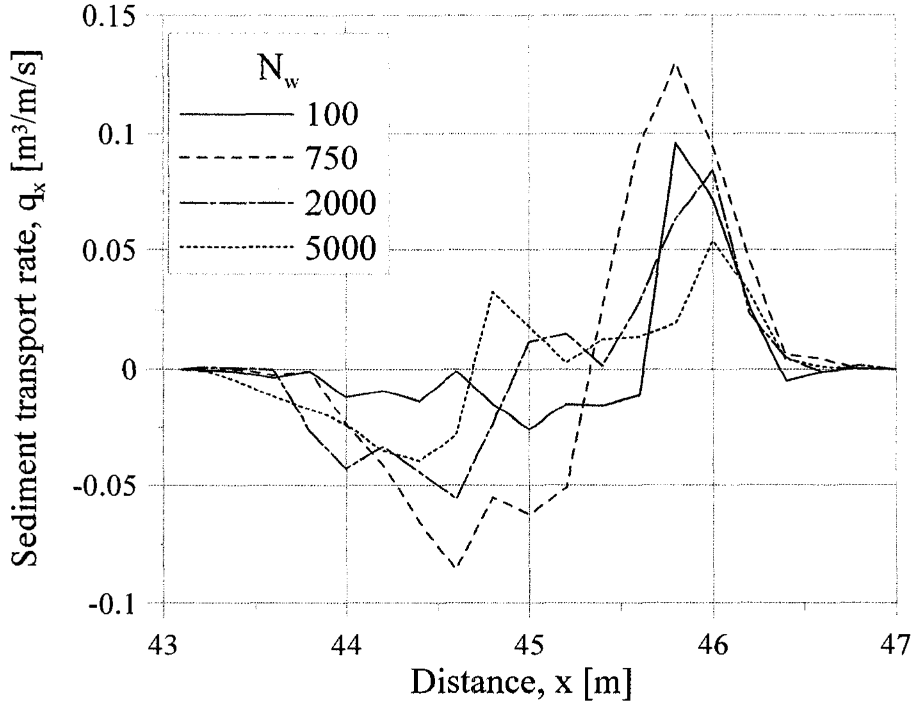

Figure D.15 – Time and space variation of the sediment transport rate, Test 15: Irregular waves, T_p = 2.5 s, H_s = 0.14 m, slope: 1:7

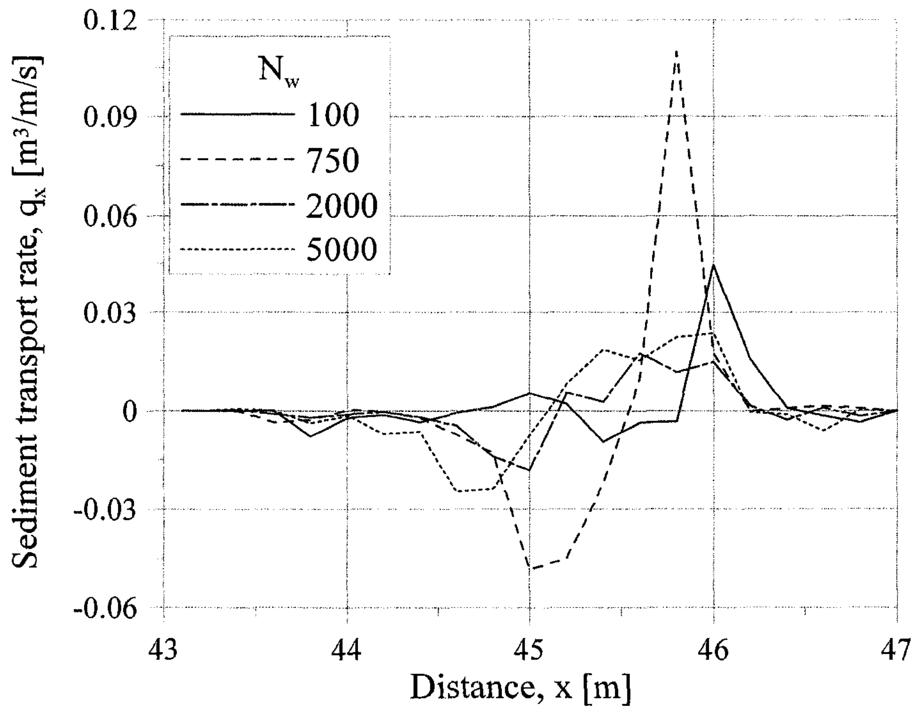

Figure D.16 – Time and space variation of the sediment transport rate, Test 16: Irregular waves, T_p = 1.5 s, H_s = 0.17 m, slope: 1:7

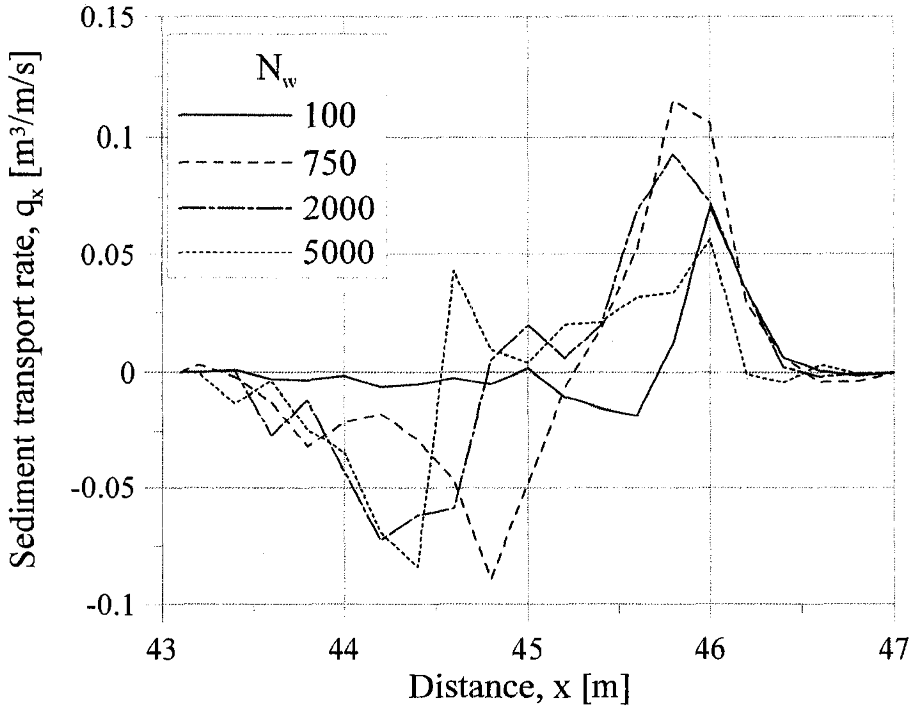

Figure D.17 – Time and space variation of the sediment transport rate, Test 17: Irregular waves, T_p = 2.2 s, H_s = 0.18 m, slope: 1:7

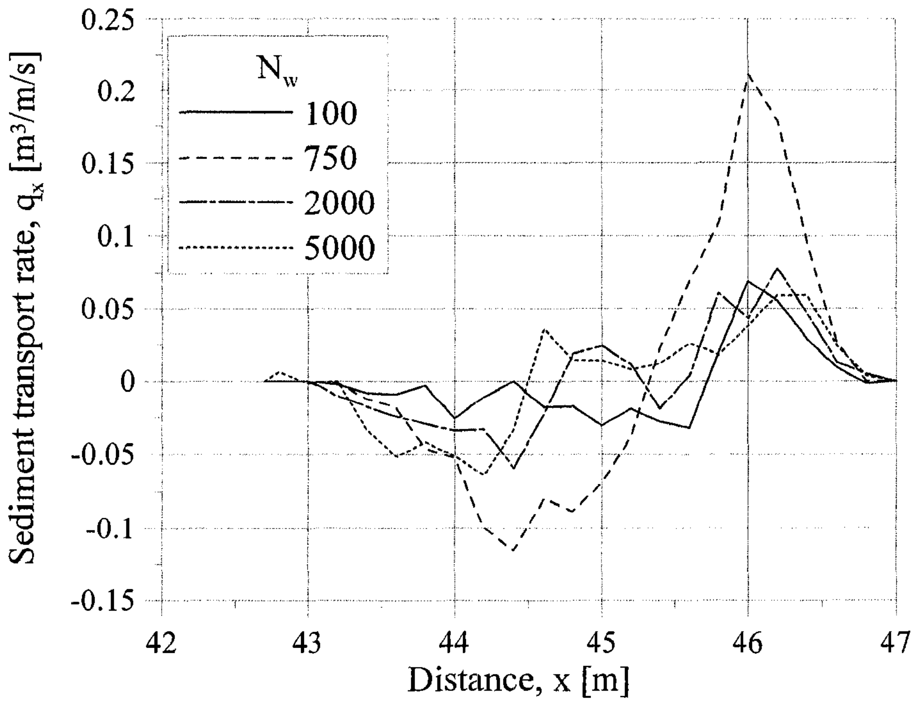

Figure D.18 – Time and space variation of the sediment transport rate, Test 18: Irregular waves, T_p = 2.5 s, H_s = 0.19 m, slope: 1:7

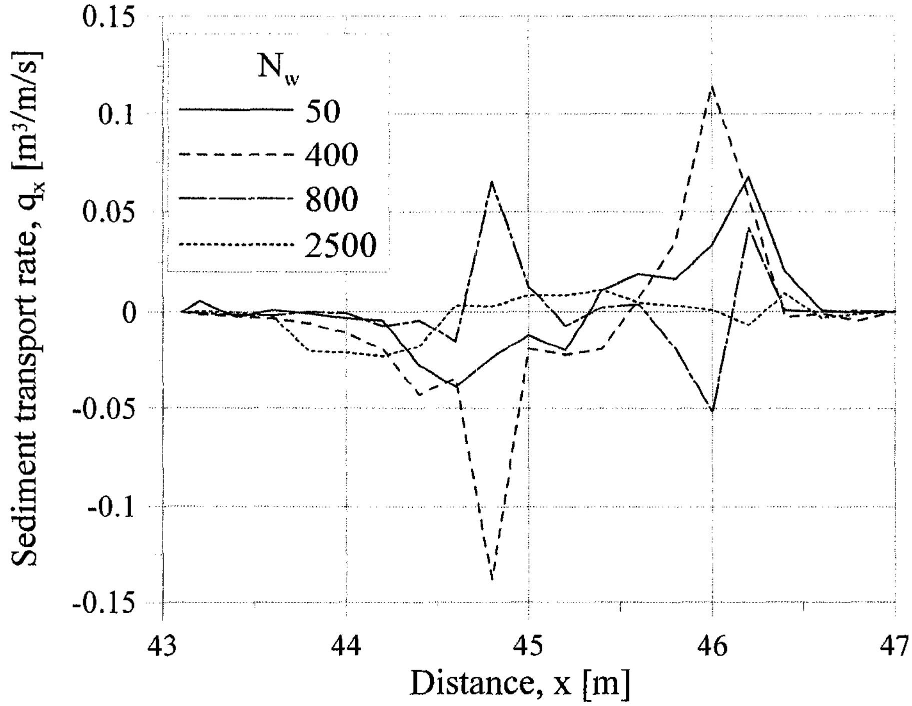

Figure D.19 – Time and space variation of the sediment transport rate, Test 19: Regular waves, T_{av} = 2.0 s, H_{av} = 0.18 m, slope: 1:7

E Outputs from Wave Gauges

Table E.1 – Average wave height for all tests with regular waves [m]

TEST 1	WG1	WG2	WG3	WG4	WG5	WG6	WG7	WG8	WG9	WG10	WG11	WG12
50	0.04	0.01	0.00	0.18	0.17	0.16	0.17	0.20	0.18	0.24	0.21	0.16
100	0.04	0.01	0.00	0.18	0.17	0.16	0.17	0.20	0.18	0.24	0.21	0.16
200	0.05	0.01	0.00	0.14	0.14	0.14	0.14	0.14	0.14	0.16	0.17	0.13
400	0.08	0.01	0.00	0.15	0.15	0.15	0.14	0.13	0.16	0.16	0.17	0.17
800	0.06	0.01	0.00	0.16	0.15	0.15	0.13	0.14	0.16	0.16	0.17	0.18
1500	0.02	0.00	0.00	0.15	0.15	0.14	0.13	0.14	0.16	0.16	0.17	0.18
2000	0.02	0.00	0.00	0.15	0.15	0.14	0.13	0.14	0.15	0.16	0.16	0.18
2500	0.02	0.00	0.00	0.15	0.15	0.14	0.13	0.14	0.15	0.16	0.16	0.18
TEST 2												
50	0.04	0.04	0.00	0.18	0.19	0.19	0.18	0.18	0.20	0.22	0.24	0.12
100	0.04	0.04	0.00	0.18	0.19	0.19	0.18	0.18	0.20	0.22	0.24	0.12
200	0.04	0.04	0.01	0.18	0.19	0.20	0.20	0.19	0.20	0.24	0.23	0.09
400	0.04	0.03	0.00	0.18	0.19	0.19	0.20	0.20	0.20	0.24	0.23	0.10
800	0.05	0.01	0.00	0.19	0.19	0.20	0.20	0.19	0.21	0.23	0.24	0.12
1500	0.07	0.01	0.00	0.20	0.19	0.18	0.17	0.19	0.21	0.22	0.22	0.15
2000	0.10	0.01	0.00	0.21	0.20	0.18	0.17	0.19	0.21	0.23	0.22	0.17
2500	0.07	0.01	0.00	0.20	0.19	0.18	0.17	0.19	0.21	0.23	0.22	0.17
3000	0.03	0.01	0.00	0.20	0.19	0.18	0.17	0.19	0.20	0.23	0.21	0.17
3500	0.02	0.00	0.00	0.19	0.18	0.17	0.17	0.20	0.19	0.24	0.21	0.17
4000	0.03	0.01	0.00	0.18	0.18	0.17	0.17	0.20	0.18	0.24	0.21	0.17
5000	NO DATA											
6000	0.02	0.00	0.00	0.18	0.17	0.16	0.17	0.20	0.18	0.24	0.21	0.16
TEST 3												
50	0.05	0.05	0.00	0.23	0.24	0.24	0.24	0.24	0.27	0.28	0.24	0.12
100	0.05	0.06	0.00	0.23	0.24	0.24	0.24	0.24	0.27	0.28	0.24	0.12
200	0.05	0.07	0.01	0.24	0.25	0.26	0.25	0.25	0.26	0.29	0.26	0.13
400	0.04	0.07	0.01	0.24	0.25	0.26	0.26	0.25	0.26	0.30	0.25	0.10
800	0.04	0.07	0.01	0.24	0.25	0.25	0.25	0.26	0.26	0.30	0.24	0.12
1500	0.06	0.01	0.00	0.27	0.27	0.28	0.27	0.25	0.29	0.29	0.24	0.13
2000	0.07	0.01	0.01	0.26	0.25	0.24	0.23	0.25	0.26	0.30	0.21	0.16
2500	0.06	0.01	0.00	0.24	0.23	0.23	0.22	0.26	0.25	0.31	0.20	0.15
3000	0.03	0.01	0.00	0.23	0.22	0.22	0.23	0.27	0.25	0.32	0.20	0.15
3500	0.02	0.01	0.00	0.23	0.22	0.23	0.23	0.27	0.24	0.32	0.21	0.15
4000	0.02	0.01	0.00	0.23	0.22	0.23	0.24	0.27	0.24	0.32	0.21	0.14
5000	0.02	0.01	0.01	0.23	0.23	0.24	0.25	0.26	0.24	0.32	0.21	0.14
6000	0.02	0.01	0.01	0.24	0.24	0.25	0.25	0.26	0.25	0.32	0.21	0.13
7000	0.02	0.01	0.01	0.24	0.25	0.26	0.26	0.25	0.25	0.31	0.22	0.13
8000	0.02	0.01	0.01	0.25	0.26	0.26	0.25	0.25	0.26	0.30	0.24	0.14
9000	0.02	0.01	0.01	0.25	0.26	0.26	0.25	0.25	0.27	0.29	0.25	0.15
10000	0.02	0.01	0.01	0.25	0.26	0.26	0.25	0.25	0.26	0.29	0.25	0.15
12000	0.02	0.01	0.01	0.25	0.26	0.26	0.25	0.25	0.26	0.29	0.26	0.14

TEST 10											
50	0.09	0.01	0.00	0.20	0.19	0.18	0.18	0.20	0.17	0.22	0.21	0.25
100	0.10	0.01	0.00	0.15	0.15	0.15	0.14	0.13	0.14	0.14	0.16	0.19
200	0.11	0.01	0.00	0.16	0.15	0.15	0.14	0.13	0.14	0.16	0.15	0.20
400	0.10	0.01	0.00	0.16	0.15	0.14	0.13	0.14	0.13	0.17	0.14	0.20
800	0.10	0.01	0.01	0.16	0.15	0.14	0.13	0.14	0.12	0.17	0.14	0.20
1500	0.10	0.01	0.01	0.15	0.15	0.14	0.13	0.14	0.12	0.18	0.15	0.21
2000	0.10	0.01	0.00	0.15	0.14	0.14	0.13	0.14	0.12	0.17	0.14	0.21
2500	0.10	0.01	0.01	0.15	0.14	0.13	0.13	0.14	0.12	0.17	0.14	0.21
TEST 11												
50	0.08	0.05	0.01	0.26	0.25	0.24	0.23	0.26	0.22	0.28	0.27	0.22
100	0.09	0.02	0.01	0.26	0.25	0.24	0.23	0.26	0.22	0.28	0.27	0.22
200	0.10	0.02	0.00	0.20	0.20	0.21	0.20	0.19	0.20	0.20	0.23	0.21
400	0.12	0.01	0.00	0.22	0.22	0.21	0.20	0.19	0.19	0.22	0.22	0.24
800	0.14	0.01	0.00	0.22	0.20	0.19	0.19	0.20	0.18	0.23	0.20	0.25
1500	0.14	0.01	0.00	0.20	0.19	0.18	0.17	0.20	0.17	0.22	0.21	0.24
2000	0.14	0.01	0.01	0.20	0.19	0.18	0.18	0.20	0.17	0.22	0.21	0.24
2500	0.15	0.01	0.00	0.20	0.19	0.18	0.18	0.20	0.17	0.22	0.21	0.24
3000	0.15	0.01	0.00	0.20	0.19	0.18	0.18	0.20	0.17	0.22	0.21	0.25
TEST 12												
50	0.08	0.06	0.00	0.09	0.09	0.09	0.09	0.09	0.09	0.09	0.09	0.09
100	0.08	0.07	0.00	0.09	0.09	0.09	0.09	0.09	0.09	0.09	0.09	0.09
200	0.09	0.03	0.00	0.25	0.25	0.25	0.25	0.26	0.24	0.25	0.29	0.15
400	0.09	0.01	0.01	0.26	0.25	0.25	0.25	0.26	0.23	0.27	0.29	0.17
800	0.11	0.01	0.01	0.26	0.25	0.24	0.24	0.25	0.22	0.29	0.27	0.21
1500	0.13	0.03	0.01	0.26	0.25	0.23	0.23	0.26	0.21	0.30	0.26	0.24
2000	0.13	0.02	0.01	0.26	0.24	0.23	0.23	0.26	0.22	0.29	0.27	0.24
2500	0.13	0.01	0.01	0.26	0.25	0.23	0.23	0.26	0.22	0.28	0.27	0.23
3000	0.13	0.02	0.01	0.26	0.25	0.24	0.23	0.26	0.22	0.28	0.27	0.22
TEST 19												
50	0.06	0.06	0.01	0.12	0.12	0.12	0.12	0.12	0.12	0.13	0.13	0.13
100	0.08	0.02	0.01	0.12	0.12	0.12	0.12	0.12	0.12	0.13	0.13	0.13
200	0.11	0.04	0.01	0.20	0.19	0.19	0.18	0.19	0.17	0.23	0.20	0.24
400	0.12	0.01	0.01	0.20	0.19	0.19	0.18	0.19	0.17	0.23	0.20	0.24
800	0.12	0.01	0.01	0.21	0.20	0.20	0.18	0.19	0.18	0.22	0.21	0.24
1500	0.12	0.01	0.01	0.21	0.20	0.19	0.18	0.19	0.18	0.22	0.21	0.25
2000	0.12	0.01	0.01	0.21	0.20	0.19	0.18	0.19	0.18	0.22	0.21	0.25
2500	0.12	0.01	0.01	0.21	0.20	0.19	0.18	0.19	0.18	0.22	0.21	0.25
3000	0.12	0.01	0.00	0.21	0.20	0.19	0.18	0.19	0.17	0.22	0.21	0.25

Table E.2 – Significant wave height for all tests with irregular waves [m]

TEST 4	WG1	WG2	WG3	WG4	WG5	WG6	WG7	WG8	WG9	WG10	WG11	WG12
100				0.13	0.14	0.14	0.13	0.13	0.13	0.13	0.14	0.11
300	0.03	0.01	0.01	0.13	0.14	0.14	0.13	0.14	0.13	0.13	0.13	0.11
750	0.02	0.01	0.01	0.13	0.13	0.13	0.13	0.13	0.13	0.13	0.13	0.11
1000	0.01			0.13	0.13	0.13	0.13	0.13	0.13	0.13	0.13	0.11
2000	0.02	0.02	0.01	0.13	0.14	0.14	0.13	0.14	0.13	0.13	0.13	0.11

3000	0.01	0.02	0.01	0.13	0.14	0.14	0.13	0.13	0.13	0.13	0.13	0.12
4000	0.01	0.02	0.01	0.13	0.14	0.14	0.13	0.13	0.13	0.13	0.13	0.12
TEST 5												
100	0.06	0.02	0.01	0.13	0.13	0.13	0.13	0.13	0.13	0.13	0.14	0.13
300	0.07	0.02	0.01	0.13	0.13	0.13	0.13	0.13	0.13	0.13	0.15	0.13
750	0.09	0.02	0.01	0.14	0.14	0.14	0.14	0.14	0.14	0.14	0.16	0.13
1000	0.06	0.02	0.01	0.13	0.13	0.13	0.13	0.13	0.14	0.14	0.16	0.14
2000	0.04	0.02	0.01	0.14	0.14	0.14	0.14	0.14	0.14	0.15	0.16	0.14
3000	0.03	0.02	0.02	0.14	0.14	0.14	0.14	0.14	0.14	0.15	0.15	0.15
4000	0.03	0.02	0.01	0.14	0.14	0.14	0.14	0.14	0.14	0.15	0.15	0.15
5000	0.03	0.02	0.01	0.14	0.14	0.14	0.14	0.14	0.14	0.15	0.15	0.14
TEST 6												
100	0.07			0.13	0.14	0.14	0.13	0.13	0.14	0.15	0.17	0.14
300	0.08	0.05	0.02	0.13	0.13	0.13	0.13	0.13	0.13	0.14	0.17	0.14
750	0.10	0.04	0.02	0.13	0.14	0.14	0.14	0.13	0.14	0.15	0.17	0.15
1000	0.06	0.02	0.02	0.14	0.14	0.14	0.14	0.13	0.15	0.15	0.18	0.15
2000	0.07	0.04	0.02	0.14	0.14	0.14	0.14	0.14	0.15	0.15	0.18	0.15
3000	0.06	0.04	0.02	0.14	0.15	0.15	0.14	0.15	0.15	0.16	0.18	0.15
4000	0.06	0.04	0.02	0.15	0.15	0.15	0.15	0.15	0.15	0.16	0.19	0.15
5000	0.06	0.04	0.02	0.15	0.15	0.15	0.15	0.15	0.16	0.16	0.19	0.15
TEST 7												
100				0.17	0.17	0.17	0.17	0.17	0.16	0.17	0.16	0.12
300	0.07	0.02	0.01	0.16	0.17	0.17	0.16	0.16	0.16	0.17	0.16	0.12
750	0.08	0.02	0.01	0.16	0.17	0.17	0.16	0.16	0.16	0.16	0.16	0.13
1000	0.07	0.02		0.16	0.17	0.17	0.16	0.16	0.16	0.16	0.16	0.13
2000	0.06	0.02	0.01	0.17	0.17	0.17	0.16	0.16	0.16	0.16	0.16	0.13
3000	0.05	0.02	0.02	0.17	0.17	0.17	0.16	0.16	0.16	0.16	0.16	0.13
4000	0.03	0.02	0.02	0.17	0.17	0.17	0.16	0.17	0.16	0.16	0.16	0.13
5000	0.03	0.02	0.02	0.17	0.17	0.17	0.16	0.17	0.16	0.16	0.16	0.13
TEST 8												
100	0.07		0.02	0.16	0.17	0.17	0.16	0.17	0.17	0.19	0.19	0.14
300	0.07	0.05	0.02	0.17	0.17	0.17	0.17	0.16	0.18	0.19	0.19	0.14
750	0.08	0.07	0.03	0.18	0.18	0.18	0.17	0.18	0.18	0.20	0.20	0.14
1000	0.07	0.04	0.02	0.17	0.18	0.18	0.17	0.17	0.18	0.20	0.19	0.15
2000	0.10	0.05	0.03	0.18	0.18	0.18	0.18	0.18	0.19	0.20	0.20	0.16
3000	0.09	0.05	0.03	0.18	0.18	0.18	0.18	0.17	0.19	0.20	0.20	0.17
4000	0.07	0.05	0.03	0.18	0.18	0.18	0.18	0.18	0.19	0.20	0.20	0.17
5000	0.05	0.04	0.02	0.18	0.18	0.18	0.18	0.18	0.19	0.20	0.20	0.17
10000	0.04	0.04	0.03	0.19	0.19	0.19	0.18	0.18	0.19	0.20	0.21	0.18
TEST 9												
100	0.07			0.17	0.18	0.18	0.18	0.17	0.19	0.20	0.22	0.15
300	0.07	0.11	0.07	0.17	0.18	0.18	0.18	0.17	0.18	0.20	0.22	0.15
750	0.08	0.13	0.06	0.18	0.18	0.18	0.18	0.18	0.19	0.20	0.22	0.16
1000	0.10	0.11	0.05	0.18	0.18	0.18	0.18	0.18	0.19	0.20	0.22	0.17
2000	0.17	0.08	0.05	0.19	0.19	0.19	0.19	0.18	0.20	0.21	0.23	0.18
3000	0.17	0.08	0.04	0.19	0.20	0.20	0.19	0.20	0.20	0.22	0.23	0.20
4000	0.18	0.07	0.04	0.20	0.20	0.20	0.20	0.20	0.20	0.22	0.23	0.20
5000	0.17	0.05	0.04	0.20	0.20	0.20	0.20	0.20	0.20	0.22	0.23	0.21

10000	0.13	0.05	0.03	0.20	0.20	0.20	0.20	0.20	0.20	0.22	0.23	0.21
TEST 13											
100				0.14	0.14	0.14	0.14	0.14	0.14	0.14	0.15	0.15
300	0.02	0.01	0.00	0.14	0.14	0.14	0.13	0.14	0.13	0.14	0.14	0.14
750	0.01	0.01	0.00	0.13	0.13	0.14	0.13	0.13	0.13	0.13	0.14	0.14
1000	0.01	0.01	0.00	0.13	0.13	0.13	0.13	0.14	0.13	0.13	0.14	0.14
2000	0.01	0.01	0.01	0.14	0.14	0.14	0.14	0.14	0.13	0.14	0.14	0.14
3000	0.01	0.01	0.01	0.14	0.14	0.14	0.14	0.14	0.13	0.14	0.14	0.14
4000	0.01	0.01	0.01	0.14	0.14	0.14	0.14	0.14	0.13	0.14	0.14	0.14
5000	0.01	0.01	0.01	0.14	0.14	0.14	0.14	0.14	0.13	0.14	0.14	0.14
TEST 14											
100	0.09	0.01	0.01	0.13	0.13	0.13	0.13	0.13	0.13	0.13	0.13	0.15
300	0.06	0.01	0.01	0.13	0.13	0.13	0.13	0.13	0.13	0.14	0.13	0.16
750	0.05	0.01	0.01	0.14	0.14	0.14	0.14	0.14	0.13	0.14	0.14	0.17
1000	0.04	0.01	0.01	0.14	0.14	0.14	0.14	0.14	0.13	0.15	0.14	0.16
2000	0.04	0.02	0.01	0.14	0.14	0.14	0.14	0.14	0.14	0.15	0.15	0.16
3000	0.04	0.01	0.01	0.14	0.14	0.14	0.14	0.14	0.14	0.15	0.15	0.16
4000	0.03	0.01	0.01	0.14	0.14	0.14	0.14	0.14	0.14	0.15	0.15	0.16
5000	0.04	0.02	0.01	0.14	0.14	0.14	0.14	0.14	0.14	0.15	0.15	0.16
TEST 15											
100	0.11	0.03	0.02	0.14	0.14	0.14	0.13	0.13	0.14	0.13	0.15	0.16
300	0.13	0.03	0.01	0.13	0.14	0.14	0.14	0.14	0.13	0.13	0.15	0.16
750	0.11	0.03	0.02	0.14	0.14	0.14	0.14	0.14	0.14	0.14	0.17	0.16
1000	0.09	0.02	0.01	0.14	0.14	0.14	0.14	0.14	0.14	0.14	0.18	0.15
2000	0.08	0.03	0.02	0.15	0.14	0.15	0.15	0.14	0.14	0.14	0.18	0.15
3000	0.07	0.02	0.02	0.15	0.15	0.15	0.15	0.14	0.14	0.14	0.17	0.15
4000	0.07	0.02	0.02	0.15	0.15	0.15	0.15	0.14	0.14	0.15	0.17	0.16
5000	0.07	0.02	0.02	0.15	0.15	0.15	0.15	0.14	0.14	0.15	0.17	0.16
TEST 16											
100				0.17	0.17	0.17	0.17	0.17	0.14	0.15	0.16	0.14
300	0.08	0.01	0.01	0.16	0.17	0.17	0.16	0.17	0.16	0.17	0.17	0.15
750	0.04	0.01	0.01	0.16	0.17	0.17	0.16	0.16	0.16	0.17	0.17	0.16
1000	0.03	0.01	0.01	0.16	0.17	0.17	0.16	0.16	0.16	0.17	0.17	0.16
2000	0.03	0.01	0.01	0.17	0.17	0.17	0.17	0.17	0.16	0.17	0.17	0.17
3000	0.03	0.01	0.01	0.17	0.17	0.17	0.17	0.17	0.16	0.17	0.17	0.17
4000	0.02	0.01	0.01	0.16	0.16	0.16	0.16	0.16	0.15	0.16	0.16	0.16
5000	0.03	0.01	0.01	0.17	0.17	0.17	0.17	0.17	0.16	0.17	0.17	0.17
TEST 17											
100	0.10	0.05	0.02	0.17	0.17	0.17	0.17	0.17	0.16	0.17	0.18	0.18
300	0.12	0.03	0.02	0.17	0.17	0.17	0.17	0.17	0.17	0.18	0.18	0.19
750	0.15	0.04	0.02	0.18	0.18	0.18	0.18	0.18	0.17	0.18	0.19	0.20
1000	0.13	0.03	0.02	0.18	0.18	0.17	0.17	0.18	0.18	0.19	0.19	0.20
2000	0.14	0.04	0.02	0.18	0.18	0.18	0.18	0.18	0.18	0.19	0.20	0.20
3000	0.10	0.03	0.02	0.18	0.18	0.18	0.18	0.18	0.18	0.19	0.20	0.20
4000	0.08	0.03	0.02	0.18	0.18	0.18	0.18	0.18	0.18	0.19	0.20	0.21
5000	0.07	0.03	0.02	0.18	0.18	0.18	0.18	0.18	0.18	0.19	0.20	0.21
TEST 18											
100	0.10	0.13		0.18	0.18	0.18	0.18	0.18	0.17	0.18	0.21	0.20

300	0.14	0.11	0.04	0.18	0.18	0.18	0.18	0.18	0.18	0.18	0.21	0.20
750	0.19	0.12	0.05	0.19	0.19	0.19	0.19	0.19	0.18	0.19	0.22	0.21
1000	0.20	0.07	0.03	0.19	0.19	0.19	0.18	0.19	0.19	0.20	0.22	0.21
2000	0.21	0.08	0.03	0.19	0.19	0.19	0.19	0.19	0.18	0.20	0.22	0.21
3000	0.21	0.06	0.03	0.19	0.19	0.19	0.19	0.19	0.18	0.20	0.22	0.22
4000	0.21	0.05	0.03	0.19	0.19	0.19	0.19	0.19	0.18	0.20	0.21	0.21
5000	0.20	0.05	0.03	0.19	0.19	0.19	0.19	0.19	0.19	0.20	0.21	0.21

Table E.3 – Average time period for all tests with regular waves [s]

TEST 1	WG1	WG2	WG3	WG4	WG5	WG6	WG7	WG8	WG9	WG10	WG11	WG12
50	2.00	2.01	2.25	2.00	2.00	2.00	2.00	2.00	2.00	2.00	1.94	1.92
100	1.94	6.16	2.25	2.00	2.00	2.00	2.00	2.00	2.00	2.00	1.94	1.92
200	2.00	2.52	2.84	2.00	2.00	2.00	2.00	2.00	2.00	2.00	2.00	1.76
400	1.98	2.32	2.34	2.00	2.00	2.00	2.00	2.00	2.00	2.00	2.00	1.96
800	2.10	1.97	1.75	2.00	2.00	2.00	2.00	2.00	2.00	2.00	2.00	1.99
1500	2.00	1.86	1.02	2.00	2.00	2.00	2.00	2.00	2.00	2.00	2.00	2.00
2000	2.01	1.91	1.21	2.00	2.00	2.00	2.00	2.00	2.00	2.00	2.00	2.00
2500	2.01	1.97	1.29	2.00	2.00	2.00	2.00	2.00	2.00	2.00	2.00	2.00
TEST 2												
50	2.26	2.79	2.00	2.00	2.00	2.00	2.00	2.00	2.00	2.00	2.00	1.57
100	2.15	2.70	2.00	2.00	2.00	2.00	2.00	2.00	2.00	2.00	2.00	1.57
200	1.98	2.16	7.36	2.00	2.00	2.00	2.00	2.00	2.00	2.00	2.00	1.45
400	1.98	2.01	4.40	2.00	2.00	2.00	2.00	2.00	2.00	2.00	2.00	1.47
800	1.78	2.75	6.64	2.00	2.00	2.00	2.00	2.00	2.00	2.00	2.00	1.62
1500	1.97	2.16	2.02	2.00	2.00	2.00	2.00	2.00	2.00	2.00	2.00	1.94
2000	2.07	2.24	2.06	2.00	2.00	2.00	2.00	2.00	2.00	2.00	2.00	1.96
2500	1.98	2.17	1.76	2.00	2.00	2.00	2.00	2.00	2.00	2.00	1.99	1.95
3000	2.00	2.12	1.84	2.00	2.00	2.00	2.00	2.00	2.00	2.00	1.99	1.95
3500	2.01	2.06	1.91	2.00	2.00	2.00	2.00	2.00	2.00	2.00	1.96	1.95
4000	2.18	2.18	2.13	2.00	2.00	2.00	2.00	2.00	2.00	2.00	1.96	1.98
5000	NO DATA											
6000	2.30	2.37	2.25	2.00	2.00	2.00	2.00	2.00	2.00	2.00	1.94	1.92
TEST 3												
50	2.58	2.68	1.99	2.00	2.00	2.00	2.00	2.00	2.00	2.00	1.95	1.59
100	2.39	2.26	1.99	2.00	2.00	2.00	2.00	2.00	2.00	2.00	1.95	1.59
200	1.79	2.00	6.75	2.00	2.00	2.00	2.00	2.00	2.00	2.00	1.98	1.57
400	1.59	2.00	8.53	2.00	2.00	2.00	2.00	2.00	2.00	2.00	1.97	1.46
800	1.34	2.00	3.76	2.00	2.00	2.00	2.00	2.00	2.00	2.00	1.96	1.71
1500	1.98	3.93	4.61	2.00	2.00	2.00	2.00	2.00	2.00	2.00	1.98	1.73
2000	1.97	2.53	4.39	2.00	2.00	2.00	2.04	2.00	2.00	2.00	1.90	1.95
2500	1.98	2.11	2.02	2.00	2.00	2.00	2.00	2.00	2.00	2.00	1.78	1.92
3000	2.05	2.11	1.87	2.00	2.00	2.00	2.00	2.00	2.00	2.00	1.75	1.86
3500	2.09	2.22	2.89	2.00	2.00	2.00	2.00	2.00	2.00	2.00	1.86	1.77
4000	2.19	2.55	3.13	2.00	2.00	2.00	2.00	2.00	2.00	2.00	1.84	1.65
5000	2.81	3.41	3.97	2.00	2.00	2.00	2.00	2.00	2.00	2.00	1.78	1.60
6000	3.46	4.47	6.26	2.00	2.00	2.00	2.00	2.00	2.00	2.00	1.77	1.58
7000	4.11	4.49	6.82	2.00	2.00	2.00	2.00	2.00	2.00	2.00	1.82	1.60

8000	4.53	6.18	7.83	2.00	2.00	2.00	2.00	2.00	2.00	2.00	1.91	1.62
9000	5.37	5.55	6.06	2.00	2.00	2.00	2.00	2.00	2.00	2.00	1.92	1.63
10000	6.29	7.19	6.23	2.00	2.00	2.00	2.00	2.00	2.00	1.99	1.97	1.59
12000	6.18	6.38	6.80	2.00	2.00	2.00	2.00	2.00	2.00	1.98	1.99	1.54
TEST 10												
50	2.00	2.21	2.08	2.00	2.00	2.00	2.00	2.00	2.00	2.00	2.00	2.00
100	2.00	4.52	2.21	2.00	2.00	2.00	2.00	2.00	2.00	2.00	2.00	2.00
200	2.00	3.06	3.75	2.00	2.00	2.00	2.00	2.00	2.00	2.00	2.00	2.00
400	2.00	2.14	1.87	2.00	2.00	2.00	2.00	2.00	2.00	2.00	2.00	2.00
800	2.03	1.87	1.97	2.00	2.00	2.00	2.00	2.00	2.00	2.00	2.00	2.00
1500	2.01	2.00	1.97	2.00	2.00	2.00	2.00	2.00	2.00	2.00	2.00	2.00
2000	2.00	2.00	1.93	2.00	2.00	2.00	2.00	2.00	2.00	2.00	2.00	2.00
2500	2.01	1.99	1.97	2.00	2.00	2.00	2.00	2.00	2.00	2.00	2.00	2.00
TEST 11												
50	2.00	3.28	4.19	2.00	2.00	2.00	2.00	2.00	2.00	2.00	1.98	1.78
100	1.96	5.77	4.19	2.00	2.00	2.00	2.00	2.00	2.00	2.00	1.98	1.78
200	2.00	4.62	4.17	2.00	2.00	2.00	2.00	2.00	2.00	2.00	2.00	1.81
400	2.00	7.30	11.52	2.00	2.00	2.00	2.00	2.00	2.00	2.00	2.00	1.93
800	2.00	2.55	1.96	2.00	2.00	2.00	2.00	2.00	2.00	2.00	2.00	1.99
1500	2.00	2.23	2.09	2.00	2.00	2.00	2.00	2.00	2.00	2.00	2.00	2.00
2000	2.00	2.36	2.11	2.00	2.00	2.00	2.00	2.00	2.00	2.00	2.00	2.00
2500	2.00	2.87	2.08	2.00	2.00	2.00	2.00	2.00	2.00	2.00	2.00	2.00
3000	2.00	2.26	2.08	2.00	2.00	2.00	2.00	2.00	2.00	2.00	2.00	2.00
TEST 12												
50	1.96	2.62	3.58	1.35	1.35	1.34	1.35	1.35	1.36	1.37	1.40	1.46
100	1.96	3.31	3.58	1.35	1.35	1.34	1.35	1.35	1.36	1.37	1.40	1.46
200	1.96	4.22	2.90	2.00	2.00	2.00	2.00	2.00	2.00	2.00	2.00	1.23
400	1.98	4.73	7.17	2.00	2.00	2.00	2.00	2.00	2.00	2.00	2.00	1.52
800	2.00	11.76	4.83	2.00	2.00	2.00	2.00	2.00	2.00	2.00	2.00	1.72
1500	2.01	8.74	4.95	2.00	2.00	2.00	2.00	2.00	2.00	2.00	1.98	1.87
2000	1.99	6.72	4.39	2.00	2.00	2.00	2.00	2.00	2.00	2.00	1.99	1.84
2500	2.00	3.95	3.28	2.00	2.00	2.00	2.00	2.00	2.00	2.00	1.98	1.82
3000	2.01	6.65	4.19	2.00	2.00	2.00	2.00	2.00	2.00	2.00	1.98	1.78
TEST 19												
50	2.00	2.81	7.89	1.77	1.78	1.75	1.74	1.80	1.87	1.85	1.90	1.87
100	1.95	3.72	7.89	1.77	1.78	1.75	1.74	1.80	1.87	1.85	1.90	1.87
200	2.00	5.89	5.21	2.00	2.00	2.00	2.00	2.00	2.00	2.00	2.00	2.00
400	2.00	2.61	5.84	2.00	2.00	2.00	2.00	2.00	2.00	2.00	2.00	2.00
800	2.00	2.22	2.05	2.00	2.00	2.00	2.00	2.00	2.00	2.00	2.00	2.00
1500	2.00	2.14	2.01	2.00	2.00	2.00	2.00	2.00	2.00	2.00	2.00	2.00
2000	2.00	2.24	2.02	2.00	2.00	2.00	2.00	2.00	2.00	2.00	2.00	2.00
2500	2.00	2.24	2.03	2.00	2.00	2.00	2.00	2.00	2.00	2.00	2.00	2.00
3000	2.00	2.26	2.08	2.00	2.00	2.00	2.00	2.00	2.00	2.00	2.00	2.00

Table E.4 – Peak wave period for all tests with irregular waves [s]

TEST 4	WG1	WG2	WG3	WG4	WG5	WG6	WG7	WG8	WG9	WG10	WG11	WG12
100	140	140	140	1.55	1.54	1.54	1.55	1.55	1.56	1.58	1.58	1.59

300	131	130	130	1.49	1.49	1.49	1.49	1.49	1.48	1.43	1.43	1.43
750	127	121	118	1.51	1.51	1.51	1.51	1.51	1.51	1.51	1.48	1.48
1000	122	61	118	1.51	1.51	1.51	1.51	1.50	1.50	1.50	1.49	1.46
2000	26	25	26	1.52	1.52	1.52	1.51	1.52	1.53	1.53	1.53	1.53
3000	26	25	36	1.52	1.52	1.52	1.51	1.53	1.53	1.53	1.54	1.53
4000	25	25	26	1.52	1.52	1.52	1.54	1.53	1.53	1.53	1.55	1.54
TEST 5												
100	176	178	176	2.07	2.07	2.06	2.11	2.11	2.09	2.14	2.18	2.18
300	34	264	180	2.00	2.02	2.02	2.00	2.00	2.09	2.08	2.09	2.98
750	28	133	45	1.95	1.95	1.95	1.93	1.95	2.10	2.03	2.64	18.59
1000	24	18	147	1.95	1.95	1.95	1.95	1.88	2.02	1.95	2.02	2.01
2000	18	18	18	1.98	1.98	2.01	2.01	1.98	1.99	2.49	18.49	18.46
3000	18	18	18	2.02	2.02	2.02	2.02	1.98	1.97	2.52	18.46	18.43
4000	18	18	18	2.06	2.06	2.11	2.02	1.98	1.93	2.10	18.44	18.43
5000	18	18	18	2.06	2.06	2.06	2.01	1.98	1.93	2.09	18.43	18.42
TEST 6												
100	208	211	210	2.48	2.48	2.48	2.48	2.48	2.57	2.58	2.76	2.76
300	35	59	65	2.48	2.48	2.48	2.48	2.48	2.50	2.50	2.59	5.15
750	36	35	35	2.46	2.42	2.42	2.42	2.48	2.49	2.48	3.66	24.11
1000	37	36	36	2.57	2.57	2.61	2.54	2.54	2.62	2.49	2.71	36.95
2000	36	36	36	2.54	2.50	2.50	2.56	2.53	3.31	37.18	37.16	25.35
3000	34	36	36	2.55	2.50	2.56	2.55	2.50	3.46	37.10	25.61	24.94
4000	35	36	36	2.54	2.50	2.56	2.55	2.49	3.50	36.98	25.57	24.95
5000	48	179	35	2.46	2.47	2.56	2.55	2.48	3.53	36.92	25.66	25.05
TEST 7												
100	140	140	140	1.61	1.61	1.61	1.61	1.61	1.60	1.62	1.60	1.60
300	69	59	68	1.50	1.50	1.51	1.51	1.48	1.43	1.43	1.43	1.89
750	120	33	122	1.51	1.51	1.51	1.51	1.51	1.54	1.54	1.54	2.08
1000	58	55	59	1.52	1.52	1.53	1.52	1.52	1.56	1.51	1.47	1.94
2000	24	19	23	1.52	1.52	1.52	1.52	1.52	1.52	1.52	1.52	18.78
3000	23	23	24	1.52	1.52	1.52	1.51	1.52	1.52	1.52	1.86	18.76
4000	23	23	24	1.52	1.52	1.52	1.51	1.52	1.52	1.52	1.85	18.73
5000	23	23	23	1.52	1.52	1.52	1.51	1.52	1.52	1.52	1.85	18.75
TEST 8												
100	173	178	177	2.24	2.15	2.14	2.14	2.14	2.18	2.18	2.18	3.18
300	38	35	159	2.11	2.11	2.11	2.07	2.10	2.20	2.15	3.42	18.70
750	18	25	25	1.91	1.91	1.91	1.92	1.92	2.76	24.17	18.44	18.39
1000	18	25	36	1.91	1.92	1.92	1.92	1.92	2.02	2.01	2.99	18.22
2000	18	18	18	2.34	2.33	2.33	2.33	2.40	2.62	18.49	18.47	18.42
3000	19	19	19	2.71	2.70	2.70	2.68	2.67	18.75	18.74	18.71	18.69
4000	18	18	18	2.61	2.96	2.97	2.74	2.74	18.45	18.43	18.42	18.40
5000	18	18	18	3.03	3.02	3.04	2.80	2.83	18.45	18.43	18.43	18.40
10000	18	18	18	3.00	3.01	2.78	2.78	2.79	18.51	18.48	18.46	18.43
TEST 9												
100	200	61	62	2.48	2.48	2.48	2.48	2.49	2.63	2.86	4.74	36.22
300	35	35	36	2.51	2.51	2.51	2.48	2.51	2.50	3.47	37.04	36.33
750	35	35	35	2.48	2.48	2.48	2.48	2.48	3.44	36.85	24.39	35.47
1000	36	37	62	2.53	2.53	2.53	2.53	2.53	2.62	3.50	37.21	36.44

2000	35	35	35	2.46	2.47	2.53	2.53	2.52	36.89	36.96	26.06	24.86
3000	35	47	177	3.59	3.60	3.59	2.52	2.63	36.74	36.74	36.74	26.06
4000	35	48	35	3.65	3.64	3.62	3.58	2.63	36.66	36.65	36.66	36.37
5000	35	35	35	3.47	3.48	3.60	3.53	2.62	36.65	36.63	36.64	36.38
10000	36	36	48	3.54	3.54	3.53	3.50	2.46	37.21	37.19	25.89	14.79
TEST 13												
100	119	120	119	1.56	1.55	1.55	1.55	1.58	1.62	1.62	1.60	1.62
300	132	132	134	1.49	1.48	1.43	1.48	1.55	1.43	1.49	1.49	1.49
750	130	130	133	1.51	1.51	1.51	1.50	1.51	1.44	1.51	1.53	1.57
1000	127	59	134	1.51	1.51	1.48	1.56	1.52	1.48	1.49	1.56	1.56
2000	37	37	37	1.52	1.52	1.54	1.54	1.54	1.52	1.52	1.53	1.53
3000	36	37	37	1.52	1.52	1.54	1.54	1.54	1.52	1.52	1.53	1.54
4000	37	37	37	1.52	1.52	1.54	1.54	1.56	1.52	1.52	1.53	1.53
5000	37	37	37	1.52	1.52	1.54	1.54	1.54	1.52	1.52	1.53	1.53
TEST 14												
100	176	178	177	2.13	2.13	2.12	2.12	2.12	2.06	2.24	2.07	2.18
300	59	262	74	1.99	1.99	1.99	1.99	2.13	2.04	2.06	2.07	2.10
750	38	38	38	1.98	1.98	1.98	2.01	1.89	2.37	2.07	37.89	2.69
1000	37	56	37	1.94	1.97	1.97	2.04	1.88	2.01	2.00	2.87	2.60
2000	36	36	36	2.04	2.04	2.02	2.01	1.98	2.39	2.02	3.23	23.24
3000	36	36	36	2.04	2.04	2.02	2.01	1.98	2.39	2.02	3.20	23.17
4000	36	36	36	2.04	2.04	2.02	1.99	1.98	2.39	2.01	3.20	23.15
5000	36	36	36	2.04	2.04	2.02	1.99	1.98	2.39	2.01	3.20	23.23
TEST 15												
100	65	214	214	2.56	2.56	2.49	2.49	2.32	2.59	2.46	2.76	2.58
300	56	55	54	2.55	2.56	2.50	2.41	2.44	2.50	2.42	2.60	38.59
750	35	36	36	2.41	2.53	2.54	2.57	2.54	2.54	38.73	2.55	28.06
1000	36	65	67	2.51	2.44	2.54	2.54	2.54	2.54	3.74	2.54	39.38
2000	51	179	37	2.52	2.60	2.58	2.57	2.54	2.54	38.64	2.56	39.01
3000	140	36	37	2.51	2.59	2.58	2.56	2.54	2.54	5.74	2.56	39.07
4000	53	36	37	2.51	2.59	2.58	2.56	2.54	2.46	5.55	2.56	39.31
5000	162	36	52	2.51	2.59	2.58	2.56	2.54	2.45	5.50	2.56	39.30
TEST 16												
100	140	140	140	1.61	1.61	1.61	1.61	1.61	1.60	1.60	1.60	1.60
300	131	132	69	1.51	1.51	1.43	1.43	1.51	1.43	1.43	1.43	1.43
750	124	123	132	1.51	1.51	1.51	1.51	1.51	1.47	1.51	1.55	1.56
1000	126	126	127	1.53	1.52	1.51	1.50	1.53	1.48	1.49	1.58	1.56
2000	36	25	25	1.55	1.55	1.55	1.54	1.57	1.54	1.52	1.58	1.85
3000	36	25	25	1.55	1.55	1.55	1.54	1.57	1.54	1.52	1.56	1.85
4000	3078	78	27	1.51	1.51	1.51	1.50	1.51	1.45	1.51	1.51	1.51
5000	25	25	25	1.55	1.55	1.55	1.54	1.57	1.54	1.52	1.54	1.84
TEST 17												
100	174	179	178	2.24	2.24	2.24	2.14	2.25	2.02	2.24	2.08	3.12
300	52	64	67	2.06	2.06	2.06	2.10	2.11	1.98	2.15	3.11	3.79
750	38	38	38	2.30	2.30	2.30	2.04	2.08	37.90	37.89	26.26	24.46
1000	37	37	37	1.90	1.90	2.01	2.01	2.01	2.38	2.72	37.64	25.63
2000	36	36	36	2.51	2.51	2.38	2.37	1.98	3.37	2.86	22.87	18.60
3000	36	58	49	2.40	2.39	2.37	2.38	1.98	3.45	2.90	22.99	18.59

4000	36	36	36	2.40	2.39	2.38	2.45	2.05	3.52	2.90	23.00	18.59
5000	36	52	36	2.40	2.39	2.38	2.45	2.05	25.98	2.91	23.06	18.59
TEST 18												
100	211	210	216	2.50	2.50	2.49	2.49	2.38	2.68	2.64	2.88	36.46
300	36	37	58	2.47	2.51	2.42	2.43	2.53	3.38	38.41	4.85	38.00
750	35	36	178	2.51	2.51	2.49	2.44	2.54	38.21	5.28	6.38	26.35
1000	37	37	37	2.44	2.43	2.43	2.45	2.54	3.96	3.22	3.96	38.89
2000	36	36	37	2.49	2.49	2.47	2.47	2.55	38.07	5.28	4.22	38.18
3000	36	54	37	2.49	2.49	2.47	2.47	2.55	38.07	5.28	4.30	38.15
4000	36	36	37	2.49	2.49	2.47	2.47	2.55	38.07	5.32	4.36	38.14
5000	36	36	36	2.49	2.48	2.46	2.47	2.55	38.07	5.35	4.39	38.16